



WATER POLLUTION CONTROL RESEARCH SERIES

● 16130DFX05/70

AN ENGINEERING - ECONOMIC STUDY OF COOLING POND PERFORMANCE

WATER POLLUTION CONTROL RESEARCH SERIES

The Water Pollution Control Research Series describes the results and progress in the control and abatement of pollution in our Nation's waters. They provide a central source of information on the research, development, and demonstration activities in the Environmental Protection Agency, through inhouse research and grants and contracts with Federal, State, and local agencies, research institutions and industrial organizations.

Inquiries pertaining to Water Pollution Control Research Reports should be directed to the Head, Publications Branch, Research Information Division, Research and Monitoring, Environmental Protection Agency, Washington, D. C. 20460.

AN ENGINEERING-ECONOMIC STUDY OF
COOLING POND PERFORMANCE

by

Littleton Research and Engineering Corporation
95 Russell Street, Littleton, Massachusetts 01460

for

Environmental Protection Agency

Project 16130DFX05/70
Contract No. 14-12-521

May 1970

EPA REVIEW NOTICE

This report has been reviewed by the Environmental Protection Agency, and approved for publication. Approval does not signify that the contents necessarily reflect the views and policies of the Environmental Protection Agency, nor does mention of trade names or commercial products constitute endorsement or recommendation for use.

ABSTRACT

A procedure for predicting the temperature of a thermally loaded captive pond is presented. Using this information, the cooling pond is shown in a special case to have an economic advantage over a cooling tower and to be not much more expensive than a natural body (stream or ocean) of water. This, with the ecological and recreational assets of a captive cooling pond, would seem to encourage their expanded use with large thermo-electric power plants.

This report was submitted in fulfillment of Contract No. 14-12-521 under the sponsorship of the Federal Water Quality Administration.

FOREWORD

There is at present a growing need for industrial cooling in the manufacturing industries, in the electric power industries and in the process industries. The primary method of effecting this heat transfer from the plant to the environment at present is to pass river, lake or sea water through heat exchangers or condensers in the plant and discharge this water directly back to its source where it will subsequently cool off by exchanging heat with the atmosphere. Our expanding industrial production combined with our relatively fixed water resources are producing substantial pressure on the ecology of our natural water resources. These waters cannot continue to accept the ever-increasing thermal waste energy without undergoing ecological change. We know that heating of natural water in excess of certain limits results in a degradation of water quality to the point where some species of aquatic life will no longer be supported. The question of accepting the death of some forms of aquatic life in favor of the added capacity of industrial cooling will be resolved, of course, by a decision-making process in which society is free to pick its choice, or degree of choice. The recently established State-Federal water quality standards have set the present tone of this decision.

The use of man-made cooling ponds has been suggested as a means of relieving the thermal pollution of our natural waters. Such captive cooling ponds were built to dissipate the waste energy from electric power plants in the early nineteen hundreds in parts of the United States where lakes and rivers were not readily available. The physical factors which control the cooling capacity of these ponds have long been of fundamental interest to workers in the field of oceanography, limnology and meteorology. As a result, considerable information relative to these factors is available in the open literature. However, this information is diffused over a large area. It is the purpose of this report to investigate the economic feasibility of using man-made cooling ponds for dissipating thermal loads. To this end the report presents a concise method, with substantiating data, for determining the thermal capacity of cooling ponds and considers the economic factors relating cooling ponds to other thermal sinks - such as cooling towers and natural water supplies. Attention has been focused on the cooling requirements of large central electric power stations in view of the fact that they must dissipate very large quantities of energy in a limited area.

SUMMARY

An analytical procedure for predicting the steady state and transient temperatures of condenser cooling water obtained from a cooling pond is presented. The predictions require knowledge of the monthly average climatic and power plant operating parameters. Measured water temperatures for several operating cooling ponds distributed over a wide region of the United States are compared to values predicted on the assumption of fully mixed ponds and slug flow ponds.

An economic analysis of the use of captive cooling ponds is presented. The factors considered in the appraisal include land costs, the influence of water temperature upon the efficiency and capital costs of the power plant, and power required to provide water pumping capacity.

Results are presented in curve form so that it is not continually necessary to return to the basic calculations.

It appears from the analyses that it is possible to obtain cooling water temperatures in a captive cooling pond which are within 5° F of the equilibrium temperature of a natural water supply with a pond area of approximately four acres per megawatt. The water requirements for a properly designed pond are not greatly different from those of a cooling tower. Where areas of adequate size are available and not too expensive, the use of a cooling pond can result in lower overall electrical costs than cooling towers and be reasonably competitive with those of a natural water supply. Cooling ponds can provide a positive contribution to the recreational, aesthetic and ecological values of a community.

TABLE OF CONTENTS

ABSTRACT	iii
FOREWORD	iv
SUMMARY	v
TABLE OF CONTENTS	vii
LIST OF FIGURES	viii
LIST OF TABLES	xi
CONCLUSIONS	1
RECOMMENDATIONS	2
INTRODUCTION	3
FACTORS REGULATING HEAT TRANSFER	5
POND OPERATING CHARACTERISTICS	19
CURVES FOR PREDICTING WATER TEMPERATURE	23
COMPARISON OF PREDICTED AND MEASURED WATER TEMPERATURE	53
CURVES FOR PREDICTING WATER LOSS BY EVAPORATION	63
APPLICATION OF DESIGN CURVES TO PARTICULAR POWER PLANTS	69
ECONOMIC ANALYSIS OF POWER PLANTS WITH COOLING PONDS	79
MULTIPURPOSE OF COOLING PONDS	99
ACKNOWLEDGEMENTS	101
REFERENCES	103
NOMENCLATURE	107
APPENDIX A - Energy Balance Equations	111
APPENDIX B - Heat Transfer by Evaporation and Convection	121
APPENDIX C - Data Collected on Operating Cooling Ponds	141

LIST OF FIGURES

Fig. No.	Title	Page
1	Energy Balance Terms for a Cooling Pond	8
2	Solar Radiation Reflectivity	10
3	Brunt Coefficient	12
4	Clear Sky Solar Radiation	12
5A	Equilibrium or Mixed Steady State Pond Temperature vs f_1 (or $f_1 + \dot{Q}_{pp}$) For $T > 32^{\circ}\text{F}$	25
5B	Equilibrium or Mixed Steady State Pond Temperature vs f_1 (or $f_1 + \dot{Q}_{pp}$) For $T < 32^{\circ}\text{F}$	26
6	Linear Temperature-Depth Profile	27
7A-G	Mixed Pond and Slug Flow Pond Transient Temperature, or Slug Flow Pond Steady State Temperature vs f_2	30-36
8	Comparison of Steady State and Transient Temperatures for a Mixed and a Slug Flow Pond	47
9	Pond Discharge Temperature vs Pond Surface Area for Mixed and Slug Flow Operation	50
10	Ratio of Mixed Pond Area to Slug Flow Pond vs Approach Temperature	51
11	Measured and Predicted Pond Temperatures for the Wilkes Plant	55
12	Measured and Predicted Pond Temperatures for the Kincaid Plant	57
13	Measured and Predicted Pond Temperatures for the Cholla Plant	58
14	Measured and Predicted Pond Temperatures for the Mt. Storm Plant	60
15	Measured and Predicted Pond Temperatures for the Four Corners Plant	61
16	Evaporation Loss Parameter for Mixed Pond in Steady State as a Function of Temperature	64

17	Evaporation Loss Parameter vs Temperature for a Slug Flow Pond Operating in Steady State	67
18	Temperature of Mixed Ponds, 2000 MW _e Plant, Design Climatic Conditions	72
19	Evaporated Water from Mixed Ponds near Phila- delphia, Pa. and Winslow, Ariz., Design Climatic Conditions	73
20	Temperature of Slug Flow Ponds for a 2000 MW _e Plant located near Philadelphia, for Design Conditions	74
21	Transient Temperature of Mixed Pond for a 2000 MW _e Plant near Philadelphia	76
22	Equipment Cost for Captive Cooling Systems	83
23	Exhaust Pressure Correction Curve	85
24	Condenser Back Pressure for a 2000 MW _e Plant near Philadelphia, Mixed Pond Cooling, Design Climatic Conditions	86
25	Condenser Back Pressure for a 2000 MW _e Plant near Philadelphia, Slug Flow Pond, Design Climatic Conditions	87
26	Lost Capacity due to Condenser Back Pressure, 2000 Megawatt Electric Plant near Philadelphia, Mixed Pond, Design Climatic Conditions	88
27	Lost Capacity due to Condenser Back Pressure, 2000 Megawatt Electric Plant near Philadelphia, Slug Flow Pond, Design Climatic Conditions	89
28	Annual Cooling Cost, Mixed Pond - 2000 MW _e Plant, Land and Development Cost - \$500/Acre of Pond, Design Climatic Conditions near Philadelphia	91
29	Annual Cooling Cost, Mixed Pond, 2000 MW _e Plant, Land and Development Cost - \$2000/Acre of Pond, Design Climatic Conditions for Philadelphia	92
30	Annual Cooling Cost, Mixed Pond, 2000 MW _e Plant, Land and Development Cost - \$5000/Acre of Pond, Design Climatic Conditions for Philadelphia	93
31	Annual Cooling Cost, Slug Flow Pond, 2000 MW _e Plant, Land and Development Cost - \$500/Acre of Pond, Design Climatic Conditions for Philadelphia	94

32	Annual Cooling Cost, Slug Flow Pond, 2000 MW Plant, Land and Development Cost - \$2000/Acre of Pond, Design Climatic Conditions for Philadelphia	95
33	Annual Cooling Cost, Slug Flow Pond, 2000 MW Plant, Land and Development Cost - \$5000/Acre of Pond, Design Climatic Conditions for Philadelphia	96
B-1	Evaporation Rate vs Wind Velocity for Lake Colorado City, Lake Hefner and the Meyer Equation	122
B-2	Comparison of Measured and Observed Pan Evaporation over the Atlantic Ocean	123
B-3	Elevation over Open Grass Land vs α_1	129
B-4	Evaporation Rate Given by Various Empirical Equations and Eq. B-16, Summer Conditions $T_w = T_a$	131
B-5	Evaporation Rate Given by Various Empirical Equations and Eq. B-16, $T_w > T_a$	132
B-6	Evaporation Rates given by Various Empirical Equations and Eq. B-16, Winter Conditions, $T_w = T_a$	133
B-7	Evaporation Rates Given by Various Empirical Equations, and Eq. B-16, Winter Conditions, $T_w > T_a$	134
C-1	Sketch of the Wilkes Plant Pond	143
C-2	Wilkes Plant: Measured Temperature-Depth Profile - January and June 1968	147
C-3	Kincaid Plant and Cooling Pond	153
C-4	Cholla Plant: Cooling Pond	155
C-5	Mt. Storm Plant and Cooling Pond	157
C-6	Mt. Storm Plant: Measured Temperature-Depth Profile, August	158
C-7	Four Corners Plant: Measured Temperature-Depth Profile, July 1969	159

LIST OF TABLES

<u>Table No.</u>	<u>Title</u>	<u>Page</u>
I	Summary of Plant Characteristics	54
II	Cost of Equipment in Millions of Dollars	82
C-1	Meteorological Data for Shreveport, La. - 1968	145
C-2	Wilkes Data - 1968	148
C-3	Meteorological Data for Springfield, Ill. - 1968	150
C-4	Kincaid Data - 1968	153
C-5	Meteorological Data for Winslow, Ariz. - 1967	157
C-6	Cholla Data - 1967 (Effective Area = 1/3 Actual Area)	158
C-7	Cholla Data, 1967 (Effective Area = Actual Area)	159
C-8	Meteorological Data for Elkins, W. Va. - 1968	161
C-9	Mt. Storm Data - 1968	166
C-10	Four Corners Data - 1967	170

CONCLUSIONS

1. The simplified technique presented in the form of design curves in the report can be used in conjunction with climatic data from nearby Weather Stations to predict the monthly average value of condenser inlet water temperature within about $\pm 5^{\circ}$ F. If this accuracy is sufficient, it is not necessary to proceed to the more particular analysis in this report.
2. Condenser inlet temperatures for a cooling pond can be made to approach temperatures associated with once-through river water cooling if the ratio of pond surface area to electric energy generation is made equal to or greater than approximately 4 acres per megawatt.
3. For regions of the United States where the humidity and rainfall are moderate to high, a cooling pond size can be selected which will result in condenser inlet water at the same temperature or lower than water from natural draft cooling towers. Likewise, for such ponds, the amount of water evaporated in the natural draft towers will exceed the difference between the water evaporated from the pond and the water gained by the pond in the form of direct precipitation.

In semi-arid regions of the United States the loss of water by evaporation from the pond surface will be substantially greater than in other locations which have the same equilibrium temperature. This additional water loss may result in an economic advantage for cooling towers in semi-arid regions.

RECOMMENDATIONS

1. Of the two analyses presented in this report, namely, a general analysis and a simplified analysis, comparisons between measured and predicted water temperatures were made only on the basis of the simplified analysis because the general analysis requires an iterative solution which is prohibitively tedious if done by hand. It is recommended that the general analysis be computerized so that it would be necessary to supply only the monthly weather conditions as obtained directly from Weather Bureau data and the monthly power plant loadings as input data in order to obtain condenser inlet water temperature and total water loss by evaporation as the output of the computer program. Furthermore, it is recommended that operating data for a longer period of time than used in the present report be sought for the two most sensitive (high ratio of thermal waste energy to pond surface area) ponds representative of high and low humidity regions respectively. Two such ponds could be the Mt. Storm pond in West Virginia and the Four Corners pond in New Mexico.

It is anticipated that the predictive technique could be refined by use of the computerized general analysis so as to make possible the prediction of cooling water temperatures to within less than $\pm 5^{\circ}\text{F}$.

2. It is recommended that a program be initiated to collect data on operating cooling towers located in various regions of the United States and compare the engineering-economic parameters of towers and cooling ponds at the various sites. The cooling tower data to be collected in this program could be used to evaluate recently developed predictive techniques for cooling towers such as that reported by Winiarski, Tichenor and Byram [31] and by Llung and Moore [32].

INTRODUCTION

At the present time the major portion of electric power is generated in thermal power plants. That remaining is generated in hydroelectric facilities. This distribution between thermal and hydroelectric plants cannot be substantially shifted to remove the load from the thermal plants and in fact will move in the other direction. As a result of this rather static distribution and with the tacit assumption that no significant breakthrough will be made in the near future on a commercial scale (electric utility level) in direct energy converting methods, considerable engineering effort is now being expended to reduce the overall cost of electric power generation in thermal plants. To date this pressure has lead to the adoption of three concepts, namely: nuclear plants, mouth-of-mine coal driven plants and very large fossil fuel plants. Unfortunately, all three concepts sharply increase the thermal pollution burden.

In the case of nuclear plants, the increased thermal pollution danger arises as a result of their lower energy conversion efficiency. Such plants are "heat-engines" in the thermodynamic sense, and are thus subject to the Carnot efficiency limit which dictates that the efficiency decreases as the temperature difference between the steam generation temperature and the surrounding (usually a river or ocean) temperature decreases. At present the temperature at which steam can be generated in a nuclear plant is considerably below the corresponding temperature in a fossil plant. As a result, the thermal energy rejected to the surroundings in the form of heat transfer to a river or ocean per unit of electric energy generated is greater in the nuclear plant. However, because nuclear thermal energy is less expensive than fossil fuel in some parts of the United States, the overall cost of generation per unit electric power may be lower in the new nuclear plants than organic plants. Nuclear plants to be economically efficient must be large units so the amount of rejected heat is large and concentrated.

In the case of mouth-of-mine coal plants, the problem of thermal pollution can be sharpened because the location of the plant is dictated by the source of coal, leaving little room for optimizing location with respect to thermal energy disposal. In this case also, economic considerations favor very large plants with large localized heat rejections.

In the case of substantially larger coal, oil and gas driven plants, the danger simply arises from the high concentration of thermal energy rejection at one location.

There is, of course, the possibility that the aquatic thermal pollution problem will be essentially eliminated if a major breakthrough were to be made (at the commercial level) with one of the direct energy converting methods which are not "heat-engines" and therefore not subject to the Carnot efficiency limitation. Anticipation of such a breakthrough in the foreseeable future does not seem to be realistic.

Faced with the economically dictated need to build large plants (on the order of 1000 to 2000 megawatts of electric power) and relatively few sources of fresh water that can accept the thermal waste from such plants without violating the State-Federal water quality standards as applied to aquatic thermal pollution, the electric power generating industry can no longer anticipate the unrestricted use of natural waters for thermal energy sinks and must now look for more acceptable heat sinks. The possibilities are the ground, the ocean, the atmosphere, and ultimately space.

This report is concerned with the use of the atmosphere as the ultimate heat sink and an isolated cooling pond as the intermediate thermal sink. In particular, predictive models are developed and their validity is assessed by comparing predicted and measured pond temperatures under various climatic conditions and power plant loads. The economic influence of the pond on the capital cost and on the operating cost of the plant is also developed.

In order that the results of this work can be readily used, they have been presented in a set of "design curves" so that it is not continually necessary to return to the basic calculations.

FACTORS REGULATING HEAT TRANSFER

A Brief Historical Review

A cooling pond serves its function as an intermediate heat sink by receiving the thermal energy rejected in the plant condensers and subsequently rejecting that energy to the atmosphere. Energy is added to the pond water by direct heat transfer in the condenser of the power plant, by absorption of short-wave solar radiation, by absorption of long wave atmospheric radiation and by make-up water that is received by the pond. Energy is removed from the pond by thermal radiation, by conduction to the atmosphere, by evaporation and by water which flows from the pond. Heat transfer between the pond water and the ground can be safely neglected when compared to the other quantities listed above.

The energy of the pond, and hence its temperature, at any time is determined by the time history of the various mechanisms that put energy into or remove energy from the pond.

The concept of calculating the temperature of a natural body of water by taking such an energy balance appears frequently in the literature. One of the earliest discussions was presented by Cummings and Richardson in 1927 [1].

Lima [2] in 1936 was one of the first workers to compare measured power plant cooling pond temperatures with predicted values. Lima developed a set of empirical curves from data collected by various power companies that had operated cooling ponds. These curves could be used to determine an overall pond-to-atmosphere heat transfer coefficient (K = heat dissipated to the atmosphere per unit area per unit time per unit difference between the water vapor pressure in the air and the water vapor pressure corresponding to the pond surface temperature) if one knew the wind speed, air temperature and power plant loading on the pond. Although Lima's empirical curves could be used to predict the temperature of the ponds used in the study to within approximately $\pm 5^{\circ}\text{F}$, they could not be confidently extrapolated to conditions beyond those studied. Likewise this empirical approach led only to the prediction of the mean pond temperature without giving insight to the influence of vertical or longitudinal temperature gradients, or the influence of the thermal capacity of the individual ponds involved in the study.

Later, in 1951, Throne [3] devised an analytical procedure for pre-

dicting cooling pond temperatures based on the energy balance concept. Throne presented his technique in a set of curves from which pond temperature could be determined if one knew the air temperature, wind speed and power plant loading. Throne compared his predicted results with data from each of 298 months of operation of a plant in Colorado. The predicted and measured values agreed within $\pm 5^{\circ}\text{F}$ for the vast majority of cases. However, in order to construct the required curves, it is necessary to know the measured equilibrium temperature of the lake in question when no waste energy load is being imposed by the power plant. In addition, the curves assume a uniform lake surface temperature and a 4°F vertical temperature variation from surface to bottom. As in the case of the empirical curves devised by Lima, Throne's technique does not account for non-steady state behavior of the pond nor is the validity of extrapolation obvious.

In 1953 Langhaar [4] presented an analytical technique, based on the energy balance concept, which was general enough to predict cooling characteristics of ponds without the necessity of measuring the equilibrium temperature of the particular pond when no waste energy load is being imposed by the power plant. Likewise, his approach was capable of being used to take into account the influence of longitudinal temperature gradients and non-steady state operation. Langhaar's work had been preceded by proposed analytical techniques for determining the cooling capacity of flowing streams by Le Bosque [5] in 1946 and by the extensive experimental energy balance study on Lake Hefner as reported, for example, by Anderson [6] in 1952. Langhaar presented his work in the form of nomographs and compared his results against a single pond in which a noticeable longitudinal (that is, in the direction of flow) temperature gradient existed in contrast to the pond investigated by Throne in which the entire pond surface was found to be at a uniform temperature.

In 1959 Velz and Gannon [7] modified the work of Langhaar and compared predicted values of temperature for a cooling pond with a pronounced longitudinal temperature gradient located in Shreveport, La., and for a river in Michigan that received waste thermal energy. In both cases the agreement between predicted and measured temperatures was within approximately $\pm 5^{\circ}\text{F}$.

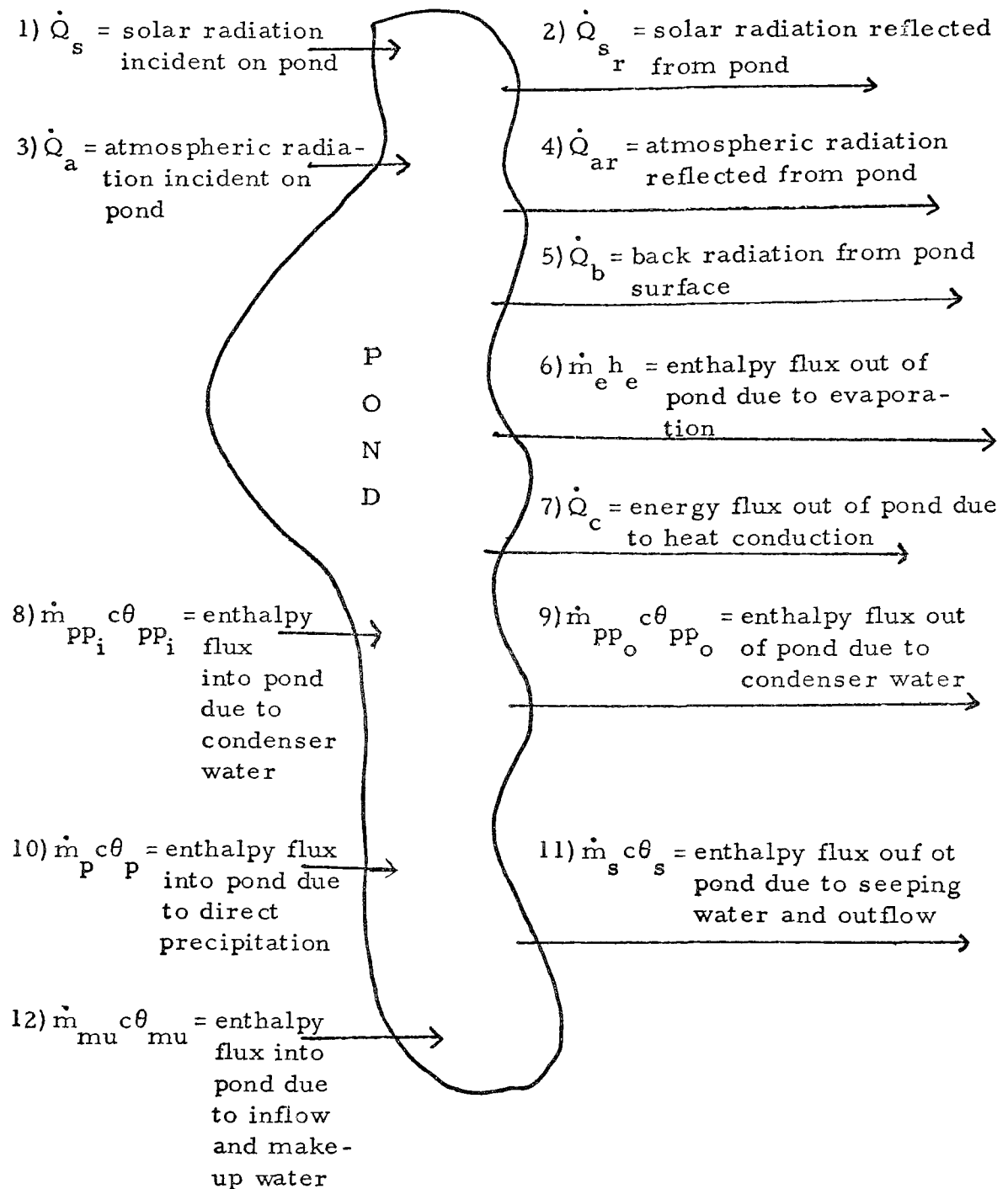
Messinger [8] reported on an experimental study on a thermally loaded stream in 1963. In this study the energy budget technique was used to predict the temperature profile along a section of the West Branch of the Susquehanna River in Pennsylvania below a point at which waste heat is added to the river. The predicted temperatures were as much as 5°F higher than measured values (based on four hour study periods).

Messinger attributed the discrepancies to inadequacies in the measurement of solar and atmospheric radiation of partially shaded water surfaces.

A comprehensive review of the energy balance technique was reported by Edinger and Geyer in 1965 [9]. Edinger and Geyer present the cooling capacity of a body of water in terms of a heat exchange coefficient by linearizing the energy balance equation. The results of this study are presented in equation, chart and table form for ponds with and without longitudinal temperature gradients. They applied the linearized energy equation to the steady state steady operation of a "mixed" pond (that is, one without longitudinal or vertical temperature gradients) and to a "flow through" pond (that is, one with a longitudinal temperature gradient but without a vertical temperature gradient) in order to compare the two modes of pond operation. Although no substantial comparison is made between predicted and measured temperatures for these two modes of operation, the authors and others [10] later, in 1968, reported on a number of field sites that have been selected for the purpose of gathering rather extensive data on the cooling characteristics of river, lake and tidal plants.

A Review of the Energy Balance Terms

The significant energy fluxes for a cooling pond are shown in Figure 1. Each flux term is discussed in the following pages; however, before considering the radiation terms, it is helpful to recall that Stefan's Law states that all bodies radiate energy by electromagnetic waves and do so at a rate proportional to the fourth power of their absolute temperature. These electromagnetic waves are not monochromatic, but rather cover a range of wavelengths. The energy transported by these waves is not the same at all wavelengths, but rather it is highly concentrated around a wavelength λ_m given by Wien's Law as $\lambda_m = C_1/T$ [11], where C_1 is a constant and T is the absolute temperature of the body radiating energy. Thus the hotter the radiating body, the shorter the wavelengths at which most of the energy is concentrated and vice versa. Thus the sun, which is at a surface temperature of approximately $11,000^{\circ}\text{R}$ will give off most of its energy at wavelengths which are short compared to wavelengths given off by the pond which has a surface temperature of approximately 500° to 570°R or, for example, compared to radiation given off by water vapor and by carbon dioxide that might be present in the atmosphere at temperatures of the order of 400° to 600°R .



Note: All terms are in units of energy per unit time per unit of pond surface area.

Figure 1 - Energy Balance Terms for a Cooling Pond

Solar Radiation (\dot{Q}_s)

According to Wein's Law the value of λ_m for the sun at a surface temperature of about $11,000^{\circ}\text{R}$ is approximately 0.5 microns. In particular, Wein's Law indicates that 99% of the sun's radiated energy is associated with wavelengths shorter than 4 microns. The amount of radiation from the sun which reaches the outer atmosphere of the earth is a function of the time of day, latitude, and the season and can be calculated without undue difficulty. However, only some of this radiation strikes the surface of the earth as short wave (4 microns or less) radiation. The amount that does strike the earth surface is called short-wave solar radiation or simply solar radiation.

Of the total radiation from the sun which strikes the outer atmosphere of the earth some is reflected back into space, some is transmitted through the atmosphere and strikes the earth surface (the solar radiation) and some is absorbed by the gases in the atmosphere, primarily by ozone in the upper atmosphere and water vapor and cloud cover. As a result of the complexity of these three possibilities, the solar radiation term (\dot{Q}_s) is more reliably measured than calculated. The instrument used to make this measurement is a pyranometer. This device consists of a flat horizontal circular disc which is housed inside a lime-glass bulb. The disc is separated into a white surface center circle and a white surface outer ring by a blackened intermediate ring. Thermopiles are used to measure the temperature difference between the black and white surface. This temperature difference is a function of the radiation flux penetrating the lime-glass bulb. The bulb material is selected so that the device will be sensitive to radiation of wavelengths equal to 4 microns or less. Selected local weather bureau stations routinely measure the solar radiation and annual summaries of these data are available from the National Weather Records Center, Asheville, North Carolina. Values of the solar radiation, averaged over a period of years, are given in map form for the United States in Ref. [12].

The solar radiation (\dot{Q}_s) averaged over a twenty-four hour period varies with the geographical location and the time of year in the range of 400 to $2800 \text{ btu}/\text{ft}^2 \text{ day}$.

Solar Radiation Reflected from the Pond Surface (\dot{Q}_{sr})

A convenient way to characterise this quantity is to state the ratio between the solar radiation reflected from the pond surface and the solar

radiation incident upon the pond surface, thus, $R_{sr} = \dot{Q}_{sr}/\dot{Q}_s$. This ratio is the solar reflectivity which has been measured and reported in the literature. In particular, empirical reflectivity curves which show the solar reflectivity as a function of the sun altitude for various cloud cover were developed in the Lake Hefner studies as reported by Anderson [6]. These empirical curves are reproduced here for convenient reference in Figure 2.

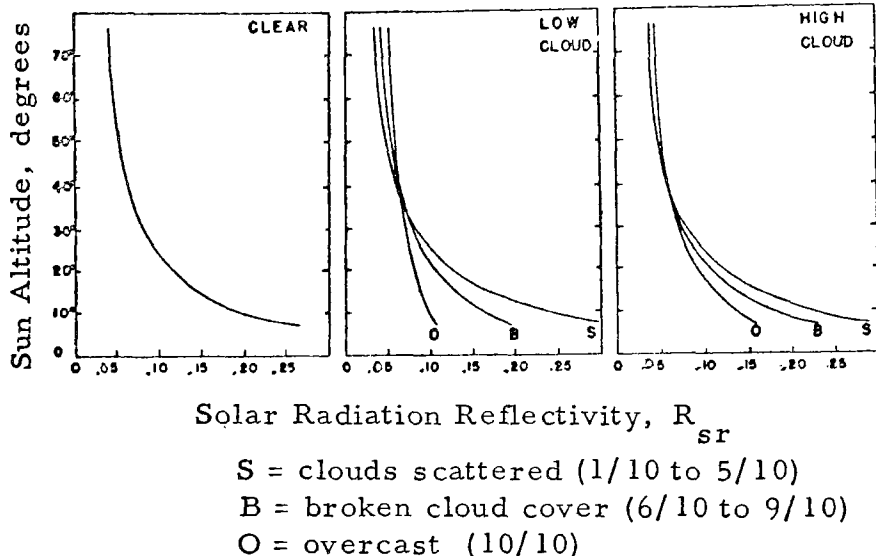


Figure 2 - Solar Radiation Reflectivity
 (after Anderson [6])

The cloud cover is characterized by the amount of cover as measured in tenths of the total visible sky covered by clouds and by the height of the cloud cover with "high" clouds designating those above 20,000 feet and "low" clouds designating those below 6500 feet. Although the solar reflectivity will vary during the day as the sun altitude changes and thus in principle the reflectivity and solar radiation should be known as a function of the time of day, an average value of each has been used in this work. The Weather Bureau reports the solar radiation, for example, as energy per day per unit area averaged over a month. The average solar reflectivity was determined from the curves by using the average sun altitude during sunlight hours for each month. Sun altitude as a function of latitude and time of day is readily available in the literature - for example, see Ref. [13].

The average value of R_{sr} is in the range of 0.04 to 0.12 for the United States.

Atmospheric radiation incident on the Pond Surface (\dot{Q}_a)

In contrast to the short wavelength (< 4 microns) associated with the solar radiation, the wavelengths associated with the electromagnetic radiation given off by the gases that constitute the earth's atmosphere are predominately long, from 4 to 120 microns. The amount of this long wave radiation which strikes the surface of the earth is known as long-wave atmospheric radiation or simply atmospheric radiation. Also in contrast to the solar radiation, the atmospheric radiation is present in the night-time as well as daytime and on completely cloudy days as well as sunny days. The intensity of this radiation is a complex function of several parameters, including the ozone, water vapor, and carbon dioxide content and distribution in the atmosphere and the atmospheric temperature. Observations indicate that the atmospheric radiation depends primarily on the air temperature and water vapor content and increases with an increase in either of these two quantities. It is this last characteristic of atmospheric radiation that results in a substantial lowering of the temperature of a pan of water left exposed to the night sky in an arid or semi-arid climate. Under these conditions there is little water vapor in the air and as a result the pan of water receives little sky radiation at night but does continue to radiate energy to space essentially as a black body and hence experiences a substantial energy or temperature depression.

Atmospheric radiation can be measured directly during the night using a Gier-Dunkle flat plate radiometer or a Thornthwaite net radiometer which measure all the radiant energy received on a blackened surface. At least in principle the atmospheric radiation can be measured in the daytime by taking the difference of two measurements, namely, the total of atmospheric and solar radiation as measured on a radiometer and the solar radiation as measured by a pyranometer. In practice these measurements are not taken routinely by the Weather Bureau stations, and the atmospheric radiation for a particular site and time must be estimated from one of the several empirical equations that have been developed [14, 15]. One such equation that has been extensively evaluated is that due to Brunt, as described by Koberg [9, 15], namely,

$$\dot{Q}_a = \sigma \epsilon (T_a + 460)^4 (C_B + .223\sqrt{P_a}) \text{ btu/ft}^2 \text{ day} \quad (\text{Eq. } 1)$$

where σ = Stefan-Boltzmann Constant = 4.12×10^{-8} btu/ft² day (°R)⁴

ϵ = surface emissivity assumed constant of .97

T_a = air temperature, °F

C_B = Brunt's coefficient. For convenience it is given in Fig. 3

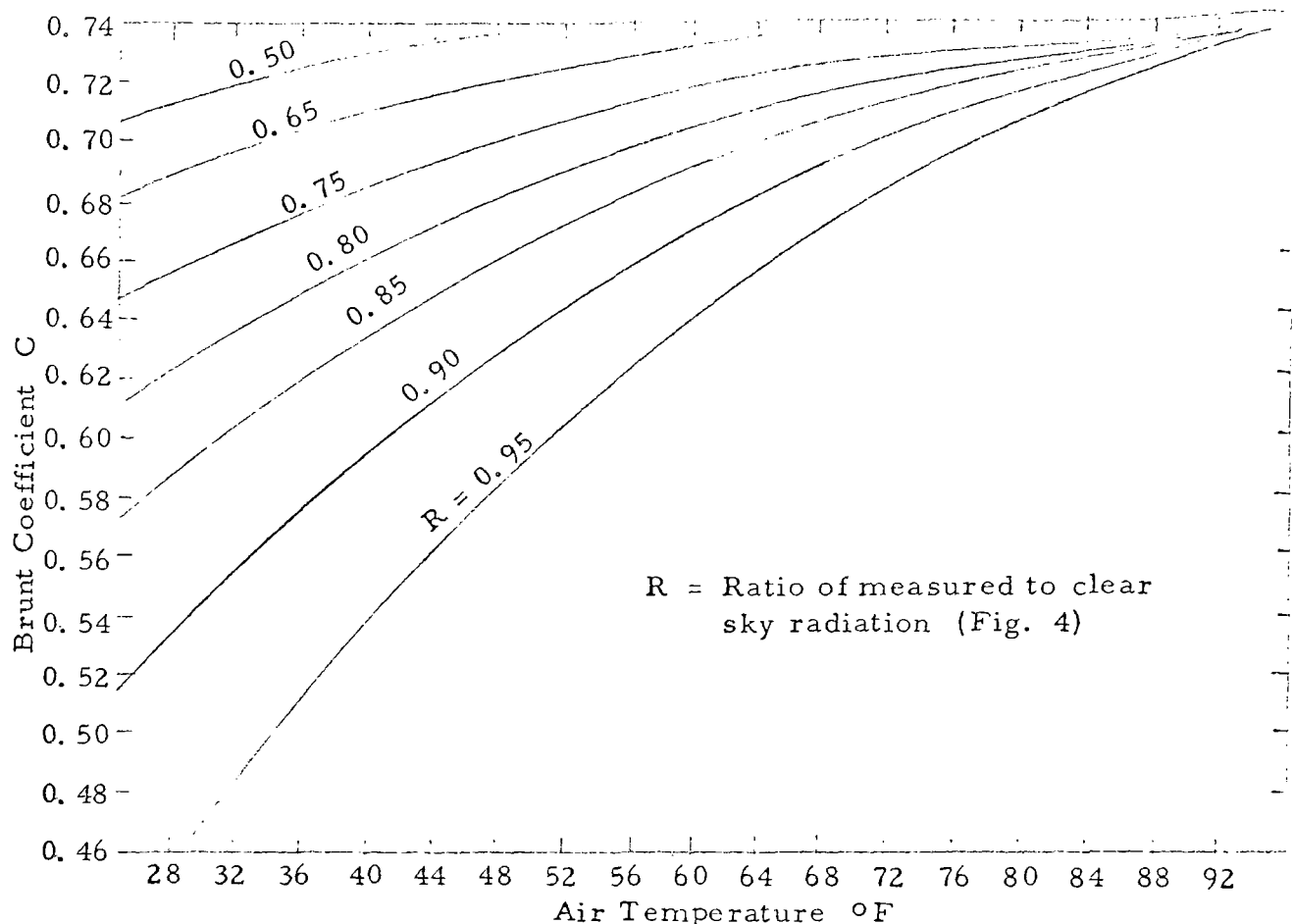


Fig. 3 - Brunt Coefficient (after Koberg - 1962)

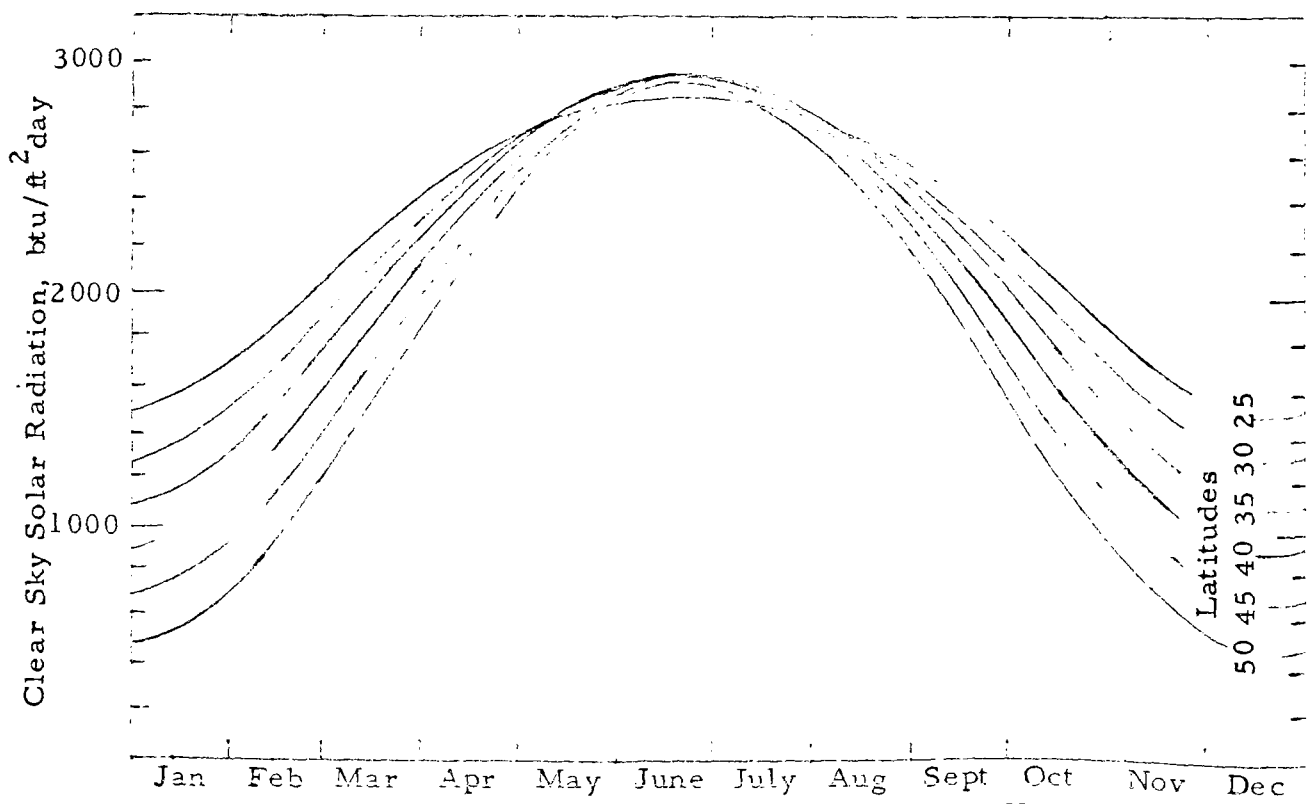


Fig. 4 - Clear Sky Solar Radiation (After Koberg - 1962)

as a function of the air temperature and the ratio of the actual measured solar radiation (as obtained from Weather Bureau data) to the solar radiation that would be received if the sky were clear (as obtained from Fig. 4).

P_a = water vapor pressure in the air, psia

The atmospheric radiation intensity will vary with climatic conditions and latitude but is approximately in the range of 1200 to 3000 btu/ ft^2 day for most parts of the United States.

Atmospheric Radiation Reflected from the Pond Surface (\dot{Q}_{ar})

The reflectivity ($= \dot{Q}_{ar}/\dot{Q}_a$) of a water surface for atmospheric radiation was shown to be approximately constant and equal to about 0.03 by Gier and Dunkle and reported in Ref. [14], pages 96-98. Thus the atmospheric radiation reflected from a water surface may be conveniently taken as $.97\dot{Q}_a$.

If a particular site that has been selected is under experimental study, it is not necessary to measure the four radiation terms given above separately, since they may be combined to give the net absorbed radiation $\dot{Q}_N = \dot{Q}_s - \dot{Q}_{sr} + \dot{Q}_a - \dot{Q}_{ar}$, which in turn can be measured directly by means of a Cummings Radiation Integrator (CRI) or with a Gier-Dunkle and Thornthwaite device. The CRI consists of a shielded shallow pan of water. The water volume is maintained at a constant level and its temperature is taken in order to measure the net radiation absorbed between specified time periods.

Back Radiation from the Pond Surface (\dot{Q}_{br})

Water radiates almost like a perfect black body and since the water temperature is in the vicinity of 50°F, the wave lengths will be long (> 4 microns) compared to the incoming solar radiation and comparable to the incoming atmospheric radiation. Thus the back radiation emitted by the water may be expressed as

$$\dot{Q}_{br} = \epsilon_w \sigma (T_s + 460)^4 \quad (\text{Eq. } 2)$$

where ϵ_w = emissivity of water surface assumed constant at .97

T_s = water surface temperature, °F

It should be noted that the energy balance terms selected for this analysis allow for the independent evaluation of each radiation flux term.

In order to emphasize this point it is helpful to consider the net amount of energy lost by radiation from a body of water (which is always maintained at some constant temperature) on a clear night and on a cloudy night. The amount of back radiation (as given by Eq. 2) will be the same for both nights; however, the incoming atmospheric radiation will be appreciably less on the clear night than on the cloudy night. As a result the net energy lost by radiation is greater during the clear night than during the cloudy night.

Since the water surface temperature may vary from 32°F to 120°F, the back radiation can vary in the range of 2400 to 4500 btu/ft² day.

Enthalpy Flux out of the Pond Due to Evaporation Water ($\dot{m}_e h_e$)

The enthalpy flux that leaves the pond as a result of evaporating water is determined by the product of two terms, namely, the specific enthalpy¹ (h_e) per pound of water vapor leaving the air-water boundary and the rate at which water vapor leaves the air-water boundary (\dot{m}_e). The first term is a well documented thermodynamic property of water and can readily be found for a given water vapor condition. The magnitude of the second term, however, depends on many factors, most notable of which are the average wind speed, vertical profile of wind speed, the water surface temperature, and the water vapor pressure in the air. The rate of evaporation of water from a natural body of water into the atmosphere has been the subject of both analytical and experimental study for a considerable length of time.

Of the analytical work the most prominent is that of Sverdrup [16] in which he compares his predicted values with values based on observed evaporation from an open pan on the deck of a ship at numerous locations.

1) The change in enthalpy between the liquid phase and the vapor phase at the same pressure and temperature is known as the latent heat of vaporization (L). It should be noted that in evaluating the energy balance on the cooling pond in the present study, the energy crossing into or out of the pond has been identified separately with the result that the latent heat vaporization, which is a difference in energy between two phases at the same temperature and pressure, does not enter the argument explicitly. This approach leads to flexibility in the analysis in the sense that the make-up water temperature can be selected or specified independent of the temperature at which water leaves the pond by evaporation.

Considerable experimental work has been done in order to formulate empirical equations for the rate of evaporation under a various climatic conditions. Although there is no way to directly measure the rate of water evaporating from the surface of a natural body of water, it is possible to obtain an indirect measure by making a water mass balance study on the body of water. This is not an easy task for it requires an accurate estimate of all inflows and outflows. The most comprehensive experimental water budget study was that undertaken at Lake Hefner, Oklahoma by a combined task force including the Geological Survey, the Weather Bureau, the U. S. Navy and the Bureau of Reclamation. Marciano and Harbeck [19] showed that for Lake Hefner the rate of evaporation could be found by use of the quasi-empirical equation

$$\dot{m}_e = N_n W (P_w - P_a) \quad (\text{Eq. } 3)$$

where N_n = an empirical coefficient for a particular lake when evaporation is averaged over n days

W = wind speed

P_w = saturation water vapor pressure corresponding to the temperature of the lake surface

P_a = water vapor pressure in the air above the lake

Equations similar to the one given above have been developed by several other workers. Prominent among these additional equations are the ones reported by Koberg et al [20] for Lake Colorado City, Texas, and the one reported by Meyer [21].

In addition to the analytical work and the water budget experimental work referred to in the above discussion, the rate at which water is evaporated from open pans placed on or somewhat above the ground has been measured and reported by the Weather Bureau. Equations are available in the literature for use in estimating the rate of evaporation from natural bodies of water based on nearby pan evaporation data.

The rate of evaporation appears to be highly dependent on the local topography because of the resulting wind structure with the result that the experimentally determined constants in the various reported semi-empirical equations vary in the order of $\pm 25\%$ or more with respect to computed versus actual evaporation rates. In addition to this variation it is noted that all of the previous work has been limited to water at the natural temperature or only a few degrees higher (as a result of other than natural heat addition).

In view of the fact that evaporation accounts for the major portion of

the energy transfer from the pond (approximately 40 to 70% depending on the time of year), it is important to be able to make reliable estimates of the rate of evaporation for ponds where specific experimental evaporation data are not available, in particular for ponds that may be subjected to sufficient heating to increase the water temperature to as much as 30°F above the natural lake temperature.

In order to provide guidelines for making such estimates, an evaporation equation was developed in Appendix B. However, it is not in convenient form to use in the simplified analysis to be developed in this report. In Appendix B it is demonstrated that the evaporation equation proposed by Meyer with a particular value of the empirical constant gives results reasonably close to those predicted by the developed equation and is much easier to use. As a result, the following form of the Meyer equation has been used to estimate the evaporation rate in the simplified analyses:

$$\dot{m}_e = (a_{12} + a_{13} W_m) (P_w - P_a) \text{ #m/ft}^2 \text{ day} \quad (\text{Eq. } 4)$$

where a_{12} , a_{13} = constants

W_m = monthly average wind speed as obtained from measurements taken at the nearest weather station about 25 feet above the surface

Energy Flux out of Pond due to Convection (\dot{Q}_c)

Since the process of convection of energy, that is, heat transfer, from the water surface into the air above is similar to the evaporation of water from the surface into the air above, it is possible to develop an expression for the ratio of energy flux due to convection to the enthalpy flux due to evaporation. Bowen [22], using diffusion theory, was the first one to develop such a ratio. He considered three special cases for which it was possible to obtain analytical solutions to his general equation. Again, in order to evaluate the influence that heated water may have on this ratio, the ratio was derived in Appendix B by making use of the known relation between the mass transfer coefficient and the heat transfer coefficient for smooth surfaces. The ratio was found to be given by the expression: [See Eq. B-31]

$$\gamma = \frac{\dot{Q}_c}{(m_e h_e)} = .00476 \frac{(T_w - T_a) P_{BAR}}{(P_w - P_a) 14.67}$$

where T_w = temperature of the water surface, $^{\circ}\text{F}$
 T_a = air temperature, $^{\circ}\text{F}$
 P_{BAR} = barometric pressure, psia

The above expression for γ is the same as that given by Bowen with the exception of the numerical coefficient which, however, is within the range of the three cases calculated by Bowen.

Enthalpy Flux into ($\dot{m}_{pp_i} c \theta_{pp_i}$) and out of Pond ($\dot{m}_{pp_o} c \theta_{pp_o}$) due to

Water Circulated through the Condenser

The rate at which cooling water is pumped through the condenser ($\dot{M}_{pp_i} = \dot{M}_{pp_o} = \dot{M}_c$) and the temperature rise across the condenser ($\theta_{pp_o} - \theta_{pp_i} = \Delta T_c$) are related to the waste thermal energy from the plant by the equation:

$$\dot{M}_c c (\Delta T_c) = \text{WTE} \quad (\text{Eq. } 5)$$

where c = specific heat of water, $1 \text{ btu}/^{\circ}\text{F} \cdot \text{lb}$

$$\dot{M}_{pp_i} = A \dot{m}_{pp_i}$$

where A = pond surface area, ft^2

\dot{m}_{pp_i} = flow rate out of condenser per unit
of pond surface area, $\text{lb}/\text{ft}^2 \text{ day}$

$$\dot{M}_{pp_o} = A \dot{m}_{pp_o}$$

where \dot{m}_{pp_o} = flow rate into condenser per unit
of pond surface area, $\text{lb}/\text{ft}^2 \text{ day}$

WTE = waste thermal energy from the plant to the pond,
 $\text{btu}/\text{ft}^2 \text{ day}$

Enthalpy Flux into Pond due to Direct Precipitation ($\dot{m}_p c \theta_p$)

The mass flow rate of direct precipitation into the pond will, of course, vary with the time of year and location. The annual average values fall between 10 inches/year in the semi-arid regions of the West and 100 inches/year in some areas of the Northwest. The direct precipitation may be in the form of water, snow or hail. Thus the specific enthalpy can be expressed as:

$$h_{p_i} = c\theta p_i \text{ btu}/\#m \text{ for rain } (\theta p_i \geq 0) \quad (\text{Eq. } 6)$$

$$h_{p_i} = -\{-.492\theta p_i + 143.3\} \text{ for ice and snow } (\theta p_i \leq 0) \quad (\text{Eq. } 7)$$

Enthalpy Flux out of Pond due to Seepage and Outflow ($\dot{m}_s c\theta_s$)

Again the specific enthalpy may be expressed in terms of the heat capacity and the temperature of the water seeping and flowing out of the pond, namely, $h_s = c\theta_s$. The rate of seepage out of the pond or lake is highly site dependent and no useful generalization can be made.

Enthalpy Flux into Pond due to Addition of Inflow and Make-up Water ($\dot{m}_{mu} c\theta_{mu}$)

The rate at which make-up water is added to the pond will depend on the source of the make-up water. For example, if the make-up is run-off water that is drained into the pond from surrounding land or is provided by the inflow of a small stream, the make-up rate will vary with the local precipitation and possible melting of snow cover. If, on the other hand, a river, a lake or a reservoir are used to provide a source of make-up, the rate may be made constant.

The specific enthalpy of the make-up water may be expressed as:

$$h_{mu} = c\theta_{mu} \quad (\text{Eq. } 8)$$

POND OPERATING CHARACTERISTICS

In addition to the climatic conditions imposed on the pond, its own hydrodynamic and energy storage behavior will influence its capacity to dissipate the waste heat received from the power plant. The complete problem of pond hydrodynamics behavior would involve specifications of the inlet and outlet geometry, water condition, the shape and depth of the pond, and the wind speed and direction. In addition, conservation of mass and energy equations and the equations of motion for the pond would have to be solved in order to determine precisely how the hot water travels through the pond, how it mixes, and finally the extent to which it is cooled in the process. Such a task is formidable if at all possible under the prescribed conditions. A simplified approach is to be taken.

Since the problem involves three dimensions and time with associated flow and turbulent mixing, it would seem helpful to break the problem into 1) longitudinal flow and mixing (that is, in the direction of water flow), 2) lateral flow and mixing (that is, perpendicular to the flow, 3) vertical flow and mixing and 4) the effect of thermal storage capacity. Each of the four above considerations is discussed below with the objective of developing a simplified approach to the complete problem.

1 & 2 The flow in the pond may, in the extreme cases, have a very pronounced flow direction with little turbulent mixing or it may have considerable turbulent mixing and no pronounced flow pattern. The first extreme is conveniently called "slug flow" since the water discharged from the condenser at a given time will tend to move through the pond as a "slug" without mixing substantially with the water ahead or behind it. The second extreme is referred to as a horizontally mixed pond in the sense that the temperature of the water will be constant in any horizontal plane as a result of horizontal (longitudinal and lateral) flowing and mixing.

Toward which of these two extremes and to what extent a given pond will operate depends on the geometry of the pond, the inlet and outlet structures and the wind.

Slug flow operation is favored by a long narrow pond with inlet and outlet at the two ends. If a pond is sufficiently long compared with its width, the temperature in a horizontal plane will, for steady state conditions, be a function of longitudinal distance only; lateral mixing due to turbulence and density currents will exert sufficient influence to

eliminate any lateral temperature gradients. The rate at which the water flows through a given pond for a given plant is proportional to the cooling water pumping rate.

Horizontally mixed pond operation is favored by a near unity ratio of length to width with the outlet structure designed to float the hot water on the surface aided by a wind that blows the discharge away from the outlet structure.

In view of the fact that the cooling capacity is a surface area phenomenon, and since the heat release from the pond by evaporation, conduction and back radiation all increase as the water temperature increases, the cooling capacity of a slug flow pond is greater than that of a mixed pond, all other conditions being held constant. The added cooling capacity of the slug flow pond is a result of the continued higher temperature at the pond inlet rather than the immediate achievement of a uniformly mixed but lower temperature. In a mathematical sense a mixed pond can be considered as a slug flow pond in which the temperature rise through the condenser is allowed to approach zero while the pumping rate is allowed to approach infinity since the temperature of the water in the slug flow pond would then be everywhere equal at a given instant.

In a given pond the surface area which is actively engaged in exchanging heat with the atmosphere may be equal to the actual water surface but in some cases will be less or more than the actual water surface. The decrease in effective area may result from channeling of the flow or from the creation of "dead-water" zones. The increase in effective area can result from wind generated waves.

3 Vertical flow is induced in water when the top water cools, becomes more dense, and subsequently sinks. In addition vertical mixing may be present as a result of turbulence. Vertical flow is inhibited and in the limit prevented when the upper layers are heated so as to become buoyant as witnessed by the development of a thermocline during the summer in natural lakes. A vigorous wind will assist in mixing the upper portion of a body of water.

The prediction of vertical temperature gradients in natural bodies of water is a complex matter which has recently come under theoretical and experimental study [23, 24]. The predictive techniques have not, however, reached the state of development where they can be conveniently incorporated into a study of the present nature. In order to estimate the influence of a vertical temperature gradient on the cooling capacity of a pond we have collected data from several operating ponds and

this experimental information will be used to characterize pond operation.

Since the cooling capacity of a pond is a surface phenomenon and increases with increasing surface temperature, it is desirable to spread the heated discharge on the surface of the pond in order to enhance the performance of the pond.

4 Before discussing the question of thermal storage capacity of a cooling pond, it is helpful to review the question of a natural pond without added heat from a power plant. When a shallow natural pond (that is, one which does not display a vertical temperature gradient) is subjected to constant climatic conditions, the water temperature will approach a steady state value known as the "equilibrium" temperature. The "equilibrium" temperature is the value to which the water will adjust itself in order to make the energy transfer into the pond exactly equal the energy transfer from the pond. Thus, when the equilibrium temperature has been achieved and the weather conditions are assumed to remain constant, there will be no additional change in the thermal energy stored in the pond water, and hence no additional change in the pond temperature.

If the natural pond is sufficiently deep, it will tend to divide into two parts as natural heating progresses from the spring into the summer. The upper region, or epilimnion, contains circulated rather turbulent water of nearly uniform temperature which approaches the "equilibrium" value. The lower region, or hypolimnion, contains relatively undisturbed water at a temperature considerably below that of the epilimnion water.

Like the natural pond, a cooling pond of the "mixed" type, if shallow and subjected to constant climatic conditions and power plant loading, will approach a constant temperature. This "steady-state" mixed pond temperature will be higher than the equilibrium temperature. The "steady-state" temperature is the temperature that the pond water will assume in order to balance the energy coming into and leaving the pond. The time required to bring the mixed pond from some given temperature to its "steady-state" value depends on the pond depth; the deeper the pond, the longer the time required. If the pond has not reached "steady-state" operation, it will be said to be in transient operation.

A cooling pond of the slug flow type may also operate in either the steady-state or transient condition. If the pond is initially at some uniform temperature when the waste thermal energy load from the

power plant is imposed and the climatic conditions are held constant, the pond outlet temperature will rise during the transient phase of operation and then reach its steady-state value. Again the steady-state outlet temperature represents the coldest temperature along the longitudinal temperature profile that the pond will assume in order to balance the energy coming into and leaving the pond. The duration of the transient flow phase will become longer as the pond is made deeper, all other conditions being held constant.

Based on the above discussion the general problem may be simplified by neglecting all lateral temperature gradients and developing a technique which will yield a solution for any combination of the remaining six conditions, namely:

Mixed pond or Slug flow pond

Vertical Temperature gradients or no vertical temperature gradients

Steady-state operation or transient operation

The next section presents such a technique in the form of design curves.

CURVES FOR PREDICTING WATER TEMPERATURE

In this section curves are presented which can be used to determine the cooling capacity of a pond operating in any one of the eight possible configurations resulting from the groups of alternates described in the previous section: name, 1) mixed or slug flow, 2) vertical or no vertical temperature gradient, and 3) steady-state or transient operation.

Case 1 - Mixed pond, steady-state, no vertical temperature gradient

For this case the conservation of energy equation is shown to reduce to the following in Appendix A (See Eq. A-15) when certain assumptions are made.

$$O = \{ \dot{Q}_{pp} + [\dot{Q}_N - a_5 - (a_{12} + a_{13}W)(a_1 - \theta_a a_{14} - P_a)] \} \\ - \{ a_6 + (a_{12} + a_{13}W)(a_2 + a_{14}) \} \theta \\ - \{ a_7 + (a_{12} + a_{13}W)(a_3) \} \theta^2 - \{ a_8 + (a_{12} + a_{13}W)(a_4) \} \theta^3 \quad (\text{Eq. 9})$$

where \dot{Q}_{pp} = the waste thermal energy imposed on the pond by the power plant in btu/(ft² of pond area), day = WTE/A

\dot{Q}_N = net radiation absorbed by the pond, in btu/ft² day

θ_a = air temperature referenced to 32° F, in ° F (i.e. above 32° F)

W = wind speed in mph

P_a = water vapor pressure in air, psia

θ = pond water temperature referenced to 32° F, in ° F

$a_1, a_2, a_3, a_4, a_5, a_{14}$ = coefficients (See Appendices A & B)

a_{12}, a_{13} = coefficients to be used in the empirical equation for rate of evaporation from the pond surface (See Appendix B)

It is convenient to label the term in the square bracket of Eq. 9 in a simple way, namely:

$$f_1 = [\dot{Q}_N - a_5 - (a_{12} + a_{13}W)(a_1 - \theta_a a_{14} - P_a)] \quad (\text{Eq. 10})$$

so that Eq. 9 can be written as:

$$\begin{aligned} \{\dot{Q}_{pp} + f_1\} &= \{a_6 + (a_{12} + a_{13}W)(a_2 + a_{14})\}\theta \\ &+ \{a_7 + (a_{12} + a_{13}W)(a_3)\}\theta^2 + \{a_8 + (a_{12} + a_{13}W)(a_4)\}\theta^3 \end{aligned} \quad (\text{Eq. 11})$$

If the value of f_1 and \dot{Q}_{pp} are determined, the pond temperature θ is easily found by solving Eq. 11. In order to avoid the need for continually finding solutions to this third order algebraic equation, the equation is presented in graph form in Figs. 5A and 5B for various values of $(a_{12} + a_{13}W)$. If the pond temperature is found to be less than 32°F ($\theta < 0$), ice would form and the use of Eq. 11 (and hence Fig. 5B) would no longer be valid. However, Fig. 5B does have an application at a later point in the analysis.

In order to demonstrate the use of Fig. 5A, consider the example data given below for the month of July in north-central United States.

$$\begin{aligned} \text{WTE} &= 35.0 \times 10^9 \text{ btu/day} \\ A &= 50 \times 10^6 \text{ ft}^2 \\ \dot{Q}_N &= [\dot{Q}_s - \dot{Q}_{sr}] + [\dot{Q}_a - \dot{Q}_{ar}] \\ &= [2050 - (.07)(2050)] + [2860 - (.03)(2860)] \\ &= 4691 \text{ btu}/\text{ft}^2 \text{ day} \\ P_a &= .294 \text{ psia} \\ \theta_a &= 75.8^\circ - 32.0^\circ = 43.8^\circ\text{F} \\ W &= 10.0 \text{ mph} \end{aligned}$$

If the value of a_{12} and a_{13} suggested in Appendix B are used; namely, $a_{12} = 3730$ and $a_{13} = 373$, then the value of the function $a_{12} + a_{13}W$ is 7460. The functions f_1 and $f_1 + \dot{Q}_{pp}$ have the following values:

$$\begin{aligned} f_1 &= [4691 - 2359 - 6714 (.089 - (43.8)(.00473) - .294)] \\ f_1 &= 5102 \text{ btu}/\text{ft}^2, \text{ day} \\ f_1 + \dot{Q}_{pp} &= 5102 + \text{WTE}/A = 5102 + \frac{35.0 \times 10^9}{50 \times 10^6} = 5,802 \text{ btu.day, ft}^2 \end{aligned}$$

Using the above values, Fig. 5A gives a steady state pond temperature of $\theta_{ss} = 79.0^\circ\text{F}$.

It should be noted that the natural equilibrium temperature (θ_{eq}) for this location and time of year can be found from Eq. 11 and hence also

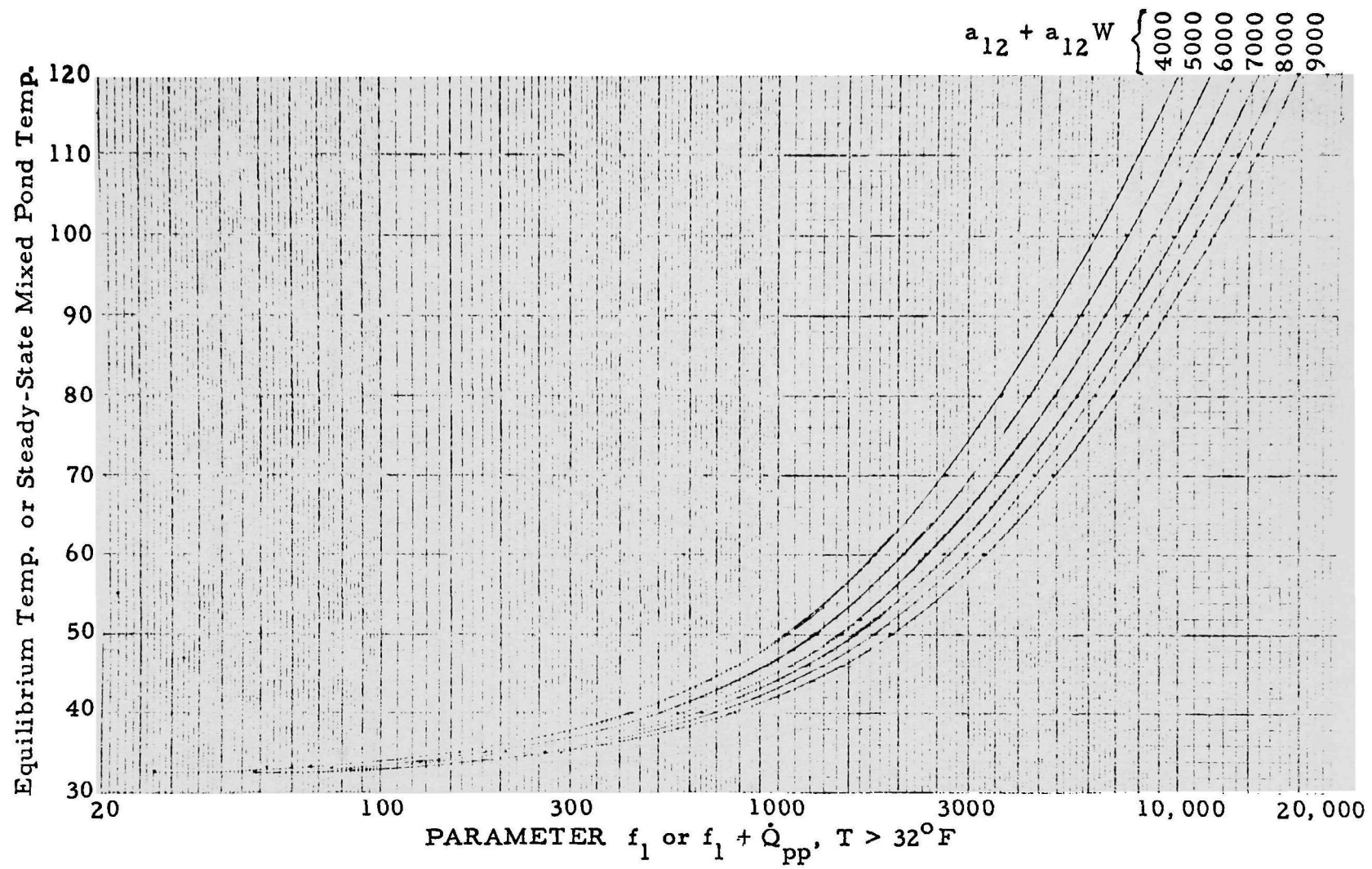


Figure 5A

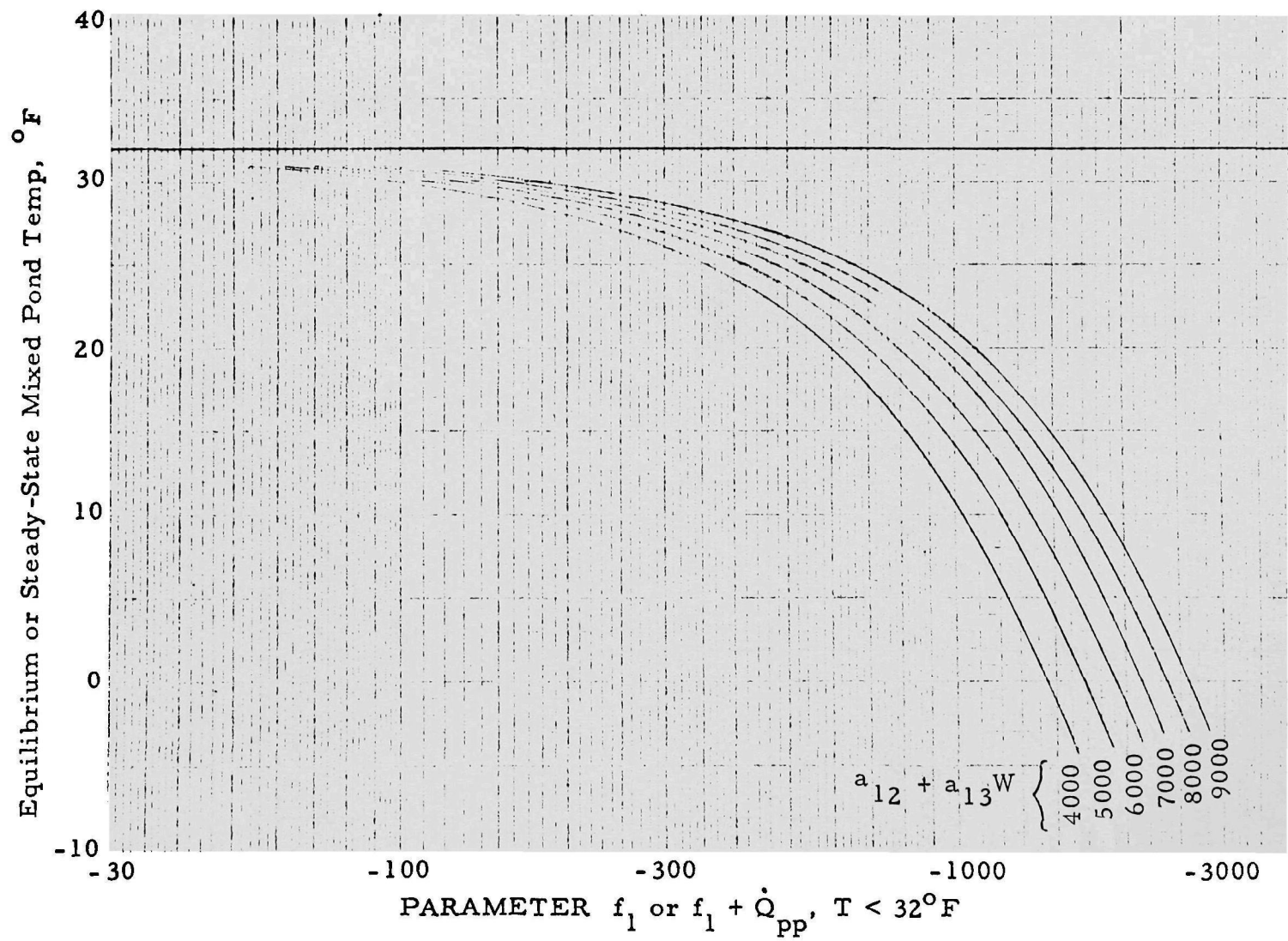


Figure 5B

Fig. 5A by letting the value of \dot{Q}_{pp} go to zero. Thus in general the natural equilibrium temperature is given by the expression:

$$f_1 = [a_6 + (a_{12} + a_{13}W)(a_2 + a_{14})]\theta_{eq} + [a_7 + (a_{12} + a_{13}W)(a_3)]\theta_{eq}^2 + [a_8 + (a_{12} + a_{13}W)(a_4)]\theta_{eq}^3 \quad (\text{Eq. 12})$$

For the example given above Eq. 12 or Fig. 5A gives an equilibrium temperature of 75.5°F .

Case II - Mixed pond, steady-state, with a specified linear vertical temperature gradient

If the pond is assumed to have a linear vertical temperature gradient as shown below in Fig. 6,

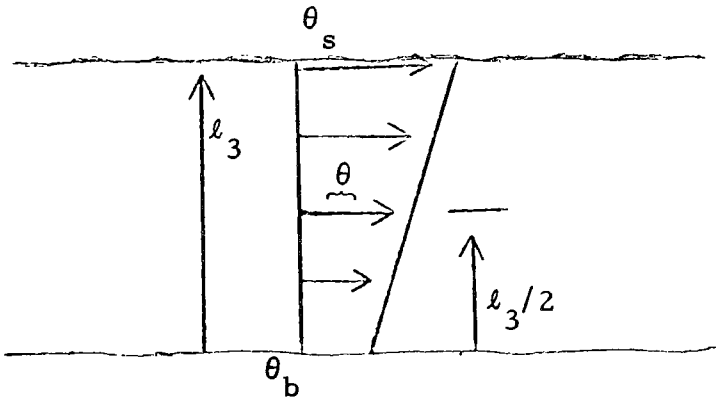


Fig. 6 - Linear Temperature - Depth Profile

then the surface temperature (θ_s) and the bulk average temperature (θ) are related by the expression:

$$\theta = \theta_s - \beta(l_3/2) \quad (\text{Eq. 13})$$

where β is the temperature decrease per unit foot of depth, or

$$\theta_s = \theta + \beta(l_3/2) \quad (\text{Eq. 14})$$

Since back radiation, evaporation and heat conduction are all surface phenomena, Eq. 12 can be expressed as:

$$\begin{aligned}
 \{\dot{Q}_{pp} + f_1\} = & \{a_6 + (a_{12} + a_{13}W)(a_2 + a_{14})\} \{\theta + \beta(\ell_3/2)\} \\
 & + \{a_7 + a_{12} + a_{13}W)(a_3)\} \{\theta + \beta(\ell_3/2)\}^2 \\
 & + \{a_8 + a_{12} + a_{13}W)(a_4)\} \{\theta + \beta(\ell_3/2)\}^3
 \end{aligned} \quad (\text{Eq. 15})$$

Comparison of Eqs. 12 and 15 shows that in steady-state operation the temperature of the pond without a vertical gradient will be the same as the surface temperature of a pond with a vertical gradient. This must be the case since all heat exchange between the water and the atmosphere has been assumed to be a surface phenomenon.

If the condenser intake water structure is so designed that it draws evenly from all levels so that the inlet water temperature is at the bulk average temperature, then for the pond with a gradient, the condenser inlet water will be lower than in the case of no gradient by the amount $\beta(\ell_3/2)$. The data presented in Appendix C indicate that β does not exceed about $1.0^\circ F/ft$ even in operating ponds that have inlet and outlet structures of such a design as to minimize mixing and enhance the flow of the hot water on the pond surface.

If a vertical gradient is anticipated, it is of course beneficial to arrange the intake structure to preferentially draw water from the lower layers. If water is drawn from the lower layers, the gradient will soon be diminished.

Case III - Mixed pond, transient operation, no vertical temperature gradients

If, as in the case of steady-state operation, certain simplifying assumptions are made, then the energy equation can be reduced to the following form (See App. A, Eq. A-13 and Eq. A-14):

$$\begin{aligned}
 (c\rho\frac{V}{A}\frac{d\theta}{dt}) = & \{\dot{Q}_{pp} + f_1\} - \{a_6 + (a_{12} + a_{13}W)(a_2 + a_{14})\}\theta \\
 & - \{a_7 + a_{12} + a_{13}W)(a_3)\}\theta^2 - \{a_8 + (a_{12} + a_{13}W)(a_4)\}\theta^3
 \end{aligned} \quad (\text{Eq. 16})$$

where c = specific heat capacity of water, $1 \text{ btu}/\#m^\circ F$

ρ = mass density of water, $62.4 \#m/\text{ft}^3$

V = volume of water in the pond

A = active surface area of pond

Eq. 16 can not be solved in closed analytical form with the result that numerical techniques must be used. In order to present the results in a generally useful way and yet avoid repetitive use of tedious methods, it is first helpful to note that the first term on the right hand side of Eq. 16 can be related to the remaining terms on the right hand side by use of Eq. 12, namely:

$$\begin{aligned} \{\dot{Q}_{pp} + f_1\} &= \{a_6 + (a_{12} + a_{13}W)(a_2 + a_{14})\}\theta_{ss} \\ &+ \{a_7 + (a_{12} + a_{13}W)(a_3)\}\theta_{ss}^2 \\ &+ \{a_8 + (a_{12} + a_{13}W)(a_4)\}\theta_{ss}^3 \end{aligned} \quad (\text{Eq. 17})$$

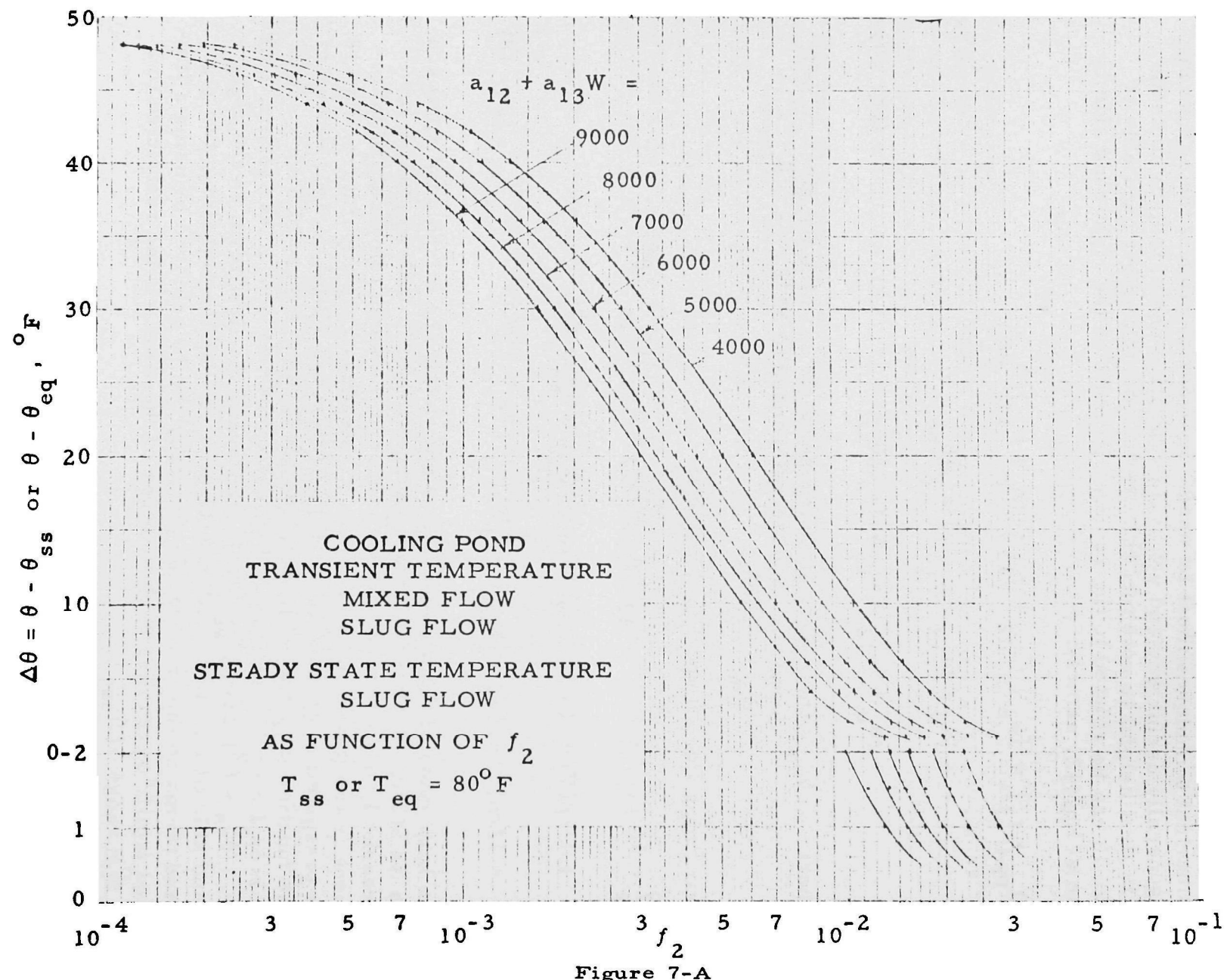
where θ_{ss} = the steady state temperature at which the given mixed pond will operate referenced to 32°F (i.e., $\theta_{ss} = T_{ss} - 32^{\circ}\text{F}$)

Combining Eq. 16 and Eq. 17 yields:

$$\begin{aligned} \frac{d\theta}{dt} &= 1/c\rho(V/A) \{a_6 + (a_{12} + a_{13}W)(a_2 + a_{14})\}\{\theta_{ss} - \theta\} \\ &+ 1/c\rho(V/A) \{a_7 + (a_{12} + a_{13}W)(a_3)\}\{\theta_{ss}^2 - \theta^2\} \\ &+ 1/c\rho(V/A) \{a_8 + (a_{12} + a_{13}W)(a_4)\}\{\theta_{ss}^3 - \theta^3\} \end{aligned} \quad (\text{Eq. 18})$$

An inspection of the above equation shows that the mixed pond approaches its steady-state temperature in an asymptotic fashion, taking progressively more time to proceed through the same temperature increment as the pond comes closer to its steady-state temperature. Eq. 18 is presented in graph form in Fig. 7A through 7G for various values of the function $(a_{12} + a_{13}W)$. In principle it is necessary to have a set of curves for each value of θ_{ss} because of the two non-linear terms, namely, $(\theta_{ss}^2 - \theta^2)$ and $(\theta_{ss}^3 - \theta^3)$. However, the first term on the right hand side of Eq. 18 is sufficiently greater than the remaining two right hand terms so that reasonable accuracy can be achieved by using a limited family of curves, each member of the family being restricted to a $\pm 5^{\circ}\text{F}$ range of θ_{ss} .

For the present case of a mixed pond in transient operation with no vertical temperature gradients, Fig. 7A through 7G was developed by multiplying Eq. 18 by dt and integrating to obtain the temperature (θ)



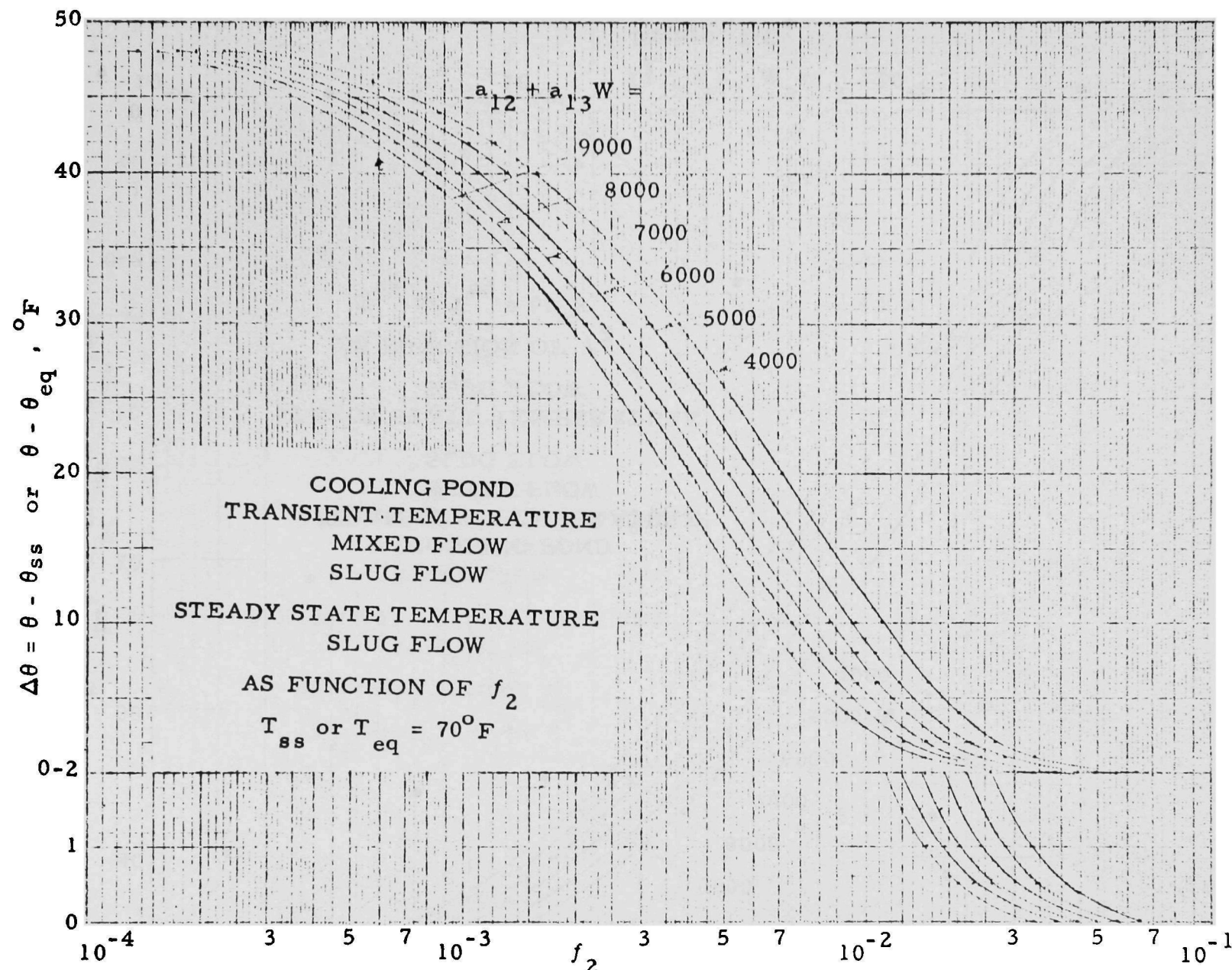


Figure 7B

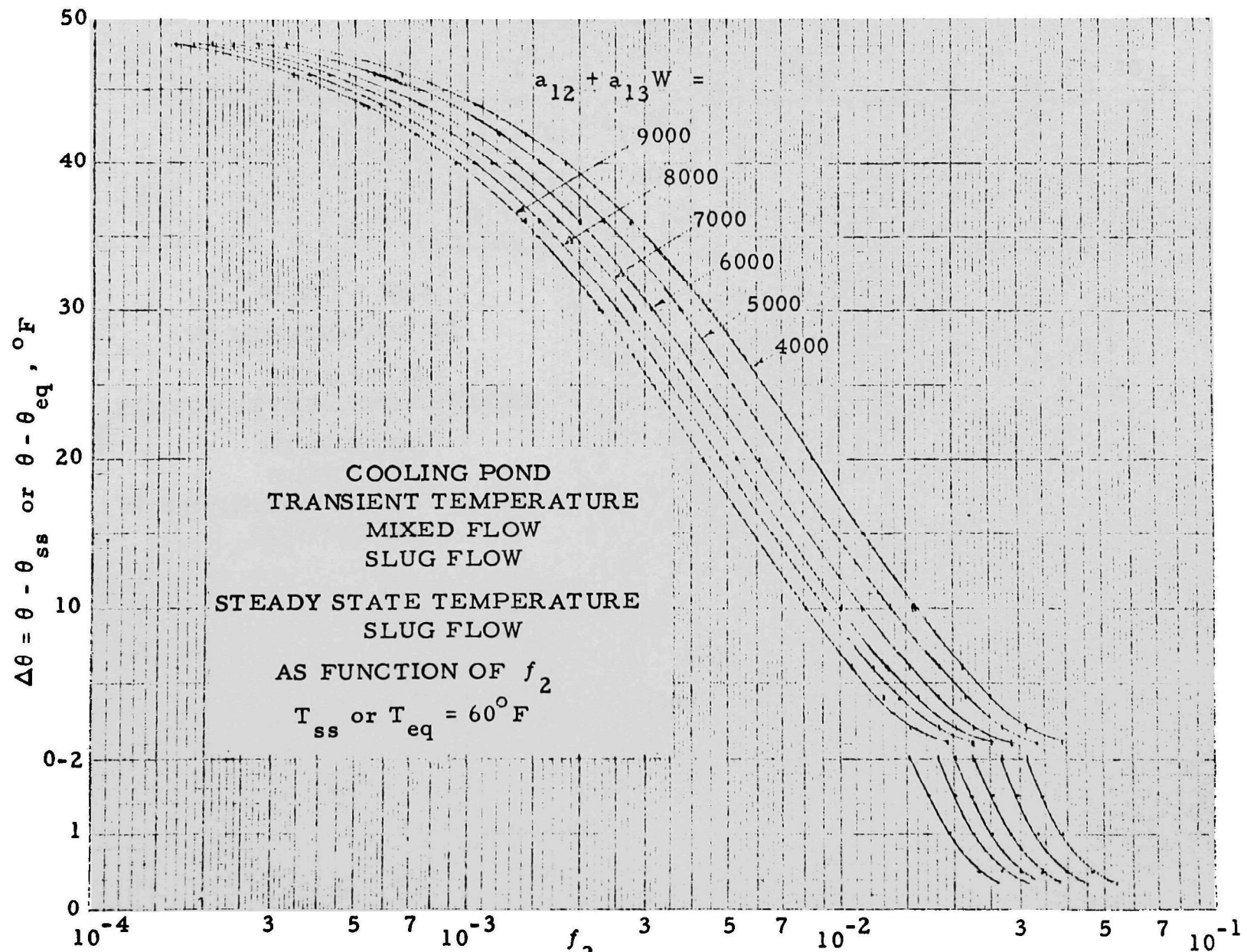


Figure 7-C

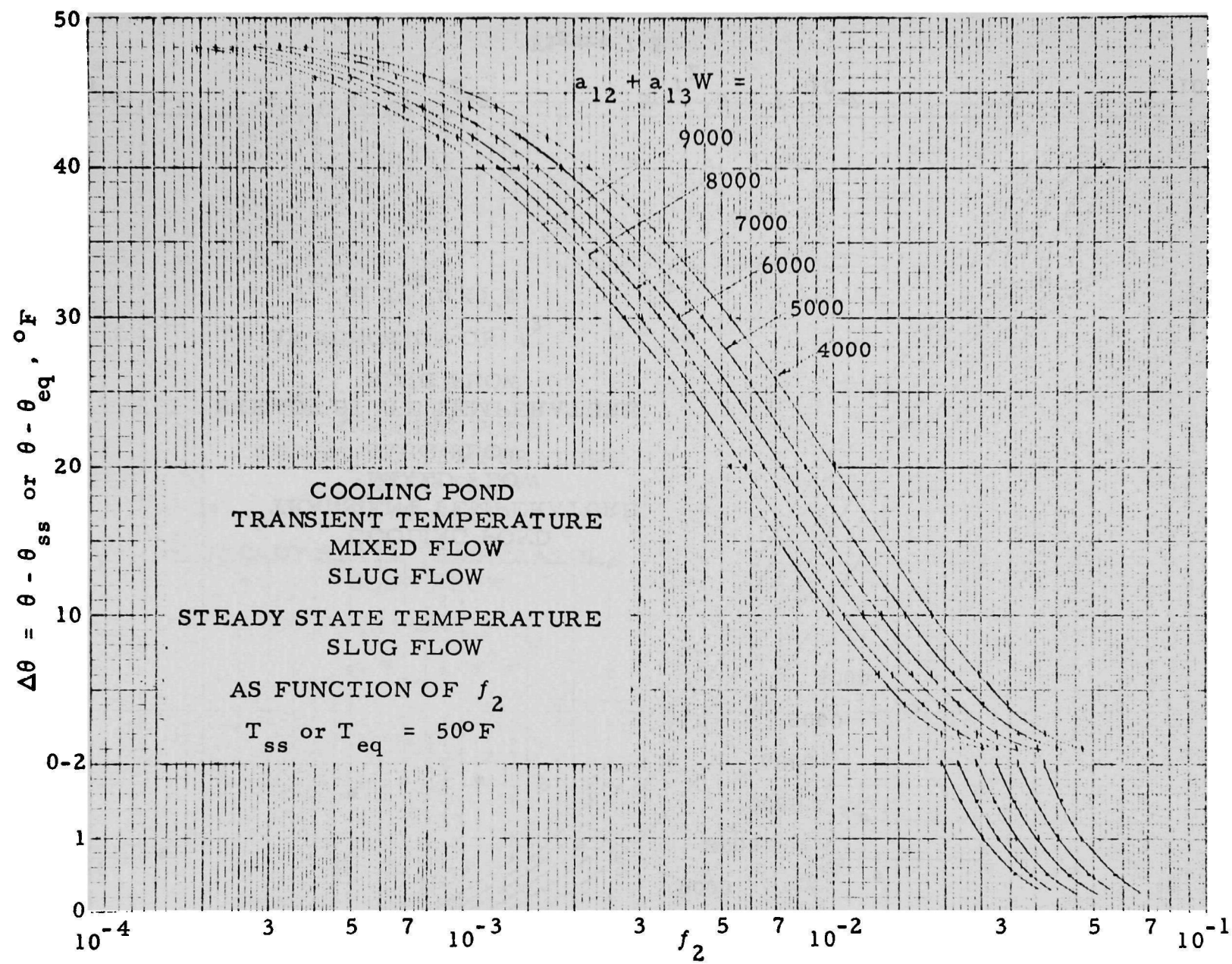


Figure 7-D

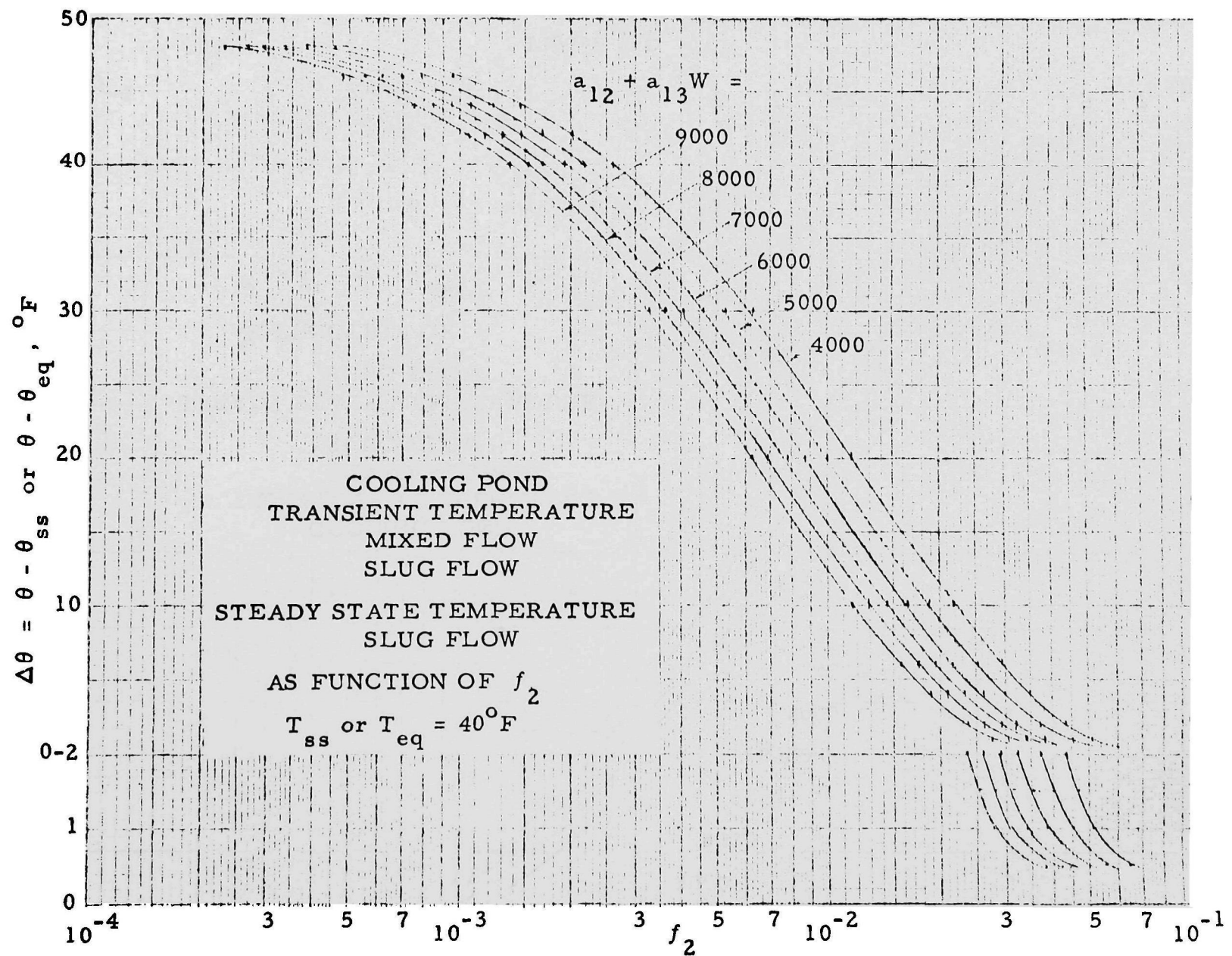


Figure 7-E

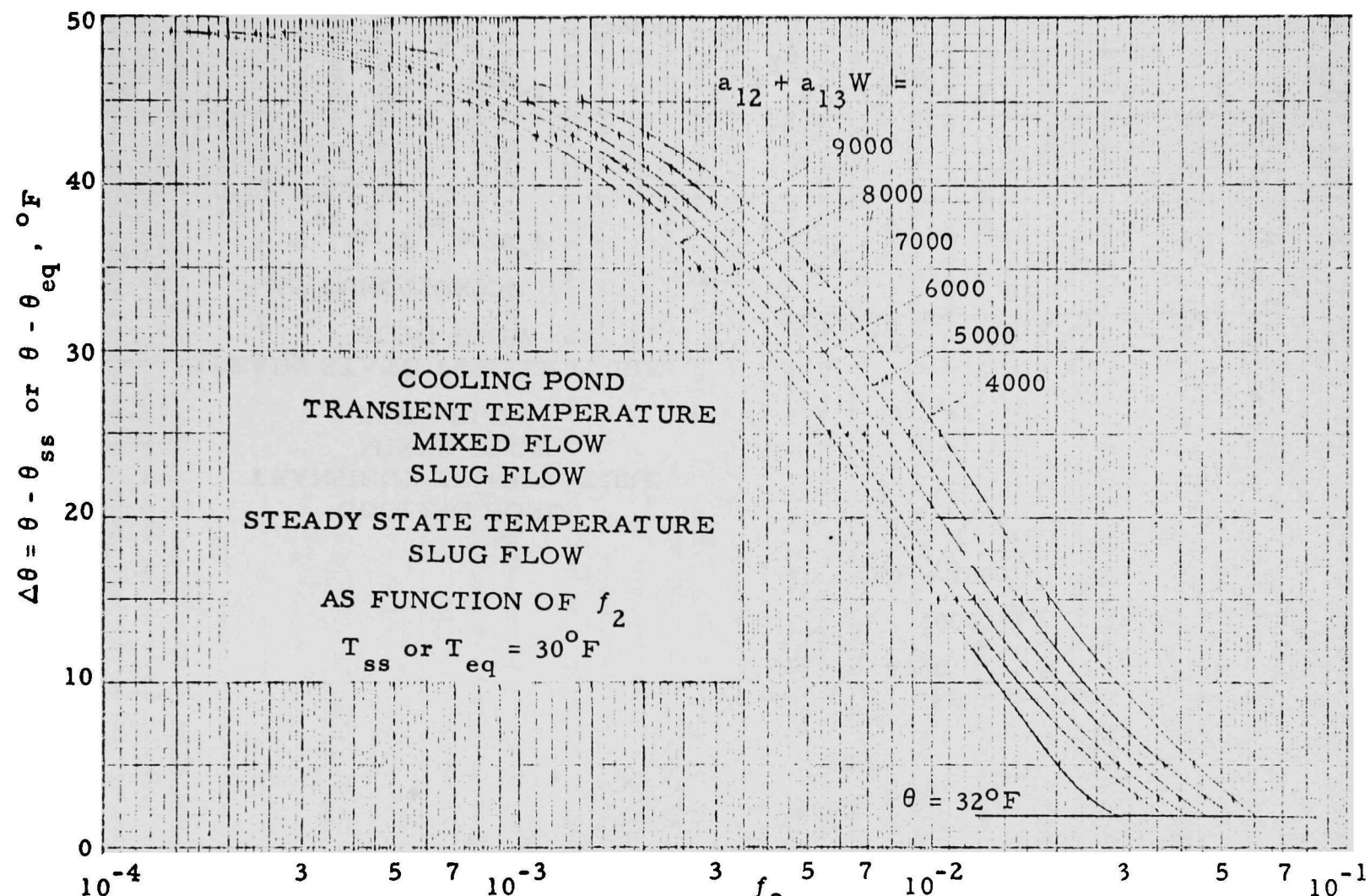


Figure 7-F

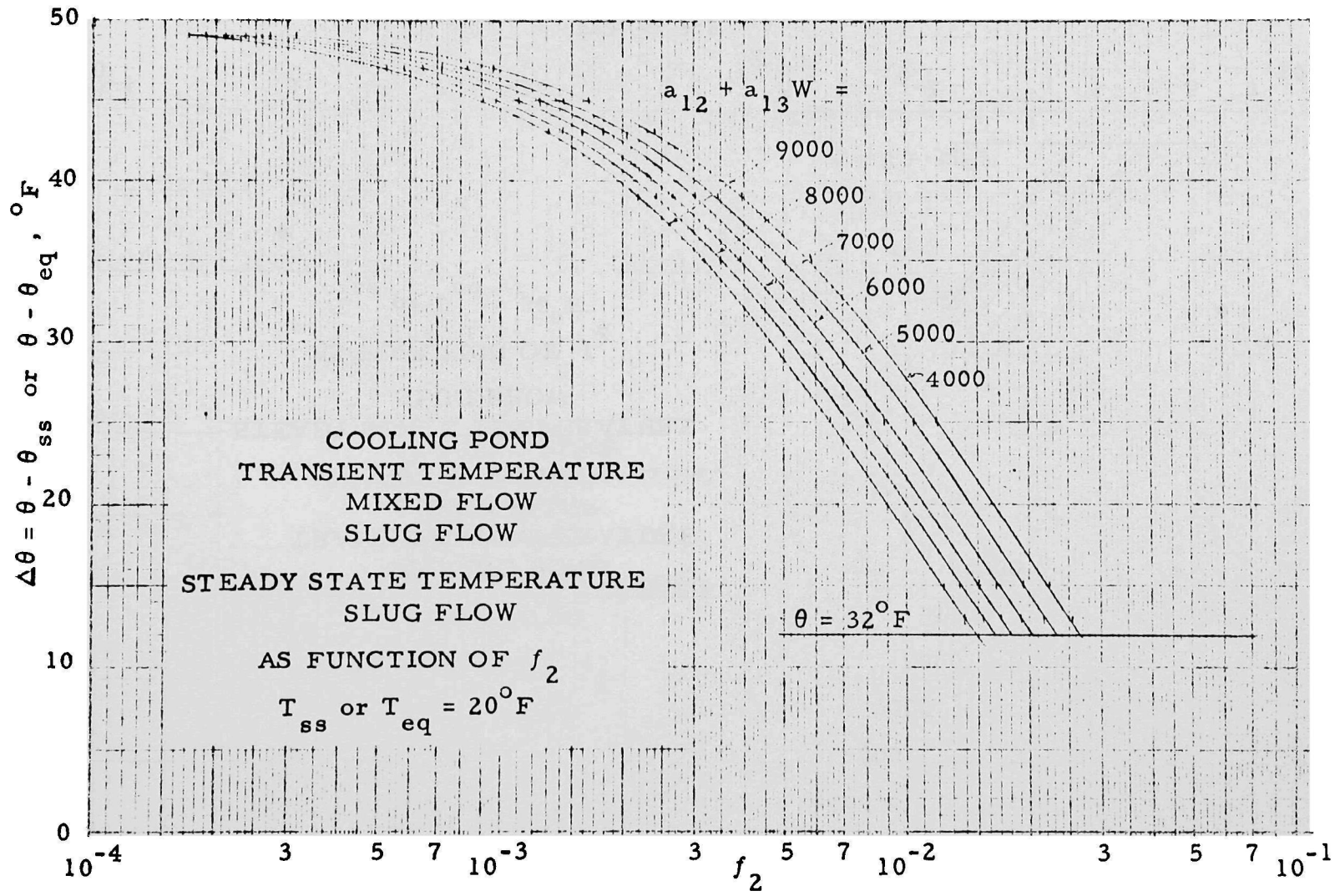


Figure 7-G

after any elapsed time (t) as given by Eq. 18-A.

$$\begin{aligned} \int_{\theta=\theta \text{ at } t=0}^{\theta} d\theta &= \int_{t=0}^{t} [\{a_6 + (a_{12} + a_{13}W)(a_2 + a_{14})\} \{\theta_{ss} - \theta\} \\ &\quad + \{a_7 + (a_{12} + a_{13}W)(a_3)\} \{\theta_{ss}^2 - \theta^2\} \\ &\quad + \{a_8 + (a_{12} + a_{13}W)(a_4)\} \{\theta_{ss}^3 - \theta^3\}] \frac{dt}{cp(V/A)} \quad (\text{Eq. 18-A}) \end{aligned}$$

Eq. 18-A cannot be integrated analytically and as a result numerical methods must be used. However, once Eq. 18-A has been integrated for a given value of $(a_{12} + a_{13}W)$ and θ_{ss} , a curve of pond temperature (θ) vs time (t) can be plotted over as wide a range of θ (or $\theta_{ss} - \theta$) as desired. In addition since $cp(V/A)$ can be assumed to be a constant for any one pond during the period of analyses, the plot of θ vs t can be made to apply to ponds of various ratios of volume to area by plotting θ vs $t/cp(V/A)$ rather than θ vs t . Fig. 7A through 7G is such a plot. The abscissa has been expressed as f_2 instead of $t/cp(V/A)$ because Fig. 7A through 7G will be used for slug flow ponds also and in this latter application f_2 will have a different definition.

To demonstrate the use of the curves presented in Fig. 7, again consider the example used in Case I. In addition to the previously given information, the pond volume is $1000 \times 10^6 \text{ ft}^3$ and the pond is assumed to be at a uniform temperature of 70°F on the last day of June. The temperature of the pond during July is to be determined under the assumption that the weather and waste thermal energy remain constant.

Since the steady-state temperature was determined to be 79.0°F , the appropriate curve to use is 7A. The following functions must be determined:

$$\text{Initial value of } (\theta_{ss} - \theta) = (79^\circ - 70^\circ) = +9^\circ\text{F}$$

$$\text{Initial value of } f_2 - \text{ This is found from Fig. 7A by using } (\theta_{ss} - \theta)_i = 9^\circ, \\ \text{and } (a_{12} + a_{13}W) = 7460.$$

$$f_{2i} = 7.30 \times 10^{-3}$$

The temperature at any day during July can now be readily found by adding to $f_{2i} = 7.30 \times 10^{-3}$ the appropriate value of $t/cp(V/A)$ and moving to the corresponding value of f_{2f} along the curve for constant $(a_{12} + a_{13}W) = 7460$. For example, on the 15th of July the pond temperature will be found at a value of f_{2f} given by:

$$f_{2_f} = f_{2_i} + \frac{t}{c\rho(V/A)}$$

$$f_{2_f} = 7.30 \times 10^{-3} + \frac{15 \text{ days}}{(1)(62.4)(1000 \times 10^6)/(50 \times 10^6)}$$

$$f_{2_f} = 7.30 \times 10^{-3} + .01205 = .01930$$

$$(\theta_{ss} - \theta)_f = +0.5^\circ F$$

$$T_f = 79 - 0.5 = 78.5^\circ F$$

Likewise on the 30th of July the temperature is found to be:

$$f_{2_f} = 7.30 \times 10^{-3} + .01930 = .02660$$

$$(\theta_{ss} - \theta)_f \approx 0.0^\circ$$

$$T_f = 79.0^\circ - 0 = 79.0^\circ F$$

Since the steady state temperature was previously found to be $79.0^\circ F$, steady state conditions have been achieved by the end of July. If the analysis were to be continued beyond this point, the new climatic and waste thermal energy loading for August would have to be used and the process continued as long as need be. The above example clearly demonstrates the asymptotic approach to steady state temperature when it is noted that the pond temperature increased by $8.5^\circ F$ in the first 15 days of July but increased only $0.5^\circ F$ in the last 15 days of July.

Case IV - Mixed pond, transient operation, with a specified linear vertical temperature gradient

Using the relationship between the bulk average temperature for the water below the surface and the surface temperature given by Eq. 14, the energy equation (Eq. 18) can be expressed as:

$$\begin{aligned} \frac{d}{dt} \left(\theta + \beta \frac{\ell_3}{2} \right) &= \frac{d\theta}{dt} \\ &= 1/c\rho(V/A) \{ a_6 + (a_{12} + a_{13}W)(a_2 + a_{14}) \} \{ [\theta_{ss} + \beta(\frac{\ell_3}{2})] - [\theta + \beta(\frac{\ell_3}{2})] \} \\ &\quad + 1/c\rho(V/A) \{ a_7 + (a_{12} + a_{13}W)(a_3) \} \{ [\theta_{ss} + \beta(\frac{\ell_3}{2})]^2 - [\theta + \beta(\frac{\ell_3}{2})]^2 \} \\ &\quad + 1/c\rho(V/A) \{ a_8 + (a_{12} + a_{13}W)(a_4) \} \{ [\theta_{ss} + \beta(\frac{\ell_3}{2})]^3 \} \end{aligned} \quad (\text{Eq. 19})$$

Fig. 7A through 7B can be used without alteration to yield solutions to the above equation if θ in Fig. 7 is replaced by $[\theta + \beta(\ell_3/2)]$.

A comparison of Eq. 18 and Eq. 19 shows that if two similar ponds, one without and one with a vertical temperature gradient, initially have the same surface temperatures, they will continue to have the same surface temperature as time goes on. However, as previously noted, if the intake structure is so arranged as to preferentially draw water from the bottom, the temperature of the incoming condenser water will be colder for the pond with a vertical gradient.

Case V - Slug flow pond, steady-state, no vertical temperature gradient

If the pond is assumed to operate in steady-state, the energy equation can be expressed as: (See Appendix A, Eq. A-24)

$$\begin{aligned} \frac{d\theta}{dA} = & \frac{\Delta T_c}{(WTE)} (f_1) - \frac{\Delta T_c}{(WTE)} [a_6 + (a_{13} + a_{13}W)(a_2 + a_{14})] \theta \\ & - \frac{\Delta T_c}{(WTE)} [a_7 + (a_{12} + a_{13}W)(a_3)] \theta^2 \\ & - \frac{\Delta T_c}{(WTE)} [a_8 + (a_{12} + a_{13}W)(a_4)] \theta^3 \end{aligned} \quad (\text{Eq. 20})$$

where ΔT_c = temperature rise experienced by the cooling water as it passes through the condenser. In steady-state this must also equal the temperature drop through the pond.

WTE = waste thermal energy from plant to pond, btu/day

$$= \dot{m}_c (\Delta T_c) c$$

$$\frac{\Delta T_c}{WTE} = \frac{1}{\dot{m}_c c}$$

where \dot{m}_c = the mass flow rate of cooling water through the condenser, #m/day

Eq. 20 can not be solved in closed form and numerical techniques must be used. However, it will be shown below that Fig. 7A - 7G can be used to solve this equation if the relation for f_1 in terms of the equilibrium temperature, as given by Eq. 12, is substituted into Eq. 20 to yield:

$$\begin{aligned}
 \frac{d\theta}{dA} = & - \frac{\Delta T_c}{WTE} [a_6 + (a_{12} + a_{13}W)(a_2 + a_{14})] [\theta - \theta_{eq}] \\
 & - \frac{\Delta T_c}{WTE} [a_7 + (a_{12} + a_{13}W)(a_3)] [\theta^2 - \theta_{eq}^2] \\
 & - \frac{\Delta T_c}{WTE} [a_8 + (a_{12} + a_{13}W)(a_4)] [\theta^3 - \theta_{eq}^3]
 \end{aligned} \quad (\text{Eq. 21})$$

If Eq. 21 is multiplied by dA and integrated to obtain the temperature (θ) after the slug has tranversed a surface area (A), the resulting expression becomes:

$$\begin{aligned}
 \int_{\theta=\theta \text{ at } A=0}^{\theta} d\theta = & \int_{A=0}^{A} - [\{a_6 + (a_{13} + a_{13}W)(a_2 + a_{14})\} \{\theta - \theta_{eq}\} \\
 & + [a_7 + (a_{13} + a_{13}W)(a_3)] \{\theta^2 - \theta_{eq}^2\} \\
 & + \{a_8 + (a_{12} + a_{13}W)(a_4)\} \{\theta^3 - \theta_{eq}^3\}] \frac{\Delta T_c dA}{(WTE)}
 \end{aligned} \quad (\text{Eq. 21-A})$$

When Eq. 21-A is compared to Eq. 18-A, it is noted that the two are identical if $(\Delta T_c dA)/WTE$ in Eq. 21-A is made equal to $dt/c\rho(V/A)$ in Eq. 18-A. As a result of this observation, Fig. 7A through 7G can be used as the solution for Eq. 21 if the abscissa (f_2) is taken as $(\Delta T_c)A/(WTE)$.

In the form of Eq. 21 the energy equation demonstrates the fact that a "slug" of water approaches the equilibrium temperature as it flows along the length of the pond. Like a mixed pond's approach to steady-state temperature, the slug approaches the equilibrium temperature in an asymptotic fashion with the downstream surface area being less effective than the upstream area.

To demonstrate the use of Fig. 7A - 7G for solving the steady-state slug flow energy equation given above, consider the example given Case I for a $\Delta T_c = 10^\circ\text{F}$. (This is referred to as the "range".) Since the natural equilibrium temperature for this case is 75.5°F , Fig. 7A is the appropriate set of curves to be used. In contrast with the mixed pond, two possible situations must be considered. The first situation arises when a given value of the condenser inlet water temperature (which is often specified as the equilibrium temperature plus a certain temperature difference called "the approach") is selected as a design criterion and the

pond area is subsequently selected to force this to be the case. The second situation arises when the following question is posed, "For a given pond area, waste thermal energy load, and climatic conditions, what will the approach temperature be?" Both situations can be dealt with by using Fig. 7A - 7G; however, the second situation requires a trial and error solution.

In order to demonstrate the procedure, both situations will be answered using the data given in the example of Case I.

First consider the case where, as a design criterion, the approach and hence the condenser inlet temperature has been selected and it is necessary to determine the surface area required to achieve this. If the approach is selected at 3.5°F , the condenser inlet water temperature will be $75.5 + 3.5 = 79.0^{\circ}\text{F}$. Since the equilibrium temperature is 75.5°F , Fig. 7A will be the appropriate set of curves to use. The following functions must be determined:

$$\text{Value of } (\theta - \theta_{\text{eq}})_i \text{ at hot end of pond} = [(79.0 + 10) - 75.5] = 13.5^{\circ}\text{F}$$

Value of f_{2i} : This is found from Fig. 7A by using

$$(\theta - \theta_{\text{eq}})_i = 13.5^{\circ}\text{F} \text{ and } a_{12} + a_{13}W = 7460$$

$$\therefore f_{2i} = .00540$$

$$\text{Value of } (\theta - \theta_{\text{eq}})_f \text{ at the cold end of pond} = [79.0 - 75.5] = 3.5^{\circ}\text{F}$$

Value of f_{2f} : This is found from Fig. 7A by using

$$(\theta - \theta_{\text{eq}})_f = 3.5^{\circ}\text{F} \text{ and } a_{12} + a_{13}W = 7460$$

$$\therefore f_{2f} = .01130$$

$$\text{Value of } \frac{A(\Delta T_c)}{WTE} = (f_{2f} - f_{2i}) = .00590$$

The pond area can now be solved by use of the last calculated value, that is:

$$A = .00590 \left(\frac{WTE}{\Delta T_c} \right)$$

$$A = .00590 \left[\frac{(35 \times 10^9 \text{ btu/day})}{10^{\circ}\text{F}} \right]$$

$$A = 20.6 \times 10^6 \text{ ft}^2$$

Thus, the slug flow pond requires less surface area than the mixed pond in order to achieve the same condenser inlet temperature.

In order to demonstrate the second situation, again consider the same example used in Case I, including the preselected surface area of $50 \times 10^6 \text{ ft}^2$. The condenser inlet water temperature is to be determined. As noted previously, this requires a trial and error solution. This solution requires that two points along the appropriate curve in Fig. 7A be fixed such that the difference between f_{2f} and f_{2i} be the required value given by the expression below and the difference between $(\theta - \theta_{eq})_f$ and $(\theta - \theta_{eq})_i$ be equal to the range, 10°F in this example.

$$f_{2f} - f_{2i} = \frac{A(\Delta T_c)}{(WTE)} \quad \text{or}$$

$$f_{2f} - f_{2i} = (50 \times 10^6 \text{ ft}^2) \frac{(10^\circ\text{F})}{(35 \times 10^9 \text{ btu/day})} = .01429$$

By trial and error, using Fig. 7A, the two required points are:

$$(\theta - \theta_{eq})_f = 0.4^\circ, \therefore T_f = 75.5^\circ + 0.4^\circ = 75.9^\circ\text{F}$$

$$(\theta - \theta_{eq})_i = 10.4^\circ, \therefore T_i = 75.5^\circ + 10.4^\circ = 85.9^\circ\text{F}$$

Thus for the slug flow pond with the same surface area as the mixed pond, the condenser inlet temperature is lower.

Case VI - Slug flow pond, steady state, with a specified linear vertical temperature gradient

As in the case of the mixed pond the energy equation is the same as for Case V except for a change of θ to the surface temperature $[\theta + \beta(\ell_3/2)]$. Thus the surface temperature is given by the following equation:

$$\begin{aligned} \frac{d(\theta + \beta \frac{\ell_3}{2})}{dA} &= \frac{d\theta}{dA} = -\frac{\Delta T_c}{WTE} [a_6 + (a_{12} + a_{13}W)(a_2 + a_{14})] [\theta + \beta \frac{\ell_3}{2}] - (\theta_{eq}) \\ &\quad - \frac{\Delta T_c}{WTE} [a_7 + (a_{12} + a_{13}W)(a_3)] [\theta + \beta \frac{\ell_3}{2}]^2 - (\theta_{eq})^2 \\ &\quad - \frac{\Delta T_c}{WTE} [a_8 + (a_{12} + a_{13}W)(a_4)] [\theta + \beta \frac{\ell_3}{2}]^3 - (\theta_{eq})^3 \end{aligned} \quad (\text{Eq. 22})$$

Case VII - Slug flow pond, transient operation with no vertical temperature gradient

This condition arises when the residence time in the pond (the time required for a slug of water to travel from pond inlet to outlet) is of the same magnitude or longer than the time over which the weather data are averaged. There are two extreme or limited cases that should be noted. First, when the residence time is very long and the ratio of V/A is small, the condenser inlet temperature will be very close to the natural equilibrium temperature associated with the time at which the water enters the condenser. This case corresponds to the use of once-through river water which has not been artificially heated upstream. The second limiting case arises when the residence time is short (compared to the time for averaging climatic conditions) and V/A is small. When this is the situation, the condenser inlet temperature will be very close to the steady state slug flow inlet temperature.

In studying the transient operation of a slug flow pond, the temperature of a slug of water will change as it flows through the pond; before it completes its pass through the pond, the average climatic conditions may change. To describe the transient operation of the pond, it is necessary to find the temperature-time relationship along the length of the pond. Although this condition is best studied with the help of a computer program, hand calculations with the aid of Fig. 7A - 7G are not excessively tedious and they help to demonstrate the technique.

The procedure is to find a limited number of temperature-time-position coordinates for a representative "slice" or "slug" of water as it travels around the pond. When the slug reaches the cold end of the pond, the range (ΔT_c) is added to its temperature (to represent passage through the condenser) and the slug is again allowed to pass through the cooling pond. If intermediate temperature-time-position coordinates are needed, additional representative slugs, appropriately spaced, can be followed through the pond. The procedure is detailed into several steps and illustrated below.

Step 1. The condenser discharge temperature must be established at some time, let this temperature be T_i and the time be $t = 0$ or t_o . Thus the slug will leave the condenser at T_i and time t_o .

Step 2. Plot the equilibrium temperature, pond residence time $t_r = (V\rho)/\dot{m}_c = [V\rho c(\Delta T_c)]/(WTE)$ and the wind parameter ($a_{12} + a_{13}W$) as a function of time.

Step 3. With the use of Fig 7A - 7G determine the temperature of the representative slug some preselected number of days (t_D) after time zero.

To determine the temperature at t_o , first find the value of f_{2i} from Fig 7A - 7G and add to it the value of $(t_D - t_o)/[\rho c(V/A)]$. The position of the slug along the pond can be found by equating the ratio of pond surface area traversed or swept by the slug to total surface area with the ratio of elapsed time to residence time. Thus the slug position at the end of t_D days is:

$$\Delta A = A \left(\frac{t_D - t_o}{t_r} \right) \quad (\text{Eq. 23})$$

where t_r = average residence time in period

t_o to t_D = days obtained from the plot

Step 4. Repeat Step 3 until the slug just reaches the cold end of the pond. The last time interval in this process will have to be selected such that the final position (the cold end) is given by $[\Sigma(\Delta A/A)] = 1.0$.

Step 5. Let the slug pass through the condenser where its temperature will increase by ΔT_c and then repeat the previous steps.

To illustrate the use of this procedure, again consider the example used in Case I. The cold end of the pond is assumed to be at 70°F on the last day of June. It is desired to find the temperature of the water arriving at the condenser intake during July. Only a few representative values will be found to illustrate the technique. In order to avoid making a plot of the equilibrium temperature, wind function and residence time so that average values of these parameters will be available in this example, it is assumed that these values are constant for July and equal to:

$$T_{eq} = 75.5^{\circ}$$

$$a_{12} + a_{13} W = 7460$$

$$t_r = \frac{V\rho c (\Delta T_c)}{(WTE)} = \frac{(1000 \times 10^6)(62.4)(1)(10)}{(35 \times 10^9)} = 17.8 \text{ days}$$

The slug which leaves the "hot" end at time, $t=0$, with a temperature of $70 + 10^{\circ} = 80^{\circ}\text{F}$ will have a lower temperature at $t = 10$ days, namely

$$f_{20 \text{ days}} = .0103$$

$$f_{210 \text{ days}} = .0103 + \frac{10 \text{ days}}{(62.4)(1)(\frac{1000 \times 10^6}{50 \times 10^6})} = .0183$$

$$\therefore (\theta - \theta_{eq})_{17.81 \text{ days}} = 0.1^\circ F$$

$$\therefore T_{17.81 \text{ days}} = 75.6^\circ F$$

After arriving at the cold end of the pond, the slug passes through the condenser where its temperature is increased by ΔT_c ($= 10^\circ F$) and subsequently flows through the pond. The temperature during this second pass is given below at the end of the next 10 days.

$$f_2^{17.8 \text{ days}} = .0065$$

$$f_2^{27.8 \text{ days}} = .0145$$

$$T_{27.8 \text{ days}} = 75.5^\circ + 1.5^\circ = 77.0^\circ F$$

$$\frac{\Delta T_{27.8 \text{ days}}}{A} = \frac{10}{17.8} = .561$$

When the slug arrives at the cold end of the pond for the second time, its temperature is:

$$f_2^{35.6 \text{ days}} = .0145 + \frac{7.81}{(62.4)(1)(\frac{1000 \times 10^6}{50 \times 10^6})} = .0208$$

$$T_{35.6 \text{ days}} = 0.4^\circ + 75.5^\circ = 75.9^\circ F$$

Since the steady state slug flow temperature was previously found to be $75.9^\circ F$ at the cold end of the pond, steady conditions have been reached; however, the climatic conditions and possibly the waste thermal energy loading must now be changed to the appropriate values for August and the process continued.

Case VIII - Slug flow pond, transient operation, with a specified linear vertical temperature gradient

Again, as for the mixed pond, the assumption of a linear temperature profile does not change the nature of the energy equation except to replace the bulk average temperature with the surface temperature. The remarks made about Case IV are also pertinent to this case.

Concluding Remarks

For ease of comparison, the steady state and transient temperature characteristics of the example pond, for both mixed and slug flow

operation, are shown in Fig. 8.

Although it is more convenient to use the steady state analysis rather than the transient analysis, such use has to be justified. The question can always be answered precisely by applying both analyses to a given problem but this is tedious. Fig. 7A - 7G can be used as a guideline in making the decision; in particular, if it is noted that a value of the function $f_2 = t/[\rho c(V/A)]$ of about 0.05 or greater, depending on θ_{ss} , for a mixed pond will produce condenser intake temperatures within a degree of the steady state pond temperature, then a rule of thumb for using steady state analysis is the requirement that:

$$t \geq 0.05 \rho c(V/A) \quad (\text{Eq. 24})$$

where t = the time duration over which conditions are averaged, in days

ρ = density of water = 62.4 lbm/ft^3

c = specific heat of water = $1.0 \text{ btu/lb, } ^\circ\text{F}$

V/A = pond volume to surface ratio

In view of the fact that weather and plant conditions are usually averaged for a period of one month, the above guideline may be rewritten as:

$$V/A \geq 10 \text{ ft} \quad (\text{Eq. 25})$$

Thus for mixed ponds of average depth of 10 ft or less, steady state analysis can be used. Although this approximate rule was devised for a mixed pond, it is also a valid guideline for slug flow ponds. As mentioned previously, a slug flow pond with sufficiently long residence time and small depth (V/A) will not only be in steady state operation, but the condenser intake temperature will be close to the equilibrium temperature. Again Figure 7 can be used to generate the guideline if it is noted that a value of the function $f_2 = [A(\Delta T_c)]/(WTE) = A/(m_c c)$ of about 0.05, or greater, depending on θ_{eq} for a slug flow pond will result in condenser intake temperatures within about 1°F of the equilibrium temperature. This observation may be expressed as

$$A \geq 0.05 \dot{m}_c c \quad (\text{Eq. 26})$$

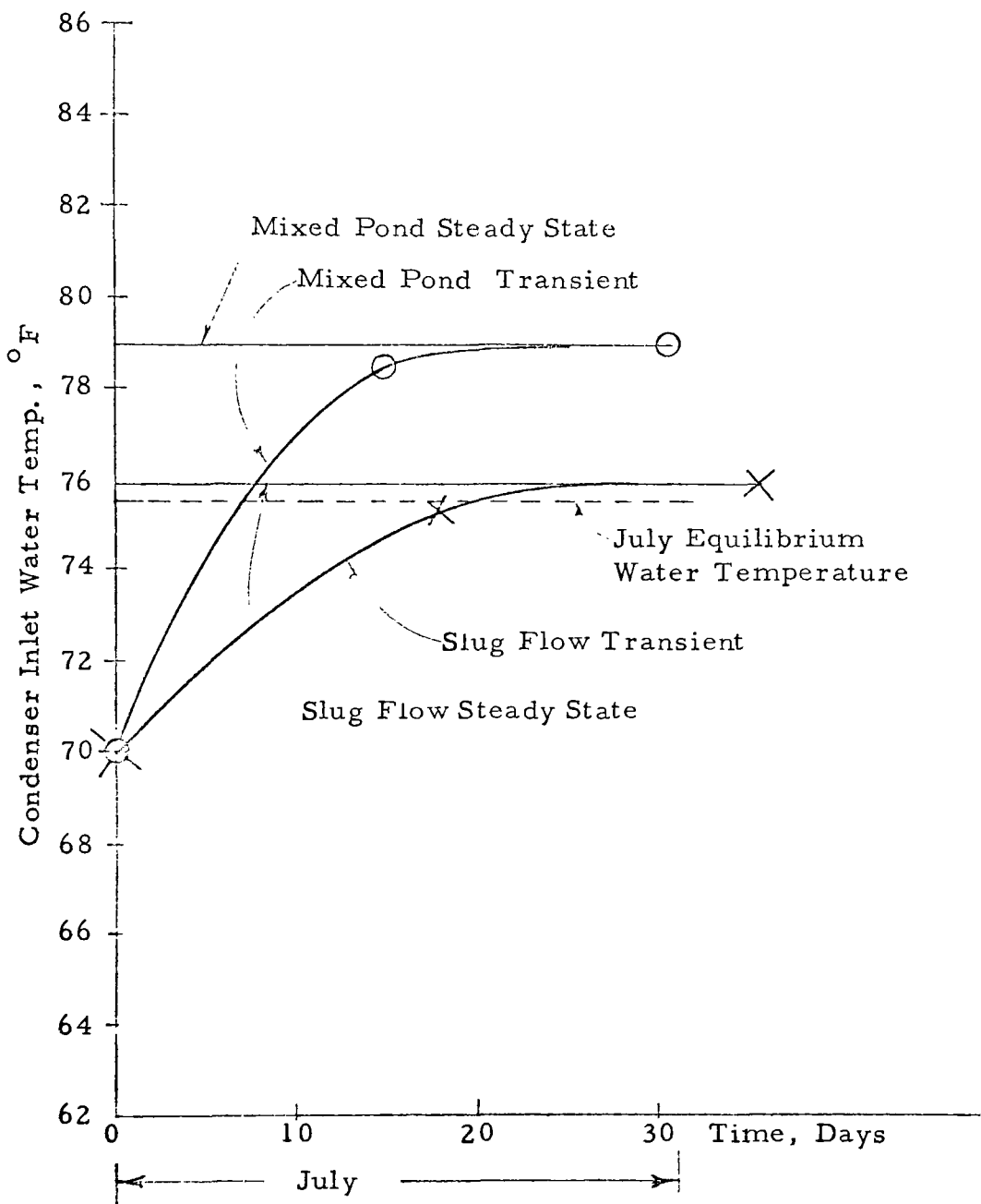
Since the residence time and pumping rate are related by the expression

$$\dot{m}_c t_r = \rho V \quad (\text{Eq. 27})$$

Equation 26 can be expressed as

$$t_r \geq 3.11 (V/A) \quad (\text{Eq. 28})$$

Thus for a 10-foot deep pond the minimum residence time that will



Comparison of Steady State and Transient Temperatures for a Mixed and a Slug Flow Pond

Figure 8

cause the water to be cooled to the lowest possible value (equilibrium temperature) is 31.1 days or one month.

An inspection of Fig. 7A - 7G shows that for the same pond surface area, the same difference in water temperature and natural equilibrium temperature at the hot end of the pond, more cooling takes place (that is to say, a lower exit temperature will result) when the equilibrium temperature is high than when the equilibrium temperature is low. Therefore, for a given pond surface area, cooling is greater in the summer than in the winter for a given geographic location; and cooling is greater in regions of high equilibrium temperature than in regions of low equilibrium temperature at a given time during the year. Since Fig. 7A - 7G also applies to the transient operation of a mixed pond when the reference temperature is not the natural equilibrium temperature but the higher "forced" steady state temperature (θ_{ss}), the above remarks also apply to the rate at which a mixed pond approaches its steady state temperature. In addition, since a mixed pond may, mathematically, be considered to be a slug flow pond in which ΔT_c approaches zero, a mixed pond of given surface area operating in steady state experiences greater cooling when the steady state temperature (θ_{ss}) is high rather than low.

To illustrate the point discussed in the above paragraph, consider the example used in Case V, namely, a waste thermal energy load of 35×10^9 btu/day imposed on a slug flow pond operating in the steady state condition. If the temperature rise through the condenser (ΔT_c) and the approach temperature are again taken as 10°F and 3.5°F respectively, the pond surface area required to achieve this approach temperature will be $20.6 \times 10^6 \text{ ft}^2$, $31.2 \times 10^6 \text{ ft}^2$, and $42.6 \times 10^6 \text{ ft}^2$ for equilibrium temperatures of 80°F , 60°F , and 40°F respectively. The physical reason for this behavior becomes apparent when it is recalled that the three means by which thermal energy is removed from the pond (other than by direct transport in escaping water), namely, 1) back radiation, 2) evaporation, 3) convection all depend on the pond surface temperature whereas the means by which thermal energy is added to the pond (other than by an inflow of water or the power plant), namely, net solar and atmospheric radiation do not depend on the water temperature.

In contrast to the greater cooling capacity at high equilibrium temperatures vs low equilibrium temperatures for a given pond surface area and the same difference between water temperature and equilibrium temperature (at the hot end of a slug flow pond), it should also be recalled that the plant efficiency decreases as the condenser temperature increases with the result that additional cooling will be required if operation at the high equilibrium temperatures increases the condenser

temperature. Thus, in general, when the equilibrium temperature is increased, two opposing trends come into play, namely, increased cooling capacity for a given pond surface and an increase in the waste thermal energy load imposed by the plant on the pond.

The sensitivity of the water temperature to pond surface area is an important consideration when considering the economics of the pond as well as when comparing predicted to measured water temperature. This sensitivity depends on the difference between the water temperature and the equilibrium temperature (for a slug flow pond) or steady state temperature (for a mixed pond). In order to demonstrate this point, the previous example is again considered, namely,

$$T_{eq} = 75.5^{\circ}\text{F}$$

$$W = 10.0 \text{ mph } (a_{12} + a_{13}) W = 7460$$

$$\text{WTE} = 35 \times 10^9 \text{ btu/day}$$

$$\text{Range} = 10^{\circ}\text{F}$$

$$f_1 = 5102 \text{ btu/ft}^2, \text{ day}$$

The pond discharge (or condenser inlet) temperature for a mixed and for a slug flow pond operating under these conditions is shown in Fig. 9 as a function of pond surface area. Again it is noted that for equal pond surface areas, the slug flow pond will deliver colder water to the condenser. It is seen from Fig. 9 that the condenser inlet temperature is not sensitive to pond surface area beyond approximately $50 \times 10^6 \text{ ft}^2$. An area of $50 \times 10^6 \text{ ft}^2$ and a waste thermal energy load of $35 \times 10^9 \text{ btu/day}$ corresponds (at 40% thermal efficiency) to pond loading of about 4 acres per megawatt of electricity produced by the plant. Therefore, in order to test the accuracy of the predicting technique, it would be helpful to have data available from ponds that have less than 4 acres per megawatts of electricity produced by the plant.

It is easier to see the relative cooling capacity of the two types of ponds if the data of Fig. 9 are replotted as the ratio of mixed pond surface area to slug flow pond surface area for the same condenser inlet water temperature as shown in Fig. 10. An inspection of Fig. 10 shows that the two ponds will have about equal cooling capacity as the difference between the condenser inlet temperature and the equilibrium temperature (that is, the approach) is increased, whereas the slug flow pond is considerably more effective at cooling the water if the condenser inlet temperature is made to approach the equilibrium temperature closely. Although Fig. 10 is for a specific equilibrium temperature (75.5°F) and for a specific WTE and ΔT_c (and hence the pumping rate), the indicated behavior is true in general.

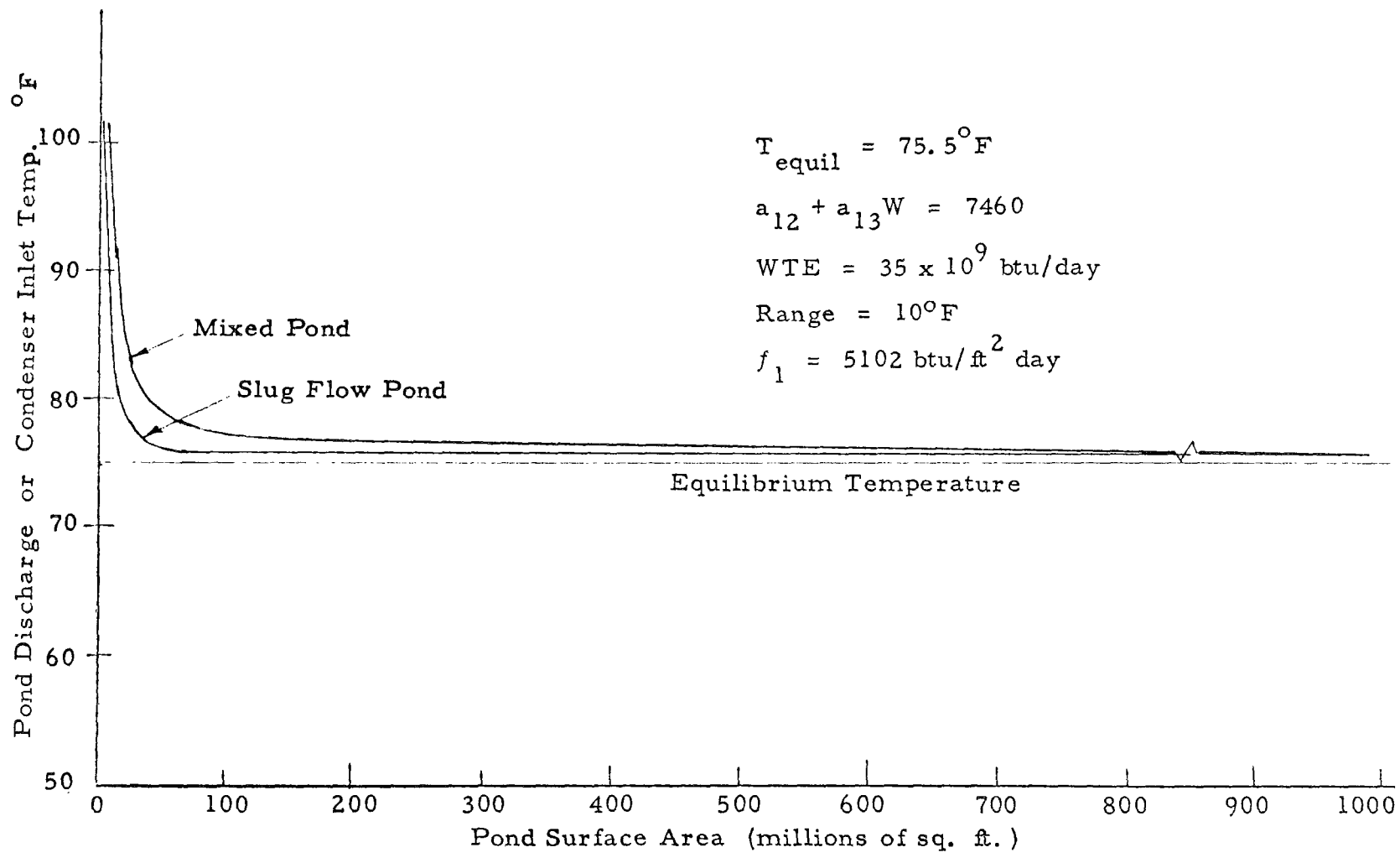


Figure 9

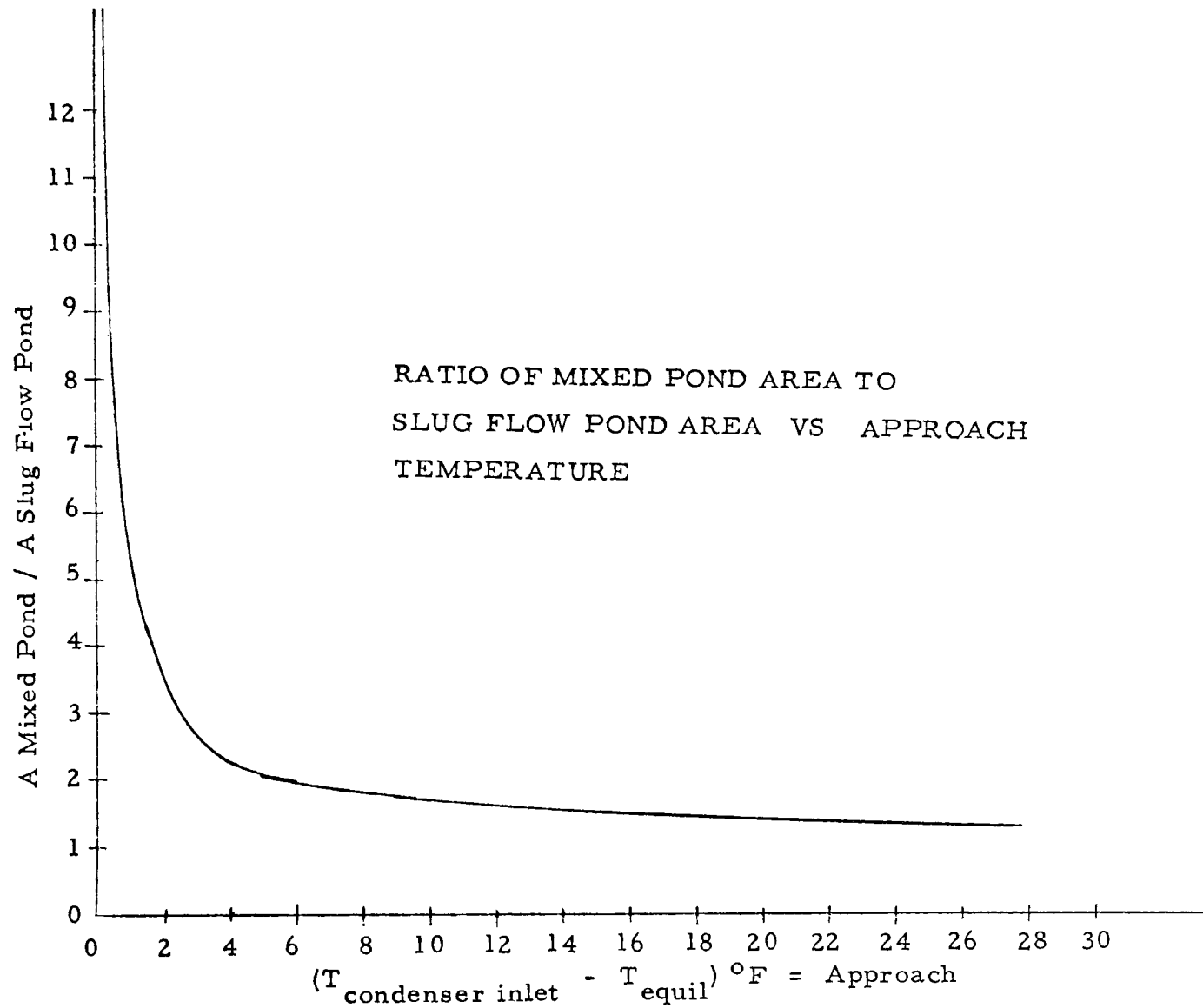


Figure 10

COMPARISON OF PREDICTED AND MEASURED WATER TEMPERATURE

Operating data of five cooling ponds were obtained from various electric power firms. These data consisted of the monthly average power generation for the plant, the monthly average condenser inlet temperature rise across the condenser, the cooling water pumping rate of plant heat rate, the nominal pond surface area, nominal pond volume or depth, pond geometry and in some cases the vertical temperature gradients.

The data obtained from the power companies together with monthly average weather conditions at nearby weather stations (obtained from the National Weather Record Center at Asheville, North Carolina) were used to predict condenser inlet temperature for each month of the year. Predicted and measured values are shown in Figs. 11 through 15. The predicted values shown are for the condition of no vertical temperature gradient in view of the fact that gradients comparable to the measured magnitude do not appear to influence the condenser temperature strongly.

The detail calculations associated with the predictions are shown in Appendix C. A brief summary of the pond characteristics is given in Table I. Each of the five plants is discussed in the following sections.

Wilkes Plant

The Wilkes Plant (179.5 MW_e) is located in Jefferson, Texas. The nearest weather station is at Shreveport, Louisiana, about 40 miles away. The summer months are warm and rather humid, the relative humidity has an average value of about 90% during the early morning and about 50% at mid-afternoon. Winter months are mild with any cold spells being limited to a few days.

The "pond" at the Wilkes Plant is in the shape of a river bend (See Appendix C). The plant removes cooling water from one end of the bend and discharges the heated water to the other end of the bend through a discharge canal. Because of the large ratio of pond surface to generating capacity ($\sim 4 \text{ acres/MW}_e$), the pond exit temperature should not be sensitive to changes in the pond surface area. In addition, since the residence time is large (compared to 3.11 V/A), the exit pond temperature will approach the natural equilibrium temperature as shown in Fig. 11.

From Fig. 11 it is seen that the measured condenser inlet temperatures are within $\pm 5^\circ$ of the average value predicted by use of the two pond

TABLE I
SUMMARY OF PLANT CHARACTERISTICS

Power Plant	Company	V/A ft	t_r days	3.11 V/A days	A/MW _e acres/MW(e)	Ratio of Width to Length in Flow direction	Comments
Wilkes	South-western Electric Power Co	15	46	46	≈ 4	~1/7	Will operate close to steady state. Condenser inlet temp. will be close to equil. temp.
Kincaid	Commonwealth Edison Co.	10	9	31	2*	~1/20	Can assume steady state operation. Condenser inlet temp. should be well above equil. temperature
Cholla	Arizona Public Service Co.	4.5	8	14	≈ 3	~1/1	Same as above
Mt. Storm	Virginia Electric & Power Co.	21 (.5V/A due to flow pattern)	16 (.5 t _r due to flow pattern)	66	≈ 1	Intake location below hot water outlet	Pond will be in transient operation
Four Corners	Arizona Public Serv. Co	40	35	124	≈ 2**	~1/1	Pond will be in transient operation

*Based on plant MW_e installed capacity in 1968. However, it is anticipated that this capacity may be eventually doubled.

**Based on plant MW_e rating in 1967. However, Unit No. 4 was put into service in July 1969 and has raised the plant MW_e rating considerably.

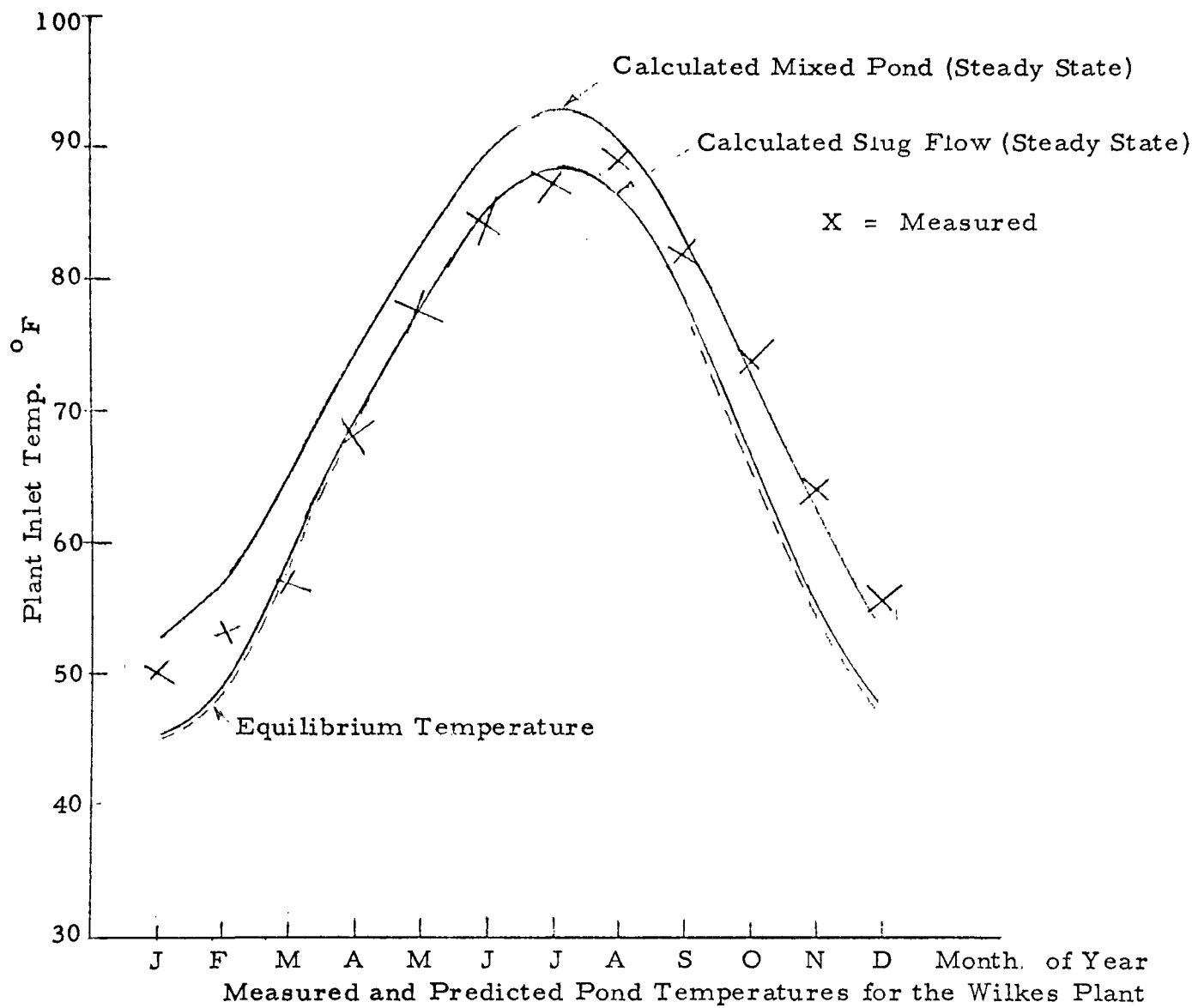


Figure 11

models.

Kincaid Plant

The Kincaid Plant ($\sim 1000 \text{ MW}_e$) is a mouth-of-mine plant located in the coal fields of Southern Illinois. The location of this plant near the center of North America results in a continental climate characterized by warm summers and fairly cold winters. Summer weather tends to be quite warm and humid. The winter does not have extended periods of severe cold; however, sharp seasonal changes do take place during the winter and summer.

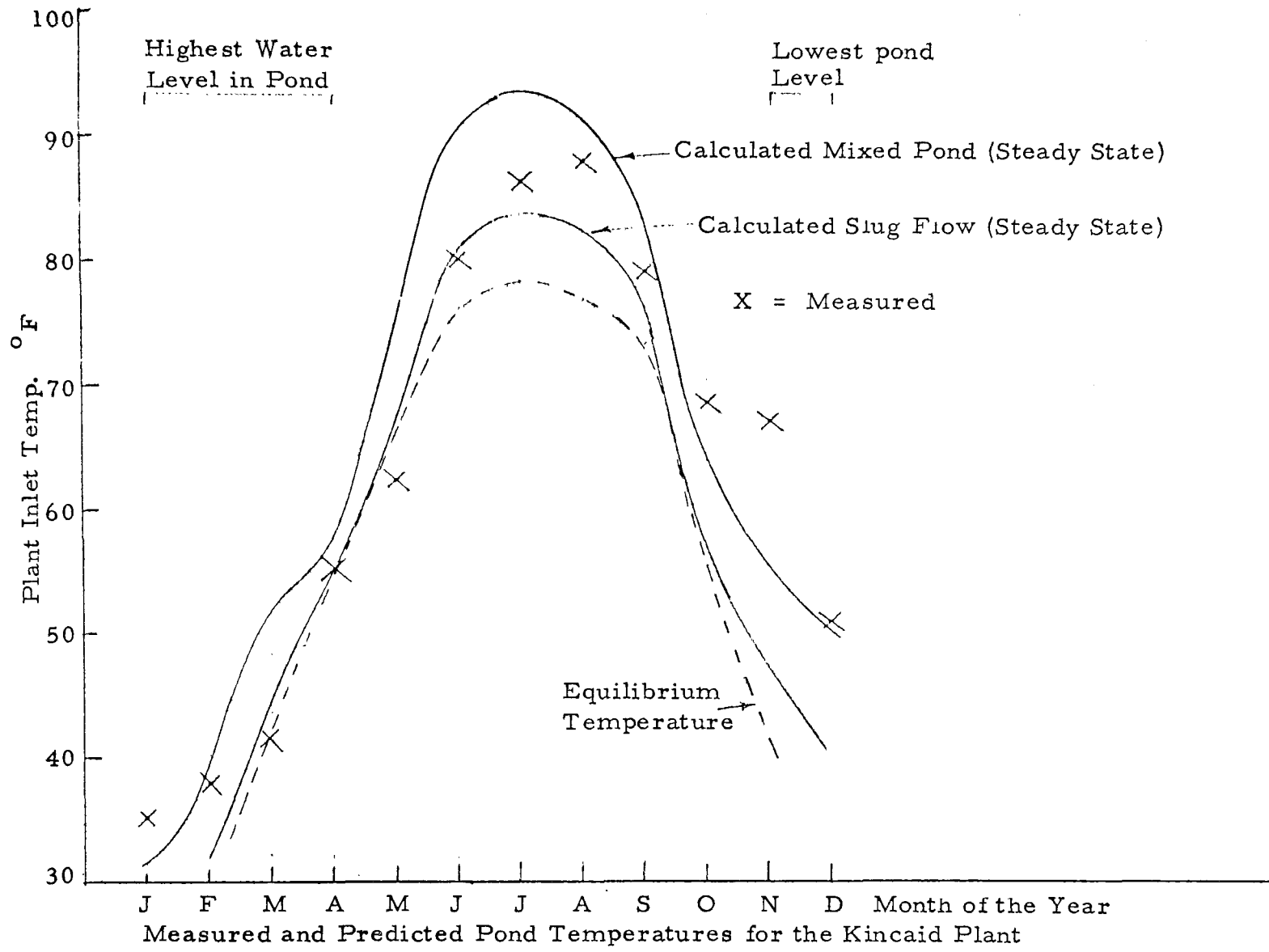
The "pond" at the Kincaid Plant is in the form of three "arms", each with a very irregular shore line (See Appendix C). The plant is located between two of the three "arms" of the pond. The heated water discharged from the condensers must flow down one arm and up the other. The third arm serves as a storage reservoir.

The predicted and measured condenser inlet temperatures are shown in Fig. 12. With the exception of the measured temperature for November, the measured values agree within $\pm 5^\circ\text{F}$ of the average temperature predicted by the two models.

Cholla Plant

The Cholla Plant is located in Joseph City, Arizona, a semi-arid climate. The nearest weather bureau is located at Winslow, Arizona, about 25 miles away. The terrain varies rapidly in the vicinity of the Cholla Plant, with the Painted Desert just to the north and the White Mountain area less than 75 miles to the southeast. As a result of rapid change in terrain, the use of weather data from the Winslow Station introduces some uncertainty. The Cholla pond is shallow (varying from inches to a maximum of 12 feet) and is divided into two parts by a dike and an associated inverted weir (See Appendix C). As a result of the pond geometry, substantial channeling of the flow may be present between the inlet and outlet with the result that not all the pond area will be effective.

The predicted and measured condenser inlet temperatures are shown in Fig. 13. The predicted values are based on the assumption that only one-third of the pond surface is effectively engaged in the cooling process as a result of channeling and subsequent dead water regions. The value of one-third was selected because it results in the best fit with the experimental data. Predicted temperatures based on the assumption that the entire pond surface is effective are also given in Table C-4



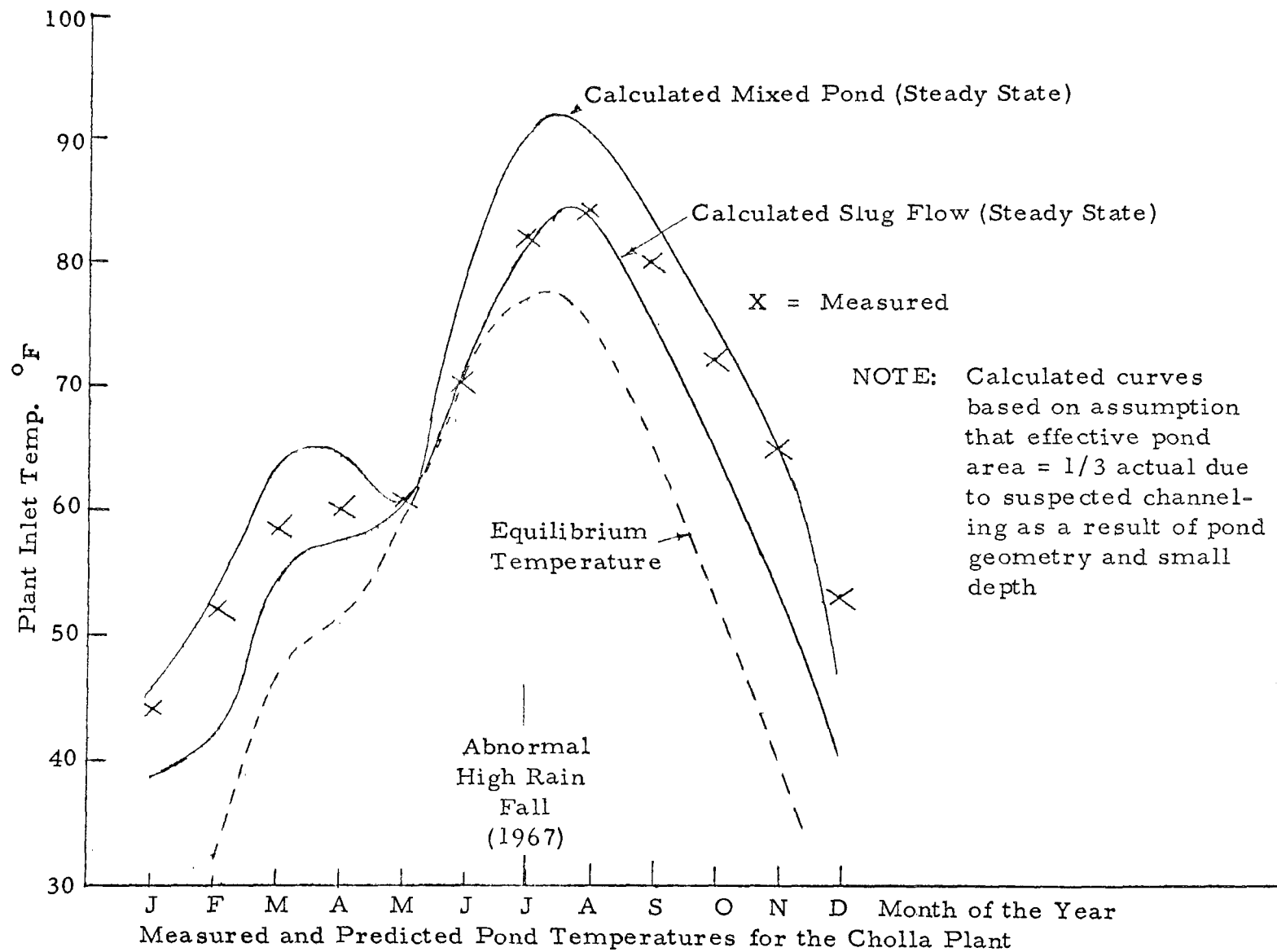


Figure 13

in Appendix C. From Fig. 13 it is seen that the measured and (average) predicted temperatures agree within $\pm 5^{\circ}\text{F}$ with one exception, namely, December.

Mt. Storm Plant

The Mt. Storm Plant is located in West Virginia near the principal storm tracks. As a result of its location it is subjected to frequent weather changes throughout the year. The summer months are warm, humid and showery. Severe cold spells do occur but do not usually last more than a few days.

The pond at the Mt. Storm Plant is quite deep (~ 100 feet) so that the pond will operate in the transient mode rather than steady state. Because of the low ratio of surface area to generating capacity (~ 1 acre per MW_e), the highest thermal loading of any pond for which we have data), the Mt. Storm reservoir provides a sensitive test for the validity of our temperature predicting techniques. The power plant is required to discharge a minimum flow of 2 cfs plus passing through the facility and any flows discharged from the West Virginia Pulp and Paper reservoir as low flow augmentation for the Potomac River.

The measured and predicted condenser inlet temperatures are shown in Fig. 14. From Fig. 14 it is noted that the measured values are within -5°F of the average of the values predicted by the two pond models, with the exception of April and May, which are -9°F and -6°C respectively from the average predicted value. In this case the predicted values overestimate the temperature which is the anticipated situation due to the use of the Meyer Equation for a heavily loaded pond as discussed in Appendix B.

Four Corners Plant

The Four Corners Plant is located in Farmington, New Mexico. The nearest weather station is at Winslow, Arizona, about 180 miles away (the same station used in evaluating the Cholla Plant). Like the nearby Cholla Plant, the Four Corners Plant is in a semi-arid environment and experiences a rainfall of about 10 inches per year. Unlike the Cholla pond, however, the Four Corners pond is relatively deep and channeling should not occur. As a result it can be assumed that the entire pond surface will be effective.

The predicted and measured condenser inlet temperatures are shown in Fig. 15. With the exception of August, the measured values agree within $\pm 4^{\circ}\text{F}$ of the average of the values predicted by the two pond models.

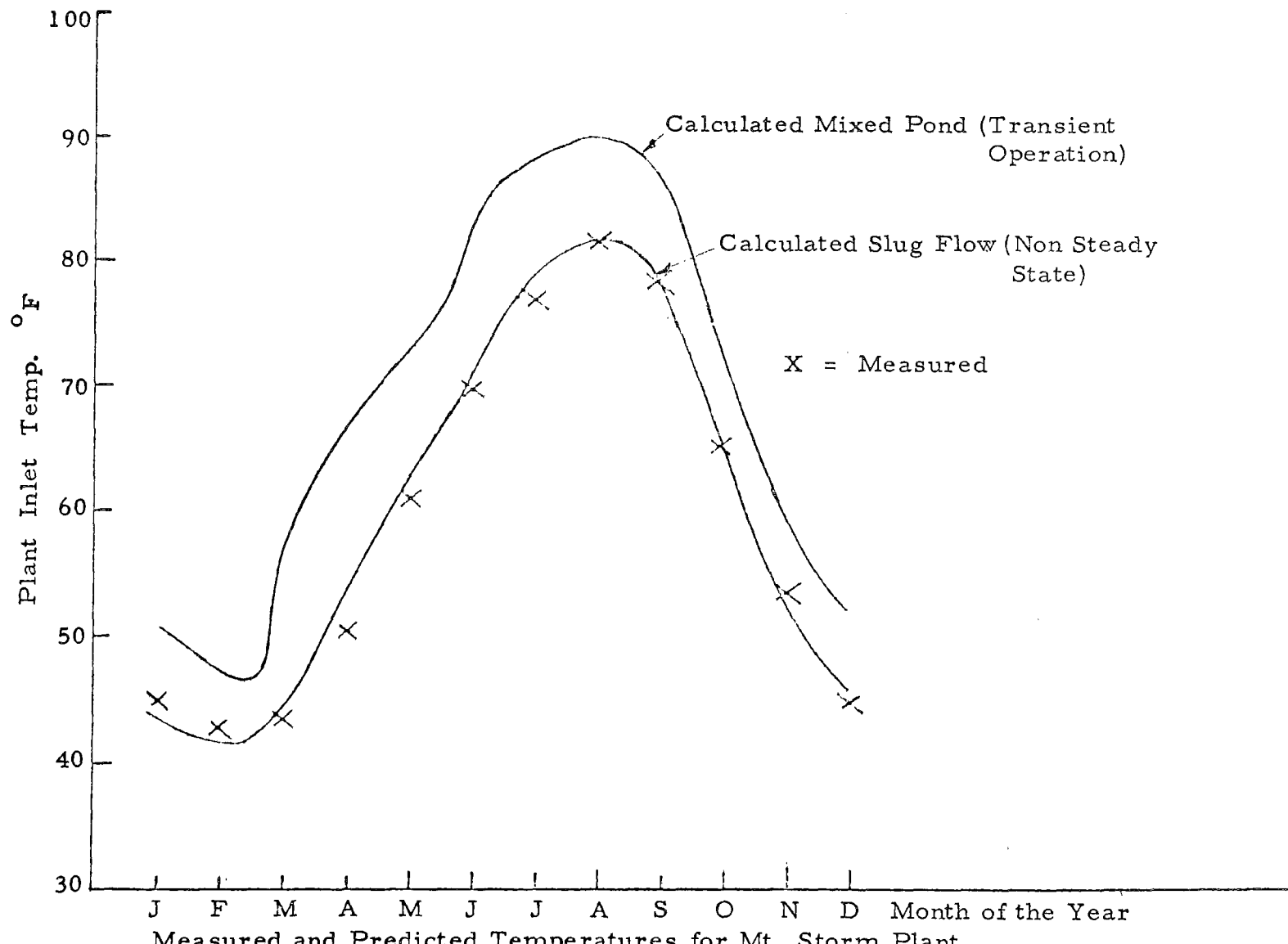


Figure 14

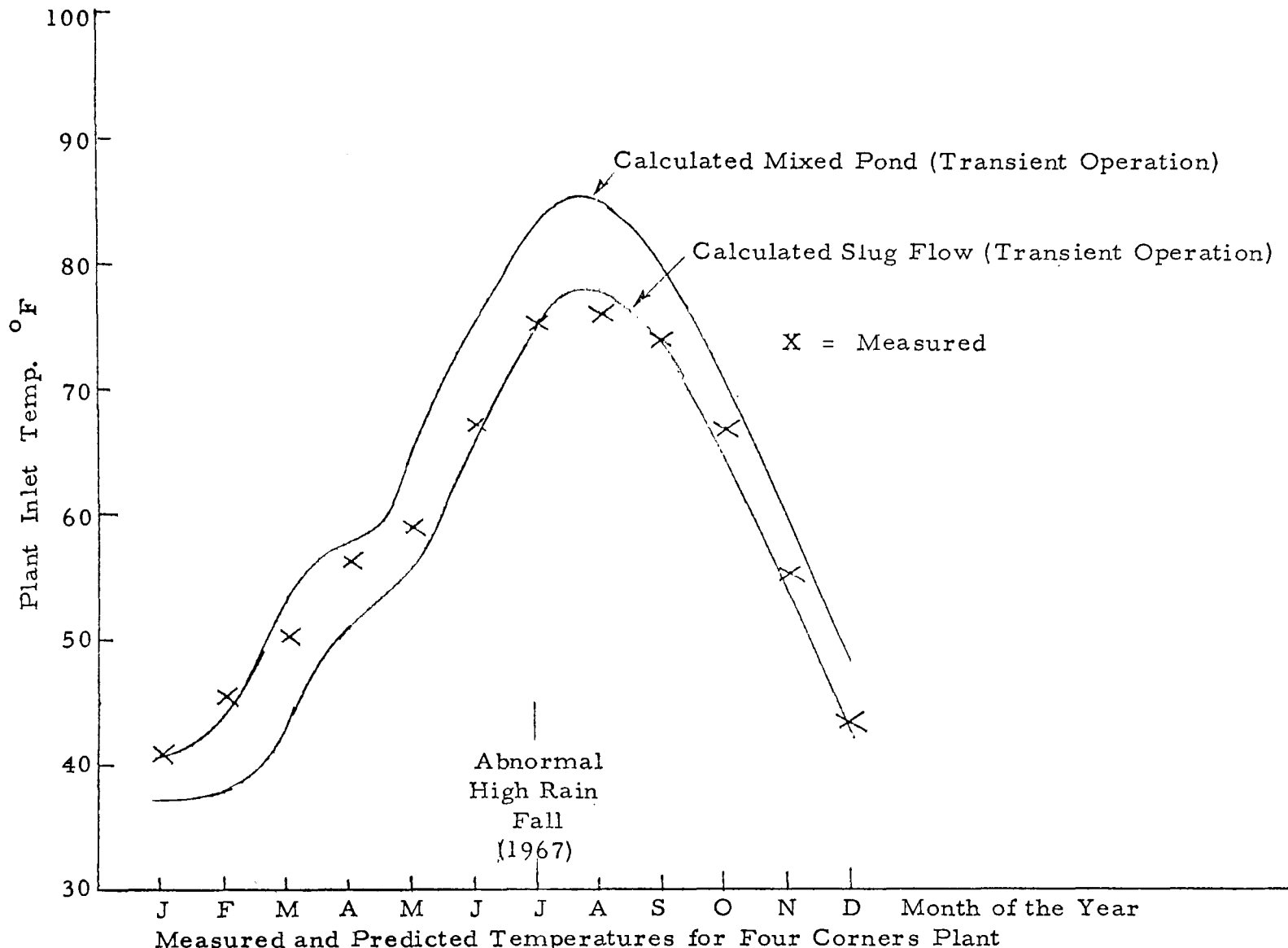


Figure 15

CURVES FOR PREDICTING WATER LOSS BY EVAPORATION

In this section the equations for predicting the water loss from the pond under both natural conditions and when the pond is receiving waste thermal energy from the power plant are presented. As a matter of convenience to the user, the results of these equations are presented in the form of curves.

For either the mixed or slug flow pond it is assumed that the rate of evaporation per unit surface area can be expressed in the simplified form suggested in Appendix B by Eq. B-33, namely:

$$\dot{m}_e = \frac{1}{1070} (a_{12} + a_{13} W) [P_w - P_a] \quad (\text{Eq. 29})$$

where $a_{12} = 3730$

$a_{13} = 373$

P_w = water saturation pressure corresponding to the temperature of the pond surface

Since the pond surface temperature is everywhere the same for the mixed pond, the amount of water lost per day in a mixed pond is:

$$\dot{m}_e = A \left(\frac{a_{13} + a_{13} W}{1070} \right) (P_w - P_a) \quad (\text{Eq. 30})$$

In order to present one set of curves to readily show this relation, Eq. 30 can be rewritten as:

$$\dot{m}_e \left(\frac{1070}{A} \right) \left(\frac{1}{a_{12} + a_{13} W} \right) = \{(a_1 + a_2 \theta + a_3 \theta^2 + a_4 \theta^3)\} - P_a \quad (\text{Eq. 31})$$

where $P_w = a_1 + a_2 \theta + a_3 \theta^2 + a_4 \theta^3$ (See Eq. B-37)

The left hand side of Eq. 31 is plotted in Fig. 16 as a function of pond surface temperature ($\theta + 32^\circ$) and air vapor pressure. To demonstrate the use of Fig. 16, consider again the example used in Case I, namely, a steady state pond temperature of 79.0°F , a pond surface of $50 \times 10^6 \text{ ft}^2$, water vapor pressure in the atmosphere of .294 psia, and a value of the wind parameter ($a_{12} + a_{13} W$) of 7460. For this case Fig. 16 gives the following value:

$$\dot{m}_e \left(\frac{1070}{A} \right) \left(\frac{1}{a_{12} + a_{13} W} \right) = .205$$

Thus the rate of evaporation from this pond is:

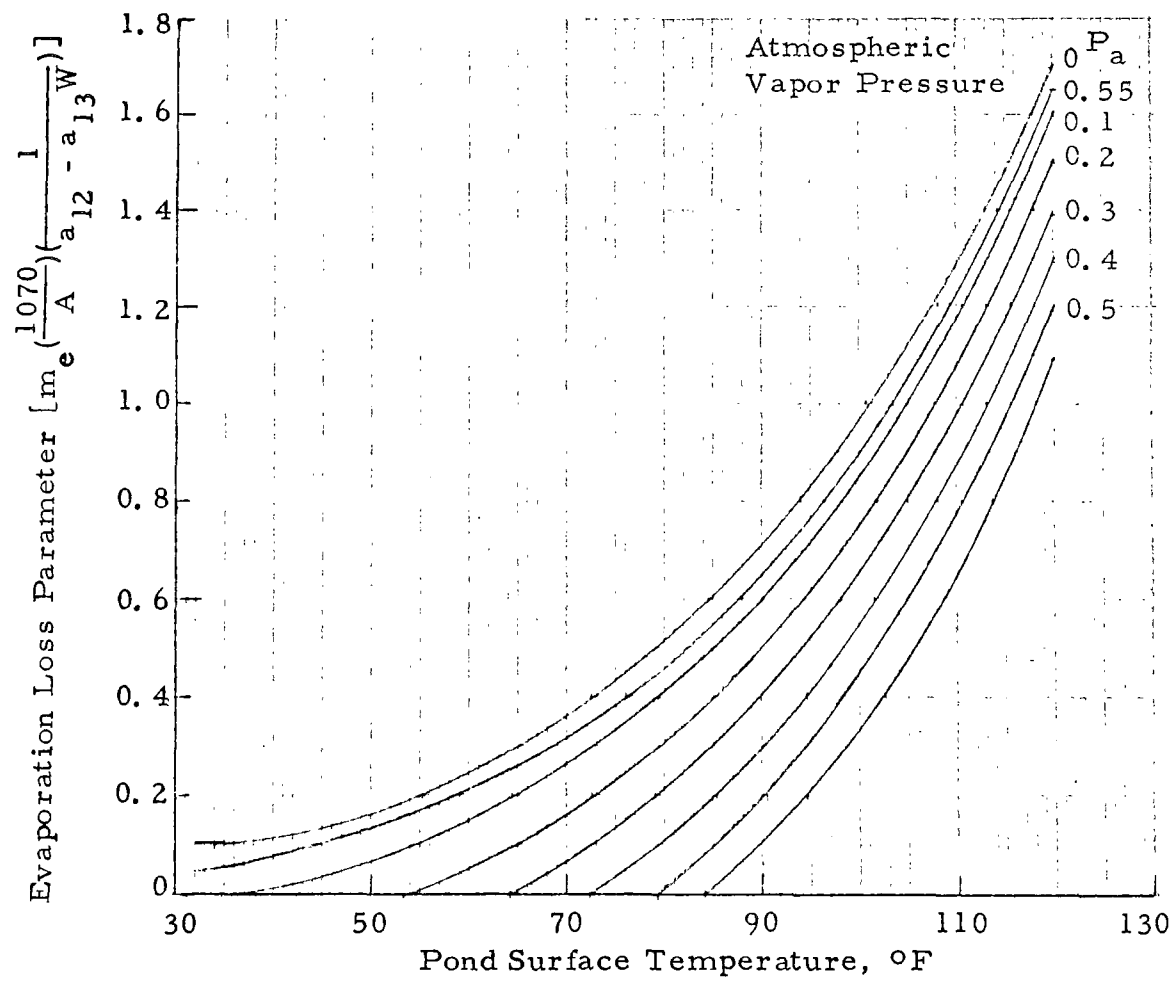


Figure 16

$$\dot{m}_e = (.205)(50 \times 10^6) \left(\frac{1}{1070}\right)(7460)$$

$$= 71.5 \times 10^6 \text{ #m/day}$$

If the waste thermal energy received by the pond is reduced to zero, then the pond temperature becomes the natural equilibrium temperature which was previously found to be 75.5°F. Again using Fig. 16, the rate of evaporation under the previous conditions but for a surface temperature of 75.5°F is found to be:

$$\dot{m}_e = (.152)(50 \times 10^6) \left(\frac{1}{1070}\right)(7460) = 53.1 \times 10^6 \text{ #, /day}$$

In the case of a slug flow pond the rate of evaporation per unit surface area changes with distance along the direction of flow and this variation must be integrated in order to determine the total water evaporated per day from the surface of the slug flow pond. Thus, integrating Eq. 30 over the pond surface yields the total rate of evaporation, namely:

$$\dot{m}_e = \int_{A=0}^A \left(\frac{a_{12} + a_{13}W}{1070} \right) (P_w - P_a) dA \quad (\text{Eq. 32})$$

Since P_a is constant along the pond surface, this equation can be re-written as:

$$\dot{m}_e = \int_{A=0}^A \left(\frac{a_{12} + a_{13}W}{1070} \right) P_w dA - \left(\frac{a_{12} + a_{13}W}{1070} \right) P_a A \quad (\text{Eq. 33})$$

Before the above equation can be integrated, the way in which the surface temperature (and hence P_w) varies with the pond area must be known. This variation is given by Eq. 21 for steady state operation. When this equation is substituted into Eq. 33, the total rate of evaporation can be found as a function of the equilibrium temperature, namely:

$$m_e = \frac{(WTE)}{\Delta T_c} (f_{3_f} - f_{3_i}) - \left(\frac{a_{12} + a_{13}W}{1070} \right) P_a A \quad (\text{Eq. 34})$$

where A at some temp. T

$$f_3 = \int_{A=\text{Reference area}}^A \left(\frac{a_{12} + a_{13}W}{1070} \right) P_w dA$$

$f_{3_i} = f_3$ for temperature at the initial or cold end of the pond where the temperature is T_i

$$f_{3_f} = f_3 \text{ for temperature at the final or hot end of the pond}$$

where the temperature is T_f

In order to facilitate the use of this procedure, values of f_3 are plotted in Fig. 17 for a selected number of equilibrium temperatures. In order to demonstrate the use of Fig. 17, again consider the previous example where $\Delta T_c = 10^{\circ}\text{F}$; $A = 50 \times 10^6 \text{ ft}^2$; $T_i = 85.9^{\circ}\text{F}$; $T_f = 75.0^{\circ}\text{F}$. For this case Fig. 17 gives the following values:

$$f_{3_i} = .0465$$

$$f_{3_f} = .0970$$

Thus the water lost by evaporation for this steady state slug flow pond is given by the expression:

$$\begin{aligned} \dot{m}_e &= \frac{(35 \times 10^9 \text{ btu/day})}{10^{\circ}\text{F}} (.0970 - .0465) - \left(\frac{7460}{1070}\right) (.294)(50 \times 10^6) \\ &= 74.5 \times 10^6 \text{ #m/day} \end{aligned}$$

As the ΔT_c for the slug flow pond is allowed to approach zero by increasing the pumping rate, the pond approaches a uniform temperature along its length which is equal to the mixed pond temperature of 79.0°F and the evaporation approaches $71.5 \times 10^6 \text{ #m/day}$.

It should be noted that the terms selected for the water mass balance on the pond allow for the estimation of each incoming and each outgoing term independently. Thus, when the water mass balance is being considered, attention must be paid to water loss from the pond by outflow and seepage in addition to the evaporation considered above as well as to water gained by the pond as a result of inflow and direct precipitation falling on the pond surface. For most cooling ponds the last item will be equal to a substantial fraction of the water lost by evaporation. To demonstrate this point it is helpful to consider the mixed pond example that was discussed above. In that example the rate of evaporation from the pond surface was shown to be $53.1 \times 10^6 \text{ #m/day}$ and $71.5 \times 10^6 \text{ #m/day}$ for waste thermal energy loads of zero and 700 btu/day ft^2 respectively. These two rates correspond to a decrease in the pond depth of 0.21 inches per day and 0.28 inches per day respectively for the $50 \times 10^6 \text{ ft}^2$ pond used in the example. An annual rainfall of 36 inches corresponds to an average increase in the pond depth of 0.10 inches per day in the form of direct precipitation.

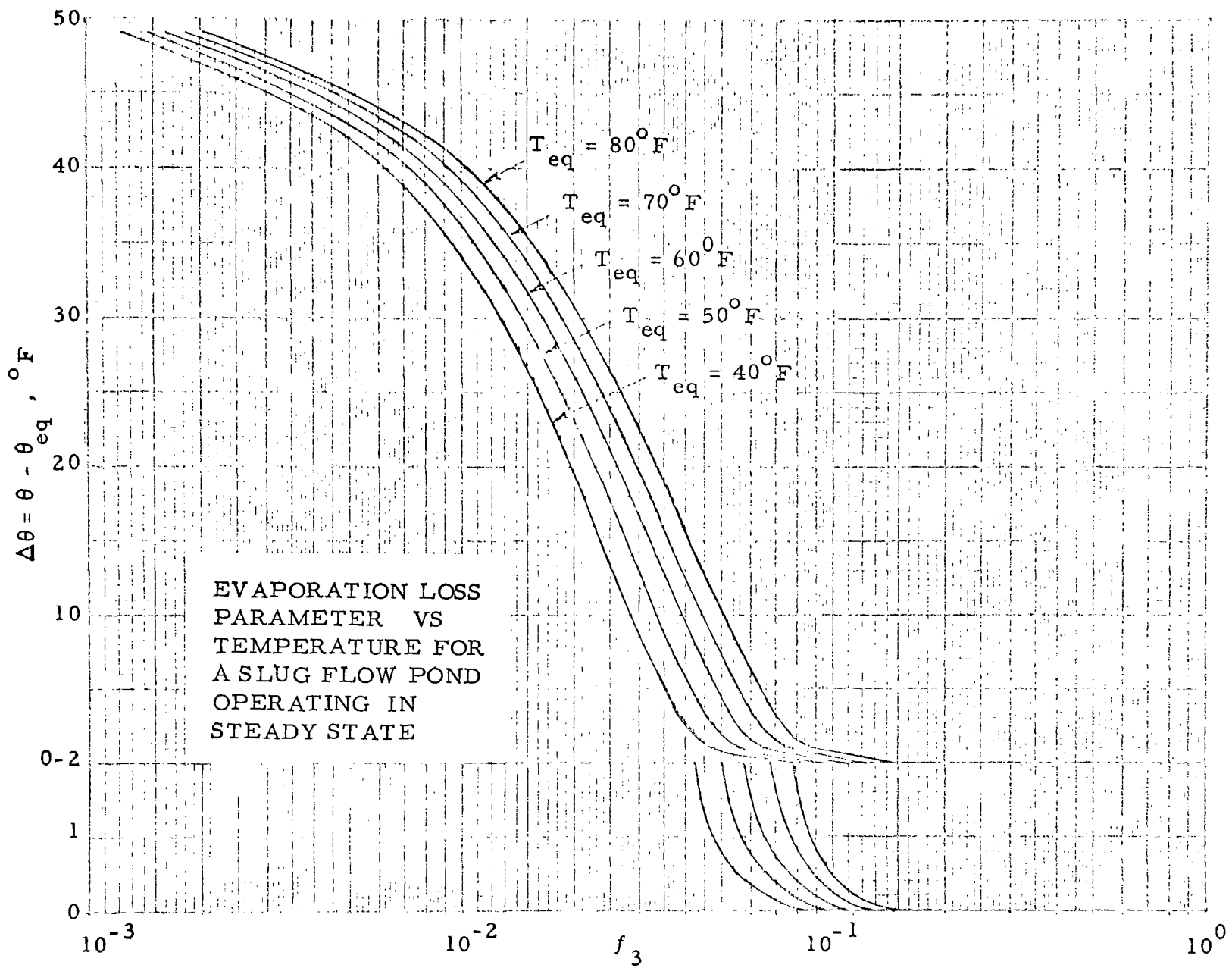


Figure 17

APPLICATION OF DESIGN CURVES TO PARTICULAR POWER PLANTS

The design curves developed previously are used to predict the performance of cooling ponds for two "typical" power plants. One of these is assumed to be located near Philadelphia, Pa. This location is nearly at sea level, has moderate temperatures, high humidity, and an adequate water supply. The other is assumed to be located near Winslow, Arizona. It is nearly a mile above sea level surrounded by even higher terrain, and has a very dry but relatively mild climate. Thus these locations represent conditions under which normal and high evaporation rates, respectively, are expected.

The power plants are assumed to generate 2000 MW_e and reject heat at the rate of 38.8×10^6 btu/day at each of these locations.

At each location the performance of two types of ponds are calculated: a mixed pond, and a slug flow pond. These types of flow are extreme models of a practical pond, the actual flow being somewhere between the extremes.

The calculation of cooling pond performance requires the knowledge of local weather conditions. These are obtained from Local Climatological Data sheets [17, 18], The Climatic Atlas [12], and Refs. [6] and [13]. Cooling pond performance is calculated for the summer months of June, July and August, considered as design conditions. At the Philadelphia plant the weather data for the summer months are summarized below, according to source.

From Local Climatological Data sheets [1]

	<u>June</u>	<u>July</u>	<u>August</u>
Wind speed, W, mph	8.7	8.1	7.8
Mean temperature, T _a , °F	71.0	75.6	73.6
Normal daily maximum temperature, T _{max} , °F	81.6	85.9	83.7
Normal daily minimum temperature, T _{min} , °F	60.4	65.2	63.5
Relative humidity, 1 AM, H ₁ , %	79	82	81
Relative humidity, 7 AM, H ₂ , %	76	79	80
Relative humidity, 1 PM, H ₃ , %	53	53	54
Relative humidity, 7 PM, H ₄ , %	60	62	65

	<u>June</u>	<u>July</u>	<u>August</u>
From Climatic Atlas [3]			
Mean daily solar radiation, \dot{Q}_s , langleys	523	510	450
Mean sky cover	0.61	0.61	0.60
From Reference [6] (See Figs. 2 and 4)			
Shortwave solar reflectivity, R_s	0.06	0.06	0.06
Clear sky solar radiation, \dot{Q}_{cs} , btu/ft ² day	2950	2850	2580
From Reference [13], page 472, after averaging:			
Sun altitude, degrees	41.7	39.7	39.0

Using the above weather data, the following quantities are calculated:

$$\begin{aligned}
 P_a &= \frac{1}{2}\{p[T_{min}, \frac{1}{2}(H_1+H_2)] + p[T_{max}, \frac{1}{2}(H_3+H_4)]\} 0.251 & 0.300 & 0.286 \\
 a_{12} + a_{13}W &= 3730(1 + W/10) & 6980 & 6750 & 6640 \\
 \theta_a &= T_a - 32^{\circ}\text{F} & 39.0 & 43.6 & 41.6 \\
 C_B & \text{(from Fig. 3)} & 0.74 & 0.74 & 0.74 \\
 \dot{Q}_a &= 4.0 \times 10^{-8}(T_a + 460)^4(C_B - 0.223\sqrt{P_a}) & 2720 & 2850 & 2820 \\
 \dot{Q}_N &= 0.97\dot{Q}_a + \dot{Q}_s(1 - R_{sr}) & 4460 & 4530 & 4290 \\
 (a_{12} + a_{13}W)(a_1 - a_{14}) & \theta_a - P_a & -2420 & -2820 & -2620 \\
 f_1 &= \dot{Q}_n - a_5 - (a_{12} + a_{13}W)(a_1 - \theta_a a_{14} - P_a) & 4521 & 4991 & 4551 \\
 (f_1)_{av} &= 4688 \\
 (a_{12} + a_{13}W)_{av} &= 6790
 \end{aligned}$$

Then with $f_1 + \dot{Q}_{pp}$, the mixed pond temperature obtained from Fig. 5A, the evaporation factor from Fig. 16, and the evaporated water equal to evaporation constant times $A(a_{12} + a_{13}W)/1070$, we obtain the following performances for mixed ponds of five sizes. The pond sizes range from 0.5 to 5 acres per MW_e, representing highly and lightly loaded ponds, respectively.

Areas, A in acres	A/MW _e	\dot{Q}_{pp}	$f_1 + \dot{Q}_{pp}$	T	Water Evap.	
					Evaporation Constant	per day in 10^9 lbs
1000	0.5	8920	13608	115	1.20	0.330
2000	1	4460	9148	99	0.64	0.351
4000	2	2230	6918	88	0.38	0.481
6000	3	1487	6175	84	0.31	0.507
10000	5	892	5580	80	0.23	0.637

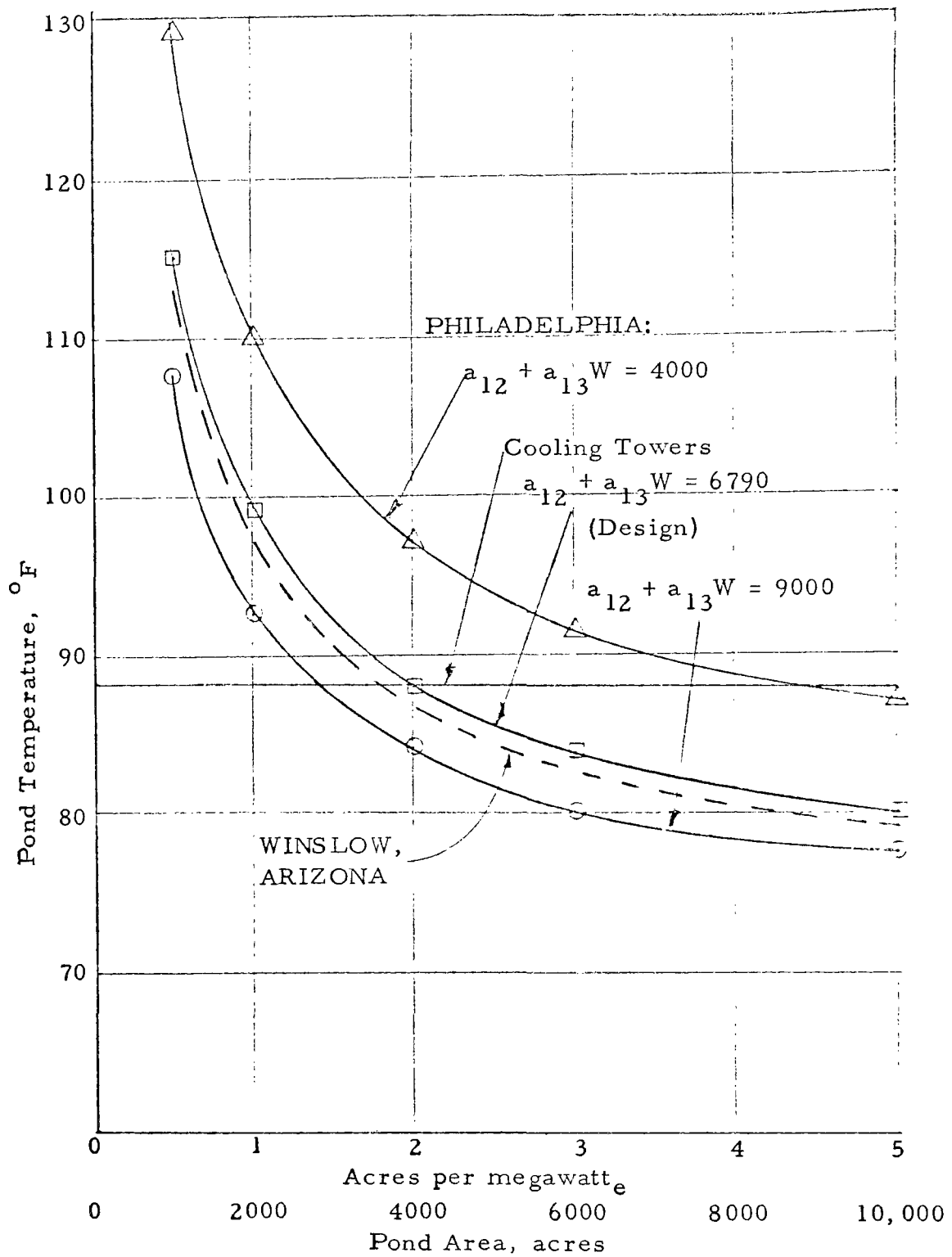
The average annual precipitation for the Philadelphia area is 40 inches. Based on this value the difference between water lost by evaporation and water gained by direct precipitation is shown below.

Area, A in acres	Water Gained by Precipitation per day in 10^9 lbs	Net Water Lost (evaporation-precipitation) per day in 10^9 lbs
1000	0. 025	0. 305
2000	0. 050	0. 301
4000	0. 099	0. 382
6000	0. 149	0. 358
10000	0. 248	0. 389

The temperature and evaporated water variation with pond area for mixed ponds at Philadelphia are shown in Figs. 18 and 19, respectively. These curves show the expected trends: the temperature of the pond increases rapidly as the heat loading increases (or equivalently as the acres per MW_e decrease) and the amount of total evaporated water increases with increasing pond size. Fig. 19 also shows an evaporation curve designated Average Over a Year. This curve is obtained by computing the evaporation rate for each month and then averaging them.

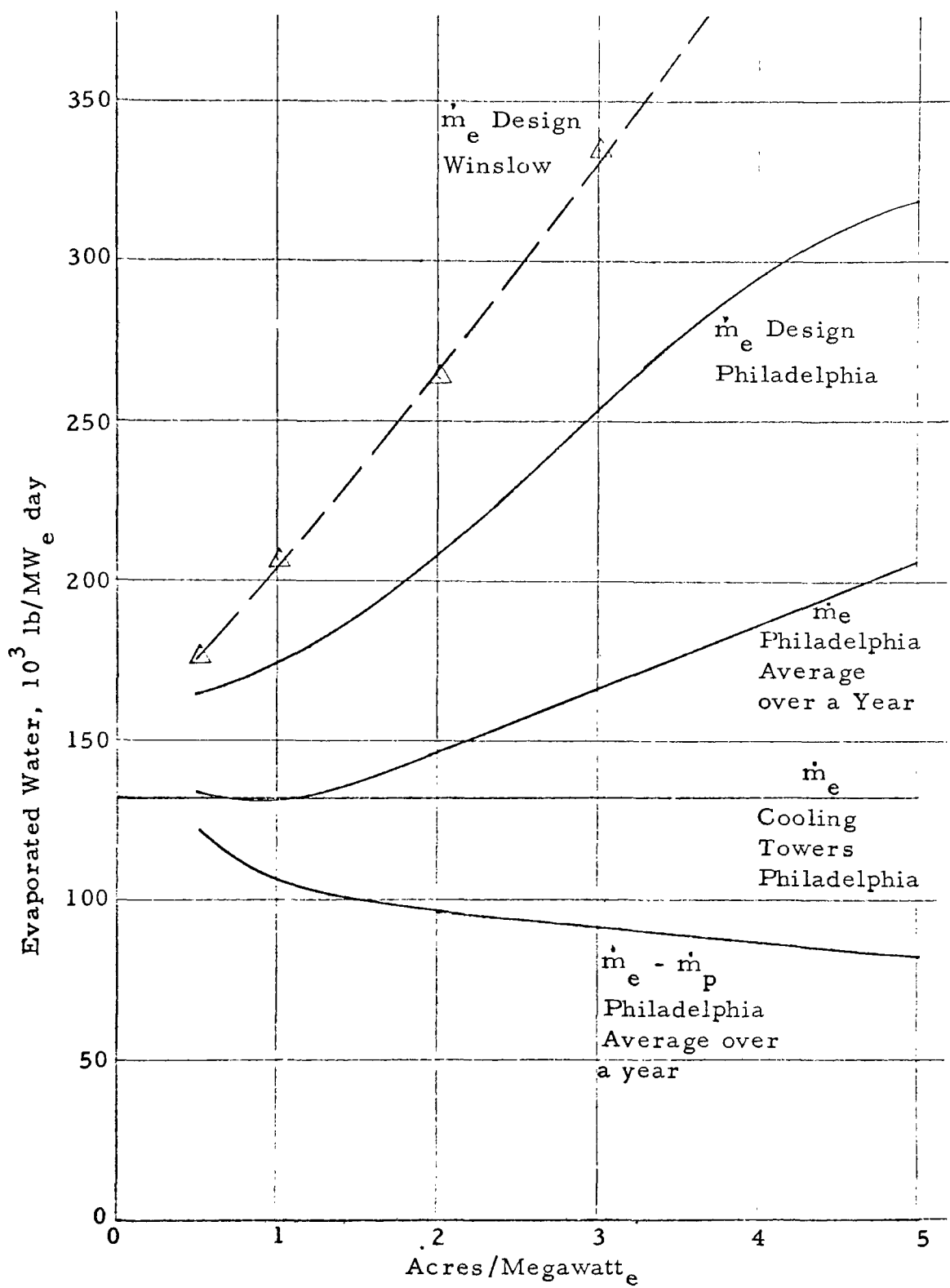
The calculation of the temperatures of the steady state and slug flow ponds requires the knowledge of the difference between inlet and outlet temperatures, or equivalently the temperature rise through the condenser. This temperature rise is a parameter in the power plant equipment design and it is determined from an economic study of the power plant operation. Such a study for the Philadelphia Plant is presented in the next section. For the present, slug flow pond temperatures are calculated for several condenser temperature rises, ranging from 10° to 30° F. The calculation of slug flow pond temperature involves the use of charts (Figs. 7A - 7G) in an iterative fashion as explained previously. The results for five pond sizes and five condenser temperature rises are presented in Fig. 20. Comparing Figs. 18 and 20, we see that the slug flow pond temperatures for corresponding pond sizes are lower than those for the mixed pond.

The sensitivity of mixed pond temperature to the wind parameter, $a_{12} + a_{13}W$, was evaluated. The results for $a_{12} + a_{13}W$ equal to 4000 and 9000, representing the extremes of the wind parameter for which curves are given, and corresponding to wind velocities of approximately 0.7 mph and 14 mph are shown in Fig. 18. We see that the sensitivity of pond temperature to the wind parameter is higher for highly loaded ponds.



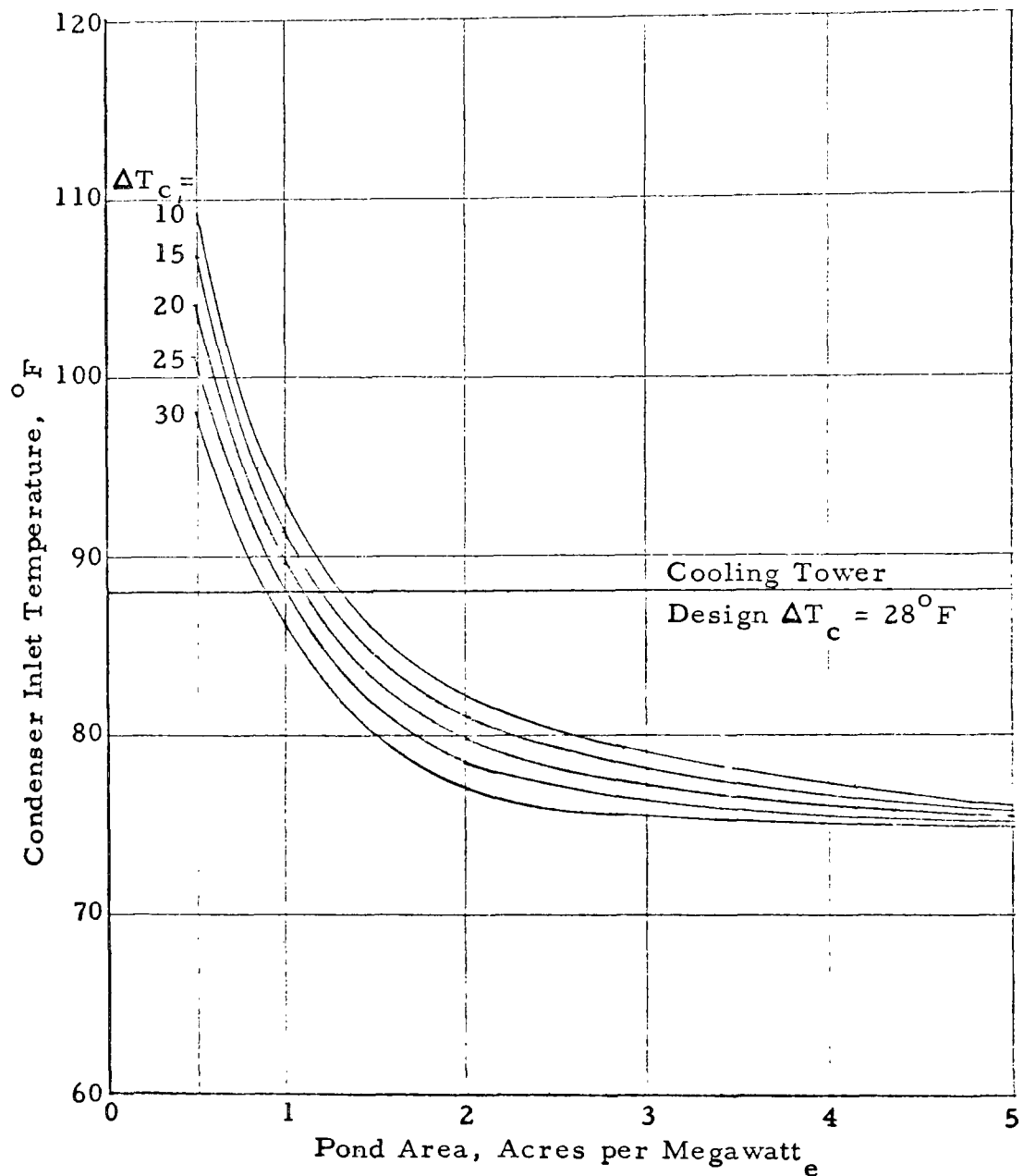
Temperature of Mixed Ponds - 2000 MW_e Plant
Design Climatic Conditions

Figure 18



Evaporated Water from Mixed Ponds Near Philadelphia, Pa., and Winslow, Ariz. - Design Climatic Conditions

Figure 19



Temperatures for Slug Flow Ponds
 2000 MW_e Plant near Philadelphia
 Design Conditions

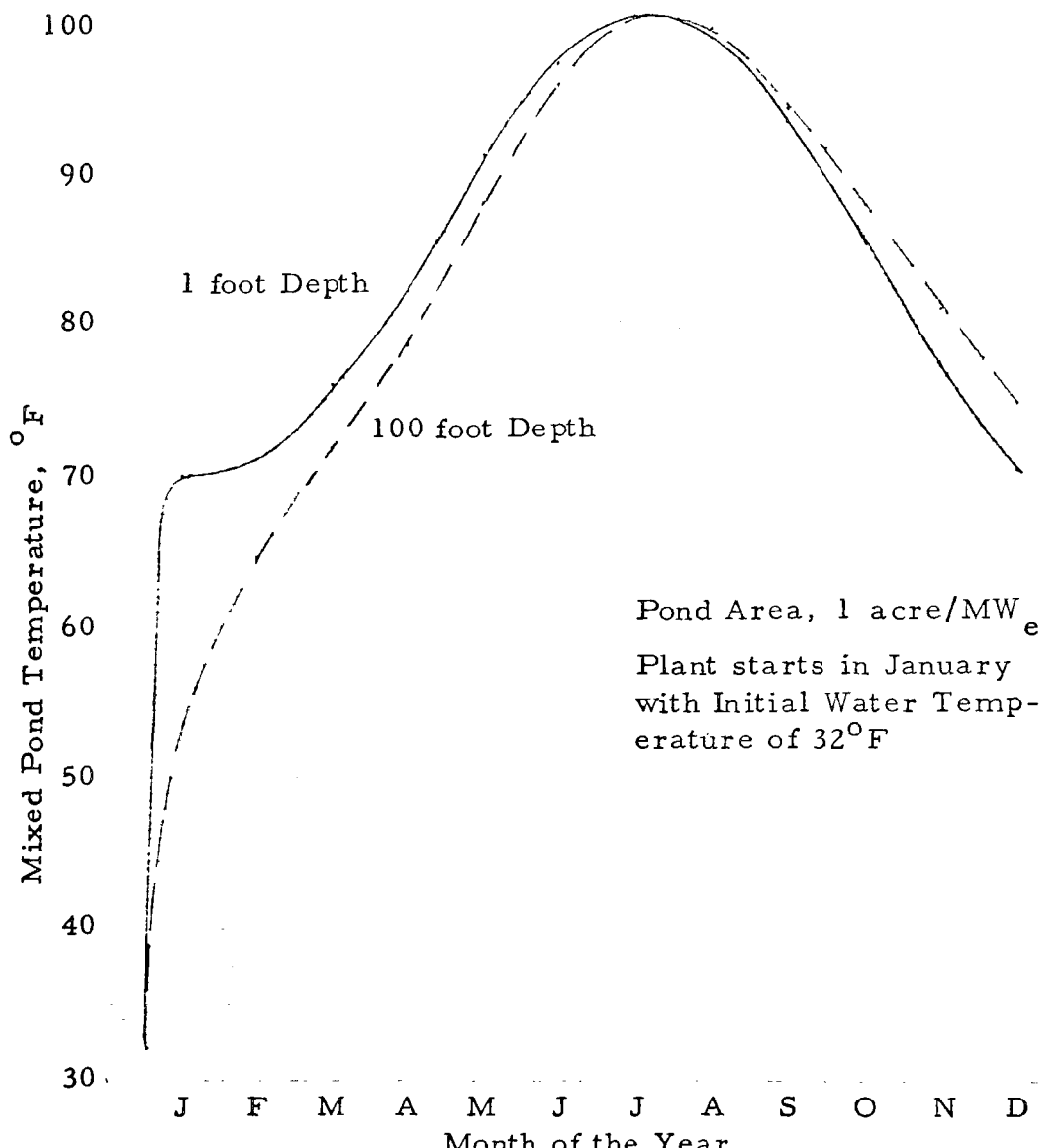
Figure 20

Transient temperatures in the mixed pond at the Philadelphia location were calculated with the aid of the charts for predicting water temperatures. The method for calculating transient temperatures consists essentially of considering the pond to operate under steady climatic and thermal waste energy for each month, and calculating the pond temperature change during the month. The final pond temperature for one month is taken as the initial temperature for the next month and a new final temperature is calculated. The whole process is carried on for a year. The temperatures for a 1-foot and 100-feet deep ponds are shown in Fig. 21. The one-foot deep pond represents steady state operating conditions, where no lag in pond temperature is expected. The 100-foot deep pond shows a temperature lag in the early months, reaches the same maximum at a slightly later time than the 1-foot deep pond, and runs at a slightly higher temperature later in the year.

The performances of the mixed and flow-through ponds at the Philadelphia location are compared with a cooling tower design for that location [28] in Figs. 18, 19 and 20. The cooling system of Ref. [28] consists of two natural draft cooling towers, each 380 feet in diameter, 380 feet high with a design range of 28°F , a design approach temperature of 16°F , and a design wet bulb temperature of 72°F . From Fig. 18 we see that the mixed pond with 2 acres per MW_e provides the same cooling as the cooling towers. Mixed ponds larger than 2 acres per MW_e perform better than the cooling tower in terms of producing lower temperature condenser cooling water. From Fig. 20 we see that slug flow ponds larger than about 1.3 acres/ MW_e perform at lower temperatures than the cooling towers. From Fig. 19 it is seen that the amount of water evaporated by the towers is greater than the net difference between water evaporated from the pond and precipitation falling directly on the pond surface for all pond sizes considered. The amount of water evaporated by the cooling towers, as shown in Fig. 19, corresponds to average conditions.

At the Winslow, Arizona, Plant the weather data taken from Ref. [18] are summarized below:

	<u>June</u>	<u>July</u>	<u>August</u>
Wind speed, W, mph	10.7	8.2	7.8
Mean temperature, T_2 , $^{\circ}\text{F}$	69.7	78.3	75.6
Normal daily maximum temperature T_{max} , $^{\circ}\text{F}$	92.0	95.7	92.4
Normal daily minimum temperature T_{min} , $^{\circ}\text{F}$	56.5	64.6	63.1
Relative humidity, 5 AM, %	38	56	67
Relative humidity, 11 AM, %	17	30	37
Relative humidity, 5 PM, %	14	27	32
Relative humidity, 11 PM, %	28	47	53



Transient Temperature of Mixed Pond for a 2000 MW_e Plant near Philadelphia

Figure 21

Then proceeding in the same way as for the mixed pond at the Philadelphia location, we obtain the performance of the mixed pond at Winslow, Arizona, summarized below and plotted in Figs. 18 and 19.

Area, A in acres	A/MW _e	T	Water evaporated per day, 10 ⁹ lbs
1000	0.5	113.0	0.352
2000	1	97.5	0.412
4000	2	86.5	0.526
6000	3	82.5	0.670
10000	5	79.0	0.944

The equilibrium temperatures of mixed ponds at Winslow, Arizona, differ from those at Philadelphia by no more than two degrees. However, ponds at Winslow evaporate much more water than at Philadelphia. In addition, the average annual rainfall in the Winslow is only 7.4 inches with the result that only about 1/6 as much water will be added to the Winslow pond by direct precipitation as at the Philadelphia pond.

ECONOMIC ANALYSIS OF POWER PLANTS WITH COOLING PONDS

The economic analysis of power plant construction and operation is a well developed subject (See, for example, Ref. 29). The costs of producing electric power are broken down into two categories: fixed charges and operating costs. The fixed charges consist of interest, taxes, insurance, and depreciation. The operating costs cover expenditures for fuel, labor, maintenance, supplies, supervision and operating taxes. The economic analysis of a power plant with a cooling pond, and the economics of the cooling pond as a subsystem of a power plant, can be subjected to such an analysis.

In order to apply the economic analysis summarized above, a power plant design, with some detail, must be available. It should be clear that the power plant design depends to some degree on the particular site selected. The power plant with a cooling pond may be significantly different from power plants with other cooling systems in that more land is required and the cooling pond may be more sensitive to the weather. Therefore, the design and economics of a power plant with a cooling pond are very much site dependent, and it is not possible, at this time, to provide an all-inclusive procedure for the economic analysis of power plants with a cooling pond without knowing the site and the details of the design.

We suggest that some insight about the economics of cooling ponds may be gained from an example. The power plant to be considered generates 2000 MW_e, is located near Philadelphia and the performance curves for the ponds for this plant are given in the previous section designated "Application of the Design Curves to Particular Plants." This particular site is selected because the construction of a power plant on the site is being considered and a plant with natural draft cooling towers has been designed [28]. Hence this example affords a realistic economic comparison between cooling ponds and cooling towers.

The design with cooling towers for this location is known with a great deal of detail [28]. The turbine is a General Electric design with a known performance curve. The condenser is of selected design with known tube size, length, gage, and material, and cooling water flow velocity. The cooling water pumps are volute pumps with known head and capacity. Cooling of water is by two very large natural draft cooling towers.

The design with a cooling pond is presented in parametric form. Essentially it is an extrapolation of the cooling tower design.

Turbine It is assumed that the turbine of the cooling tower design is used in the cooling pond design. There is a disadvantage to the cooling pond in doing so, since the turbine is selected for a high temperature rise through the condenser. For some ponds where the range of the condenser is lower, a different turbine would be more economical.

Condenser The condenser design is extrapolated from that for the cooling tower design. The basis of the extrapolation is the formulae of Ref. [30]. The following are assumed to be known:

$$\text{Heat transferred, } Q = 1.568 \times 10^{10} \text{ btu/hr}$$

$$\text{Tube diameter, } D = 1 \frac{1}{4}''$$

$$\text{Tube thickness, } t = 0.049''$$

$$\text{Tube length, } L = 96'$$

Tube material - Admiralty brass

$$\text{Material factor, } C_m = 1.0$$

$$\text{Tube cleanliness factor, } C_c = 0.85$$

$$\text{Cooling water flow velocity, } V = 7 \text{ ft/sec}$$

Thus with the formulae of Ref. 30 we obtain

$$A_c = 4.33 \times 10^7 / R \quad (\text{Eq. 35})$$

$$G = 3.136 \times 10^7 / R \quad (\text{Eq. 36})$$

$$T_v = T_i + R(1 - e^{-1.61C_t}) \quad (\text{Eq. 37})$$

where A_c = condenser area, sq. ft

G = cooling water flow, gpm

R = temperature range, $^{\circ}\text{F}$

T_i = condenser inlet water temperature, $^{\circ}\text{F}$

T_v = saturation temperature in condenser, $^{\circ}\text{F}$

C_t = temperature correction factor, given in Ref. 30

The condenser area and the pumping rate for five temperature rises are given below and compared with the cooling tower design:

	$R (^{\circ}\text{F})$	$A_c (10^6 \text{ sq. ft})$	$G (10^6 \text{ gpm})$
Cooling Pond Design	10	4.33	3.14
	15	2.89	2.09
	20	2.16	1.57
	25	1.73	1.25
	30	1.44	1.05
Cooling tower design	28	1.53	1.12

Cooling water pumps The head loss in feet of water through 1 1/4" tubes is 0.25" per foot of travel [30]. The length of tubes is 96'. The head loss in water boxes is 1.4' [30]. For the head loss in the pond and conduits, take 10% of the sum of losses in tubes and water boxes. Thus the total pump head required is:

$$H = [0.25(96) + 1.4] 1.1 = 28'$$

The power required is:

$$\text{bhp} = \frac{GH\gamma}{3960\eta} = \frac{G(28)(1.0)}{3960(0.85)} = 0.00832 G$$

or

$$kw = 0.7457 \text{ bhp} = 0.0062 G \quad (\text{Eq. 38})$$

where
bhp = brake horsepower
G = pumping rate, gpm
 γ = fluid density
 η = pump efficiency, assumed to be 85%
kw = power required, kilowatts

Cooling Pond

Both mixed and flow through ponds are considered. The design of these is characterized by the performance curves for the Philadelphia site presented in Figs. 18 and 20.

The remaining equipment, buildings, and facilities of the cooling tower and cooling pond design are assumed to be the same. They are omitted from the economic study. Thus the economic study is based on the capital cost and operating expenditures for that equipment which is different in the cooling tower and cooling pond designs, namely, condensers, cooling water pumps, cooling towers/ponds. The measure of economy is the annual cost and operation of such equipment expressed in dollars. It should be remembered then, that percentage differences between the costs of the two designs are meaningless.

Cost of Equipment From Ref. [28] we find that for the cooling tower design, the cost of condenser fabrication and installation is \$4.90 per square foot of condenser area, and the cost of pumps is \$1.50 per gpm. For the cooling pond design, assume that the condensers also cost \$4.90 per square foot, but that the pumps cost \$0.50 per gpm, because the required head is about one-third of that required for the towers. The cooling towers cost \$15,920,000 [28]. The cost of the cooling pond will include all expenditures for its construction such as the cost of land, site preparation, construction of dams and dikes. Since this cost is highly

site dependent, three values of pond cost will be considered: \$500, \$2000. and \$5000 per acre of effective pond area. These pond costs are considered to cover the extremes and the average.

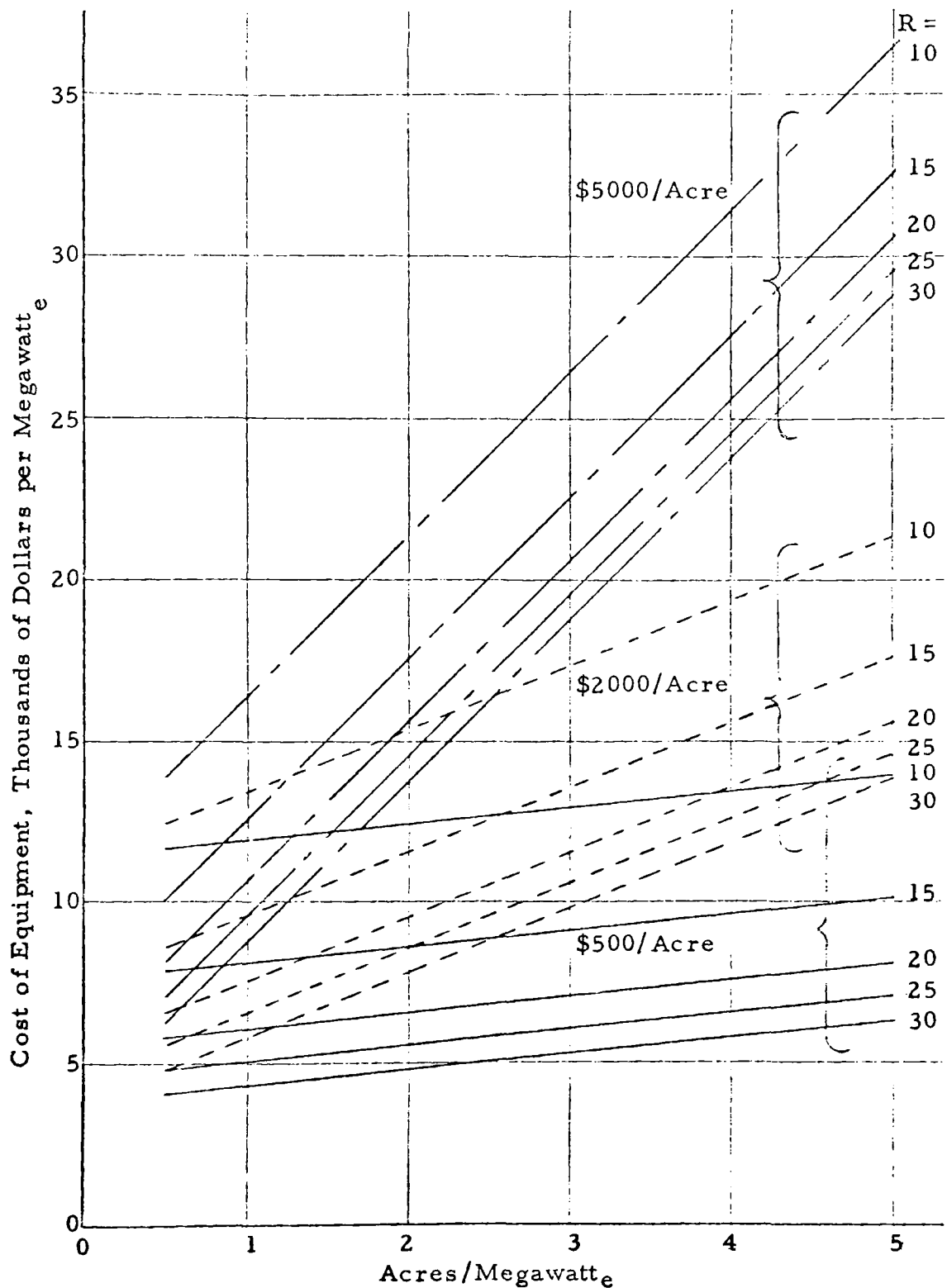
The cost of equipment for plants with cooling towers and cooling ponds is summarized below. For cooling ponds five temperature rises through the condenser, five pond areas, and three pond costs are considered.

TABLE II
COST OF EQUIPMENT IN MILLIONS OF DOLLARS

	Cooling Tower	Cooling Pond					
		R° F	10	15	20	25	30
Condensers	7.51	21.200	14.151	10.400	8.500	7.080	
Pumps	1.68	1.570	1.045	0.785	0.625	0.525	
Cooling Tower	15.92						
Cooling Pond		(acres)	1000	2000	4000	6000	10000
\$500/acre			0.5	1.0	2.0	3.0	5.0
\$2000/acre			2.0	4.0	8.0	12.0	20.0
\$5000/acre			5.0	10.0	20.0	30.0	50.2

The above equipment costs are presented in Fig. 22.

As the condenser cooling water temperature increases, the turbine back pressure will increase correspondingly. Subsequently the turbine efficiency will decrease and less electric energy will be produced per given unit of fuel energy expended. This loss of capacity due to increased turbine back pressure can be a substantial factor in the operating expense of a cooling pond facility. In order to assess the magnitude of this loss of capacity, the turbine "exhaust pressure correction curve" (that is, the curve showing decrease in output electric energy per unit fuel energy input as a function of back pressure) must be known. It should be pointed out that the "exhaust pressure correction curve" will vary from one particular turbine to another. Since the cost of lost capacity due to increased back pressure is one of the more significant terms contributing to operating cost of a cooling pond facility, a particular "exhaust pressure correction curve" (and hence a particular turbine) must be selected in order to execute the economic analysis and thus the economic analysis becomes a "cut-and-try" process. In principle a number of possible turbines should be selected for the task of conducting an economic analysis to yield the optimum pond size. In selecting the group of turbines, the assumption should be made that the average operating back pressure may turn out to be quite low (as, for example, if the cooling pond were to be very lightly loaded and located in the extreme



Equipment Cost for Captive Cooling Systems

Figure 22

north-central United States, say, northern Minnesota) or quite high (as for example, if the the cooling pond were to be very heavily loaded and located in a zone of high equilibrium temperature, say, in Louisiana).

Although in principle a number of possible turbines should be selected for the study, only one will be used in the present example, namely, General Electric Co. designation TC6F-38, thermodynamic rating 1, 112, 215 kw (See Fig. 23).

With the use of Eq. 37 and the pond temperatures given in Fig. 18 for the mixed ponds and Fig. 20 for the slug flow ponds, the condenser back pressure can be determined as a function of pond area. These values are shown in Figs. 24 and 25.

With the back pressure established as a function of pond area, the "exhaust pressure correction curve" shown in Fig. 23 can be used to determine the lost electrical capacity due to increased back pressure as a function of pond area. These values are shown in Figs. 26 and 27.

With the data in Figs. 22, 26 and 27, equations 36 and 38, and a maintenance cost for ponds of \$2/acre, the economics of a power plant with a cooling pond, as compared with a cooling tower, can be computed for various temperature rises of cooling water, pond sizes, and pond costs. An example is given below for a mixed pond.

1. Temperature range, $\Delta T_c = 10^\circ$
2. Pond size, $A = 1000 \text{ acres} = 0.5 \text{ acres/MW}_e$
3. Pond cost = \$2000/acre of effective pond area.
4. Pumping rate = $3.14 \times 10^6 \text{ gpm}$
5. The cost of equipment = $\$24.77 \times 10^6$ (Fig. 22)
6. Interest rate = 11.5%
7. Capital cost = $24.77 \times 10^6 (1.115) = \$2.848 \times 10^6 / \text{yr}$
8. Lost capacity due to back pressure = $80.6 \times 10^3 \text{ kw}$ (Fig. 26)
9. Cost of lost capacity due to back pressure* = $80.6 \times 10^3 (10.40)$
= $\$0.839 \times 10^6 / \text{yr}$
10. Lost capacity due to pumping** = $0.0062(3.14 \times 10^6) = 19.5 \times 10^3 \text{ kw}$
11. Cost of lost capacity due to pumping*** = $19.5 \times 10^3 (10.40)$
= $\$0.202 \times 10^6 / \text{yr}$

* Based on a loss rate of \$10.40/kw-yr due to increased turbine back pressure above the turbine design pressure. [28]

** See Eq. 38.

*** Based on a loss rate of \$10.40/kw-yr due to loss in capability because of power required for pumps and fans. [28]

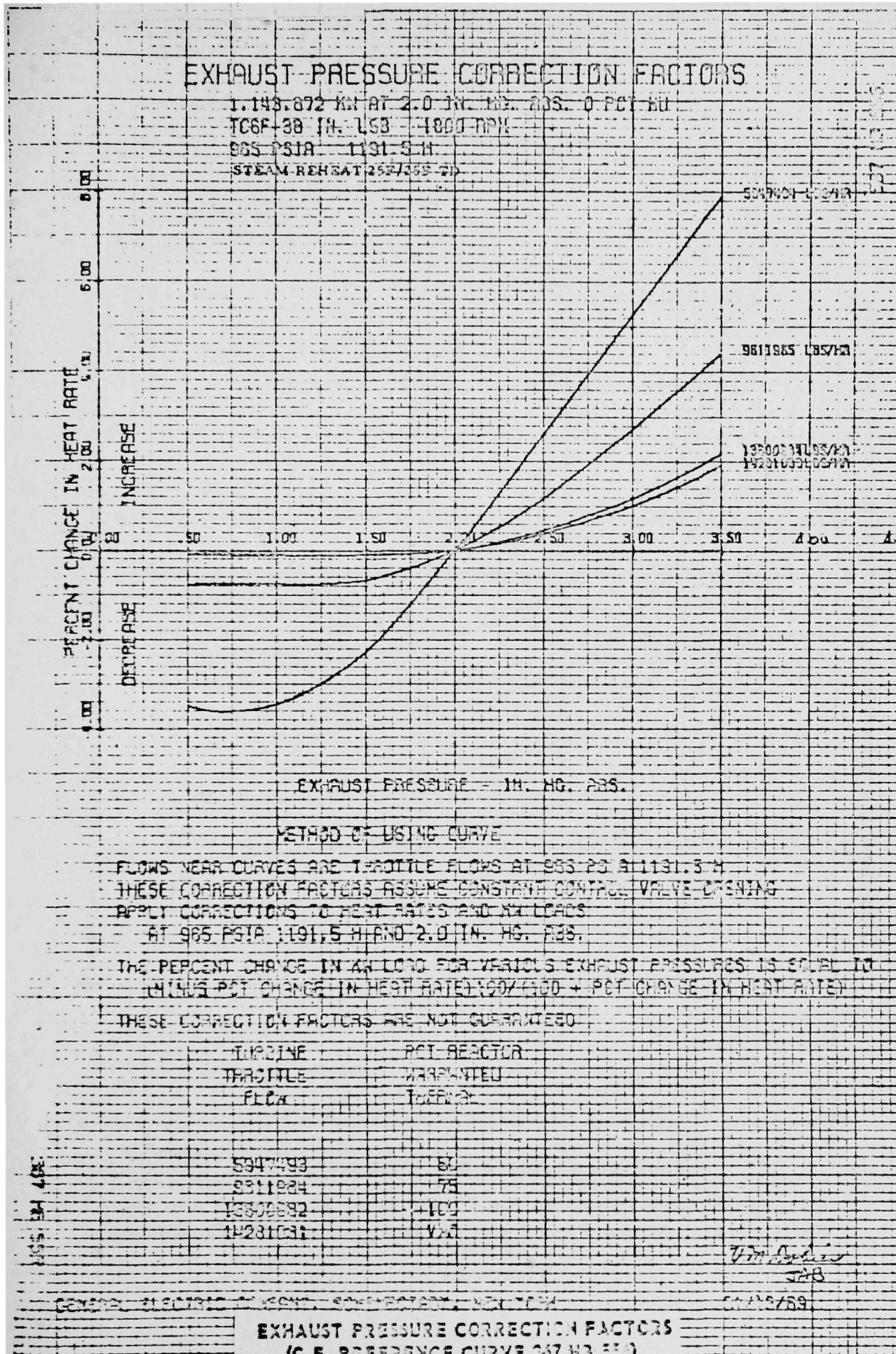
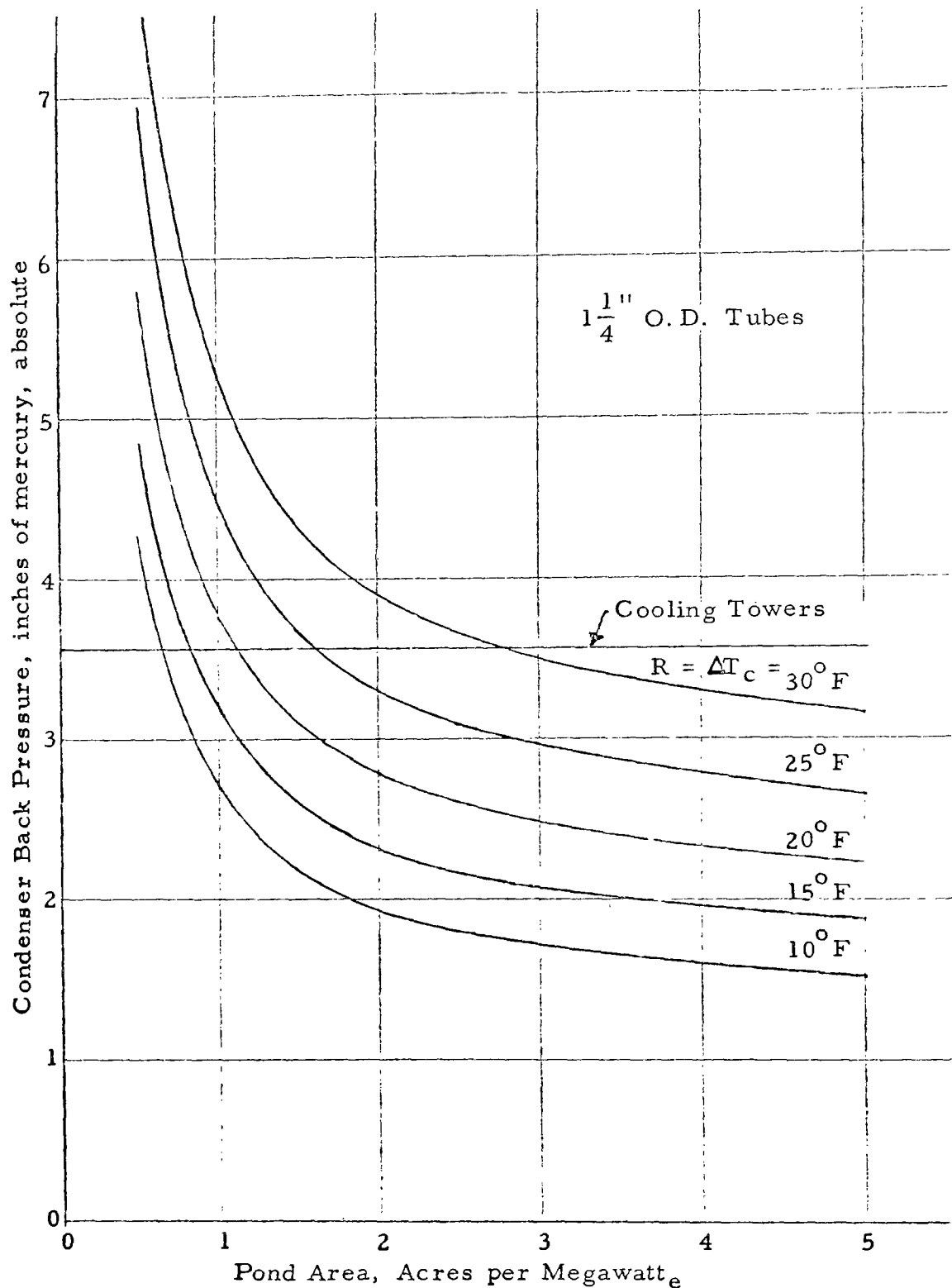
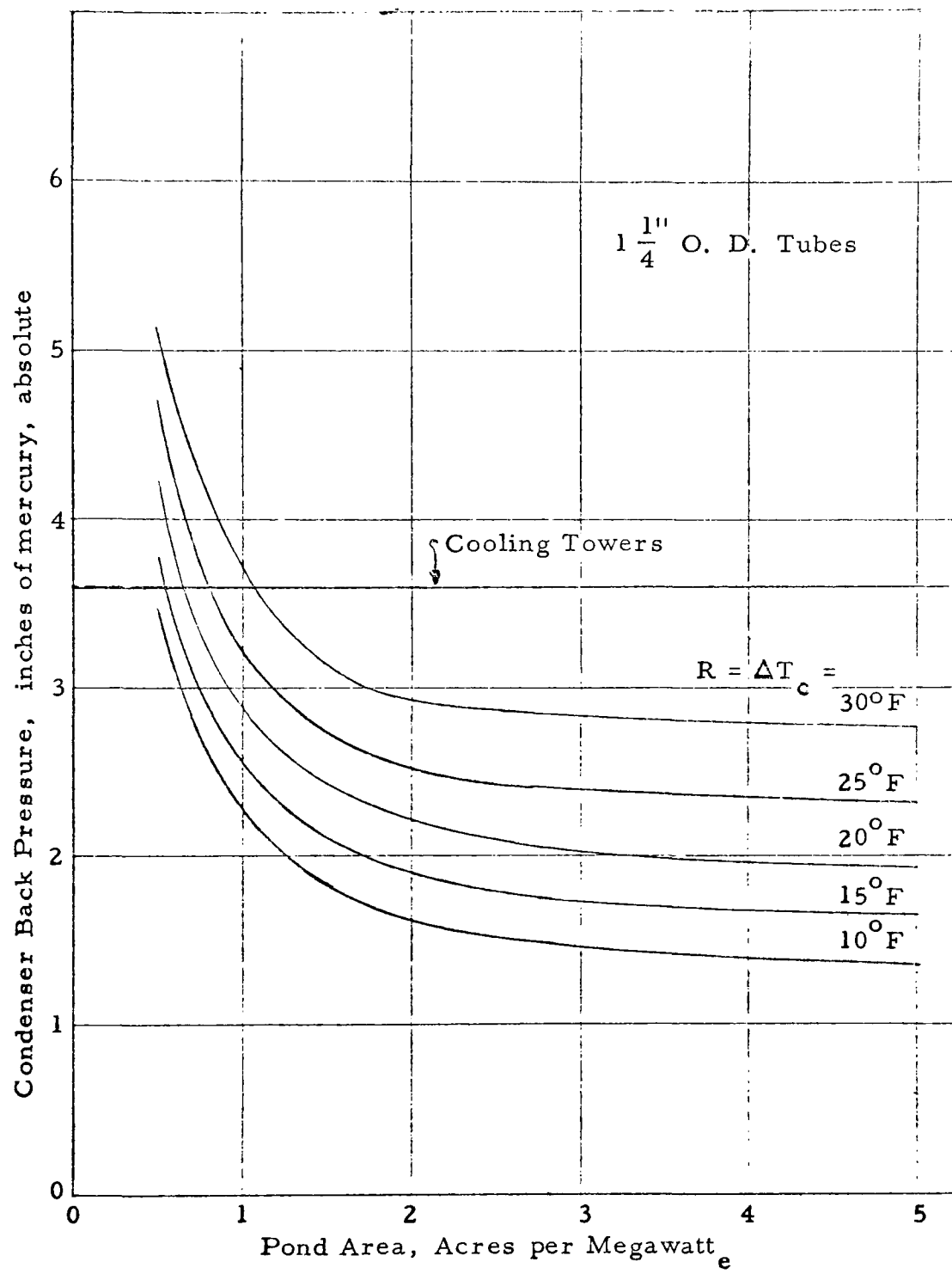


Fig. 23 - Exhaust Pressure Correction Curve



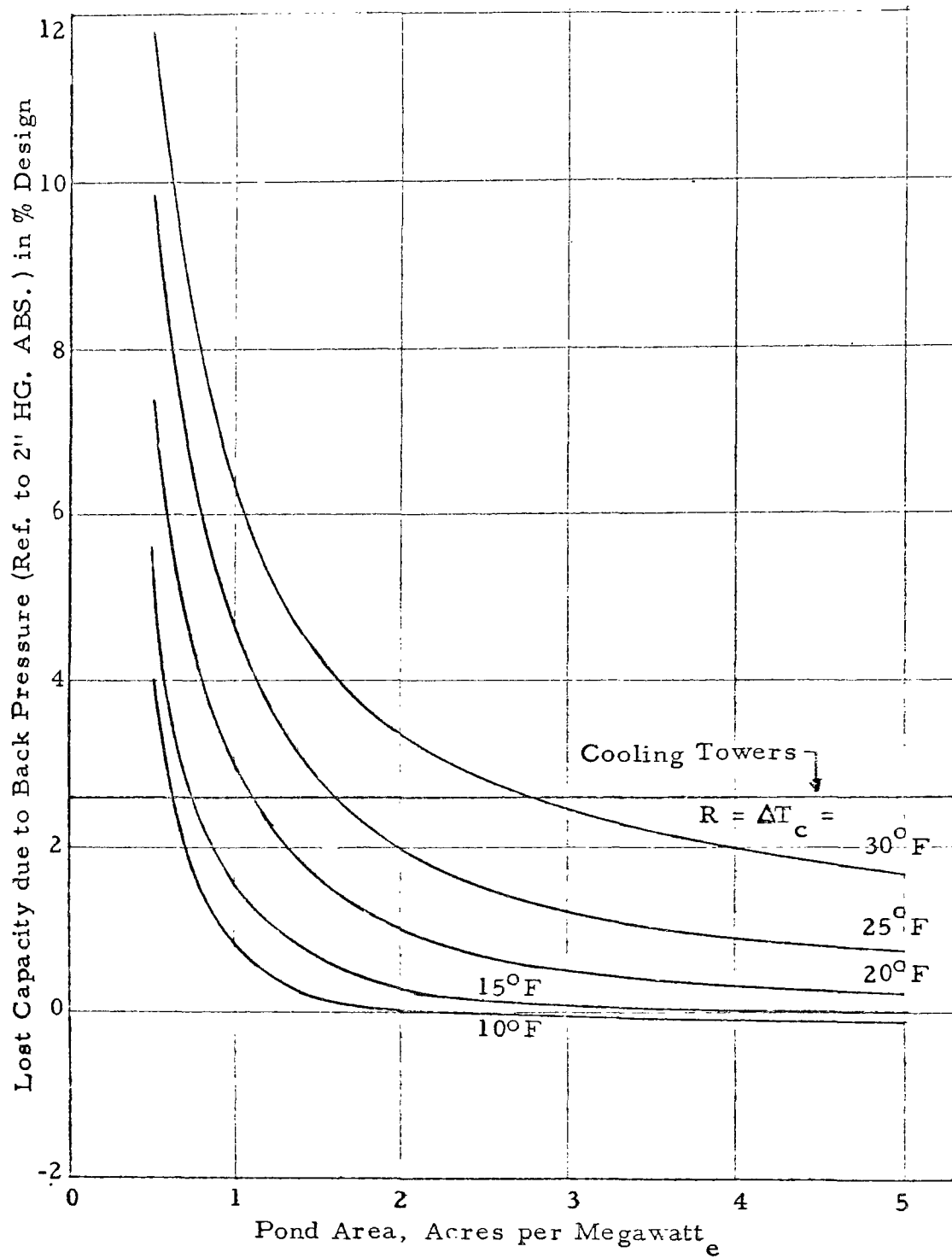
Condenser Back Pressure for a 2000 MW_e Plant near
Philadelphia, Mixed Pond Cooling, Design Climatic Conditions

Figure 24



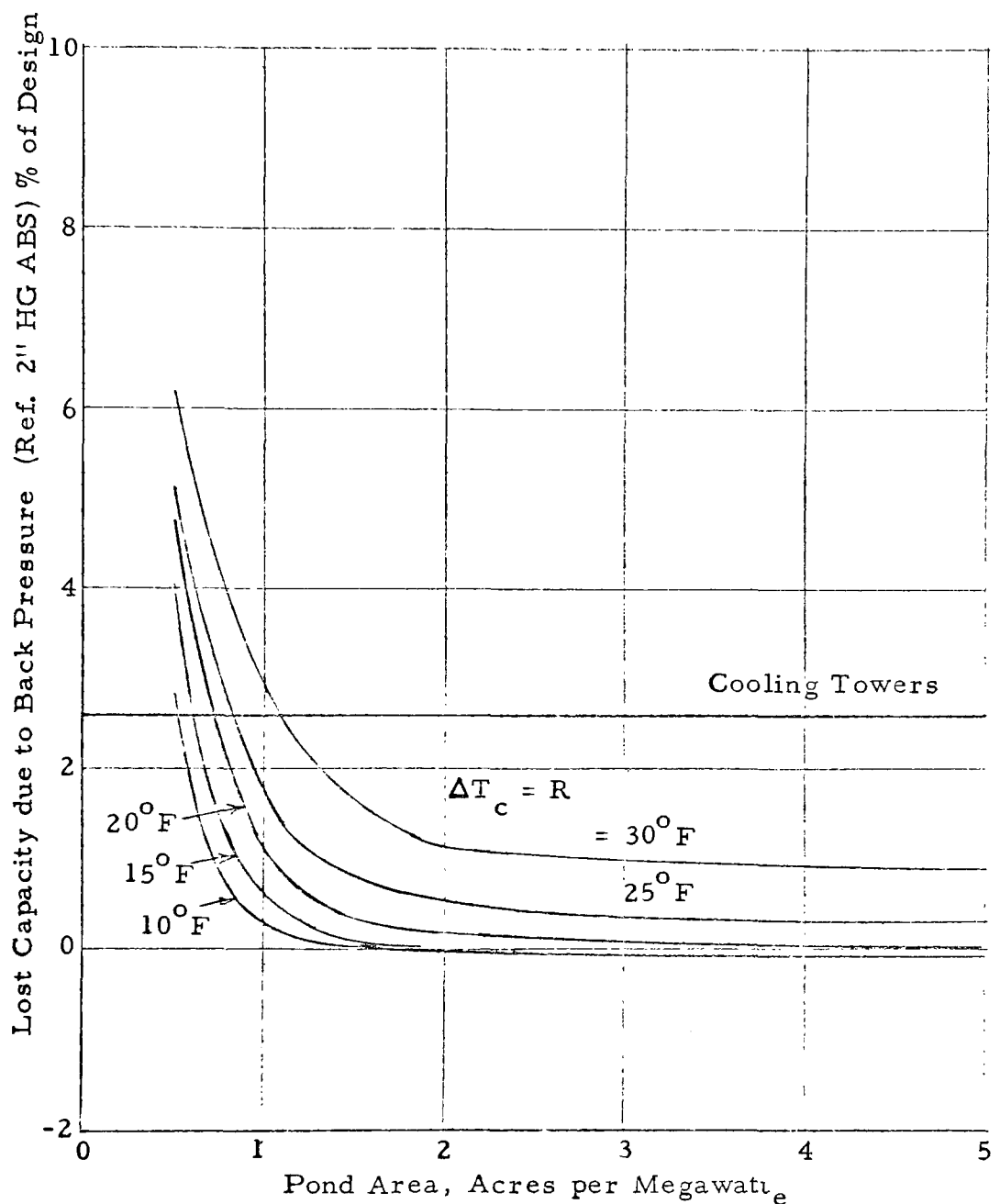
Condenser Back Pressure for a 2000 MW Electrical Plant
near Philadelphia, Slug Flow Pond, Design Climatic Con-
ditions

Figure 25



Lost Capacity due to Condenser Back Pressure, 2000 Megawatt Electric Plant near Philadelphia, Mixed Pond, Design Climatic Conditions

Figure 26



Lost Capacity due to Condenser Back Pressure,
2000 Megawatt Electric Plant near Philadelphia. Slug Flow
Pond, Design Climatic Conditions

Figure 27

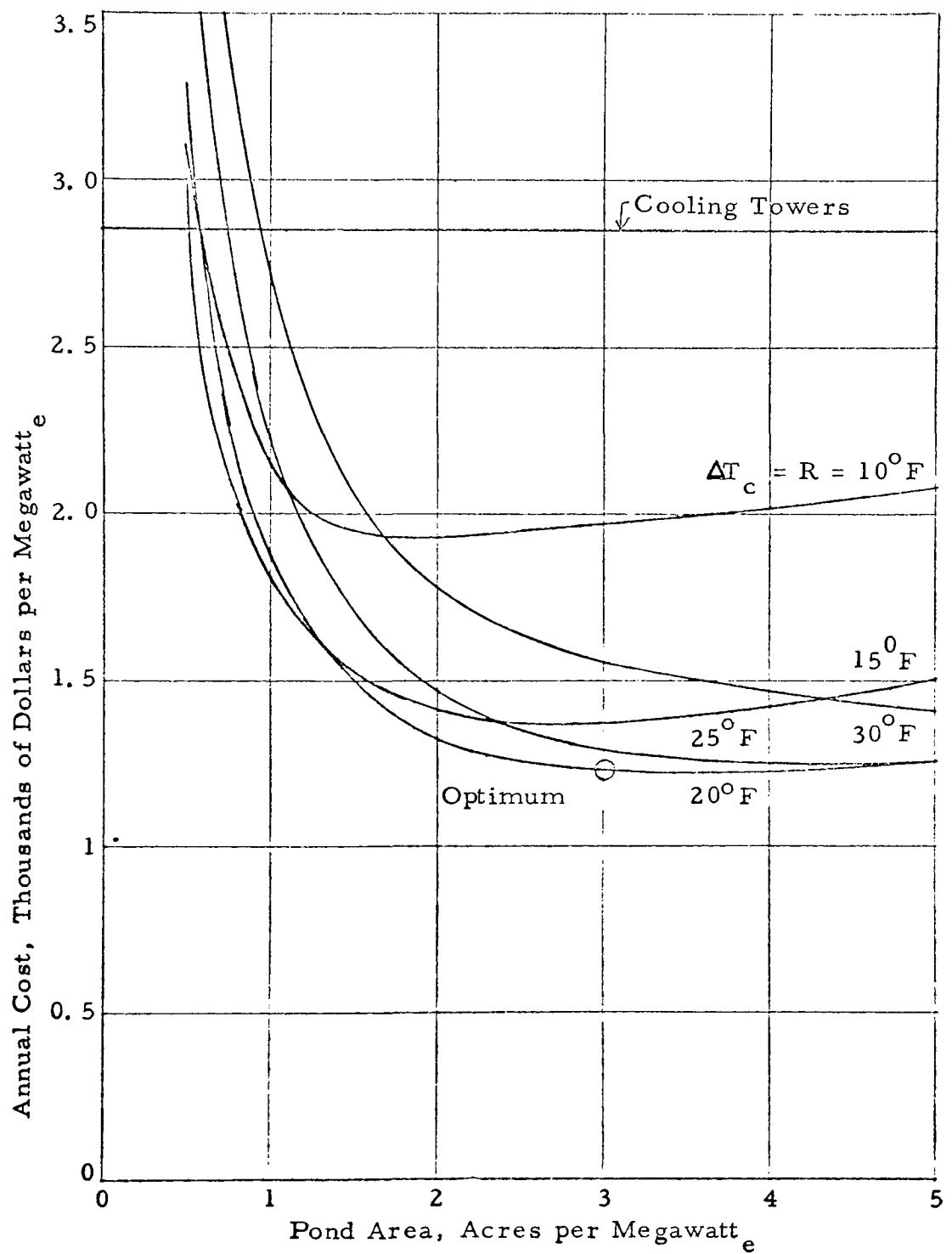
12. Replacement cost of lost power* = $(80.6 + 14.5) 10^3$ (21.00)
 = $\$2.10 \times 10^6/\text{yr}$
13. Cost of power for pumps* = 19.5×10^3 (21.00) = $\$0.409 \times 10^6/\text{yr}$
14. Maintenance = $2(1000)$ = $\$0.002 \times 10^6/\text{yr}$
- Total cost = sum of items 7, 9, 11, 13, 14 = $\$6.40 \times 10^6$

The cost of a power plant with cooling towers can be evaluated similarly except that equipment cost should be taken from Table II, and the pumping head is approximately three times higher.

The economics of cooling ponds of various sizes with five temperature rises through the condenser, and different unit pond costs, together with their comparison with the economics of cooling towers is presented in Figs. 28, 29 and 30 for mixed ponds, and Figs. 31, 32 and 33 for slug flow ponds. For the mixed ponds the optimum temperature rise through the condenser is 20°F and the pond size is approximately 3, 2 and 1.5 acres/MW_e for pond costs of \$500, \$2000 and \$5000 per acre of effective pond area, respectively. For the slug flow ponds, the optimum temperature rise through the condenser is 25°F and the pond size is approximately 2.5, 1.5 and 1 acre/MW_e for the above pond costs, respectively. The optimum for a practical cooling pond would be somewhere between those for the mixed and the flow through ponds. Figs. 28 through 33 show that the cooling pond, for reasonable land costs, is competitive with cooling towers at locations where an adequate supply of cooling water is available. At site locations where the climate is dry and cooling water is scarce, the cost of replacing evaporated cooling water should be considered.

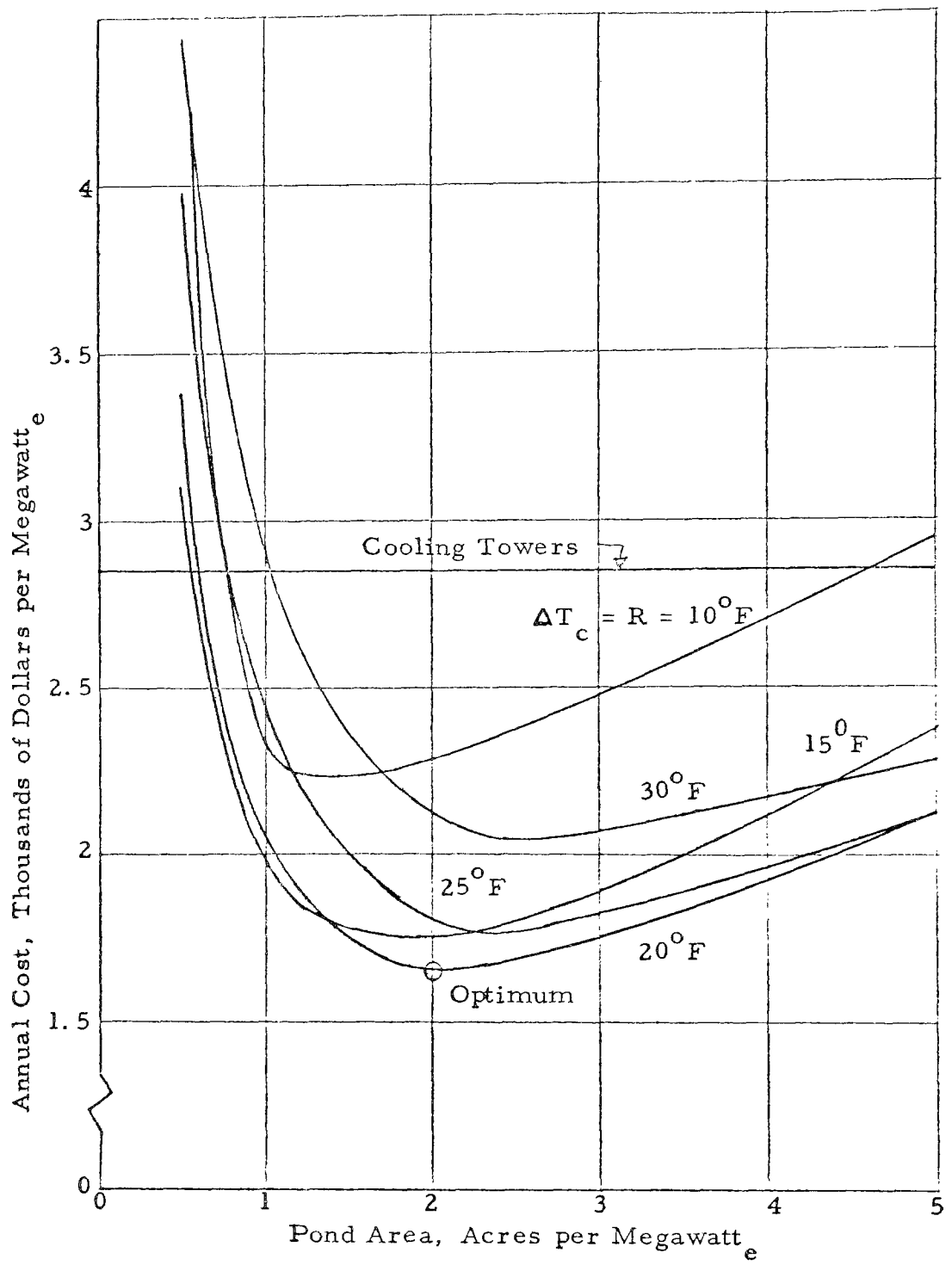
It should be noted that the values in Figs. 28 through 33 are based on annual cost for constant design conditions (that is, average summer conditions). Since the summer time imposes the most adverse conditions, the back pressure on which these figures are based is higher than what the actual back pressure will be for a considerable part of the year. As a result, the pond operating cost tends to be overestimated. However, the technique presented herein can be readily extended by considering the average climatic conditions for each of the four seasons or, if desired, by considering the average climatic conditions for each month. When the economic evaluation is extended in this manner, a family of turbines and condensers must be included in order that the optimum hardware can be selected on the basis of seasonal or monthly average climatic conditions (as well as power plant loading). Since the economics

* Based on 7000 hours of operation per year at an energy cost of \$0.003/kw-hr, or \$21.00/kw-yr.



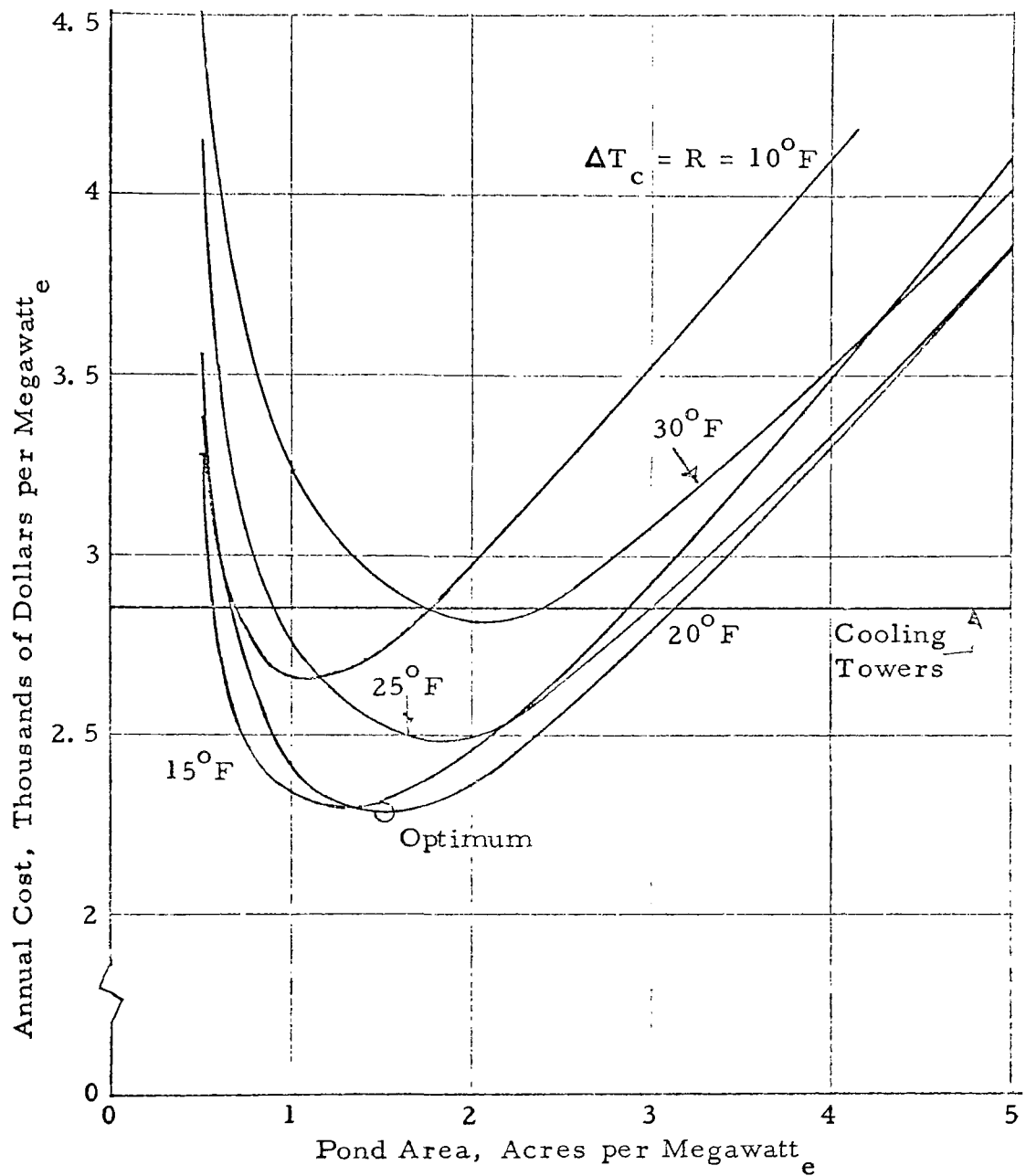
Annual Cooling Cost, Mixed Pond, 2000 MW_e Plant
 Land and Development Cost - \$500 per Acre of Pond
 Design Climatic Conditions for Philadelphia

Figure 28



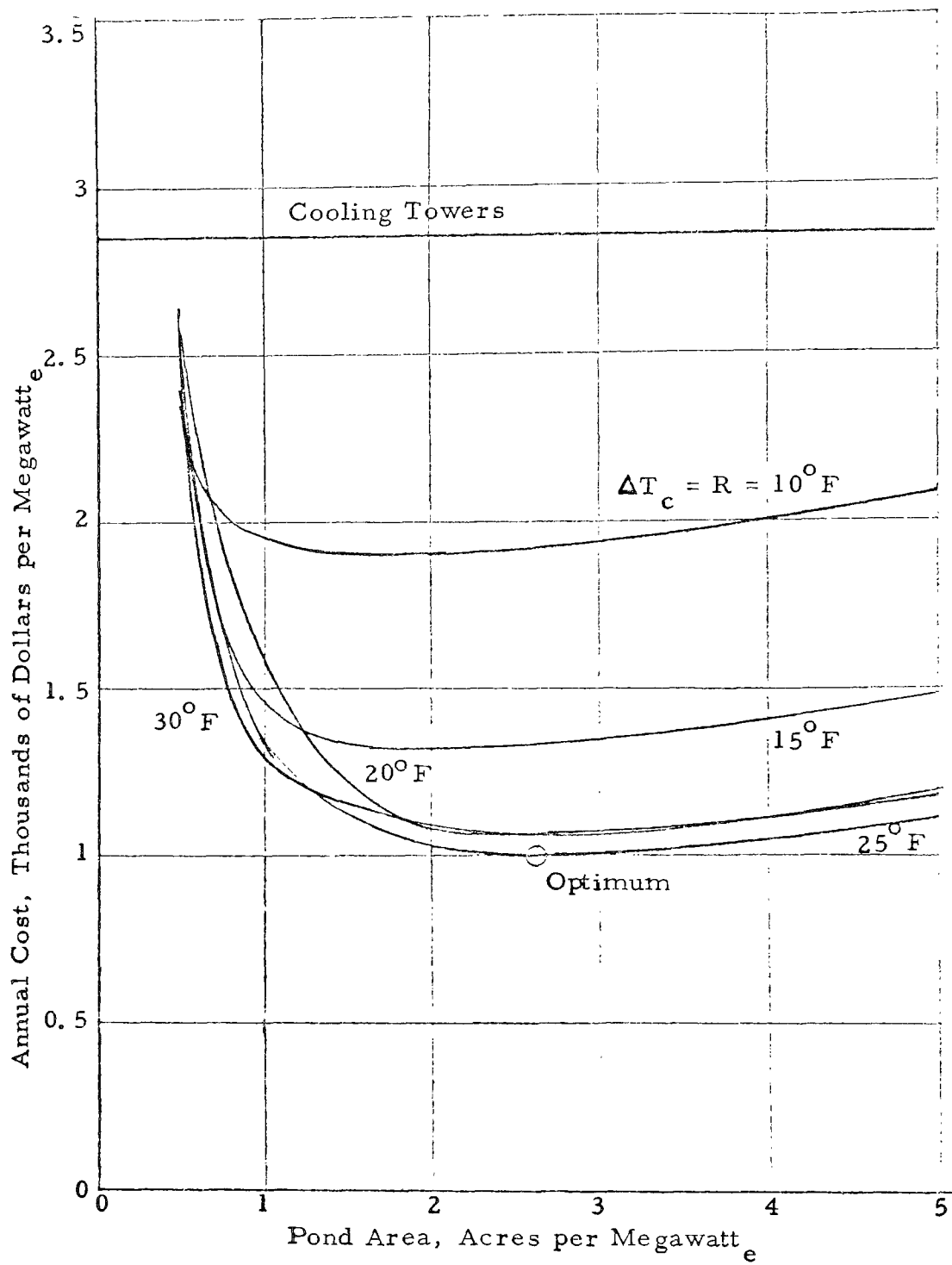
Annual Cooling Cost, Mixed Pond, 2000 MW_e Plant
 Land and Development Cost - \$2000 per Acre of Pond
 Design Climatic Conditions for Philadelphia

Figure 29



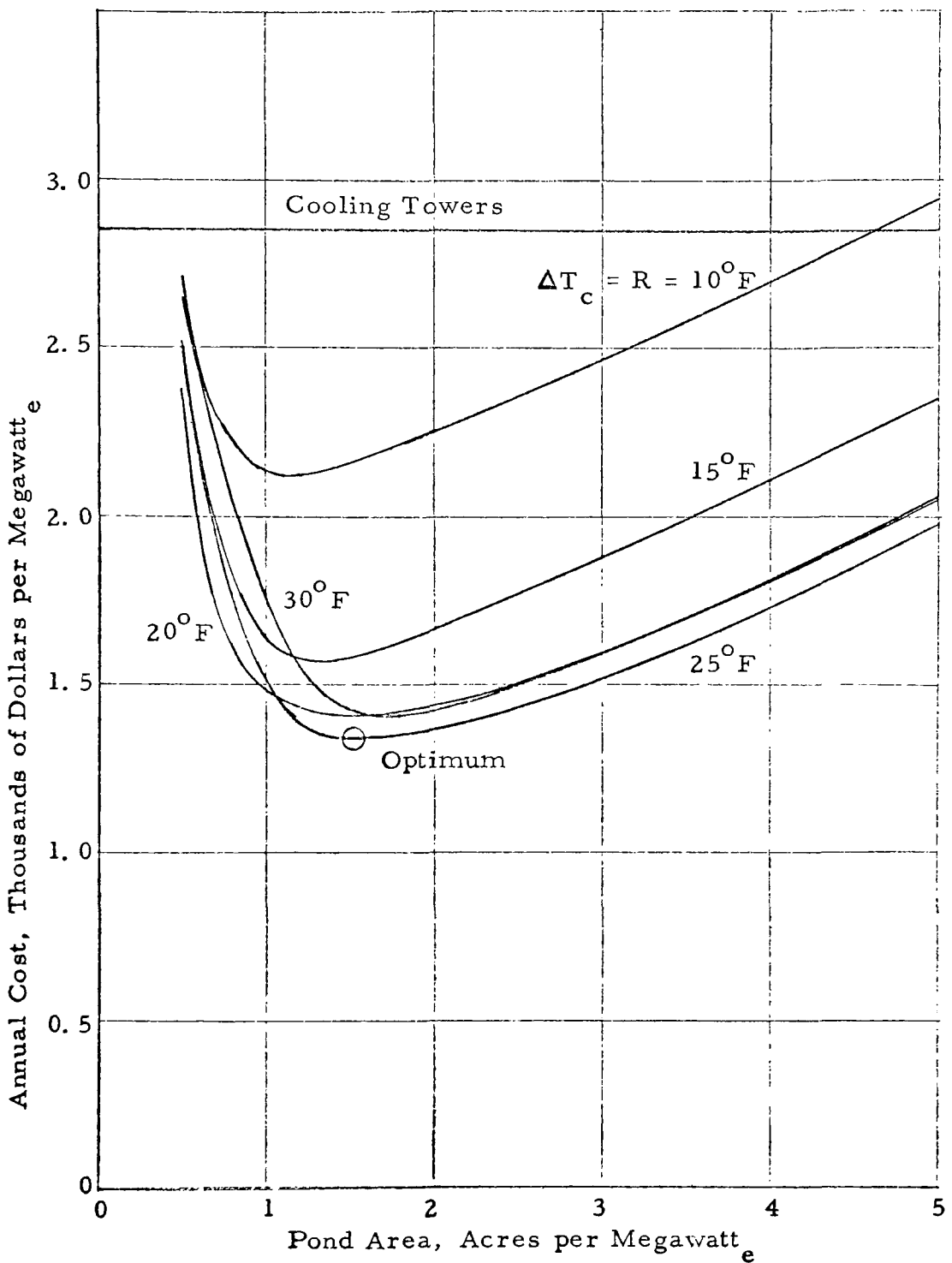
Annual Cooling Cost, Mixed Pond, 2000 MW_e Plant
 Land and Development Cost - \$5000 per Acres² of Pond
 Design Climatic Conditions for Philadelphia

Figure 30



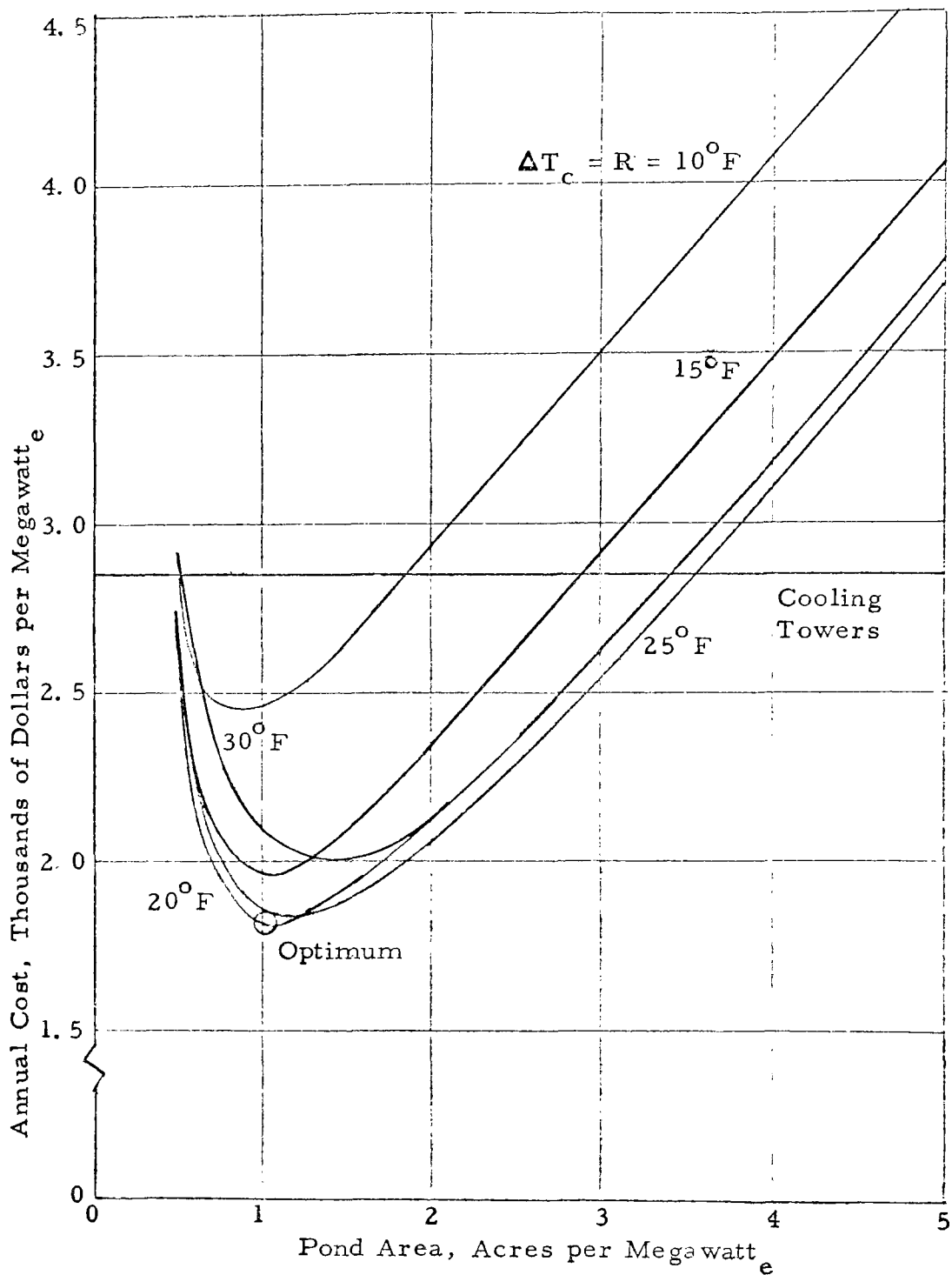
Annual Cooling Cost, Slug Flow Pond, 2000 MWe Plant
 Land and Development Cost - \$500 per acre of Pond
 Design Climatic Conditions for Philadelphia

Figure 31



Annual Cooling Cost, Slug Flow Pond, 2000 MW_e Plant
 Land and Development Cost - \$2000 per Acre
 Design Climatic Conditions for Philadelphia

Figure 32



Annual Cooling Cost, Slug Flow Pond, 2000 MW_e Plant
 Land and Development Cost - \$5000 per Acre
 Design Climatic Conditions for Philadelphia

Figure 33

of the pond are dependent on the turbine back pressure characteristics, the variation of climatic condition during the year and the variation on power plant loading during the year, the task of identifying optimum plant equipment and pond size are strongly coupled problems and are substantially site dependent.

MULTI-PURPOSE USE OF COOLING PONDS

The economic production of electric power is complicated by the fact that it cannot be stored economically in large quantities and must therefore be produced at a rate corresponding to the demand. The demand varies considerably with the time of day. However, from the viewpoint of the total cost, capital plus operating cost, it is desirable to structure an electrical power system such that the fossil or nuclear driven power plants operate at capacity in as steady a fashion as possible. When operating in this steady mode, the plants are referred to as "base-loaded" plants. One technique that has been used to allow base-loading of major size fossil (or nuclear) plants in a particular power system and still match the system's electrical power output with the peak in the customer's demand curve is to include hydroelectric plants in the system. Since energy used to drive the hydroelectric plants, namely, water at the top of an abrupt elevation change, can be "stored" to some extent and since such plants can be started and stopped quickly compared to steam plants, the hydroelectric plants can be used to provide the power to accommodate the demand peaks. Such peaking power plants are restricted to power systems that are fortunate enough to be located near feasible sites for the construction of hydroelectric plants.

A more generally applicable method for making it possible to base-load the major plants in a system is to use the surplus electric power generated by the base-loaded plants during periods of low consumer demand to pump water from a lower level to a high level. Subsequently this energy is used to generate electric power during periods of high consumer demand by allowing the pumped water to return to the low level by passing through the same hydraulic and electrical machine functioning in this case as a turbine and generator. The overall efficiency of this storage system can be of the order of 70%.

Within recent years large reversible pump-turbines are being developed for peaking power plants. These are generally of the variable pitch Kaplan type so that the same electrical equipment is used both as a motor or a generator and the same hydraulic equipment as a pump or turbine. The direction of rotation is changed for pumping or generating and a wide range of flows and corresponding power levels for the same synchronous rpm (except sign) can be handled by changing the pitch of the pump-turbine.

It is desirable to use the combination of storage ponds that are required for the pumped storage system for cooling of the condenser water. If one of the water reservoirs is a river or lake in which thermal pollution is unacceptable, the power plant can be located on the upper

reservoir which will function as a cooling pond. In this case the channel to the pump-turbine should be on the inlet side of the condenser so that cool water is interchanged with the lower reservoir, and only the upper reservoir is significantly above the ambient temperature. The location of a fossil fuel power plant on the upper level is desirable for air pollution reasons. It will be necessary to locate the hydraulic peaking power plant at the lower level because the pump cannot lift water more than a few feet without cavitating.

It will generally be desirable to have the power capacity of the hydraulic peaking power plant about the same size as that of the power plant. It will be found that at this rating the flow in the peaking power plant will be much larger than that required for the condenser cooling water and if the upper reservoir is not deep, the required storage capacity will provide adequate surface area for cooling. In this case there is no additional cost for the cooling pond.

At the end of a long power demand it might be anticipated that the level of the upper reservoir will be down so that there will be a reduced surface area for cooling the condenser water. However, since the flow rates of the cooling water is only a small percentage of that of the storage water*, the water for the turbines will be primarily the cooler subsurface water and the warmed condenser water will not reach the turbine intake. Even when operating at a small percentage of rated capacity as a pump, the hydraulic unit will deliver cool water to the condenser.

The water lost by evaporation, as shown earlier, is only slightly greater than that lost by natural evaporation, and so a significant saving in water is attained when the cooling pond is combined with the pumped storage project.

* The water required by the condensers = $0.0152 [KW \times (1 - \eta_t) / \eta_t \Delta T]$ cfs where η_t = plant thermal efficiency (neglecting stack losses) The water flowing in the pumped storage system = $11.8 [KW \eta_p / \Delta h]$ cfs, as a pump where η_p = efficiency of pump plus motor plus duct; Δh = ft difference in head between reservoirs and = $11.8 KW / (\Delta h \eta_g)$ cfs, as a generator.

ACKNOWLEDGEMENTS

The authors wish to acknowledge the advice and helpful information provided by Mr. Walter Shade and the technical staff of Gilbert Associates, Reading, Pennsylvania.

The cooperation of the following electric power companies which utilized captive ponds for condenser water cooling is appreciated. These companies provided month by month information regarding thermal loading and water temperature in their cooling ponds:

Southwestern Electric Power Company
Commonwealth Edison Company
Arizona Public Service Company
Virginia Electric and Power Company
Mississippi Power and Light Company
Texas Power and Light Company
South Carolina Public Service Authority

REFERENCES

1. Cummings, N. W. and Richardson, B., Evaporation from Lakes, Physical Review, Vol. 30, October 1927
2. Lima, D. O., Pond Cooling by Surface Evaporation, Power, March, 1936
3. Throne, R. F., How to Predict Lake Cooling Action, Power, Sept., 1951
4. Longhaar, J. W., Cooling Pond May Answer Your Water Cooling Problem, Chemical Engineering, August 1953
5. Le Bosquet, M., Cooling-Water Benefits from Increased River Flows, Journal of New England Water Works Association, 60, 2, June 1946
6. Anderson, E. R., Energy Budget Studies in Water-Loss Investigations, Volume I - Lake Hefner Studies, Technical Report, U. S. Geological Survey Circ. 229, Washington, D. C., 1952 (See also Ref. 19)
7. Velz, C. J. and Gannon, J. J., Forecasting Heat Loss in Ponds and Streams, Journal W. P. C. F., Vol. 32, No. 4, April 1960
8. Messinger, H., Dissipation of Heat from a Thermally Loaded Stream, U. S. Geological Survey Professional Paper 475-C (Article 104), Washington, D. C. 1963
9. Edinger, J. E. and Geyer, J. C., Heat Exchange in the Environment, Edison Electric Institute Project No. 49, Edison Electric Institute, New York, N. Y., June 1965
10. Geyer, J. C., Edinger, J. E., Graves, W. L. and Brady, D. K., Field Sites and Survey Methods, Report No. 3 - Edison Electric Institute Research Project No. 49, Edison Electric Institute, New York, N. Y., June 1968
11. Page, L., Introduction to Theoretical Physics, D. Van Nostrand Co., New York, N. Y., 1945
12. Climatic Atlas of the United States, U. S. Dept. of Commerce, Environmental Science Services Admin., Washington, D. C., June 1968

13. ASHRAE - Handbook of Fundamentals, American Society of Heating, Refrigeration and Air Conditioning Engineers, New York, N. Y., 1967, pp. 470-474
14. Hutchinson, G. D., A Treatise on Limnology, John Wiley and Sons, Inc., New York, N. Y., 1957, pg. 377
15. Koberg, G. E., Methods to Compute Long Wave Radiation from the Atmosphere and Reflected Solar Radiation from a Water Surface, U. S. Geological Survey Professional Paper, Washington, D. C., 1962
16. Sverdrup, H. U., On the Evaporation from the Oceans, Journal of Marine Research, 1937-38.
17. Local Climatological Data for Philadelphia, Pennsylvania - 1968, U. S. Dept. of Commerce, Environmental Science Service Admin., Asheville, North Carolina
18. Local Climatological Data for Winslow, Arizona - 1967, U. S. Dept. of Commerce, Environmental Science Service Admin., Asheville, North Carolina
19. Marciano, J. J. and Harbeck, G. E., Mass Transfer Studies in Water-Loss Investigation: Lake Hefner Studies, U. S. Geological Survey Professional Paper 269, Washington, D. C., 1954
(This material previously published as U. S. Navy Electronics Lab. Report No. 327 and U. S. Geological Survey Circ. No. 229, 1952)
20. Koberg, G. E., Harbeck, G. E. and Hughes, The Effect of the Addition of Heat from a Power Plant on the Thermal Structure and Evaporation of Lake Colorado City, Texas, U. S. Geological Survey, Professional Paper No. 272-B, 1959
21. Linsley, R. K., Kohler, M. A. and Paulhus, J. L., Hydrology for Engineers, McGraw Hill Book Co., New York, N. Y., 1958, pg 98, Also see Ref. 7.
22. Bowen, I. S., The Ratio of Heat Losses by Conduction and by Evaporation from any Water Surface., Physical Review, Vol. 27, June 1926

23. Sunderam, T. R., Easterbrook, C. C., Prech, K. R. and Rudinger, G., An Investigation of the Physical Effects of Thermal Discharges into Cayuga Lake, Cornell Aeronautical Lab., No. VT-2616-0-2, Buffalo, N. Y., November 1969
24. Beer, L. P. and Piper, W. O., Environmental Effects of Condenser Water Discharge in Southwest Lake Michigan, Waukegan Study on Lake Michigan, Commonwealth Edison Co., Chicago, Ill.
25. Steam-Electric Plant Construction Cost and Annual Production Expenses - Twentieth Annual Supplement, Federal Power Commission, Washington, D. C. 1968
26. Chemical Engineers' Handbook, Edited by John H. Perry, McGraw Hill Book Co., New York, N. Y., 1963, pp. 14-20, 21
27. Holman, J. P., Heat Transfer, McGraw Hill Book Co., New York, N. Y., 1963, pg. 383
28. Private Communication from Walter Shade, Gilbert Associates, Inc., Reading, Pennsylvania.
29. Skrotzki, B. G. A. and Vopat, W. A., Power Station Engineering and Economy, McGraw Hill Book Co., New York, N. Y., 1960
30. Standard Handbook for Mechanical Engineers, Seventh Edition, Edited by T. Baumeister, McGraw Hill Book Co., New York, N. Y., 1967
31. Winiarski, L. D., Tichenor, B. A. and Bryan, K. V., A Method for Predicting the Performance of Natural Draft Cooling Towers, U. S. Dept. of Interior, FWPCA - Pacific Northwest Water Lab., Corvallis, Oregon, January 1970
32. Leung, P. and Moore, R. E., Water Consumption Determination for Steam Power Plant Cooling Towers: A Heat-and-Mass Balance Method, Presented at the Winter Annual Meeting of ASME, Los Angeles, Calif., November 1969

NOMENCLATURE

a	a constant coefficient
A	pond surface area
c	specific heat of water
c_B	Brunt's Coefficient
c_f	friction coefficient
c_p	specific heat of air at constant pressure
c_1	constant in Wien's Law
C	concentration of water vapor per unit volume
D	diffusion coefficient
f_1	a term in the energy balance equation defined as $[Q_N - a_5 - (a_{12} + a_{13}W)(a_1 - \theta_a a_{14} - P_a)]$
f_2	a parameter used to plot the steady state behavior of a slug flow pond (in which case $f_2 = A(\Delta T_c)/WTE$, or to plot the transient behavior of a mixed or slug flow pond (in which case $f_2 = t/\rho c(V/A)$.
f_3	a parameter used to plot the water lost from a slug flow pond by evaporation
g	acceleration of gravity
h_e	specific enthalpy of water as it leaves the pond by evaporation (with respect to the reference point $h_e = 0$ at 32°F)
h_D	mass transfer coefficient
h_p	specific enthalpy of precipitation (with respect to the reference point $h_p = 0$ at 32°F)
Δh	change in the specific enthalpy of water between the liquid state at the make-up temperature and the vapor state at the pond surface temperature
Δh_T	change in the specific enthalpy of water between the liquid state and vapor state at constant temperature
H. R.	annual average power plant heat rate
ℓ_1	pond width at $x=0$
ℓ_2	pond length at $y=0$

ℓ_3	pond depth at a given location
\dot{m}	mass flow rate per unit surface area
\dot{m}_c	mass flow rate through the condenser
\dot{m}_e	mass flow rate per unit surface area out of pond due to evaporation
\dot{m}_{mu}	mass flow rate per unit surface area into pond in the form of make-up water
\dot{m}_p	mass flow rate per unit surface area into pond in the form of precipitation
\dot{m}_s	mass flow rate per unit surface area out of pond due to seepage
M_a	molecular weight of air
M_w	molecular weight of water
\dot{M}	mass flow rate
\dot{M}_{mu}	mass flow rate into pond in the form of make-up water
\dot{M}_{pp_i}	mass flow rate into pond from condenser
\dot{M}_{pp_o}	mass flow rate out of pond to condenser
MW_e	net electrical power produced by the plant in megawatts
N_n	empirical coefficient used to relate evaporation rate to the wind speed and relative humidity
P_a	water vapor pressure in the atmosphere
\dot{P}_{BAR}	barometric pressure
P_w	saturated water vapor pressure corresponding to the temperature of the water at the pond surface
Q_a	atmospheric radiation incident on pond
Q_{ar}	atmospheric radiation reflected from pond
Q_{br}	back radiation emitted from pond surface
Q_c	energy flow rate per unit surface area
Q_N	net absorbed radiation
Q_s	solar radiation incident on pond
Q_{sr}	solar radiation reflected from pond

R_{ey}	Reynolds Number
R_{sr}	ratio of reflected to incident solar radiation
R_u	universal gas constant
S_c	Schmidt Number
t	time
t_r	residence time of water in the pond
T	temperature
T_{aa}	absolute air temperature
T_{wa}	absolute water temperature
ΔT_c	temperature rise through the condenser
u	fluid velocity
V	pond volume
w	humidity ratio
W	wind speed
W_C	wind speed in Colorado City Equation
W_H	wind speed in Lake Hefner Equation
W_M	wind speed in Meyer Equation or mean speed for one month
WTE	waste thermal energy from a power plant
x	a coordinate distance
y	a coordinate distance
z	pond depth
α	thermal diffusivity
β	linear temperature profile gradient
ϵ	emissivity
ϵ_w	emissivity of water
θ	temperature measured with respect to 32° F ($\theta = T - 32^{\circ}\text{F}$)
θ_{eq}	equilibrium pond temperature measured from 32° F ($\theta_{eq} = T_{eq} - 32^{\circ}\text{F}$)
θ_{pi}	temperature of direct precipitation measured from 32° F ($\theta_{pi} = T_{pi} - 32^{\circ}\text{F}$)

θ_{pp_i}	temperature of water leaving the condenser measured from 32°F ($\theta_{pp_i} = T_{pp_i} - 32^{\circ}\text{F}$)
θ_{pp_o}	temperature of water entering the condenser measured from 32°F ($\theta_{pp_o} = T_{pp_o} - 32^{\circ}\text{F}$)
θ_s	water surface temperature measured from 32°F ($\theta_s = T_s - 32^{\circ}\text{F}$)
θ_{ss}	steady state mixed pond water temperature measured from 32°F ($\theta_{ss} = T_{ss} - 32^{\circ}\text{F}$)
λ	pond width
λ_m	wavelength
ν	kinematic viscosity
ρ	density
$\rho_{\text{B. L.}}$	density of boundary layer material
σ	Stefan-Boltzmann constant

APPENDIX A
ENERGY BALANCE EQUATIONS

Completely mixed pond, no vertical temperature gradient

In the case of the completely mixed pond, it is assumed that the inlet-outlet structure, the wind, turbulence, and vertical currents resulting from cooling at the surface and subsequent sinking of the denser fluid result in complete vertical mixing so that no temperature difference exists between the water at the top and at the bottom of the pond.

Water is lost from the pond by evaporation to the atmosphere and by seepage into the surrounding ground. Water is added to the pond by precipitation on the pond surface, by precipitation run-off that flows directly into the pond and by the addition of make-up water which may be obtained from a stream, a storage reservoir or wells. For the purpose of analysis, it is assumed that the flow of make-up water into the pond is continuously adjusted so that the volume of water in the pond remains constant. To check the reasonableness of this assumption, it is helpful to note that based on two acres of pond surface per megawatt of electricity, a 35% thermal efficiency and 2/3 of the cooling to result from evaporation, the pond volume decreases by only 0.2 inches per day due to the extra thermal load in the absence of seepage. On the average, for an annual rainfall of 36", direct precipitation would add 0.1 inches per day of water to the pond.

The mass balance for the entire pond is given by the expression:

$$[\dot{M}_{mu} + \dot{M}_{pp_i} + \dot{m}_p] - [\dot{M}_{pp_o} + \dot{m}_s + \dot{m}_e] = \frac{\partial}{\partial t} (\rho V) = 0 \quad (\text{Eq. A-1})$$

where

\dot{M}_{mu} = flow of makeup and inflow water into the pond, #m/day

\dot{M}_{pp_i} = flow of water from the power plant condenser into the pond, #m/day

\dot{m}_p = precipitation flux falling directly on the pond surface, #m/day ft²

\dot{M}_{pp_o} = flow of water from the pond to the power plant condenser, #m/day

\dot{m}_s = flux of water from the pond through outflow and to the ground by seepage, #m/day ft²

\dot{m}_e = flux of water from the pond to the atmosphere by evaporation, #m/day ft²

$$A = \text{pond surface, ft}^2$$

$$\rho = \text{density of water, lbm/ft}^3$$

$$V = \text{volume of pond water, ft}^3$$

The energy balance for the entire pond can be expressed as: (See Fig. 1)

$$\begin{aligned} & \{\dot{M}_{mu} c\theta_{mu} + \dot{M}_{pp_i} c\theta_{pp_i} + A\dot{m}_p h_p + A[(\dot{Q}_s - \dot{Q}_{sr}) + (\dot{Q}_a - \dot{Q}_{ar})]\} \\ & - \{\dot{M}_{pp_o} c\theta + A\dot{m}_s c\theta + A[\dot{Q}_{br} + h_e \dot{m}_e + \dot{Q}_c]\} \\ & = \frac{\partial}{\partial t} \iiint \rho c \theta \, dv \end{aligned} \quad (\text{Eq. A-2})$$

- where c = specific heat of water at constant pressure,
 $1.0 \text{ btu/lbm}^\circ\text{F}$
- θ = pond temperature in excess of $32^\circ\text{F} = T - 32^\circ\text{F}$, $^\circ\text{F}$
- \dot{Q}_s = solar radiation incident on pond surface, btu/day ft^2
- \dot{Q}_{sr} = solar radiation reflected from pond surface, btu/day ft^2
- \dot{Q}_a = atmospheric radiation incident on pond surface,
 btu/day ft^2
- \dot{Q}_{ar} = atmospheric radiation reflected from pond surface,
 btu/day ft^2
- \dot{Q}_{br} = energy radiated from pond surface, btu/day ft^2
- \dot{m}_e = mass flux from the pond to the atmosphere by evaporation, lbm/day ft^2
- h_e = enthalpy of evaporated water, btu/lbm (Ref. 32°F . fluid)
- \dot{Q}_c = energy transfer from the pond to the atmosphere by convection, btu/day ft^2
- h_p = enthalpy of precipitation (Ref. 32°F , fluid)
- \dot{m}_p = $c\theta_{pi}$, $\text{btu/lbm}^\circ\text{F}$, if $T > 32^\circ\text{F}$
 P_i $= +0.492(\theta) - 143.3$, $\text{btu/lbm}^\circ\text{F}$, if $T < 32^\circ\text{F}$
 P_1

Since the temperature is everywhere equal in the pond at a given instant, the right hand side of Eq. A-2 may be expressed as:

$$\frac{\partial}{\partial t} \iiint \rho c \theta \, dv = \frac{\partial}{\partial t} (\rho c \theta V) = c \theta \frac{\partial}{\partial t} (\rho V) + c (\rho V) \frac{\partial \theta}{\partial t} \quad (\text{Eq. A-3})$$

However, the first term on the right hand side of the last equation is

zero as a result of the assumption applied in Eq. A-1, thus the last equation becomes:

$$\frac{\partial}{\partial t} \iiint \rho c \theta \, dv = c(\rho V) \frac{\partial \theta}{\partial t} \quad (\text{Eq. 2-4})$$

The first term in Eq. A-2 represents the energy introduced into the pond by the addition of make-up water and can be expressed with the aid of Eq. A-1, as:

$$\dot{M}_{mu} c \theta_{mu} = A(\dot{m}_s + \dot{m}_e - \dot{m}_p) c \theta_{mu}$$

where $\dot{m}_{pp_i} - \dot{m}_{pp_o} = 0$, since there is no loss of cooling water in the condenser.

Thus,

$$\dot{M}_{mu} c \theta_{mu} = A(\dot{m}_s - \dot{m}_p) c \theta_{mu} + A(\dot{m}_e h_{mu}) \quad (\text{Eq. A-5})$$

where $h_{mu} = c \theta_{mu}$ = enthalpy of the water added as make-up

Substituting Eq. A-4 and Eq. A-5 into Eq. A-2, the energy equation becomes:

$$\begin{aligned} & \{A[\dot{m}_s - \dot{m}_p] c \theta_{mu} + \dot{M}_{pp_i} c \theta_{pp_i} + A \dot{m}_p h_p + A[(\dot{Q}_s - \dot{Q}_{sr}) + (\dot{Q}_a - \dot{Q}_{ar})]\} \\ & - \{\dot{M}_{pp_o} c \theta + A \dot{m}_s c \theta + A(\dot{Q}_{br}) + A[\dot{m}_e (h_e - h_{mu}) + \dot{Q}_c]\} = c(\rho V) \frac{\partial \theta}{\partial t} \end{aligned} \quad (\text{Eq. A-6})$$

It is now helpful to express the terms in Eq. A-6 as polynomials of θ and then collect all terms of equal order.

Term I represents the energy introduced into the pond by the addition of water to compensate for seepage and precipitation and is not a function of the pond temperature.

Terms III and IV do not depend on the pond temperature, θ , and may be left as they are.

Terms II and V may be combined and expressed as:

$$\dot{M}_{pp_i} c \theta_i - \dot{M}_{pp_o} c \theta = \text{waste thermal energy} = \text{WTE, btu/day} \quad (\text{Eq. A-7})$$

Term VI is already expressed as a function of the pond temperature to

the first power.

Term VII represents the energy radiated from the pond surface, and since water radiates as almost a black body, this term may be expressed as:

$$\dot{Q}_{br} = A \epsilon_w \sigma (\theta + 32 + 460)^4 \quad (\text{Eq. A-8})$$

where ϵ_w = emissivity of water = .97

σ = Stefan-Boltzman constant 4.15×10^{-3} btu/day ft² (°R⁴)

Eq. A-8 can be expanded in binomial form to give the expression:

$$\dot{Q}_{br} = A \epsilon_w \sigma (492)^4 [1 + 4(\frac{\theta}{492}) + 6(\frac{\theta}{492})^2 + 4(\frac{\theta}{492})^3 + (\frac{\theta}{492})^4] \quad (\text{Eq. A-9})$$

At the cost of introducing an error of less than 7/10 of one percent for pond temperature up to 100°F, the last term on the right hand side of Eq. A-9 may be neglected. Thus Term VII may be expressed as:

$$Q_{br} = A \{a_5 + a_6 \theta + a_7 \theta^2 + a_8 \theta^3\} \text{ btu/day} \quad (\text{Eq. A-10})$$

where $a_5 = 2358.74$ btu/day ft²

$a_6 = 19.176$ btu/day ft² (°F)

$a_7 = 5.850 \times 10^{-2}$ btu/day ft² (°F)²

$a_8 = 7.923 \times 10^{-5}$ btu/day ft² (°F)³

Term VIII represents the heat transfer to the atmosphere as a result of evaporation and convection, and may be expressed as:

$$A \{[\dot{m}_e (h_e - h_{mu}) + \dot{Q}_c]\} = A \{\dot{m}_e (\Delta h) + \dot{Q}_c\} \quad (\text{Eq. A-11})$$

where $\dot{m}_e \Delta h$ = net energy transfer that results from water evaporating from the pond and being replenished. The value of Δh depends on the temperature of the evaporating water and make-up water. Since the make-up water temperature can vary from 32°F to about 90°F, and the maximum pond temperature will be about 25°F above the make-up water, Δh could vary from 1085.7 to 1053.6. Thus within an error of $\pm 1.5\%$, the value of Δh may be taken as a constant equal to 1070 btu/#m.

In Appendix B it is shown (Eq. B-39) that Eq. A-11 can be expressed in the form of a polynomial in θ , namely,

$$A\{\dot{m}_e \Delta h + Q_c\} = A\{(a_{12} + a_{13}W)(a_1 - \theta_a a_{14} - P_a) + (a_{12} + a_{13}W)(a_2 + a_{14})\theta \\ + (a_{12} + a_{13}W)(a_3)\theta^2 + (a_{12} + a_{13}W)(a_4)\theta^3\} \quad (\text{Eq. A-12})$$

(See Appendix B for values of coefficients)

where P_a = water vapor pressure in atmospheric air, psia

θ_a = air temperature referenced to 32°F ($\theta_a = T_a - 32^\circ\text{F}$)

Substituting Eqs. A-7, A-10 and A-12 into the energy balance equation, A-6, yields:

$$c\rho\left(\frac{V}{A}\right)\frac{d\theta}{dt} = \{\dot{m}_p(h_p - c\theta_{mu}) - \dot{m}_s(c\theta - c\theta_{mu})\} \\ + \{\dot{Q}_{pp} + [\dot{Q}_N - a_5 - (a_{12} + a_{13}W)(a_1 - a_{14}\theta_a - P_a)]\} \\ - \{a_6 + (a_{12} + a_{13}W)(a_2 + a_{14})\}\theta \\ - \{a_7 + (a_{12} + a_{13}W)(a_3)\}\theta^2 \\ - \{a_8 + (a_{12} + a_{13}W)(a_4)\}\theta^3 \quad (\text{Eq. A-13})$$

where \dot{Q}_{pp} = WTE/A, btu/ ft^2 day

$\dot{Q}_N = [(\dot{Q}_s - \dot{Q}_{sr}) + (\dot{Q}_a - \dot{Q}_{ar})]$

If in addition to the previous assumptions it is assumed that the enthalpy of the precipitation and seepage are equal to the enthalpy of the water in the pond, then the first terms on the right hand side of the above equation will go to zero, namely:

$$\{\dot{m}_p(h_p - c\theta_{mu}) - \dot{m}_s(c\theta - c\theta_{mu})\} = 0 \quad (\text{Eq. A-14})$$

Completely mixed pond, simplified case, steady state operation

The general energy balance equation can be simplified considerably if Eq. A-14 is assumed to be valid and if the ratio of volume to area of the pond is assumed to be very small (or if the time over which weather

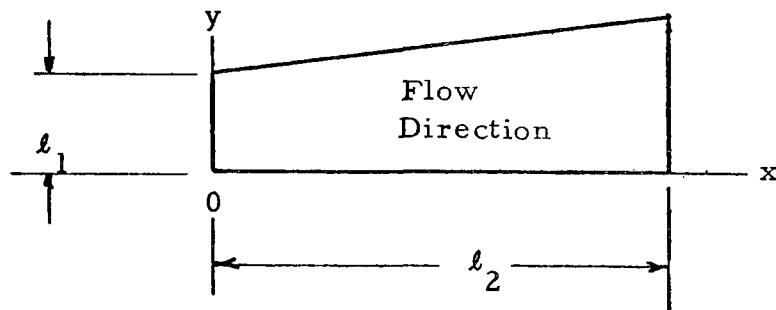
conditions are averaged is long compared to the residence time in the pond). These assumptions lead to the steady state energy equation:

$$0 = \{\dot{Q}_{pp} + [\dot{Q}_N - a_5 - (a_{12} + a_{13}W)(a_1 - a_{14}\theta_a - P_a)]\} \\ - \{a_6 + (a_{12} + a_{13}W)(a_2 + a_{14})\} \theta \\ - \{a_7 + (a_{12} + a_{13}W)(a_3)\} \theta^2 \\ - \{a_8 + (a_{12} + a_{13}W)(a_4)\} \theta^3 \quad (\text{Eq. A-15})$$

Slug flow pond, no vertical temperature gradients

For this situation it is helpful to look not at the entire pond as was done for the mixed pond, but at a differential control volume which moves at the constant velocity, u , imposed by the plant pumping rate at any given time. Water is lost from the control volume by evaporation to the atmosphere and by seepage into the surrounding ground. Water is added to the control volume by precipitation directly on the exposed surface and by precipitation run-off that flows into the control volume and by additional make-up water which may be obtained from a storage reservoir, a stream or wells. Again as in the case of the mixed pond, it is convenient for the purpose of analysis to assume that the flow of make-up water into the control volume takes place continuously at such a rate that the volume of water in the control volume remains constant.

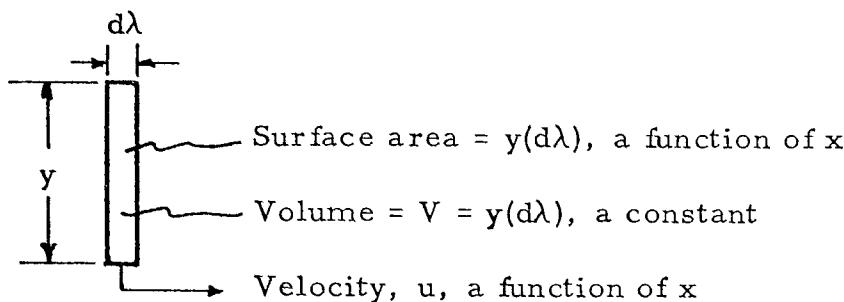
The mass and energy balance for the moving control volume can be developed in a way similar to that used for the completely mixed pond. However, in this case we must make allowances for variable temperature rise across the condenser, variable pond depth and variable pond width. The pond geometry is sketched below along with the control volume.



z = depth at any x dimension

ℓ_2 = length at $y=0$

ℓ_1 = length at $x=0$



The mass balance for the moving control volume is:

$$y(d\lambda)[\dot{m}_{mu} + \dot{m}_p] - y(d\lambda)[\dot{m}_s + \dot{m}_e] = \frac{\partial}{\partial t}[\rho y_z)(d\lambda)] = 0 \quad (\text{Eq. A16})$$

where \dot{m}_{mu} = flux of make-up water into control volume, #m/ ft^2 day

Eq. A-16 can be solved for the rate of flow of make-up water required to maintain a constant water volume in the pond and yields:

$$\dot{m}_{mu} = \dot{m}_s + \dot{m}_e - \dot{m}_p \quad (\text{Eq. A-17})$$

The energy balance for the control volume is:

$$y(d\lambda)\{\dot{m}_{mu}c\theta_{mu} + \dot{m}_p c\theta_p + [(\dot{Q}_s - \dot{Q}_{sr}) + (\dot{Q}_a - \dot{Q}_{ar})]\} - y(d\lambda)\{\dot{m}_s c\theta + \dot{Q}_{br} + \dot{m}_e h_e + \dot{Q}_c\} = \frac{\partial}{\partial t}[c\theta\rho zy d\theta] \quad (\text{Eq. A-18})$$

However, the right hand side of Eq. A-18 can be expressed as:

$$\frac{\partial}{\partial t}[c\theta\rho zy d\lambda] = \rho c(yz d\lambda) \frac{\partial\theta}{\partial t} \quad (\text{Eq. A-19})$$

since $\frac{\partial}{\partial t}(yz d\lambda) = 0$ from Eq. A-16.

Thus, by substituting Eq. A-19 and A-17 into A-18, the energy equation can be expressed as:

$$\begin{aligned}
 & \text{I} \quad \text{III} \quad \text{IV} \\
 \{(\dot{m}_s - \dot{m}_p) c\theta_{mu} + \dot{m}_p c\theta_p + [(\dot{Q}_s - \dot{Q}_{sr}) + (\dot{Q}_a - \dot{Q}_{ar})]\} \\
 & \text{VI} \quad \text{VII} \quad \text{VIII} \\
 - \{\dot{m}_s c\theta + \dot{Q}_{br} + [\dot{m}_e (h_e - h_{mu}) + \dot{Q}_c]\} = c\rho_z \frac{\partial \theta}{\partial t} \quad (\text{Eq. A-20})
 \end{aligned}$$

When the differential equation is solved for this case, it yields the temperature of the fluid in the moving control volume. Subsequently the temperature at any location along the pond flow length at any desired time can be found from the relationship between time and distance traveled, namely:

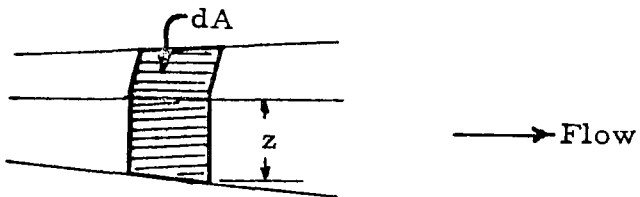
$$x = \int_{t=0}^t u dt \quad (\text{Eq. A-20A})$$

where u = water velocity in longitudinal direction, ft/sec

Since the terms in Eq. 19 correspond to the like labeled terms in Eq. A-6, Eq. 19 can also be expressed as:

$$\begin{aligned}
 c\rho_z \frac{d\theta}{dt} = & \{\dot{m}_p (h_p - c\theta_{mu}) - \dot{m}_s (c\theta - c\theta_{mu})\} \\
 & + \{\dot{Q}_N - a_5 - (a_{12} + a_{13}W)(a_1 - a_{14}\theta_a - P_a)\} \\
 & - \{a_6 + (a_{12} + a_{13}W)(a_2 - a_{14})\} \theta \\
 & - \{a_7 + (a_{12} + a_{13}W)(a_3)\} \theta^2 \\
 & - \{a_8 + (a_{12} + a_{13}W)(a_4)\} \theta^3 \quad (\text{Eq. Q-21})
 \end{aligned}$$

It is usually more convenient to find the temperature not after a certain longitudinal distance, x , has been traveled by the control volume or "slug", but to find the temperature when the slug has swept out a certain amount, A , of pond area. Thus for the variable width and depth pond under consideration



the continuity equation yields:

$$(dt) (\dot{m}_c) = \rho z dA \quad (\text{Eq. A-22})$$

or

$$dt = \frac{\rho z}{\dot{m}_c} dA \quad (\text{Eq. A-23})$$

Substituting Eq. A-23 into Eq. A-21 yields the desired form of the energy equation, namely:

$$\begin{aligned} \dot{m}_c c \frac{d\theta}{dA} &= \{ \dot{m}_p (h_p - c\theta_{mu}) - \dot{m}_s (c\theta - c\theta_{mu}) \} \\ &+ \{ \dot{Q}_N - a_5 - (a_{12} + a_{13}W)(a_1 - a_{14}\theta_a - P_a) \} \\ &- \{ a_6 + (a_{12} + a_{13}W)(a_2 + a_{14}) \} \theta \\ &- \{ a_7 + (a_{12} + a_{13}W)(a_3) \} \theta^2 \\ &- \{ a_8 + (a_{12} + a_{13}W)(a_4) \} \theta^3 \end{aligned} \quad (\text{Eq. A-24})$$

where $\dot{m}_c c = \frac{WTE}{\Delta T_c}$, btu/day ${}^{\circ}\text{F}$

Again as in the case of the mixed pond, the first term on the right hand side of Eq. A-24 will go to zero if the enthalpy of the precipitation and seepage are equal to the enthalpy of the water in the control volume (Eq. A-14).

Slug flow pond, simplified case, steady state operation

Again as in the case of the mixed pond, if Eq. A-14 is assumed to be valid and if the time over which the weather conditions are averaged is long compared to the time required for a slug to flow through the pond (the residence time, $t_r = (\rho V)/\dot{m}_c$), then the energy balance equation reduces to the steady state case and the pond operates in the steady state mode given by the equation:

$$\begin{aligned}
 \frac{d\theta}{dA} = & \frac{\Delta T_C}{WTE} \{ \dot{Q}_N - a_5 - (a_{12} + a_{13}W)(a_1 - a_{14}\theta - P_a) \} \\
 & - \frac{\Delta T_C}{WTE} \{ a_6 + (a_{12} + a_{13}W)(a_2 + a_{14}) \} \theta \\
 & - \frac{\Delta T_C}{WTE} \{ a_7 + (a_{12} + a_{13}W)(a_3) \} \theta^2 \\
 & - \frac{\Delta T_C}{WTE} \{ a_8 + (a_{12} + a_{13}W)(a_4) \} \theta^3
 \end{aligned} \tag{Eq. A-25}$$

where the temperature decrease experienced by the water as it flows through the pond must be equal to the temperature rise (ΔT_C) experienced by the water as it passes through the condenser for steady state operation. This demand of equality determines the magnitude of the inlet and outlet pond temperature for given climatic and plant conditions.

APPENDIX B

HEAT TRANSFER BY EVAPORATION AND CONVECTION

Evaporation

Many empirical relationships have been developed in order to predict the rate of evaporation from a natural water surface exposed to the atmosphere [19, 20, 21]. However, all the experimental data for large bodies of water exposed to the atmosphere are limited to unheated or very slightly heated water, with the result that these data have been collected under conditions where the equilibrium temperature and water temperature differ by only a few degrees. Since it is a matter of experience that the equilibrium temperature and air temperature generally differ by only a few degrees, it may then be said that these data were collected for conditions of only a few degrees difference between air and water temperature. In view of the above considerations, the empirical equations developed on the bases of these data can not, *a priori*, be extrapolated to the anticipated situation where the water temperature may be as much as 30°F in excess of the air temperature as a result of heavy thermal energy loading on the pond. In addition, evaporation rates predicted by the various empirical formulae differ by more than a factor of two among each other. (See Fig. B-1). Likewise, equations based on fundamental principles have been devised, of which the work by Sverdrup is the most notable [16]. Nevertheless, when he used his method to compute evaporation rates in various regions of the Atlantic Ocean and compared the results to measurements made by Wust, the computed values differed from the measured values by as much as + 20% and - 35% (See Fig. B-2).

In view of the fact that evaporation accounts for the major portion of the heat transfer from the pond (approximately 40 to 70%), it is important to be able to make accurate estimates of the evaporation rate for ponds where specific experimental evaporation data are not available, - in particular, for heated ponds with temperature substantially above natural pond temperatures. It is therefore desirable to develop an analytical expression which displays reasonable agreement with some of the known measurements in the range of their validity, but which can be extrapolated to regions of present interest.

In order to develop the desired relationship, the analogy between mass and momentum transfer will be used. The relationship will be developed on the basis that the water surface can be assumed to be a smooth surface.

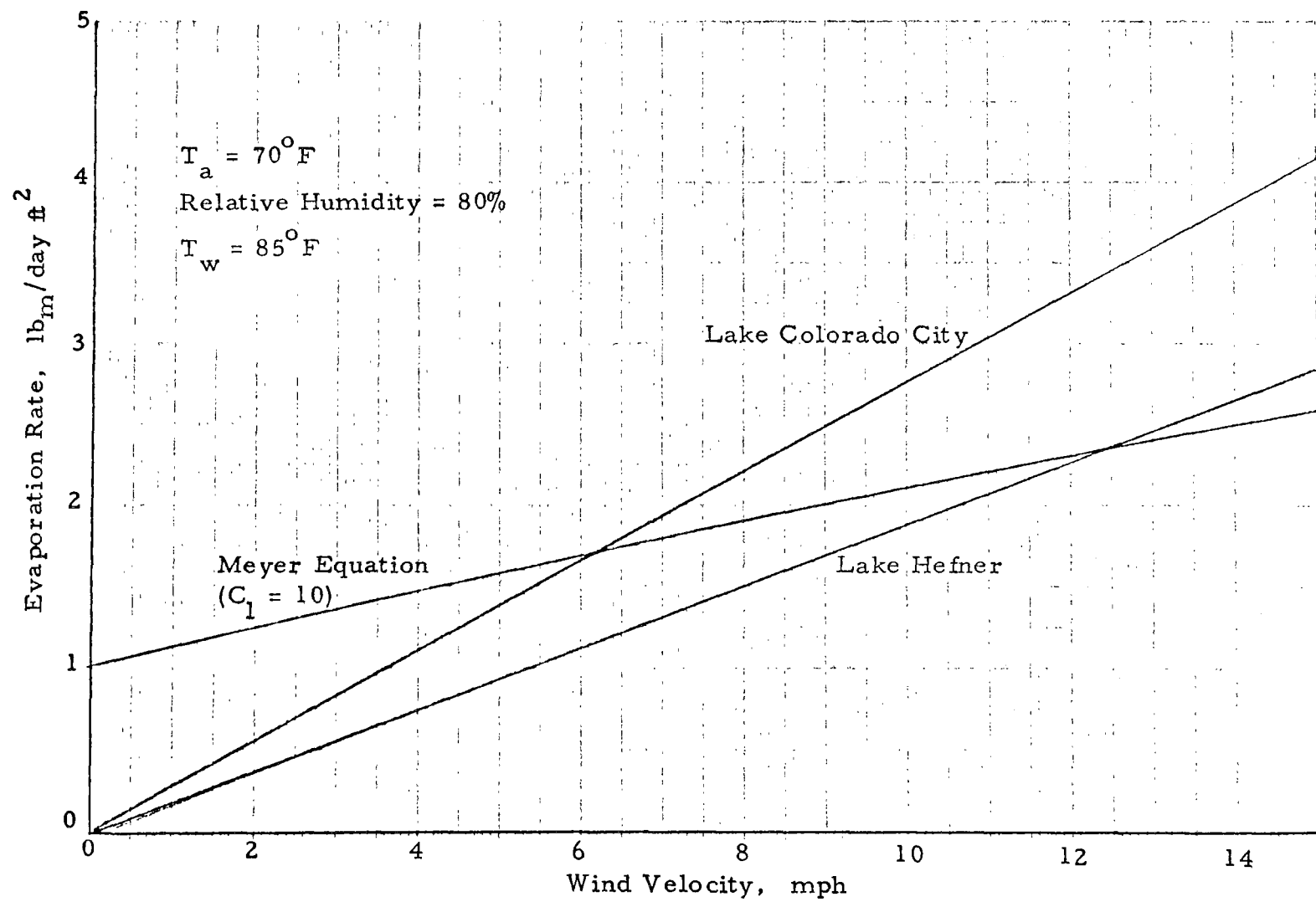
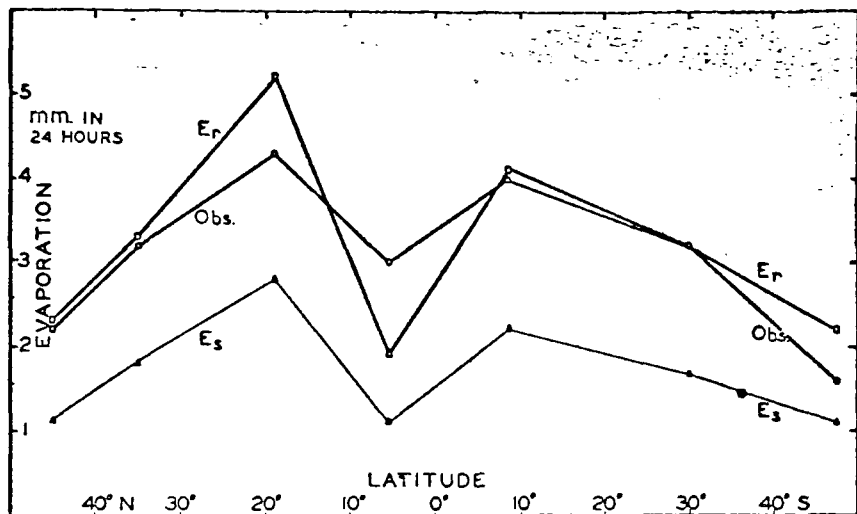


Figure B-1



NOTE: Predicted curves are based on the assumption that the sea surface is characterized by a constant roughness parameter (E_r) or by a smooth surface (E_s). [After Sverdrup, Ref. 16]

Fig. B-2 - Comparison of Measured Pan Evaporation and Observed Values over the Atlantic Ocean

If it is assumed that the water surface can be represented by a smooth flat surface, the analogy between mass and momentum transfer can be expressed as: [27, p. 337]

$$\text{For Laminar Flow: } \frac{h_D S_c^{2/3}}{U_\infty} = \frac{c_f}{2} = 0.332 \text{Rey}_x^{-1/2} \quad (\text{Eq. B-1})$$

$$\text{For Turbulent Flow: } \frac{h_D S_c^{2/3}}{U_\infty} = \frac{c_f}{2} = 0.0288 \text{Rey}_x^{-1/5} \quad (\text{Eq. B-2})$$

where c_f = local friction coefficient

h_D = mass transfer coefficient, ft/sec

S_c = Schmidt Number

= ν/D (ν = kinematic viscosity, ft²/sec,
 D = diffusion coefficient, ft²/sec)

U_∞ = free stream air velocity, ft/sec

Rey_x = Reynolds Number at a distance, x , from the leading edge or $\text{Rey}_x = (U_\infty x)/\nu$

If it is assumed that the boundary layer starts at the edge of the water surface, the local value of the average mass transfer coefficient up to any distance, $x = L$, from that leading edge is found by combining Eq. B-1 and Eq. B-2 to yield:

$$h_{D_{ave}} = \frac{1}{L} \left\{ \int_{x=0}^{x=300,000} \frac{\nu}{U_\infty} \text{MAX} \frac{U_\infty}{S_c^{2/3}} (.332) \left(\frac{U_\infty x}{\nu} \right)^{-1/2} dx + \int_{x=300,000}^{\text{Rey}_L \left(\frac{\nu}{U_\infty} \right) \text{MAX}} \frac{U_\infty}{S_c^{2/3}} (.0288) \left(\frac{U_\infty x}{\nu} \right)^{-1/5} dx \right\} \quad (\text{Eq. B-3})$$

The first term on the right hand side represents the contribution to the diffusion coefficient over the zone where the boundary layer is laminar and the second term represents the contribution where the boundary layer is turbulent. However, before the second term can be integrated, the upper limit of integration must be established. If the water and the atmosphere were not exchanging heat, and if in addition, the wind was steady and moving parallel to the water surface, the turbulent boundary

layer would continue to thicken and the upper limit of x would be the length of the lake. However, even in the absence of heat exchange between the water and the atmosphere, the wind will not be steady but will gust and may not be moving parallel to the water surface. These conditions are likely to vary rapidly in time, but most likely result in substantially smaller influences than the combination of averaging the wind speed over as much as 30 days and the effect of heat exchange from water to the atmosphere. Thus, it seems reasonable as a first approximation to take as the upper limit for x that distance at which the heated and therefore buoyant boundary layer tends to rise vertically from the pond surface, with the result that free stream air fills in to form the beginning of new boundary layer material. The distance at which this happens, x_0 , can be estimated by setting the ratio of buoyant force to inertia force equal to unity. Thus:

$$\frac{B.F.}{I.F.} = 1 \approx \frac{\rho_\infty g x_0^3 - \rho_{B.L.} g x_0^3}{\frac{U_\infty^3}{\rho_{B.L.} x_0^3 (\frac{x_0}{U_\infty})}} \quad (Eq. B-4)$$

where ρ_∞ = free stream air density

$\rho_{B.L.}$ = density of material in the heated boundary layer

g = acceleration due to gravity

U_∞ = air free stream velocity

Solving Eq. B-4 for the boundary layer thickness at $x = x_0$ yields:

$$x_0 = \frac{U_\infty^2}{\frac{g(\frac{\rho_\infty}{\rho_{B.L.}})}{(P_{BAR})(144)}} \quad (Eq. B-5)$$

$$\text{where } \frac{\rho_\infty}{\rho_{B.L.}} = \frac{\frac{(P_{BAR})(144)}{(53.34)(T_{aa})}}{\frac{(P_{BAR} - P_w)(144)}{(53.34)(T_{wa})}(1+w)} \quad (Eq. B-6)$$

$$\frac{\rho_\infty}{\rho_{B.L.}} = \left(\frac{T_{wa}}{T_{aa}} \right) \frac{P_{BAR}}{(P_{BAR} - P_w)(1+w)} \quad (Eq. B-7)$$

where T_{aa} = absolute air temperature, $^{\circ}\text{R}$
 T_{wa} = absolute water temperature, $^{\circ}\text{R}$
 w = humidity ratio
 P_{BAR} = barometric pressure, psia
 P_w = water vapor pressure corresponding to saturation at the temperature of the water surface, psia

Using Eq. B-5 as the upper limit for integrating Eq. B-3 results in the expression:

$$h_{D_{\text{ave}}} = \frac{1}{x_o} \frac{U_{\infty}}{S_c^{2/3}} \left\{ .322 \left(\frac{\nu}{U_{\infty}} \right)^{1/2} \left[(3 \times 10^5) \frac{\nu}{U_{\infty}} \text{MAX} \right]^{1/2} \right. (2) \\ \left. + .0288 \left(\frac{\nu}{U_{\infty}} \right)^{1/5} \left(\frac{5}{4} \right) [x_o - (3 \times 10^5) \frac{\nu}{U_{\infty}}]^{4/5} \right\} \text{ft/sec} \quad (\text{Eq. B-8})$$

Eq. B-8 may be solved for specific climatic conditions and substituted into the expression for the net diffusion of water vapor into the atmosphere given below:

$$\dot{m}_e = h_{D_{\text{ave}}} (C_{A_1} - C_{A_2}) (3600 \times 24) \text{ #m/day ft}^2 \quad (\text{Eq. B-9})$$

where C_{A_1} = concentration of water vapor in $\text{#m}/\text{ft}^3$ corresponding to saturation at the temperature of the water surface
 C_{A_2} = concentration of water vapor in $\text{#m}/\text{ft}^3$ corresponding to the actual conditions in the free stream air, psia

If water vapor is treated as a perfect gas, Eq. B-9 can be re-written as:

$$\dot{m}_e = h_{D_{\text{ave}}} \left\{ \frac{M_w (144)}{R_u T_{wa}} (P_w - P_a) \right\} (3600 \times 24) \text{ #m/day ft}^2 \quad (\text{Eq. B-10})$$

$$m_e = (1.678) h_{D_{\text{ave}}} \frac{(P_w - P_a)}{T_{wa}} (8.64 \times 10^4) \text{ #m/day ft}^2 \quad (\text{Eq. B-11})$$

where P_a = water vapor pressure corresponding to actual conditions in the free stream air, psia

M_w = molecular weight of water = 18.0 $\text{#m}/(\text{#m-mole})$

R_u = universal gas constant = 1545 $\text{#f-ft}/(\text{#m-mole})^{\circ}\text{R}$

Eq. B-11 could be solved for a given water temperature and given climatic conditions; however, before doing so, it is helpful to note that the laminar boundary layer extends for only a distance of $3 \times 10^5 \nu / U_\infty$, which at 70°F and 5 mph is equal to

$$3 \times 10^5 \frac{(1.7 \times 10^{-4} \text{ ft}^2/\text{sec})}{7.34 \text{ ft/sec}} = 6.95 \text{ ft}$$

Since this is small compared to the anticipated pond dimensions and since the air will be initially turbulent, we can approximate Eq. B-11 as if the boundary layer were turbulent from the edge of the pond.

Thus the expression for $h_{D_{ave}}$ from Eq. B-8 becomes:

$$h_{D_{ave}} = \frac{U_\infty}{S_c^{2/3}} \{ .0288 \left(\frac{\nu}{U_\infty} \right)^{1/5} \left(\frac{5}{4} \right) \left[\frac{1}{x_0} \right]^{1/5} \} \quad (\text{Eq. B-12})$$

When Eq. B-5 and B-7 are substituted into Eq. B-12 and the results are substituted into Eq. B-11, the expression for evaporation becomes:

$$\dot{m}_e = (1.047 \times 10^4) \left(\frac{1}{S_c} \right)^{2/3} \nu^{1/5} U_\infty^{2/5} \\ \times \left[\frac{T_{wa}(P_{BAR})}{T_{aa}(P_{BAR}) - P_w(1+w)} - 1 \right]^{1/5} \left[\frac{P_w - P_a}{T_{wa}} \right] \quad (\text{Eq. B-13})$$

where $S_c = \frac{\nu}{D}$ and since D varies approximately at $T_{abs}^{3/2}$ [Ref. 26]

$$= \nu \left(\frac{1}{D_{77^\circ F}} \right) \left(\frac{537}{T_{aa}} \right)^{3/2} \\ D = 2.75 \times 10^{-4} \text{ ft}^2/\text{sec at } 77^\circ F \quad [\text{Ref. 27}]$$

Thus Eq. B-13 becomes:

$$\dot{m}_e = [0.0815] \frac{U_\infty^{2/5}}{\nu^{7/15}} \left[\frac{T_{aa}}{T_{wa}} \right] \left[\frac{T_{wa}(P_{BAR})}{T_{aa}(P_{BAR}) - P_w(1+w)} - 1 \right]^{1/5} \left[\frac{P_w - P_a}{T_{wa}} \right] \quad (\text{Eq. B-14})$$

Since the wind velocity is measured at some height, b , (often ~ 26 ft), Eq. B-14 must be corrected for the velocity profile effect by substituting into Eq. B-14 the expression:

$$U_{\infty} = \left(\frac{1}{\alpha_1}\right) U_b \quad (\text{Eq. B-15})$$

where U_b = velocity of the wind at some specified elevation above the water surface, b feet, ft/sec
 U_{∞} = free stream wind velocity, ft/sec
 α_1 = ratio of wind speed at elevation b to free stream wind speed. This ratio will depend on U_{∞} and location. The value of α_1 as measured above open grassland is shown in Fig. B-3. Although α_1 will vary with specific location, a variation of $\pm 50\%$ results in a variation of the evaporation rate of only $\pm 18\%$.

Thus, the final expression for the rate of evaporation is:

$$\dot{m}_e = [-815] \left[\frac{1}{\alpha_1} \right]^{2/5} \frac{U_b^{2/5}}{\nu^{7/15}} \left[\frac{T_{aa}}{T_{wa}} \right] \left[\frac{T_{wa}(P_{BAR})}{T_{aa}(P_{BAR} - P_w)(1+w)} - 1 \right]^{1/5} \times [P_w - P_a] \quad (\text{Eq. B-16})$$

Of the formulae available in the literature, two have been selected which have no zero wind velocity term, namely, an equation from the Lake Hefner study and one from the Lake Colorado City study, and one formula with a zero wind velocity term, namely, the Meyer Equation. In each of these three cases, the rate of evaporation is given as a function of local wind speed and the difference between the saturation vapor pressure corresponding to the water surface temperature and the water vapor pressure some distance above the surface. The three equations are:

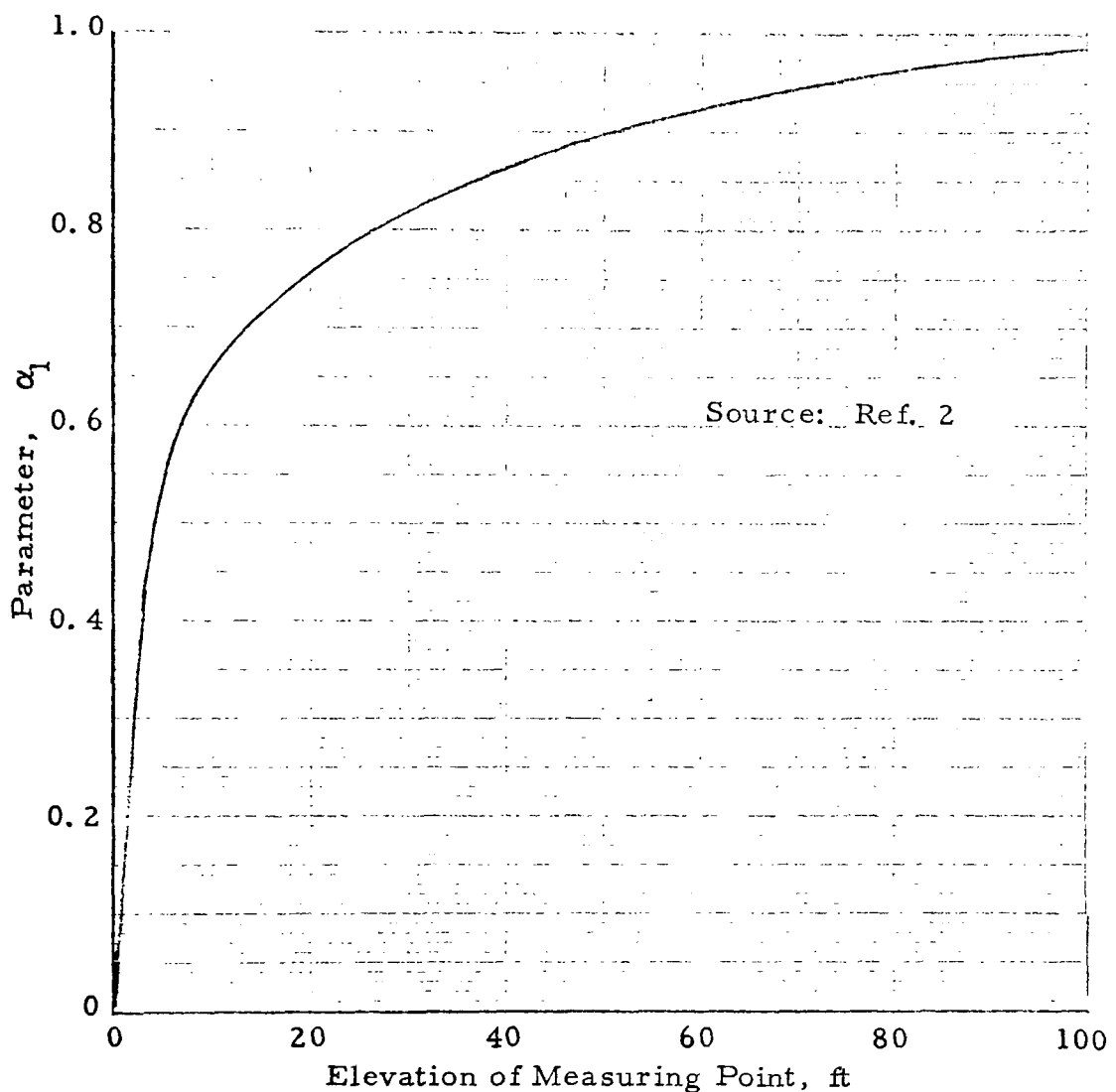
$$\text{Lake Hefner Eq. [19]: } \dot{m}_e = (.614) W_H (P_w - P_a) \text{ #m/day ft}^3 \quad (\text{Eq. B-17})$$

$$\text{Lake Colorado City [20]: } \dot{m}_e = (.897) W_c (P_w - P_a) \text{ #m/day ft}^2 \quad (\text{Eq. B-18})$$

The Meyer Equation [21]:

$$\dot{m}_e = C_1 (.349) \left(1 + \frac{m}{10}\right) (P_w - P_a) \text{ #m/day ft}^2 \quad (\text{Eq. B-19})$$

where C_1 is a constant for a given location and ranges from 10 to 15 depending on depth and exposure of the water under study as well as the frequency of the available meteorologic measurements. For surface accumulation, C is taken near the higher value whereas for large deep



Elevation Over Open Grass Land vs α_1

Figure B-3

bodies of water, C is taken near the lower limit.

W = wind speed, mph

W_H = W in Lake Hefner Equation measured about 26 feet above the ground and taken as the average over a three-hour period

W_C = W in Lake Colorado City Equation measured about 26 feet above the ground and taken as the average over a 24-hour period

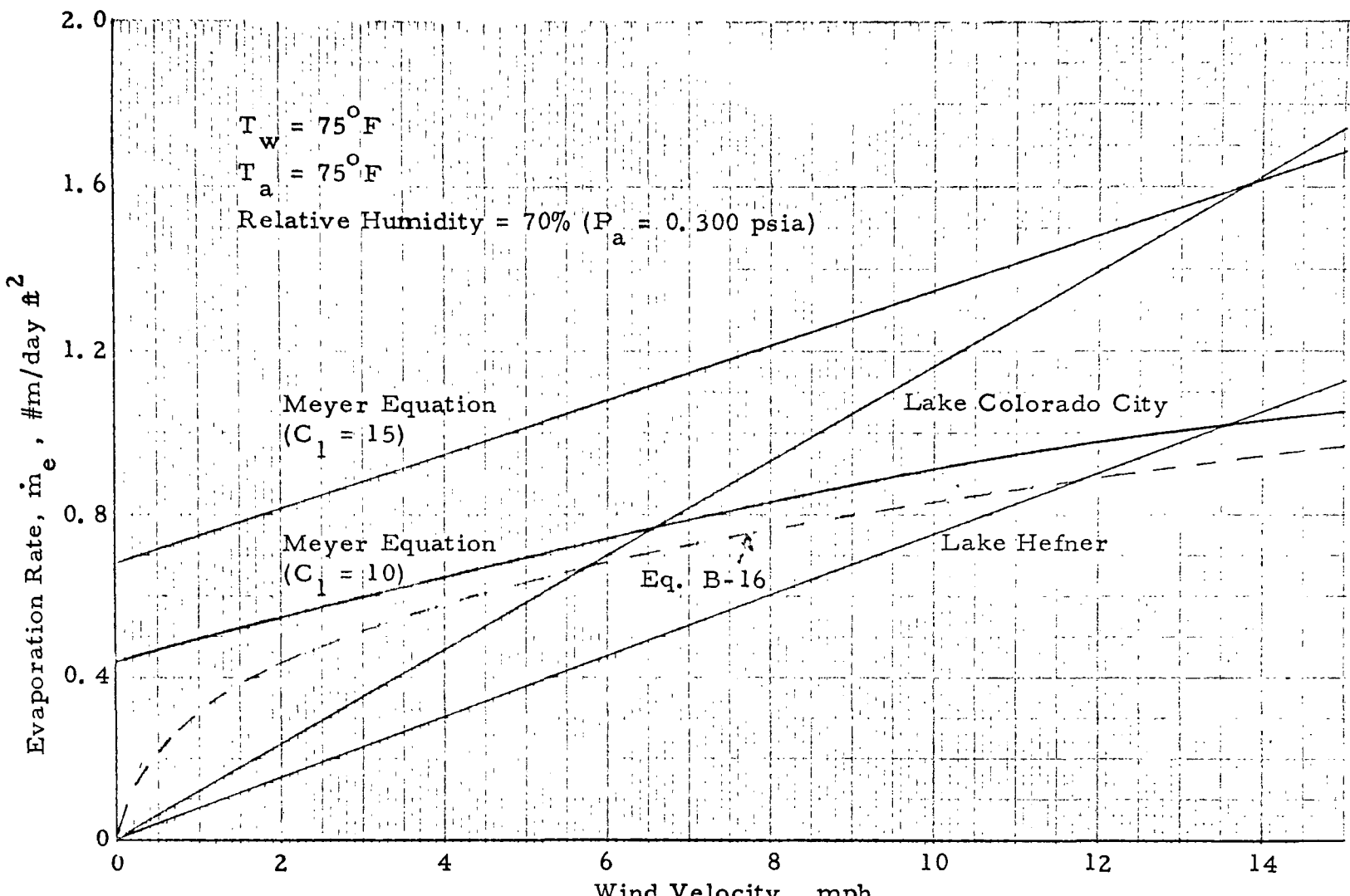
W_M = W in the Meyer Equation and taken as the monthly average wind speed value from measurements made at the nearest Weather Station about 25 feet above the surface

P_w = equilibrium, or saturated, vapor pressure corresponding to the temperature of the water at some specified point near the surface

P_a = water vapor pressure of the atmospheric air, measured at the same height and averaged in the same way as the wind speed, psia

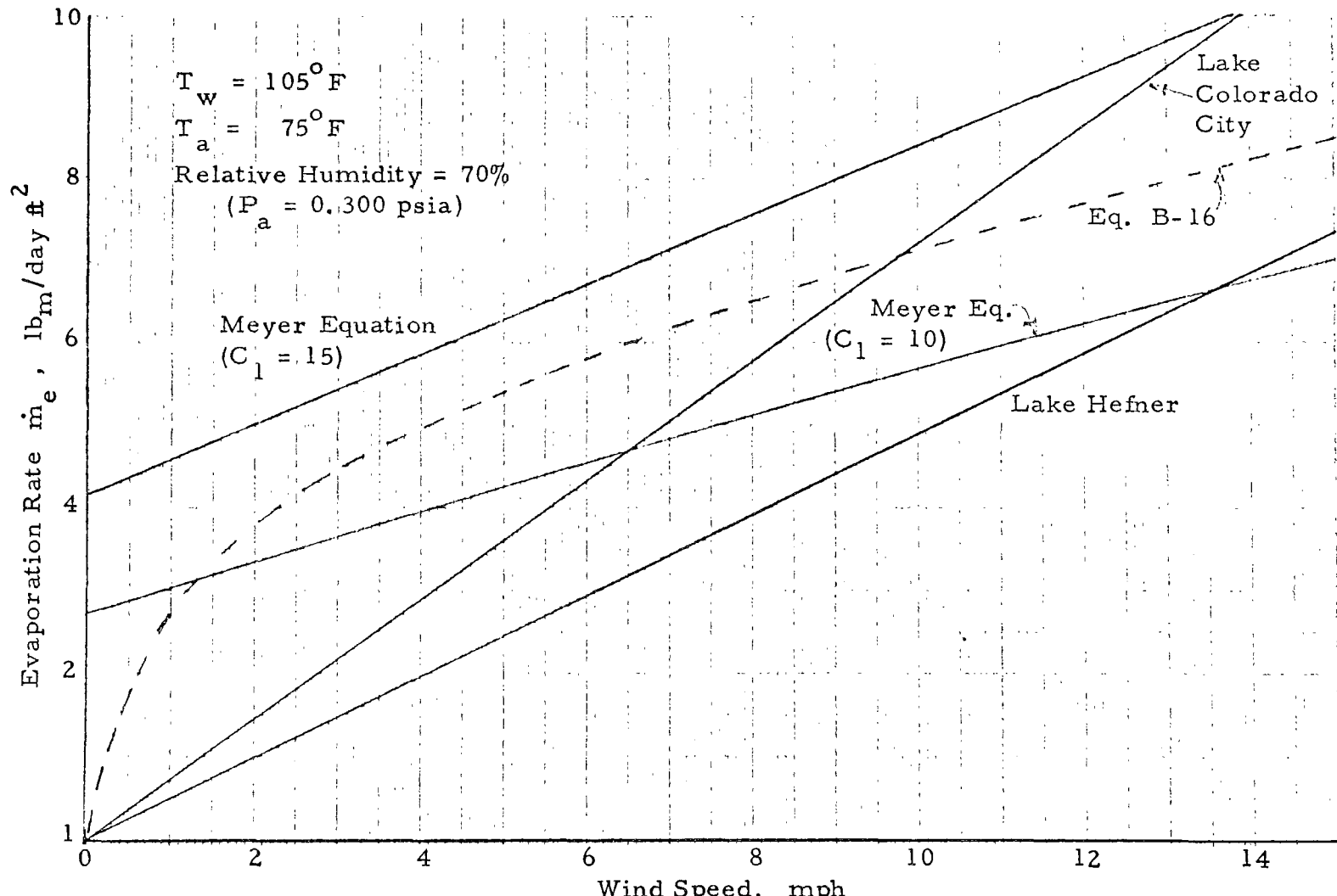
Figs. B-4, B-5, B-6 and B-7 show a comparison of the three empirical equations and the analytical solution, Eq. B-16, based on the analogy between mass and momentum transfer for heated water under summer and winter conditions respectively with $T_w = T_a$ and with $T_w > T_a$.

Since $T_w = T_a$ in both Fig. 4 and Fig. 6, the condition under which the original experimental data were collected (that is, water near the equilibrium temperature) is satisfied. From Fig. 4 and Fig. 6 it is noted that the evaporation rates predicted by Eq. B-16 for the cases where $T_w = T_a$ follow the trend of the Meyer Equation with $C_1 = 10$ closely over the range of wind speeds pertinent to monthly average values (~ 4 to 15 mph), but are somewhat lower (about 10 to 20%). Whereas in Fig. 5 and Fig. 7 (with T_w greater than T_a by 30°F) the evaporation ratio predicted by Eq. B-16 also follows the trend of the Meyer Equation with $C_1 = 10$ over the wind speed range of present interest, but are somewhat higher (about 20%). On the basis of these observations it appears reasonable to use the Meyer Equation with $C_1 = 10$ to determine the evaporation ratio for pond temperatures that are only slightly above air or equilibrium temperature. However, for heavily loaded ponds, the water temperature will be well in excess of the equilibrium temperature and the rates should be estimated by use of Eq. B-16. If the simpler Meyer Equation is used for heavily loaded



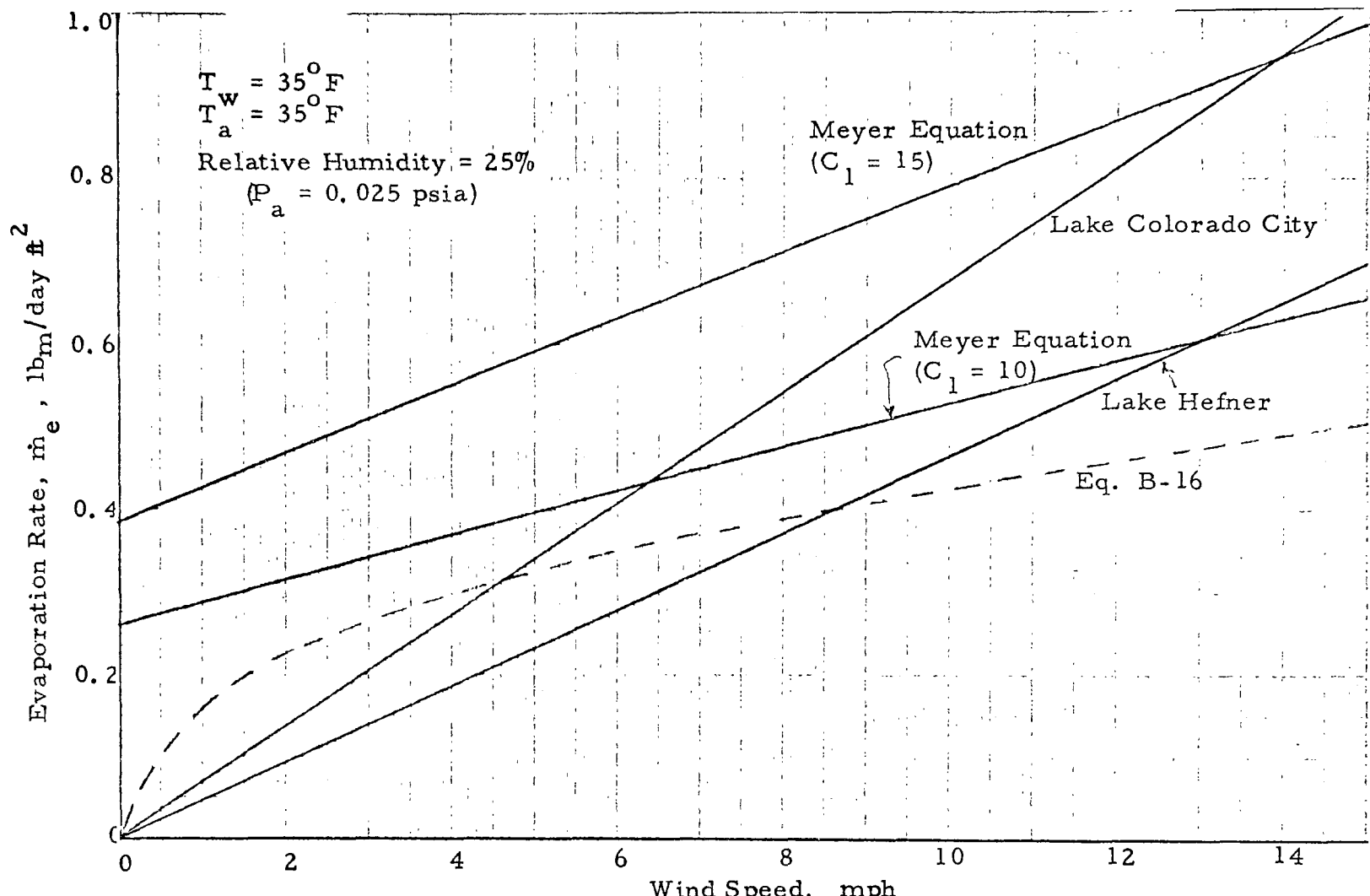
Evaporation Rate Given by Various Empirical Equations and Eq. B-16
 Summer Conditions $T_w = T_a$

Figure B-4



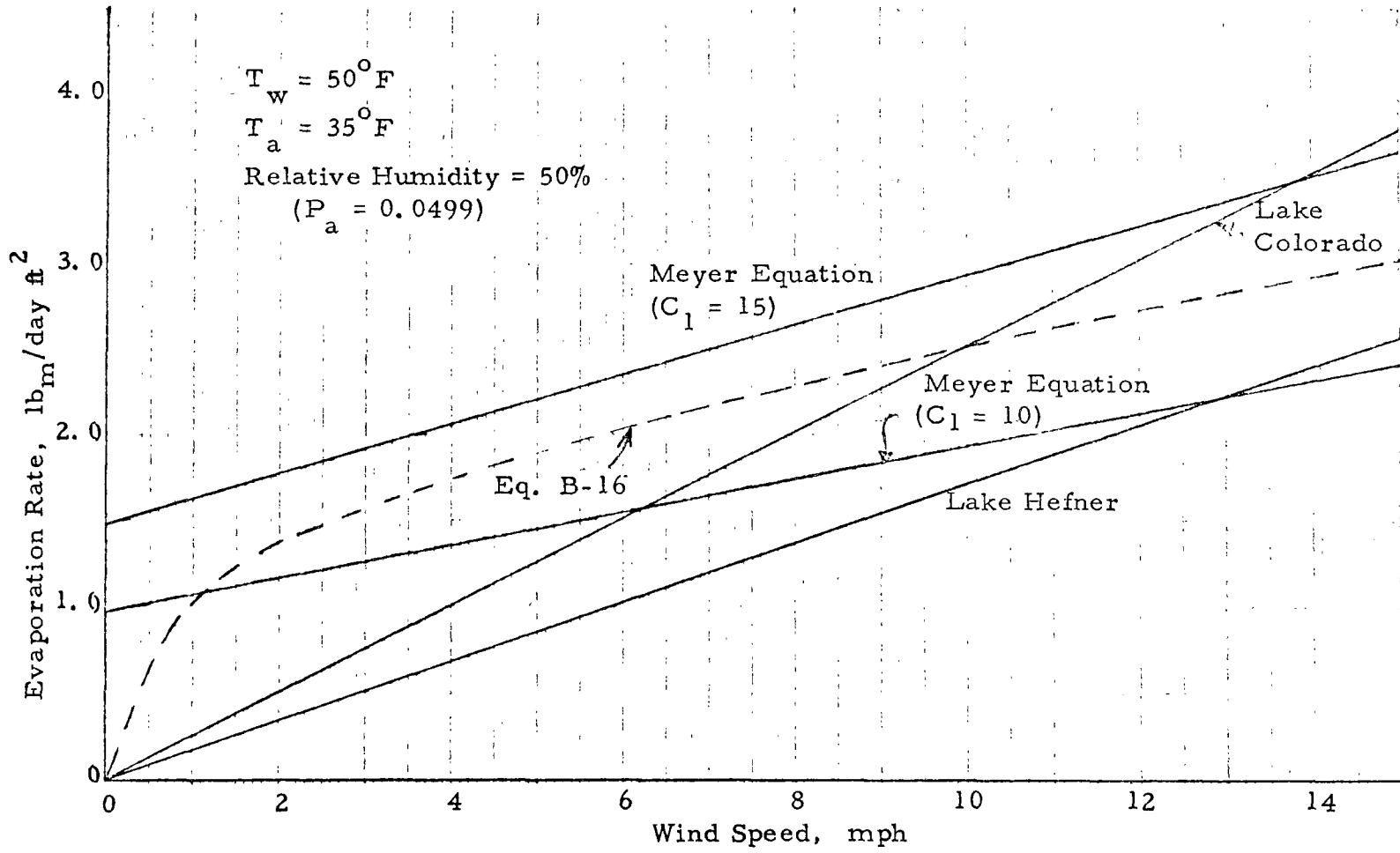
Evaporation Rate Given by Various Empirical Equations and Eq. B-16
 $T_w > T_a$

Figure B-5



Evaporation Rates given by Various Empirical Equations and Eq. B-16
Winter Conditions, $T_w = T_a$

Figure B-6



Evaporation Rates Given by Various Empirical Equations and Eq. B-16
Winter Conditions, $T_w > T_a$

Figure B-7

ponds, the predicted temperatures will be too high.

When comparing the curves in Figs. 34 through 37, it is helpful to note that coefficients were also calculated for the Lake Hefner and Lake Colorado City equations by using data from the nearest weather station, as in the case of the Meyer Equation, and these coefficients were found to agree within 5% with the previous ones. This agreement is not surprising if the only substantive difference in the two measurements is the height at which the observations are made in view of the fact that the 26-foot height is well above the laminar and buffer zone of the boundary layer and is thus in an area of active turbulent mixing and relatively slow velocity change with elevation as can be seen from Fig. B-3. The apparent difference between the various empirical curves, however, is far more significant. The difference amounts to a factor of almost 1.5 between the two curves that do not have a zero wind velocity term, and to a considerably higher factor when equations without the zero wind term are compared to the equation with the zero term at speeds below 5 mph. A major portion of these apparent discrepancies most likely result from the differences in local topography and the inherent difficulties of estimating the mass of evaporated water by the indirect process of making a mass balance.

Convection

Bowen [22] developed an expression for the ratio of heat transfer by convection to heat transfer as a result of evaporation on the basis of diffusion theory. He was able to find analytical solutions to his equations for three special cases and subsequently selected one of these cases as the most probable for application to bodies of water, namely:

$$\gamma = \frac{\dot{Q}_c}{\dot{Q}_e} = .00494 \left(\frac{T_w - T_a}{P_w - P_a} \right) \frac{P}{14.67} \quad (\text{Eq. B-20})$$

Bowen pointed out that the above equation was valid only "for values of T_w low enough that the [specific] volume of the air is not appreciably increased by the water vapor evaporating into it." In order to provide a valid method of estimating the ratio \dot{Q}_c/\dot{Q}_e under conditions where the water temperature, T_w , is high, it is convenient to write the analogy between mass transfer and momentum transfer and then the analogy between heat transfer and momentum transfer. Again assuming the water surface can be represented as a smooth surface, the former is given by the expression (See page 337, Ref. 27) :

$$\frac{h_{D_x}}{U_\infty} (S_c)^{2/3} = \frac{c_f}{2} \quad (\text{Eq. B-21})$$

where c_f = local friction coefficient

h_{D_x} = local mass transfer coefficient, ft/sec

and the latter is given by the expression (See page 136, Ref. 27):

$$\frac{h_x}{\rho c_p U_\infty} P_r^{2/3} = \frac{c_f}{2} \quad (\text{Eq. B-22})$$

where h_x = local coefficient of heat transfer, btu/sec ft² °F

P_r = Prandtl number = ν/α

α = thermal diffusivity, ft²/sec

When both mass and heat transfer take place simultaneously as they do at the air-water interface, the ratio of the heat transfer coefficient to the mass transfer coefficient can be found by dividing Eq. B-22 by Eq. B-21 to yield:

$$\frac{h}{h_D} = \rho c_p \left(\frac{\alpha}{D}\right)^{2/3} \quad (\text{Eq. B-23})$$

The subscript designating local conditions has been dropped from Eq. B-23 for convenience since the equation is valid for local values and average values over a length x .

The heat transfer rate by convection may be expressed as:

$$\dot{Q}_c = h(T_w - T_a) (3600 \times 24) \text{ btu/day ft}^2 \quad (\text{Eq. B-24})$$

where T_w = water surface temperature, °F

T_a = air free stream temperature, °F

The heat transfer rate by evaporation at constant temperature may be defined as:

$$\dot{Q}_e = \dot{m}_e (\Delta h_T) \quad (\text{Eq. B-25})$$

where \dot{m}_e = mass rate of water being evaporated

Δh_T = change in enthalpy between the vapor and liquid state at the same temperature. This varies from about 1075 btu/#m at 32°F to 1037 btu/#m at 100°F

If the expression given in Eq. B-10 for m_e is substituted into the above equation, the value of Q_e is given as:

$$\dot{Q}_e = (\Delta h_T) h_D \left\{ \frac{M_w(144)}{R_u T_{wa}} (P_w - P_a) \right\} (3600 \times 24) \text{ btu/day ft}^2 \quad (\text{Eq. B-26})$$

The desired ratio, γ , can now be found by dividing Eq. B-24 by Eq. B-26 and substituting Eq. B-23 into the resulting expression:

$$\gamma = \frac{\dot{Q}_c}{\dot{Q}_e} = \frac{\frac{P_{BAR} M_a C_p (\alpha/D)^{2/3} (T_w - T_a)}{M}}{T_{aa} \left\{ (\Delta h_T) \frac{M_w}{T_{wa}} (P_w - P_a) \right\}} \quad (\text{Eq. B-27})$$

where $\rho = \frac{P_{BAR} M_a(144)}{R_u T_{aa}}$, here it is assumed that $P_a = P_{BAR}$
and M_a = molecular weight of air,
 $28.8 \text{ #m}/\text{#m-mole}$

Since both the thermal diffusivity, α , and the diffusion coefficient, D , vary as the absolute temperature raised to the 3/2 power (to within 5% over the temperature range of interest), the value of α/D can be expressed as its value at any one temperature, say, 77°F.

$$\frac{\alpha}{D} = \left(\frac{\alpha}{D} \right)_{77^\circ F} = \left(\frac{2.34 \times 10^{-4}}{2.75 \times 10^{-4}} \right) = 851 \quad (\text{Eq. B-28})$$

Substituting this value into Eq. B-27 together with the values of M_a and M_w lead to:

$$\gamma = \frac{5.05}{\Delta h_T} \left[\frac{T_{wa}}{T_{aa}} \right] \frac{(T_w - T_a)}{(P_w - P_a)} \left[\frac{P_{BAR}}{14.67} \right] \quad (\text{Eq. B-29})$$

In order to compare Eq. B-29 with the expression proposed by Bowen as the most probable when T_w was not excessively high, it is convenient to note that for modest values of T_w compared to T_a (say within 10°F), the ratio of (T_{wa}/T_{aa}) can be assumed to equal unity within an error of about 2%, with the result that Eq. B-29 becomes:

$$\gamma = \frac{5.05}{\Delta h_T} \frac{(T_w - T_a)}{(P_w - P_a)} \frac{P_{BAR}}{14.67} \quad (\text{Eq. B-30})$$

If in addition to the above assumption the value of Δh_T is taken to be the value of saturation condition corresponding to 69°F, namely, $\Delta h_T = 1060 \text{ btu}/\text{#m}$, Eq. B-30 becomes:

$$\gamma = 0.00476 \frac{(T_w - T_a)}{(P_w - P_a)} \frac{P_{BAR}}{14.67} \quad (\text{Eq. B-31})$$

The value of .00476 for the coefficient in Eq. B-31 is in reasonable agreement with the value of .00494 in Bowen's most probable equation as given in Eq. B-20. When T_{wa} is appreciably greater than T_{aa} , the use of Eq. B-29 for γ is recommended over the simpler form given by Eq. B-30.

Combined Convection and Evaporation

General Case

The combined heat transfer by evaporation and convection can be expressed by combining the appropriate expression for evaporation heat transfer and Eq. B-29. In the most general form, Eq. B-16 would be used for the evaporation heat transfer rate to yield the following expression for combined energy transfer by evaporation and conduction:

$$\dot{Q}_e + \dot{Q}_c = [0.0815] \left[\frac{1}{\alpha_1} \right]^{2/5} \frac{U_b^{2/5}}{v^{7/5}} \left[\frac{T_{wa}(P_{BAR})}{T_{aa}(P_{BAR} - P_w)(1+w)} - 1 \right]^{1/5} \\ \times \left[\left(\frac{T_{aa}}{T_{wa}} \right) (P_w - P_a) \right] \left[1 + \left(\frac{5.05}{\Delta h_T} \right) \left(\frac{T_w - T_a}{P_w - P_a} \right) \left(\frac{P_{BAR}}{14.67} \right) \right] \quad (\text{Eq. B-32})$$

Simplified Case

The mathematical difficulties associated with the use of Eq. B-32 can be avoided at the expense of making approximations for \dot{m}_e by using Eq. B-19, with a value of $C_1 = 10$ selected as a result of an examination of Fig. B-4 through Fig. B-7, in place of the analytical expression given by Eq. B-16. Thus:

$$\dot{m}_e = (3.49 + 0.349W)(P_w - P_a) \quad (\text{Eq. B-33})$$

and

$$\dot{Q}_e = \Delta h_T (3.49 + 0.349W)(P_w - P_a) \quad (\text{Eq. B-34})$$

If in addition to the above assumption Eq. 30 is used in place of Eq. 29 (for water temperature 30°F in excess of air temperature this represents an error of 5% in the ratio Q_c/Q_e), the expression for combined energy transfer by evaporation and convection becomes:

$$\dot{Q}_e + \dot{Q}_c = \Delta h_T (3.49 + 0.349W)(P_w - P_a) \left[1 + \frac{5.05}{\Delta h_T} \frac{(\theta - \theta_a)}{(P_w - P_a)} \frac{P_{\text{BAR}}}{14.67} \right] \quad (\text{Eq. B-35})$$

However, in the generalized analysis presented in the text of the report, it is more convenient to have the combined net transfer of energy that results from convection (\dot{Q}_c) and from water evaporating from the pond at the pond surface as discussed in Appendix A, Eq. A-11. This net transfer of energy can readily be found by using Eq. B-35. Thus:

$$\dot{m}_e (\Delta h) + Q_c = \Delta h (3.49 + 0.349W)(P_w - P_a) \left[1 + \frac{5.05}{\Delta h} \frac{(\theta - \theta_a)}{(P_w - P_a)} \frac{P_{\text{BAR}}}{14.67} \right]$$

where $\Delta h = 1070 \text{ btu}/\#m$ (See Eq. A-11) (Eq. B-36)

In order to obtain the final form of the energy equation as a polynomial in θ , the water vapor pressure corresponding to saturation conditions at the temperature of the pond surface, P_w , in Eq. B-35, can be expressed by the following equation with an error of less than 2%.

$$P_w = a_1 + a_2 \theta + a_3 \theta^2 + a_4 \theta^3 \quad (\text{Eq. B-37})$$

where $a_1 = .089$ for $0 \leq \theta < 70$; $a_1 = .089$ $-32 < \theta \leq 0$
 $a_2 = 3.50 \times 10^{-3}$ for $0 \leq \theta < 70$; $a_2 = 4.00 \times 10^{-3}$ $-32 < \theta \leq 0$
 $a_3 = 5.68 \times 10^{-6}$ for $0 \leq \theta < 70$; $a_3 = 7.30 \times 10^{-5}$ $-32 < \theta \leq 0$
 $a_4 = 1.13 \times 10^{-6}$ for $0 \leq \theta < 70$; $a_4 = 5.20 \times 10^{-7}$ $-32 < \theta \leq 0$

where $\theta = \text{pond temperature in excess of } 32^{\circ}\text{F}$
 $\theta = T - 32^{\circ}\text{F}$

In order to reduce the number of variables in the final energy balance equation without introducing errors greater than 5% in the Q_c term for elevations up to 1000 feet above sea level (Q_c is itself only about 10%

as much as $\dot{m}_e \Delta h$ with the result that the total error introduced by this approximation is small), the value of $P_{BAR}/14.67$ in Eq. 36 can each be taken as a constant, namely;

$$\frac{P_{BAR}}{14.67} = 1, \quad \text{that is, sea level conditions are assumed.}$$

Using this assumption, the coefficient a_{14} is defined as:

$$a_{14} = \frac{5.05}{\Delta h} \frac{P_{BAR}}{14.67} = \frac{5.05}{1070} \left(\frac{14.67}{14.67} \right) = .00473 \quad (\text{Eq. B-38})$$

When Eq. B-38 and Eq. B-37 are substituted into Eq. B-36, the final simplified expression for the net transfer of energy that results from convection (\dot{Q}_c) and from water evaporating from the pond at the pond surface temperature and being replaced by water at the make-up temperature ($\dot{m}_e \Delta h$) becomes:

$$\begin{aligned} \dot{m}_e (\Delta h) + \dot{Q}_c &= (a_{12} + a_{13} W)(a_1 - a_{14} \theta_a - P_a) \\ &\quad + (a_{12} + a_{13} W)(a_2 + a_{14}) \theta \\ &\quad + [(a_{12} + a_{13} W) a_3] \theta^2 \\ &\quad + [(a_{12} + a_{13} W) a_4] \theta^3 \end{aligned} \quad (\text{Eq. B-39})$$

where $a_{12} = \Delta h (3.49) = 3730$

$a_{13} = \Delta h (.349) = 373$

θ_a = air temperature in excess of $32^\circ F$ or

$$\theta_a = T_a - 32^\circ F$$

APPENDIX C

DATA COLLECTED ON OPERATING COOLING PONDS

Several electric power companies furnished data on cooling ponds presently in operation. Sufficient data to allow a comparison of predicted and measured temperatures were made available on five plants, namely,

1. Wilkes Plant - Jefferson, Texas
2. Kincaid Plant - Kincaid, Illinois
3. Cholla Plant - Joseph City, Arizona
4. Mt. Storm Plant - Mt. Storm, West Virginia
5. Four Corners Plant - Farmington, New Mexico

The data for each plant are discussed in the following section.

Wilkes Plant

Southwestern Electric Power Company supplied data for their Wilkes Plant in Jefferson, Texas, together with an aerial photograph of the pond. These data are shown below together with a sketch of the pond site (Fig. C-1).

CIRCULATING WATER REPORT 1968

Month	Average Temperature, °F			Average Monthly Load (MW _e)
	IN	OUT	ΔT _c	
January	50	87	37	174.2
February	53	91	38	173.9
March	57	93	36	174.1
April	69	96	27	173.0
May	77	98	21	173.3
June	84	105	21	176.9
July	87	108	21	173.5
August	89	110	21	173.8
September	82	103	21	171.4
October	74	94	20	164.6
November	64	85	21	175.3
December	55	92	37	173.7

JOHNSON CREEK DAM AND RESERVOIR
Wilkes Power Plant

Water Temperatures

Drainage Area: 11.0 sq. miles

Capacity: 10,100 Acre feet

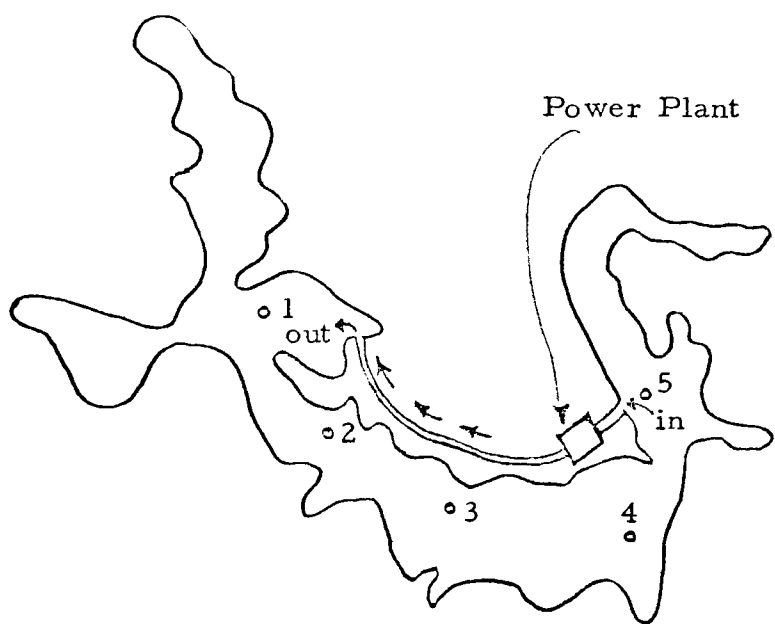
Area of Lake: 651 Acres

Average Depth: 15.5 feet

Max. Depth: 43.0 feet

Min. Depth: 0.0 feet

Station		Jan.	Feb.	Mar.	Apr.	May	June	July	Aug.	Sept.	Oct.	Nov.	Dec.
1	Surface	58	67	65	78	88	95	93	96	89	79	68	70
	2'	61	64	64	76	88	95	93	95	88	79	66	65
	5'	49	55	63	67	87	95	93	91	82	74	64	58
	10'	48	54	57	66	78	89	87	89	80	72	62	57
	15'	47	54	55	65	75	82	84	87	80	72	62	56
	19'4"	46	54	54	63	73	78	82	84	79	72	62	56
2	Surface	52	58	66	71	85	93	89	92	86	75	63	63
	2'	52	58	61	71	85	93	89	92	85	75	63	62
	5'	47	56	57	70	83	92	89	90	81	73	63	57
	10'	46	55	56	66	77	87	88	88	79	72	60	56
	15'	45	55	56	65	75	80	84	86	79	72	60	56
	18'6"	45	55	56	65	72	75	81	80	78	72	60	56
3	Surface	50	57	54	74	82	91	98	92	85	75	64	61
	2'	50	57	54	74	82	91	88	92	85	75	64	60
	5'	48	56	54	73	81	91	88	91	82	74	62	58
	10'	47	54	54	66	78	88	86	88	80	72	61	56
	15'	46	54	54	65	75	81	84	86	80	72	61	56
	22'9"	46	54	54	63	66	67	71	71	75	72	61	56
4	Surface	48	53	54	70	80	89	86	89	82	73	63	62
	2'	48	53	54	70	80	89	86	89	82	73	63	60
	5'	47	53	54	69	80	89	86	88	81	73	63	57
	10'	47	53	54	66	78	87	85	88	79	72	63	56
	15'	46	52	54	65	74	79	84	87	79	72	62	56
	32'6"	45	51	52	57	57	59	58	58	59	60	61	55
5	Surface	46	52	54	65	80	89	86	89	74	73	63	55
	2'	46	52	54	65	80	89	86	89	79	73	63	55
	5'	45	52	54	65	80	89	86	89	79	73	63	55
	10'	45	52	54	65	80	89	85	89	79	73	63	55
	15'	44	52	54	65	79	81	85	88	79	72	62	54
	23'8"	44	52	54	60	62	65	65	69	71	72	61	54



SKETCH OF THE WILKES PLANT POND

Fig. C-1

In addition to these data, the energy conversion efficiency of the plant must be known in order to determine the waste thermal energy load imposed on the pond. For the Wilkes Plant the average annual heat rate (btu of chemical energy into the plant per kw-hr of net generation) is given as 9,854 in Ref. 25. Of this 9,854 btu, 3413 btu are converted to electric energy; a small fraction (say α_2) is rejected directly to the atmosphere primarily in the exhaust gases and the remainder is rejected to the condenser cooling water.

The waste thermal energy (WTE) rejected to the pond can then be expressed:

$$WTE = [(H.R.) (1 - \alpha_2) - 3413] (MW_e) (24 \times 10^3) \text{ btu/day} \quad (\text{Eq. C-1})$$

where H.R. = annual average heat rate in btu per kw-hr

α_2 is assumed to be constant at 10% for the plants under consideration.

However, the heat rate will vary somewhat with the time of year. This variation is usually small ($\sim \pm 2\%$). Here it has been approximated as eight hundredths of one percent for each $^{\circ}\text{F}$ deviation of the condenser cooling water from its yearly average value. Thus the heat rate to be used to calculate the waste thermal energy as given by Eq. C-1 for any given time of the year becomes:

$$(heat rate) = (heat rate)_{\substack{\text{annual} \\ \text{average}}} + .0008 (T_{\substack{\text{ave} \\ \text{condenser} \\ \text{outlet}}} - T_{\substack{\text{condenser} \\ \text{outlet}}}) \quad (\text{Eq. C-2})$$

where $T_{\substack{\text{ave} \\ \text{condenser} \\ \text{outlet}}} = 96.9^{\circ}\text{F}$ for the Wilkes Plant

The climatic data were obtained from the nearest Weather Station at Shreveport, Louisiana, about 40 miles away, and are given in Table C-1.

Since the measured solar radiation was not available in the "Annual Summary" given in Table C-1, values had to be taken as the average value over a period of years as given in Ref. 7 and repeated below.

TABLE C - 1

SHREVEPORT, LOUISIANA

METEOROLOGICAL DATA FOR 1968

LATITUDE 32° 28' N
 LONGITUDE 93° 49' W
 ELEVATION (ground) 254 Feet

Month	Temperature								Degree days	Precipitation						Relative humidity							
	Averages				Extremes					Total	Greatest in 24 hrs.	Date	Total	Greatest in 24 hrs.	Date	Total	Greatest in 24 hrs.	Date	Total	Greatest in 24 hrs.			
	Daily maximum	Daily minimum	Monthly	High heat	Date	Lowest	Date	Degree days		Total	Greatest in 24 hrs.	Date	Total	Greatest in 24 hrs.	Date	Total	Greatest in 24 hrs.	Date	Total	Greatest in 24 hrs.			
JAN	53.2	37.5	45.4	76	31	18	8	604	8.33	2.85	8-9	1-0	1.0	8	83	87	73	75	71	78	54	52	
FEB	54.4	32.8	43.6	69	27	21	22	614	2.22	0.97	14-15	0.4	0.4	22-23	80	88	60	58	80	85	57	59	
MAR	67.3	44.4	55.9	82	10	23	1	308	1.89	0.78	21-22	1.5	1.5	21-22	79	85	57	59	81	86	62	60	
APR	76.5	56.4	66.5	85	22	39	6	49	9.38	2.50	27-28	0.0	0.0	0.0	81	89	58	62	83	89	62	60	
MAY	82.2	63.1	72.7	90	24	51	1	U	6.05	1.38	9-10	0.0	0.0	0.0	83	89	58	62	71	78	54	52	
JUN	89.6	70.5	80.1	97	12	59	27	0	2.78	1.63	26	0.0	0.0	0.0	83	89	58	62	80	88	60	58	
JUL	90.4	71.5	81.0	96	18	62	5	0	4.68	2.12	18	0.0	0.0	0.0	83	88	60	61	83	87	57	64	
AUG	91.5	72.4	82.0	95	25+	64	29	0	1.89	1.09	10-11	0.0	0.0	0.0	82	88	57	62	82	85	52	64	
SEP	83.8	63.4	73.6	92	2	56	27+	0	9.59	5.14	14-15	0.0	0.0	0.0	82	88	57	62	82	88	57	62	
OCT	78.0	55.2	66.6	88	2+	38	29	57	1.90	0.94	9	0.0	0.0	0.0	82	85	52	64	80	86	57	67	
NOV	64.4	42.9	53.7	83	1	28	12	346	5.85	1.65	30	0.0	0.0	0.0	80	86	57	67	72	77	56	59	
DEC	57.0	36.2	46.6	70	27	24	24	560	3.27	1.39	12	T	T	22	72	77	56	59	80	85	59	62	
YEAR	74.0	53.9	64.0	97	12	18	JAN.	8	2538	57.83	5.14	14-15	2.9	1.5	21-22	80	85	59	62	80	85	59	62

Month	Wind								Sunrise to sunset	Number of days						Temperatures					
	Resultant		Average speed		Fastest mile		Percent of possible sunshine	Average sky cover sunrise to sunset		Precipitation			Thunderstorms			Maximum		Minimum			
	Direction	Speed	Direction	Speed	Direction	Date				Clear	Partly cloudy	Cloudy	0.1 inch or more	Snow, Sleet	1.0 inch or more	Heavy fog	90 and above	32 and below	22 and below	0 and below	
JAN	09	2.0	8.5	23	30	13+	31	8.2	4	3	24	15	1	1	3	0	0	0	13	15	
FEB	35	2.6	8.5	23	32	29	60	5.9	11	3	15	6	0	0	0	0	0	0	15	6	
MAR	19	3.1	9.3	22	29	20+	47	7.3	5	5	21	11	1	4	0	0	0	0	0	0	
APR	16	2.7	9.0	22	34	27	49	6.7	7	6	17	12	0	7	1	1	0	0	0	0	
MAY	17	3.2	8.0	30	34	17	57	6.2	7	10	14	12	0	9	1	1	0	0	0	0	
JUN	17	3.5	6.8	29	16	24	59	6.4	6	11	13	10	0	6	0	20	0	0	0	0	
JUL	16	2.3	6.3	28	13	18+	63	6.4	7	12	12	8	0	9	0	22	0	0	0	0	
AUG	16	2.8	6.1	30	35	7	68	5.3	11	12	8	11	0	8	1	24	0	0	0	0	
SEP	12	1.2	6.1	21	3	15+	68	4.8	13	8	9	6	0	4	2	7	0	0	0	0	
OCT	18	0.8	6.4	21	36	9+	67	4.6	12	12	7	5	0	2	3	0	0	0	0	0	
NOV	25	1.2	8.6	32	25	15	53	5.6	10	6	14	9	0	6	1	0	0	2	1	0	
DEC	20	1.4	9.0	33	28	27	52	6.1	11	4	16	9	0	2	1	0	0	11	0	0	
YEAR	17	1.5	7.7	33	28	27	57	6.1	104	92	170	114	2	58	13	74	2	47	0	0	0

Solar Radiation for Shreveport, Louisiana

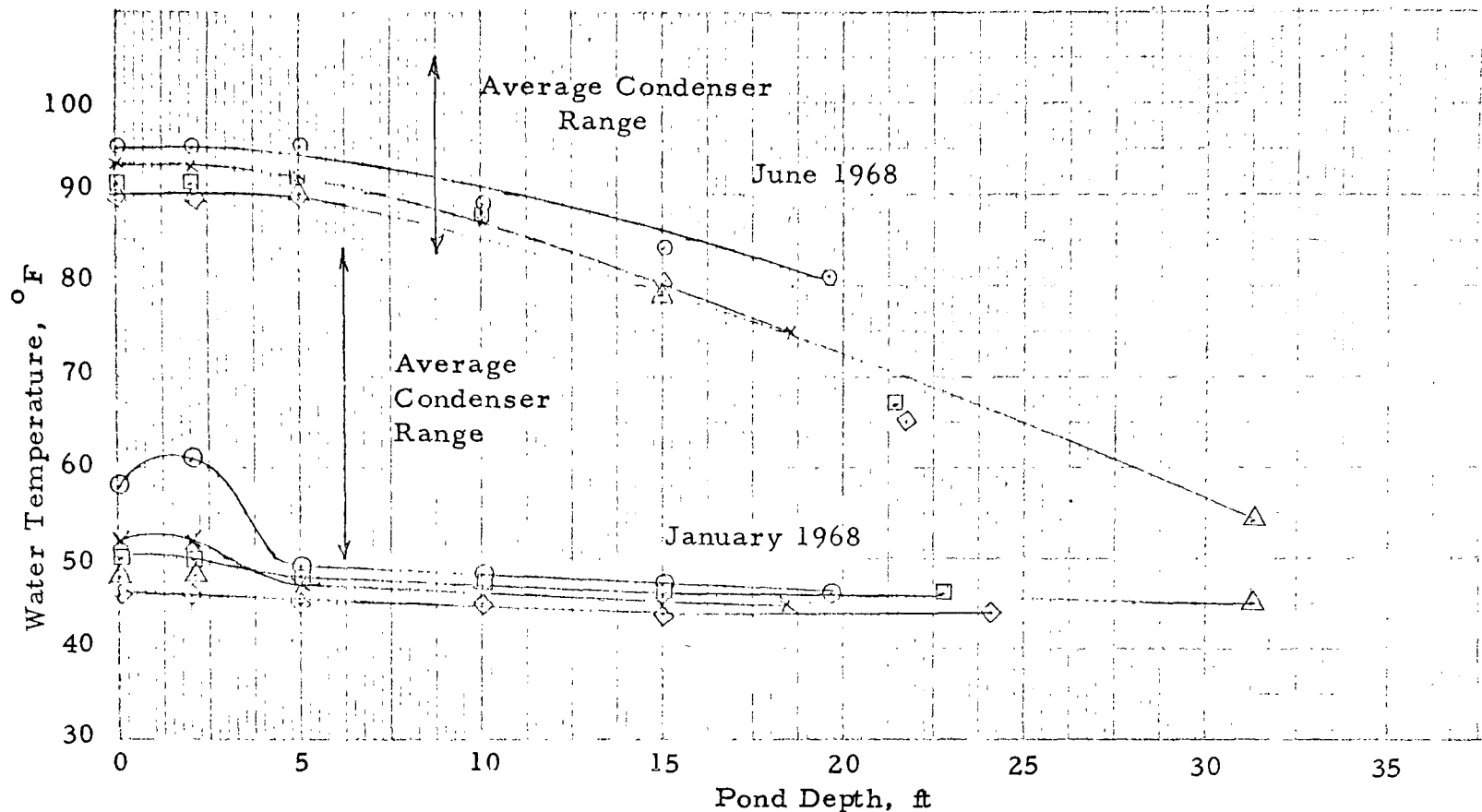
Month	Solar Radiation, Q_a (Langley's/day)
January	232
February	292
March	384
April	446
May	558
June	557
July	578
August	528
September	414
October	354
November	254
December	205

The parameters necessary to use the curves presented in the text of the report can be calculated from the above data and the desired temperatures determined. The results are shown in Table C-2 for steady state pond operation.

Fig. C-2 shows the measured temperature-depth profile for the various stations along the flow direction for January and June. From this figure it can be concluded that considerable lateral and longitudinal mixing occurs near the hot end of the pond where the heated water enters the pond from the discharge canal. It is also apparent that the upper few feet (up to 5 feet) of water is well mixed vertically so that the temperature in this upper region at any one station is essentially uniform.

If the measured temperature-depth profile is approximated with a straight line, the slope of the line (β) would be approximately $0.3^{\circ}\text{F}/\text{ft}$ for January and $1.0^{\circ}\text{F}/\text{ft}$ for June.

L41



See Sketch of Plant Site for Station Locations
(Fig. C-1)

Wilkes Plant: Measured Temperature - Depth Profile - January and June 1968

Figure C-2

TABLE C-2 - Wilkes Data 1968

	Jan	Feb	Mar	Apr	May	June	July	Aug	Sep	Oct	Nov	Dec
Q_N btu/ft ² day	2880	3202	3670	4108	4820	5240	5260	5050	4458	3818	3132	281
T_a , °F	45.4	43.6	55.9	66.5	72.7	80.1	81.0	82.0	73.6	66.6	53.7	46.0
P_a , psia	.105	.114	.156	.245	.280	.384	.417	.386	.322	.228	.150	.120
W, mph	8.5	8.5	9.3	9.0	8.0	6.8	6.3	6.1	6.1	6.4	8.6	9.0
$a_{12} + a_{13} W =$ $3730 + 3730 W / 10$	6900	6900	7190	7080	6720	6260	6080	6000	6000	6110	6920	7080
$-3730(1+W/10)$ $\times (.089)$ $- \theta_a (.0042) - P_2$	515	552	1293	2260	2570	3130	3470	3200	2610	1850	1140	841
$\dot{Q}_{pp} = WTE/A$	776	787	792	792	801	79	821	834	805	750	778	788
f_1	1036	1395	2604	4009	5031	6011	6371	5891	4709	3309	1913	1299
$f_1 + \dot{Q}_{pp}$	1812	2182	3396	3801	5832	6802	7192	6725	5514	4059	2691	2087
$A(\Delta T_c)/WTE$.0475	.0481	.0454	.0340	.0263	.0265	.0255	.0251	.0261	.0266	.0269	.0472
ΔT_c , °F	37	38	36	27	21	21	21	21	21	20	21	37
T_{equil} , °F	45.2	48.8	58.8	69.4	77.2	85.5	88.0	86.0	78.5	67.6	54.1	47.3
T_{mixed} , °F (steady state)	53.2	56.3	65.0	75.0	82.5	90.0	92.7	90.6	83.5	73.3	60.3	54.7
$T_{slug flow}$, °F (steady state)	45.4	49.0	59.9	69.5	77.3	85.5	88.0	86.0	78.6	67.9	54.9	47.7

Kincaid Plant

Commonwealth Edison Company supplied data for their Kincaid Plant in southern Illinois together with a map of the site. These data together with a sketch of the site follow.

Monthly Average Power Generation - 1968 - Kincaid

Month	Gross Generation	Condenser Inlet Water Temp °F	Actual Heat Rate btu/net kw-hr
January	239, 530 MWHR	35	10, 200
February	259, 072 "	38	10, 470
March	232, 382 "	41	10, 570
April	65, 256 "	55	
May	329, 160 "	62	10, 800
June	556, 984 "	80	10, 340
July	535, 687 "	86	10, 340
August	608, 715 "	88	10, 390
September	395, 030 "	79	10, 200
October	293, 811 "	68	10, 150
November	364, 708 "	67	10, 300
December	635, 320 "	51	10, 140
Total	124, 515, 655 "		
1968 Avg.	376, 304. 6 "		

Total Surface Area of Cooling Lake - 2700 acres

Average depth of cooling lake - 10 feet

Total volume of cooling lake - 35,000 acre-ft

ΔT_c = about 18°F at full load

Eq. C-1 was used to determine the waste thermal energy rejected to the pond from the given heat rate and electric energy generating rate.

The climatic data (except for solar radiation which was taken as the average monthly values from Ref. 12) were obtained from the nearest Weather Station at Springfield, Illinois. These data are given in Table C-3, followed by the data for solar radiation.

TABLE C - 3

SPRINGFIELD, ILLINOIS

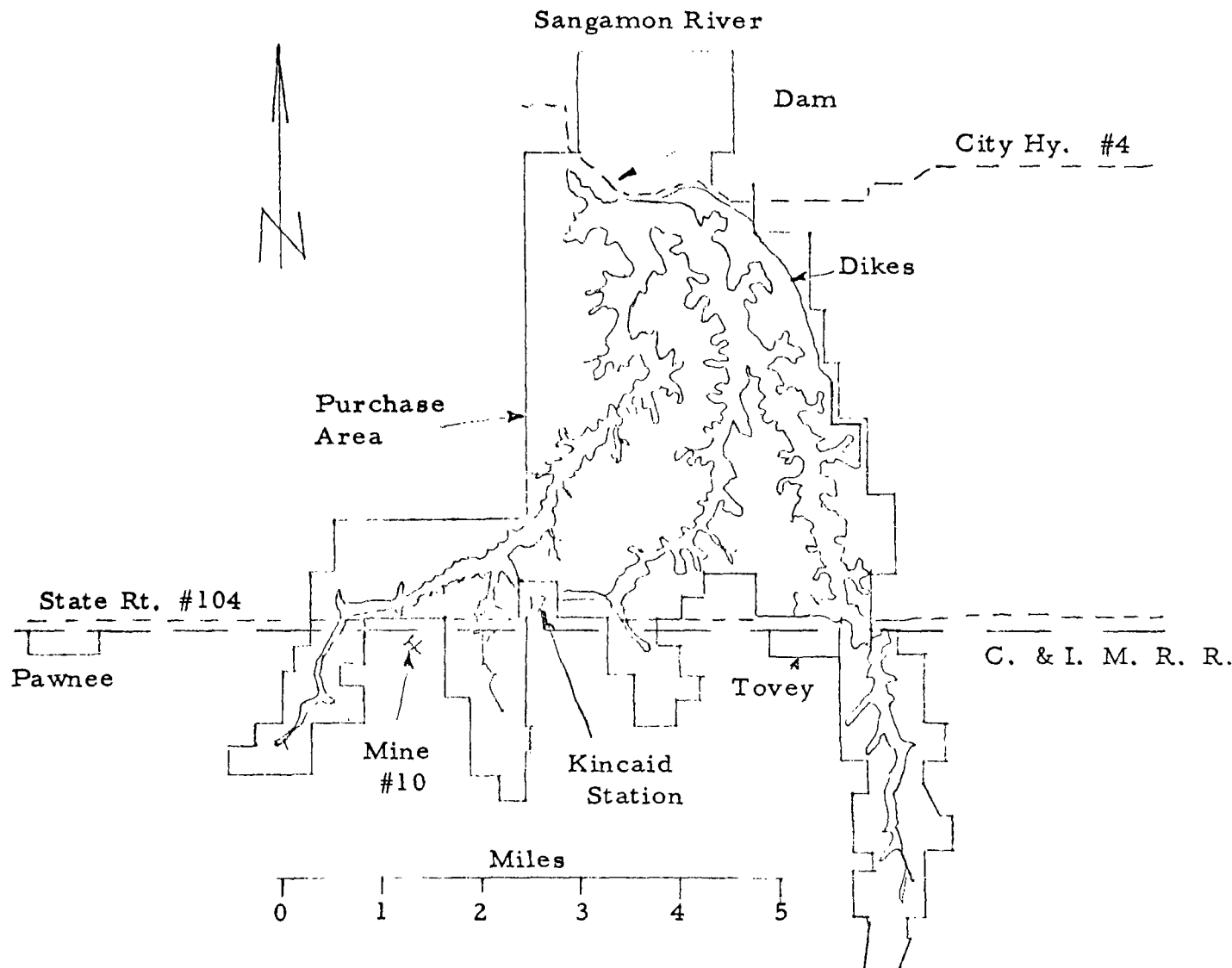
METEOROLOGICAL DATA FOR 1968

LATITUDE 39° 50' N
 LONGITUDE 89° 40' W
 ELEVATION (ground) 588 Feet

SPRINGFIELD, ILLINOIS
 CAPITAL AIRPORT
 1968

Month	Temperature								Precipitation								Relative humidity			
	Averages				Extremes				Degree days				Snow, Sleet				Mid.			
	Daily maximum	Daily minimum	Monthly	Highest Date	Lowest Date	Degree days Total	Greater in 24 hrs.	Date	Total	Greater in 24 hrs.	Date	Standard time used: CENTRAL	8 AM	Noon	6 PM					
JAN	31.1	16.4	23.8	57 29 -14 7	1271	1.79	0.52	13-14+	13.0	5.4	12-13	76	76	72	74					
FEB	34.6	16.6	25.6	59 1 22	1134	1.15	1.08	31-1	1.7	0.8	6-7	69	70	51	54					
MAR	54.1	31.4	42.8	78 28 3 13	684	1.25	0.55	15	4.5	3.4	12	65	70	52	51					
APR	64.1	41.7	52.9	79 30+ 29 6	358	2.44	1.87	3	1.7	1.7	5	66	73	50	50					
MAY	69.3	48.7	59.0	87 15+ 37 6	203	5.69	2.38	22-23	0.0	0.0	74	77	58	58						
JUN	85.5	63.5	74.5	96 30+ 50 28+	8	3.25	2.63	14-15	0.0	0.0	70	74	50	50						
JUL	96.4	65.2	75.8	95 13 51 3	1	4.67	1.41	27	0.0	0.0	77	80	54	57						
AUG	85.4	65.0	75.2	96 23+ 49 28	2	0.99	0.52	3-4	0.0	0.0	80	86	56	60						
SEP	78.5	54.8	66.7	88 22+ 44 27+	31	3.29	1.69	17-18	0.0	0.0	81	86	54	62						
OCT	66.7	42.9	54.8	86 15 26 29	353	1.43	1.03	13	0.0	0.0	74	81	51	56						
NOV	48.7	33.9	41.3	74 1 19 13	703	3.08	1.47	28	0.7	0.3	80	83	66	73						
DEC	36.5	21.6	29.1	54 12 -5 31	1107	2.64	1.07	27-28	4.7	1.5	30	78	80	68	72					
YEAR	61.7	41.8	51.8	96 AUG- 23+ -14 7	5855	31.67	2.63	14-15	24.6	5.4	JUN- 14-15	74	78	57	60					

Month	Wind								Number of days								Temperatures				
	Resultant		Fastest mile		Sunrise to sunset				Precipitation				Thunderstorms				Maximum		Minimum		
	Direction	Speed	Average speed	Speed	Direction	Date	Percent of possible sunshine	Average sky cover sunrise to sunset	Clear	Partly cloudy	Cloudy	Precipitation .01 inch or more	Snow, Sleet .10 inch or more	Heavy log 90° and above	32° and below	32° and below	0 and below				
JAN	19	1.7	11.4	28	S	5	51	6.4	9	6	16	10	5	1	5	0	17	27	2	7	
FEB	29	7.4	12.4	32	NW	16	66	4.7	15	3	11	6	2	1	1	0	12	28	2	2	
MAR	24	4.0	14.7	36	NE	12	60	6.4	7	9	15	8	0	3	2	2	16	5	0	0	
APR	19	5.1	13.5	41	W	23	61	5.8	7	11	12	9	0	3	1	0	0	0	0	0	
MAY	22	2.2	11.4	35	SW	15	53	6.9	5	9	17	15	0	9	1	0	0	0	0	0	
JUN	20	4.7	9.6	29	W	14	74	4.8	15	5	10	7	0	5	0	10	12	13	0	0	
JUL	19	2.2	8.0	34	SW	14	69	5.2	12	7	12	10	0	0	11	0	12	0	0	0	
AUG	19	3.4	8.7	20	SW	24	71	5.3	11	8	12	5	0	5	1	0	13	0	0	0	
SEP	19	4.1	9.0	26	SE	18	66	5.4	12	6	12	9	0	3	0	0	0	0	0	0	
OCT	20	6.2	11.4	32	SW	27	71	4.7	14	7	10	8	0	3	0	0	0	0	0	0	
NOV	28	3.2	10.8	34	SW	28	30	8.1	3	6	21	12	0	0	0	0	0	0	0	0	
DEC	23	5.5	14.6	42	W	23+	38	7.2	6	6	19	12	3	0	0	11	0	15	0	0	
YEAR	22	3.3	11.3	42	W	DEC-	60	5.9	116	83	167	111	10	42	17	35	42	120	10		



Kincaid Plant and Cooling Pond

Figure C-3

Solar Radiation for Springfield, Illinois

Month	Solar Radiation btu/ ft^2 day
January	608
February	885
March	1200
April	1513
May	1883
June	2070
July	2050
August	1870
September	1582
October	1132
November	738
December	534

Although the pond surface is 2700 acres, only two arms of the three-arm "pond" is involved in the cooling circuit; the third arm provides storage. In addition to the question of effective area due to the three-arm shape of the "pond", the highly irregular shape also increases the uncertainty of the effective area because of the possibility of zones of dead water. From the map provided with the data it was estimated that 60% of the 2700 acres (or 1620 acres) was effective. The predicted pond temperatures, based on an active surface area of 1620 acres, are shown in Table C-4 for steady state operation.

TABLE C-4 - Kincaid Data 1968

	Jan	Feb	Mar	Apr	May	June	July	Aug	Sept	Oct	Nov	Dec
Q_N , btu/ ft^2day	2060	2345	3008	3560	4033	4620	4690	4440	3940	3270	2565	2138
T_a , $^{\circ}\text{F}$	23.8	25.6	42.8	52.9	59.0	74.5	75.8	75.2	66.7	54.8	41.3	29.1
P_a , psia	.024	.041	.082	.119	.166	.256	.294	.302	.229	.1385	.102	.059
W, mph	11.4	12.4	14.7	13.5	11.4	9.6	8.0	8.7	9.0	11.4	10.8	14.6
$a_{12} + a_{13} W$ $= (3730 + 3730W/10)$	7980	8350	9200	8760	7960	7300	6710	6960	7090	7980	7750	4160
$-3730(1+W/10)$ $x[.089 - \theta_a x(.00473) - P_a]$	-830	-650	406	1125	1630	2690	2770	2910	2790	1340	465	0394
$\dot{Q}_{pp} = WTE/A$	988	1202	1013	304	1485	2520	2260	2580	1745	1208	1635	2610
f_1	-1061	-585	1152	2429	3434	5071	5241	5121	4493	2359	744	-549
$f_1 + \dot{Q}_{pp}$	-49	617	2165	2733	5064	7761	8011	7701	6238	3567	2379	2061
$A(\Delta T_c)/WTE$.0182	.0149	.0177	.0593	.0121	.0071	.0080	.0070	.0103	.0149	.0110	.0069
ΔT_c , $^{\circ}\text{F}$	18	18	18	18	18	18	18	18	18	18	18	18
T_{equil} , $^{\circ}\text{F}$	19.0 will ice	25.5 will ice	43.2	54.6	63.5	75.8	77.0	77.0	73.1	55.5	44.8	26.2 will ice
T_{mixed} , $^{\circ}\text{F}$ (steady state)	32.0	38.8	51.6	57.1	74.2	90.2	93.5	91.2	83.0	64.5	56.1	50.5
$T_{slug flow}$, $^{\circ}\text{F}$ (steady state)	23.0	32.0	44.9	54.6	66.8	80.8	83.4	82.2	76.6	57.2	47.8	40.4

Cholla Plant

Arizona Public Service Co. supplied data for their Cholla plant in Joseph City, Arizona, together with a sketch of the site. These data are given below and in Fig. C-4.

1967 Station Net Output (MW-HR)

Jan	53, 341.8	July	70, 303. 9
Feb	54, 562.8	Aug	88, 501. 9
Mar	64, 635.1	Sept	81, 903. 9
April	63, 488.2	Oct	72, 289. 6
May	1, 377.5	Nov	77, 748. 9
June	40, 978.0	Dec	65, 024. 1

Average 61, 176. 3 MW-HR

Pond surface area: 380 acres

Total plant rating in megawatts: 115 MW

Average Temperature into Condenser by Month - 1967

<u>Month</u>	<u>°F</u>	<u>Month</u>	<u>°F</u>
Jan	44	July	82
Feb	52	Aug	84
Mar	58	Sept	80
Apr	60	Oct	72
May	60	Nov	65
June	70	Dec	53

Average depth of pond: 4. 5 ft

Maximum depth of pond: 12 ft

Minimum depth of pond: 1 in.

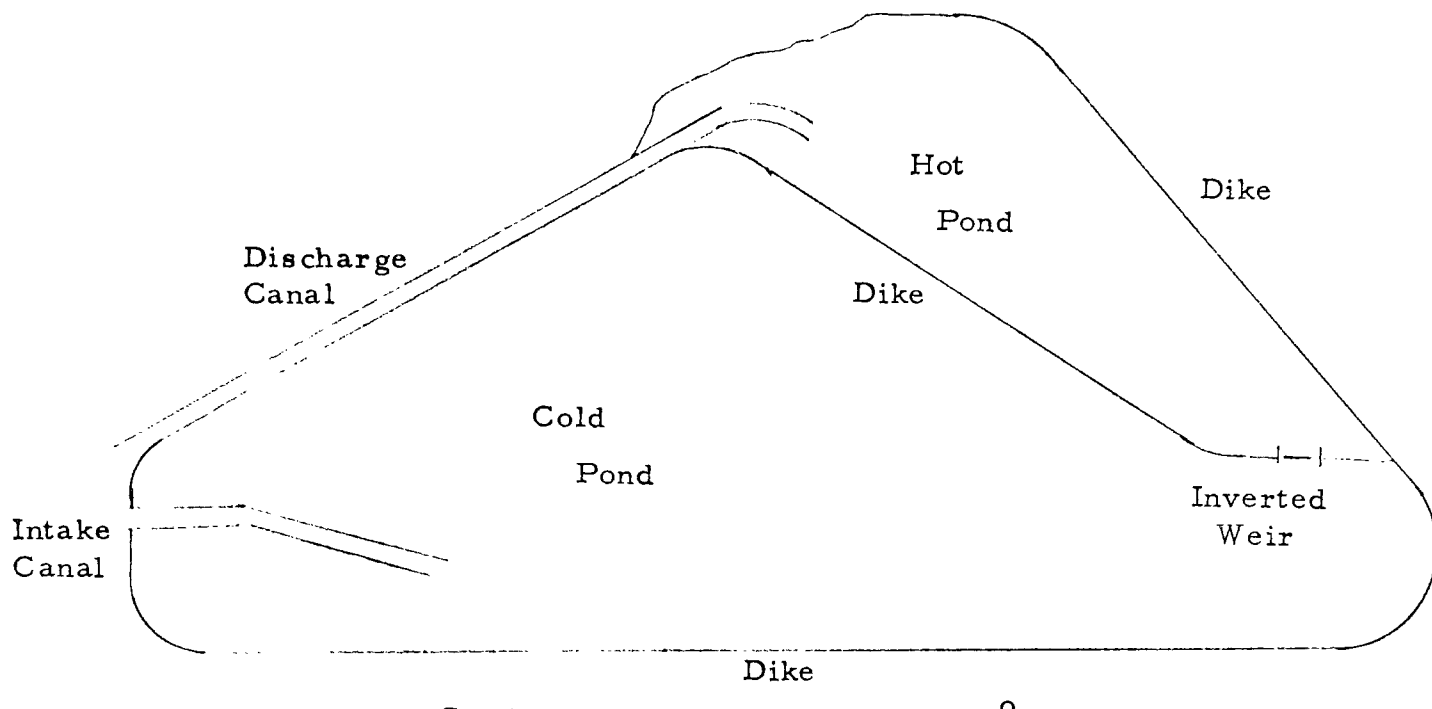
Typical temperature depth profiles in pond:

(Pond too shallow for enough variation in temperature to matter)

Temperature rise across the condenser: 20°

For the Cholla Plant the average heat rate is given as 9, 838 btu/kw-hr in Ref. 25. The waste thermal energy rejected to the pond was calculated by use of Eq. C-1 and C-2 where for this plant

$$T_{\text{average condenser outlet}} = 84.9^{\circ}\text{F}$$



Cholla Plant: Cooling Pond

Figure C-4

The climatic data ~~were~~ obtained from the summary of the Winslow, Arizona, Weather Station for 1967, about 25 miles away, except for the solar radiation (not available at Winslow) which was obtained from the records at Albuquerque. These data are given in Table C-5 (Solar radiation data given below).

Because of the shallowness of this pond together with the pond shape, it is most likely that substantial channeling of the flow occurs with the result that only some of the pond surface area will effectively take part in the cooling circuit. It is assumed that only 1/3 of the total pond area of 380 acres (or 127 acres) will be effective. The tabulated parameters and predicted temperatures are shown in Table C-6 for steady state pond operation.

If it is assumed that the entire pond surface is effective in transmitting energy to the atmosphere, the predicted pond temperatures will be lower than the values given in Table C-6 and are given in Table C-7.

Solar Radiation for Albuquerque

<u>Month</u>	<u>Solar Radiation (Langley's/day)</u>
January	303
February	386
March	505
April	618
May	695
June	729
July	677
August	624
September	541
October	440
November	325
December	274

TABLE C - 5

WINSLOW, ARIZONA

METEOROLOGICAL DATA FOR 1967

LATITUDE 35° 01' N
 LONGITUDE 110° 44' W
 ELEVATION (ground) 4895 Feet

WINSLOW, ARIZONA
 MUNICIPAL AIRPORT
 1967

Month	Temperature								Degree days	Precipitation						Relative humidity							
	Averages				Extremes					Total	Greatest in 24 hrs.	Date	Snow, Sleet			Total	Greatest in 24 hrs.	Date	5 AM	11 AM	5 PM	11 PM	
	Daily maximum	Daily minimum	Monthly Highest	Date	Lowest	Date	Degree	hrs.					AM	PM	AM	PM	AM	PM	Standard time used:	MOUNTAIN			
JAN	47.5	14.9	31.2	67	30	5	2		1038	0.10	0.10	23	T	T	25	+ 75	58	37	66				
FEB	57.1	21.7	39.4	71	13	10	8		711	0.01	0.01	20	0.1	0.1	20	46	29	18	33				
MAR	67.0	31.2	49.1	80	23	13	13		485	0.24	0.19	29	0.1	0.1	5	45	22	17	33				
APR	68.3	32.1	50.2	79	3	22	20		440	0.10	0.05	9	0.4	0.4	12	46	21	17	34				
MAY	77.9	42.2	60.1	92	23+	24	1		182	0.27	0.25	30	0.0	0.0	31	17	14	25					
JUN	85.9	53.5	69.7	96	30+	43	6		6	1.06	0.69	18-19	0.0	0.0	40	23	18	32					
JUL	92.2	64.4	78.3	101	3+	59	8+	0	2,67	0.78	12	0.0	0.0		56	36	34	49					
AUG	90.6	60.6	75.6	96	26+	55	21	0	1,09	0.48	28	0.0	0.0		59	39	30	49					
SEP	84.3	54.2	69.3	92	4	43	14	11	0.49	0.21	24	0.0	0.0		61	38	29	52					
OCT	76.0	38.0	57.0	87	1	25	30	252	0.11	0.11	3	0.0	0.0		44	24	15	31					
NOV	63.4	30.8	47.1	75	15	23	14	528	0.36	0.29	22	0.2	0.2	29	54	37	27	46					
DEC	33.0	9.8	21.4	59	7	-12	22	1344	3.73	1.51	13-14	39.6	17.0	13-14	76	65	63	73					
YEAR	70.3	37.8	54.1	101	3+	-12	22	4997	10.23	1.51	13-14	40.4	17.0	13-14	53	34	27	44					

Month	Wind								Percent of possible sunshine	Number of days						Temperatures						
	Resultant		Average speed	Fastest mile				Average sky cover sunrise to sunset		Sunrise to sunset			Precipitation	Snow, Sleet	1.0 inch or more	Thunderstorms						
	Direction	Speed		Speed	Direction	Date	Clear			Partly cloudy	Cloudy	0.1 inch or more				90 and above	32 and below	32 and below	0 and below	below		
JAN	20	2.7	7.0	43	20	5	5.1	14	6	11	1	1	0	0	0	0	0	0	0	28	5	
FEB	26	2.6	8.2	44	22	14	3.5	16	6	6	1	1	0	0	0	0	0	0	25	0		
MAR	20	6.7	10.8	46	19	29	5.7	12	6	13	3	1	0	0	0	0	0	0	17	0		
APR	20	10.1	13.3	52	18	12	3.2	20	4	6	3	3	0	0	0	0	0	0	22	0		
MAY	23	5.1	10.0	30	23	5	4.1	16	8	7	3	3	0	0	0	0	0	0	4	0		
JUN	21	6.4	10.7	37	19	5	3.0	19	8	3	3	3	5	0	0	0	0	0	0	0		
JUL	23	3.6	8.2	35	26	4	6.5	5	12	14	11	0	16	0	0	20	0	0	0	0	0	
AUG	14	1.4	7.8	35	30	23	4.9	12	10	9	9	0	14	0	0	21	0	0	0	0	0	
SEP	19	1.7	8.3	32	21	24	4.2	14	11	5	7	0	7	0	0	4	0	0	0	0	0	
OCT	24	2.0	7.6	26	34	29	2.5	21	7	3	1	0	0	0	0	0	0	0	7	0		
NOV	19	2.3	7.0	29	19	28	3.7	16	9	5	3	3	0	0	0	0	0	0	22	0		
DEC	23	3.1	7.8	39	22	16	4.5	16	4	11	6	4	0	0	0	0	0	0	31	9		
YEAR	21	3.7	8.9	52	18	12	4.2	181	91	93	51	5	45	4	57	20	156	14				

TABLE C-6 - Cholla Plant - 1967

	Jan	Feb	Mar	Apr	May	June	July	Aug	Sept	Oct	Nov	Dec
\dot{Q}_N , btu/ ft^2 day	2212	2615	3300	3825	4450	5270	5030	4750	4160	3450	2700	2085
T_a , °F	31.2	39.4	49.1	50.2	60.1	69.7	78.3	75.6	69.3	57.0	47.1	21.4
P_a , psia	.024	.025	.050	.052	.058	.097	.206	.193	.154	.084	.062	.041
W, mph	7.0	8.2	10.8	13.3	10.0	10.7	8.2	7.8	8.3	7.6	7.0	7.8
$a_{12} + a_{13} W + (3730 + 3730W/10) - 3730(1 + W/10)$	6350	6780	7750	8690	7450	7710	6780	6640	6820	6550	6350	6640
$x[.089 - \theta_a \times (.00473) - P_a]$	-438	-203	364	425	758	1432	2260	2050	1640	740	280	-664
$\dot{Q}_{pp} = WTE/A^*$	1599	1680	2034	2004	45	1338	2385	3030	2766	2355	2505	2010
f_1	-585	53	1305	1891	2849	4343	4931	4991	3441	1831	621	-938
$f_1 + \frac{\dot{Q}_{pp}}{WTE}$	1014	1733	3339	3895	2894	5681	7316	7471	6207	4186	3126	1072
$A(\Delta T_c)/WTE$.0125	.0119	.0098	.0099	.444	.0148	.0084	.0066	.0068	.0085	.0080	.0099
ΔT_c , °F	20	20	20	20	20	20	20	20	20	20	20	20
T_{equil} , °F will ice	23.5	32.2	46.5	50.8	60.0	70.0	76.6	74.3	66.8	53.5	40.6	18.6 will ice
T_{mixed} (steady state)	45.0	52.6	63.7	64.7	60.2	78.2	90.3	91.5	84.0	73.1	66.0	45.8
$T_{slug flow}$ (steady state)	39.0	41.0	53.5	56.8	60.0	71.2	80.6	84.3	76.8	64.5	54.6	41.0

*The effective area, A, is assumed to be 1/3 of actual surface area.

TABLE C-7 - Cholla Plant, 1967 (Cont.)

	Jan	Feb.	Mar	Apr	May	June	July	Aug	Sept	Oct	Nov.	Dec.
$\dot{Q}_{pp} = WTE/A^*$	532	559	675	668	15	432	786	1010	915	778	828	665
$f_1 + \dot{Q}_{pp}$	-53	612	1980	2559	2864	4775	5717	5451	4356	2609	1449	-273
T _{mixed} (Steady state)	31.5 will ice	40.2	52.7	56.0	60.1	76.8	81.5	80.2	72.9	60.7	50.0	28.1 will ice

* Effective area is assumed to equal actual surface area of pond.

Mt. Storm Plant

Virginia Electric and Power Co. provided data on their Mt. Storm plant at Mt. Storm, West Virginia, together with a sketch of the cooling pond (Fig. C-5). Some of these data are presented below.

Circulating Water Temperature, °F

Month	Intake	Discharge	Net Generation for Month, kw-hr
January	45.0	64.3	718,415,900
February	43.5	62.8	576,140,500
March	43.5	62.8	705,117,000
April	50.0	69.3	582,202,600
May	61.0	80.3	577,455,100
June	69.0	88.3	603,031,300
July	77.0	96.3	533,818,300
August	81.5	100.8	594,162,000
September	78.0	97.3	519,600,000
October	64.5	83.8	204,414,500
November	53.0	72.3	311,167,000
December	44.0	63.3	462,693,000

Pond surface area = 1125 acres (at full pool)

Pond volume = 48,000 acre-ft (at full pool)

Temperature rise across the condenser - 19.3°F at full load

Using the same assumptions as for the Wilkes and Cholla plants and the yearly average heat rate of 9,405 btu from Ref. 25, the waste thermal energy can again be expressed by Eq. C-1 and Eq. C-2 where:

$$T_{\text{average condenser outlet}} = 78.4^{\circ}\text{F}$$

The climatic data were obtained from the data collected at the Weather Station at Elkins, West Virginia, about 70 miles away. Solar radiation data had to be taken from the maps in Ref. 12. The weather station data is given in Table C-8.

Solar Radiation - Elkins

Month	btu/ $\text{ft}^2 \text{ day}$	Month	btu/ $\text{ft}^2 \text{ day}$	Month	btu/ $\text{ft}^2 \text{ day}$
Jan	725	May	1620	Sept	1520
Feb	1133	June	2170	Oct	892
Mar	1392	July	2010	Nov	555
Apr	1732	Aug	1850	Dec	545

TABLE C - 8

ELKINS, WEST VIRGINIA

METEOROLOGICAL DATA FOR 1968

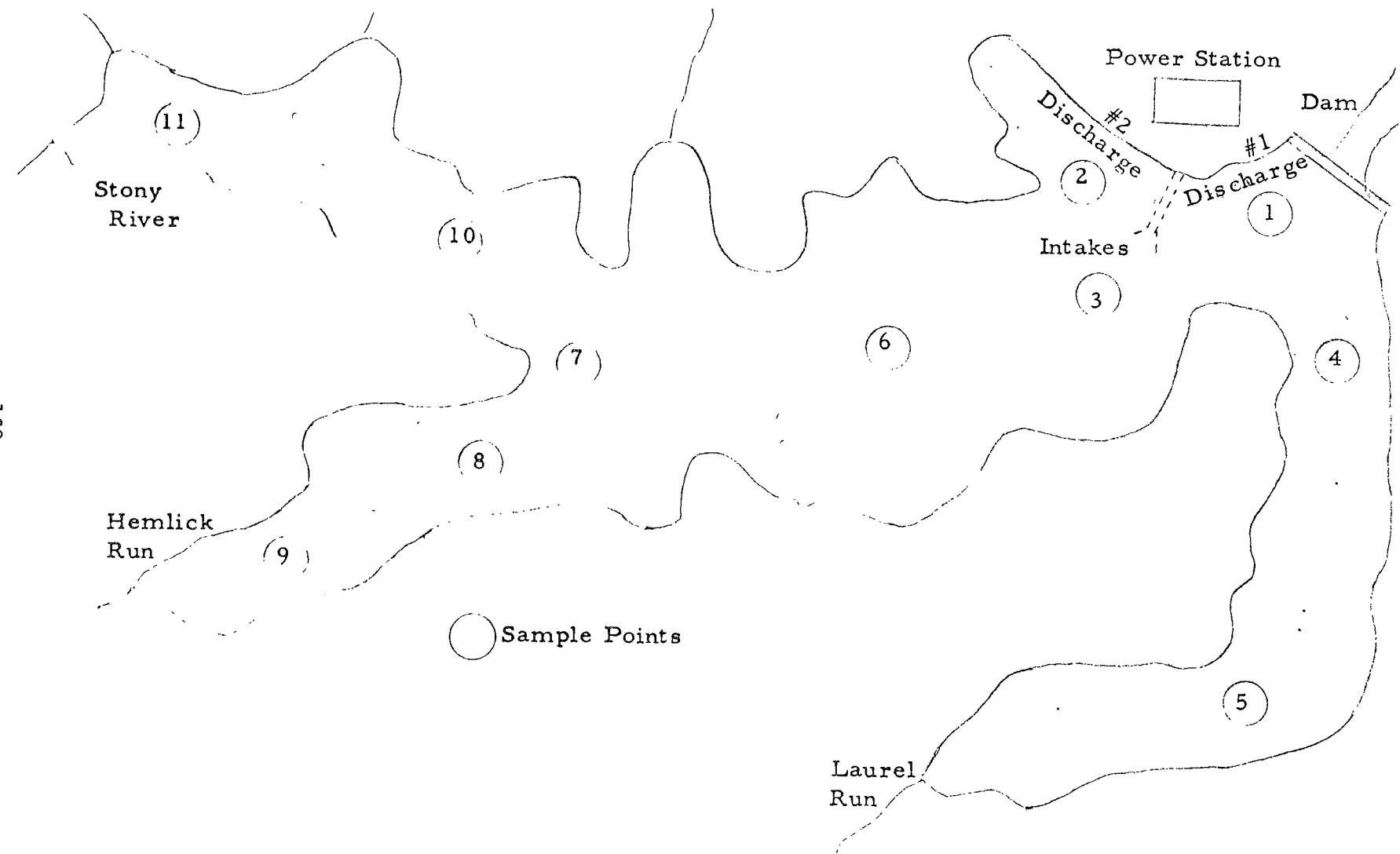
LATITUDE 38° 53' N
 LONGITUDE 79° 51' W
 ELEVATION (ground) 1970 Feet

ELKINS, WEST VIRGINIA
 ELKINS-RANDOLPH CO AP
 1968

Month	Temperature								Degree days	Precipitation								Relative humidity			
	Averages				Extremes					Total	Greatest in 24 hrs.	Date	Snow, Sleet								
	Daily maximum	Daily minimum	Monthly	Highest Date	Lowest Date	Degree days	Total	Greatest in 24 hrs.	Date				Total	Greatest in 24 hrs.	Date						
JAN	38.6	11.4	25.0	54 22	-17 2	1233	1.88	0.76	13-14	14.1	4.6	13-14	83	86	65	75					
FEB	33.0	11.0	22.0	59 1	-5 23+	1239	1.80	0.69	29	24.1	8.6	20-21	70	74	49	56					
MAR	55.5	28.1	41.8	79 22	7 14	711	4.28	1.28	12-13	10.3	8.3	29-1	77	83	53	57					
APR	64.0	35.8	49.9	78 14+	21 2	444	1.54	0.45	4-5	0.1	0.1	11	81	86	52	48					
MAY	66.9	44.6	55.8	80 15+	25 7	279	7.30	1.86	23-24	0.0	0.0		84	87	60	65					
JUN	78.7	51.9	65.3	89 30	39 21	67	2.05	0.42	11	0.0	0.0		96	95	57	72					
JUL	82.1	56.2	69.2	98 18+	40 5	16	3.46	1.01	25	0.0	0.0		97	97	55	69					
AUG	81.0	58.8	69.9	87 23+	39 29	46	4.07	1.24	0.0	0.0	0.0		97	97	62	77					
SEP	74.4	48.1	61.3	83 24	34 30	122	3.01	1.29	10	0.0	0.0		98	59	82						
OCT	63.5	39.0	51.3	78 14	20 31	425	3.21	1.05	18-19	0.5	0.5	29	95	56	76						
NOV	51.7	32.7	42.2	73 1	15 14	673	3.20	0.97	6-7	11.9	8.9	12	89	67	79						
DEC	39.0	18.1	28.6	51 28	-5 11	1121	3.04	0.69	4	19.7	4.0	18	82	70	77						
YEAR	60.7	36.3	48.5	39 30	-17 2	6376	38.84	1.86	23-24	80.7	8.9	NOV.	89	59	69						

NOTE: Station operated less than full time after July. Summary based on available data.

Month	Wind								Percent of possible sunshine sunrise to sunset	Number of days								Temperatures				
	Resultant		Fastest mile				Sunrise to sunset			Precipitation		Snow, Sleet		Thunderstorms		Heavy fog						
			Speed	Average speed	Speed	Direction	Date	Clear	Partly cloudy	Cloudy	1/1 inch or more	1/10 inch or more	1/100 inch or more	Thundershowers	90° and above	32° and below	32° and below	0° and below				
JAN	28	2.2	6.9	31	30	7	7.1	8	3	20	15	6	0	3	0	0	8	28	5			
FEB	28	5.7	9.6	29	31	17	6.3	7	9	13	11	7	0	1	14	29	5					
MAR	28	5.0	9.5	37	28	23	7.2	6	5	20	17	3	3	2	0	2	18	0				
APR	27	2.8	7.8	40	30	14	7.7	4	5	21	14	7	3	2	0	0	13	0				
MAY	27	3.4	8.4	37	31	3	8.4	2	4	25	18	0	4	4	0	0	4	0	0			
JUN	28	2.5	5.5	25	12	8	7.7	3	9	18	13	0	9	14	0	0	0	0				
JUL				21	30	22	7.0	5	9	17	10	0	8	13	0	0	0	0				
AUG				35	25	7	7.0	3	13	15	13	0	0	0	0	0	0	0				
SEP	?			16	16	18+	7.0	4	12	14	7	0	0	0	0	0	0	0				
OCT				23	14	18	6.5	8	7	16	11	0	0	0	0	0	0	8	0			
NOV				30	30	19	9.1	1	4	25	17	2	2	0	0	0	2	15	0			
DEC				35	28	5	8.7	2	6	23	22	8	0	0	0	0	10	30	3			
YEAR				40	30	14	7.5	53	86	227	168	26	0	0	0	0	36	145	13			



Mt. Storm Plant and Cooling Pond

Figure C-5

RESERVOIR TEMPERATURES
MT. STORM RESERVOIR

ALL TEMPERATURES IN DEGREES FARENHEIT

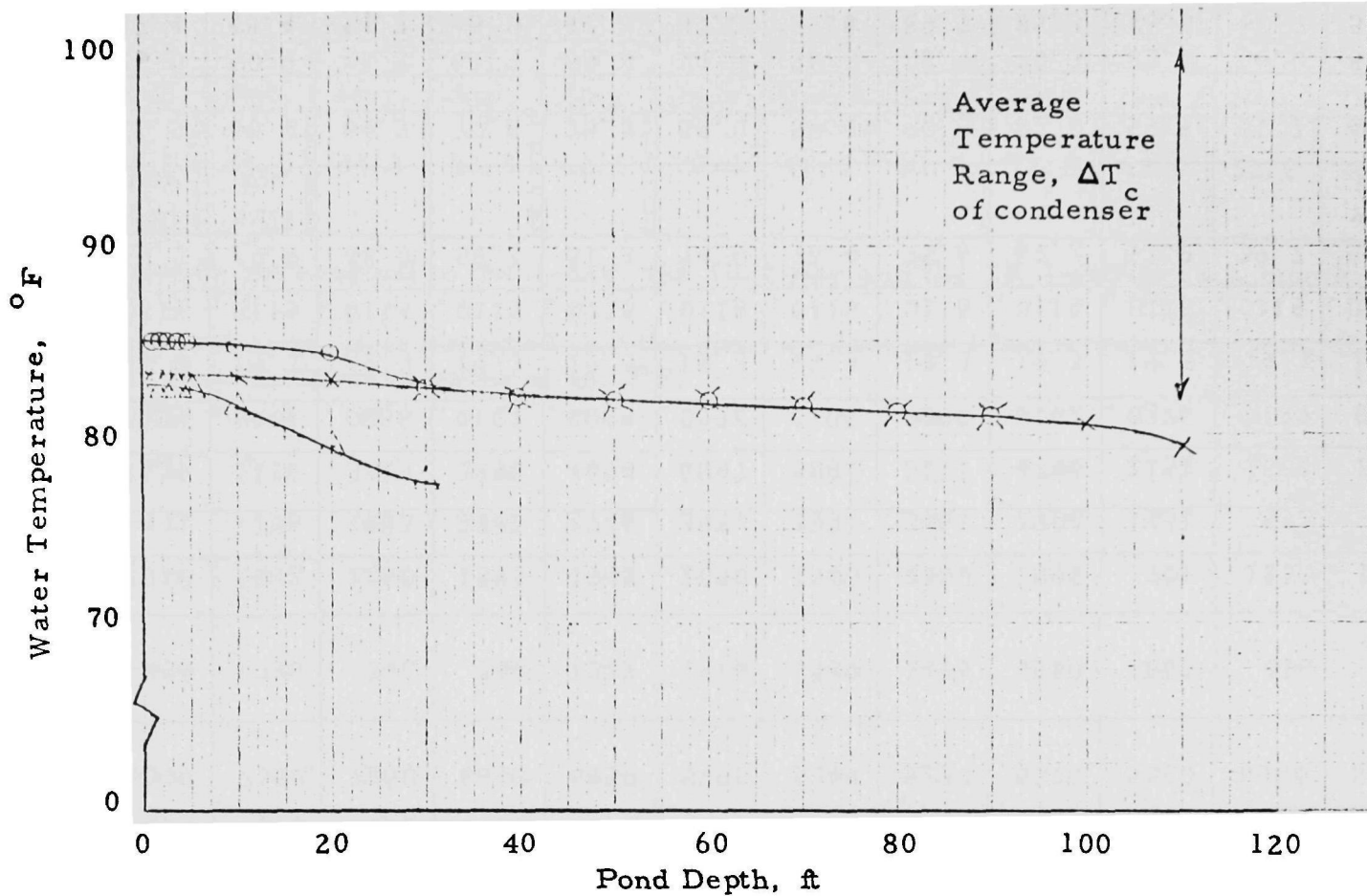
Date	8-28-68	8-28-68	8-28-68	8-28-68	8-28-68	8-28-68	8-28-68	8-28-68	8-28-68	8-28-68	8-28-68
Buoy	#1	#2	#3	#4	#5	#6	#7	#8	#9	#10	#11
Time	9:25 A	11:20 A	9:52 A	10:20 A	10:30 A	11:40 A	1:30 P	1:45 P	1:55 P	2:35 P	2:50 P
Depth											
1	85.0	84.4	83.4	83.0	83.4	84.4	83.8	82.6	82.0	83.6	83.3
2	85.0	84.4	83.4	83.0	83.4	84.4	83.8	82.6	82.0	83.6	83.3
3	85.0	84.4	83.4	83.0	83.4	84.4	83.8	82.6	82.0	83.6	83.3
4	85.0	84.6	83.5	83.4	83.5	84.2	83.5	82.5	82.0	83.6	82.8
5	85.0	84.6	83.5	83.4	83.5	84.2	83.5	82.5	82.0	83.6	82.8
10	84.8	84.0	83.2	83.4	83.2	84.1	83.0	81.5	81.3	83.3	82.7
20	84.4	83.1	83.0	83.0	82.7	83.2	82.3	79.0	79.6	82.1	
30	82.6	82.5	82.8	82.8	82.4	82.8	81.6	77.5		81.8	
40	82.0	82.2	82.3	82.5	82.2	82.2	81.3			81.5	
50	81.8	81.8	81.8	82.0		81.8				80.5	
60	81.8	81.4	81.6	81.8		81.2				80.5	
70	81.5	81.0	81.4			80.6					
80	81.0	80.6	81.2			80.1					
90	80.9		81.0								
100			80.6								
110			79.1								
120											
130											
140											
Bottom											
Ft & °F	92' 80.0°	88° 79.9°	117° 75.5°	65° 81.5°	47° 81.6°	87° 79.8°	45° 81.0°	30° 77.5°	22° 78.0°	59° 82.3°	15° 82.3°

The "pond" at Mt. Storm is very deep with the intake and outlet located in the same region of the pond. The intake structure is 93 feet below the surface and the two discharge structures are near the surface. As a result of this geometry, when considering the slug flow operation, it is necessary to consider the pond to be divided into two ponds each with a depth of 1/2 the actual value. In the upper "pond" the slug flows away from the intake, and in the lower "pond" the slug flows toward the intake structure. As a result of this assumption, the slug spends only one half of its time exchanging heat with the atmosphere and spends the other half returning undercover to the intake structure.

The tabulated parameters and predicted temperatures are shown in Table C-9 for steady state and transient operation.

Fig. C-6 shows the measured temperature-depth profile for the Mt. Storm pond in August. From Fig. C-6 it is noted that although the condenser range is 19.3°F (the average inlet and outlet condenser temperatures for August were 81.5°F and 100.8°F respectively), the measured points show relatively small temperature variation (small compared to 19.3°F) with either depth or horizontal displacement. As a result it can be concluded that considerable mixing in all three directions takes place in this pond. It should be pointed out that the intake and discharge structure for the Mt. Storm Plant consists of large diameter pipes rather than canals as in the Wilkes and Four Corners Plants. As a result, stronger mixing would be anticipated in the Mt. Storm pond.

The upper few feet (up to about 5 ft) of water at any given station is essentially uniform in temperature. If the measured temperature-depth profile was to be approximated as a straight line, the slope of the line would be about $0.05^{\circ}\text{F}/\text{ft}$.



Station 1 (Near outlet, outlet near surface)

See Fig. C-5

Station 9

for Station

Station 3 (Near inlet, inlet near bottom)

Locations

Mt. Storm Plant: Measured Temperature - Depth Profile, August

Figure C-6

TABLE C-9 - Mt. Storm Data, 1968

	Jan.	Feb.	Mar.	Apr.	May	June	July	Aug.	Sept.	Oct.	Nov.	Dec.
Q_N' , btu/ft ² day	2180	2335	3075	3620	3790	4500	4410	4320	3763	2950	2495	2190
T_a , °F	25.0	22.0	41.8	49.9	55.8	65.3	69.2	69.9	61.3	51.3	42.2	28.6
P_a , psia	.044	.035	.090	.116	.164	.246	.277	.291	.231	.152	.108	.062
W, mph	6.9	9.6	9.5	7.8	8.4	5.5	4.3	4.1	4.4	5.0	6.9	6.9
$a_{12} + a_{13} W =$ $(3730 + 3730W/10)$	6300	7300	7260	6640	6850	5790	5340	5250	5370	5590	6300	6300
$-3730(1+W/10)$ $[.089 - \theta_a$ $\times (.00473) - P_a]$	-490	-736	342	744	1315	1816	1940	1475	1500	860	416	-69
\dot{Q}_{pp} = WTE/A	2310	1842	2260	1893	1948	2090	1900	2150	1890	701	1030	1523
f_1	-6/1	-706	1053	2005	2746	395/	3991	3961	2904	1451	552	-238
$f_1 + \dot{Q}_{pp}$	1629	1136	3313	3898	4694	6047	5891	6111	4794	2152	1582	1285
$A(\Delta T_c)/WTE$.0083	.0105	.0086	.0107	.0099	.0092	.0105	.0090	.0102	.0275	.0187	.0126
ΔT_c , °F	19.3	19.3	19.3	19.3	19.3	19.3	19.3	19.3	19.3	19.3	19.3	19.3
$(t_{30.5})/C_p(V/A)$.0115	.0115	.0115	.0115	.0115	.0115	.0115	.0115	.0115	.0115	.0115	.0115
T_{equil} , °F	23.3 will ice	23.0 will ice	44.5	55.1	61.3	74.0	76.4	75.6	67.2	51.9	39.7	31.0 will ice
T_{mixed} , °F (steady state)	51.5	45.4	64.3	70.8	75.5	88.0	89.1	90.5	82.0	59.5	51.7	48.2
T_{mixed} , °F (transient*)	45.0 47.4 48.9	50.9 48.4 47.2	46.5 54.2 58.7	61.3 66.0 68.4	69.4 72.6 74.0	74.6 81.2 84.8	86.3 87.8 88.4	88.7 89.3 90.0	90.3 86.3 84.1	83.0 75.5 69.8	66.0 60.7 57.9	55.5 53.0 51.2

TABLE C-9 - Mt. Storm Data, 1968 (Cont.)

	Jan.	Feb.	Mar.	Apr.	May	June	July	Aug.	Sept.	Oct.	Nov.	Dec.
T Slug flow °F (transient operation)	43.5	41.5	44.5	53.5	62.5	70.5	78.5	81.5	78.5	65.0	52.0	45.5

*The three temperatures correspond to the 1-day, the 10. 2-day and the 20. 4-day of each month.

NOTE: For the transient case, it is assumed that the pond on January 1 has a water temperature equal to the measured intake value of 45. 0°F.

Four Corners Plant

Together with data for the Cholla Plant, Arizona Public Service Co. also supplied data for their Four Corners Plant in Farmington, New Mexico, together with a sketch of this site. These data are given below.

1967 Station Net Output (MW-HR)

Jan	371,666.1	July	406,318.8
Feb	356,133.5	Aug	373,721.1
Mar	355,936.1	Sept	363,212.1
April	300,292.0	Oct.	357,595.8
May	393,629.6	Nov	244,555.4
June	377,698.1	Dec.	319,519.1

Average 351,607.3 MH-HR

Pond surface area: 1200 acres

Total Plant rating in megawatts: 575 MW *

Average Temperature into Condenser by Month, 1967

<u>Month</u>	<u>°F</u>	<u>Month</u>	<u>°F</u>
January	41	July	75
February	45	August	76
March	50	September	74
April	56	October	66
May	58	November	55
June	67	December	43

Average depth of pond: 40 feet

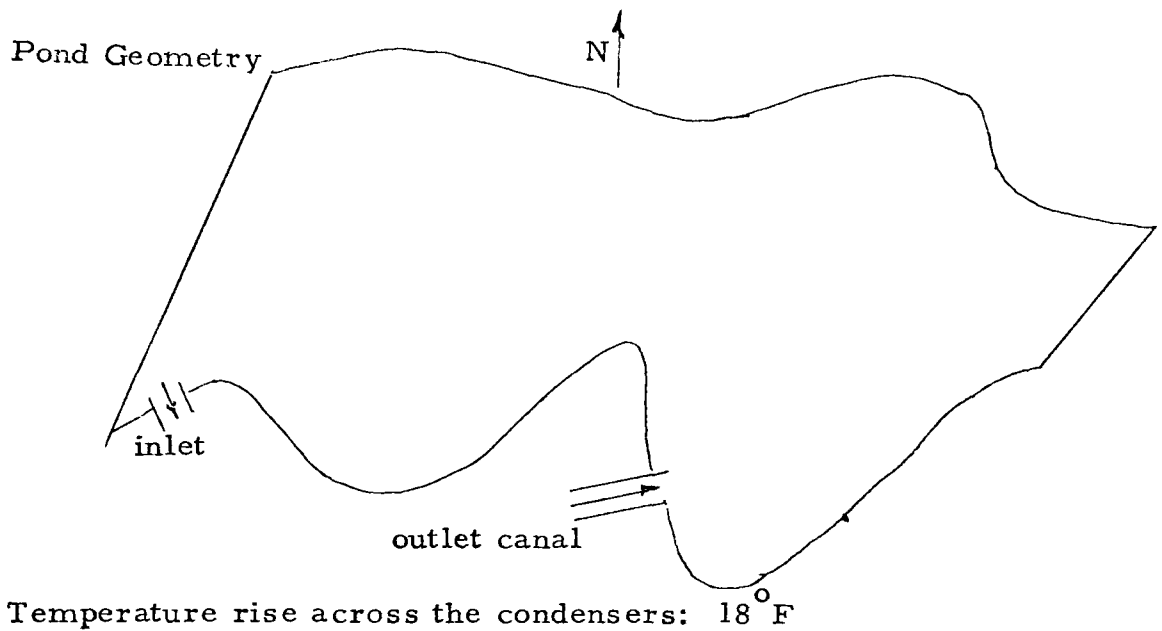
Maximum depth of pond: 110 feet

Minimum depth of pond: 3 feet

Typical Temperature-Depth Profiles in Pond, 1969

<u>Depth</u>	<u>°F</u>	<u>Depth</u>	<u>°F</u>
1'	82.5	50'	76.5
10'	82.0	60'	71.5
20'	81.5	70'	64.5
30'	81.0	80'	58.0
40'	79.0		

*Unit 4 was put into operation July, 1969. This will raise the plant rating considerably. However, not enough time has elapsed to give the data required, relative to cooling pond involving No. 4.



Using the same assumptions as for the Cholla and Wilkes plants and the yearly average heat rate of 10,278 btu from Ref. 25, the waste thermal energy can again be computed by Eqs. C-1 and C-2 where

$$T_{\text{average condenser outlet}} = 76.8^{\circ}\text{F}$$

The climatic data were the same data used for the Cholla Plant since these two plants are within a distance of about 175 miles of each other and the Winslow station is the nearest Weather Bureau.

Since this pond is relatively deep and of a regular shape, it is assumed that all 1200 acres of pond surface effectively enter into the cooling process. The tabulated parameters and predicted temperatures are shown for transient and steady state pond operation in Table C-10.

Fig. C-7 shows a typical measured temperature-depth profile for the Four Corners Pond in July. The closer the water is to the surface, the slower the temperature changes with depth. If the measured profile is approximated with a straight line, the slope (β) would be about $0.3^{\circ}\text{F}/\text{ft}$.

TABLE C-10 - Four Corners Data - 1967

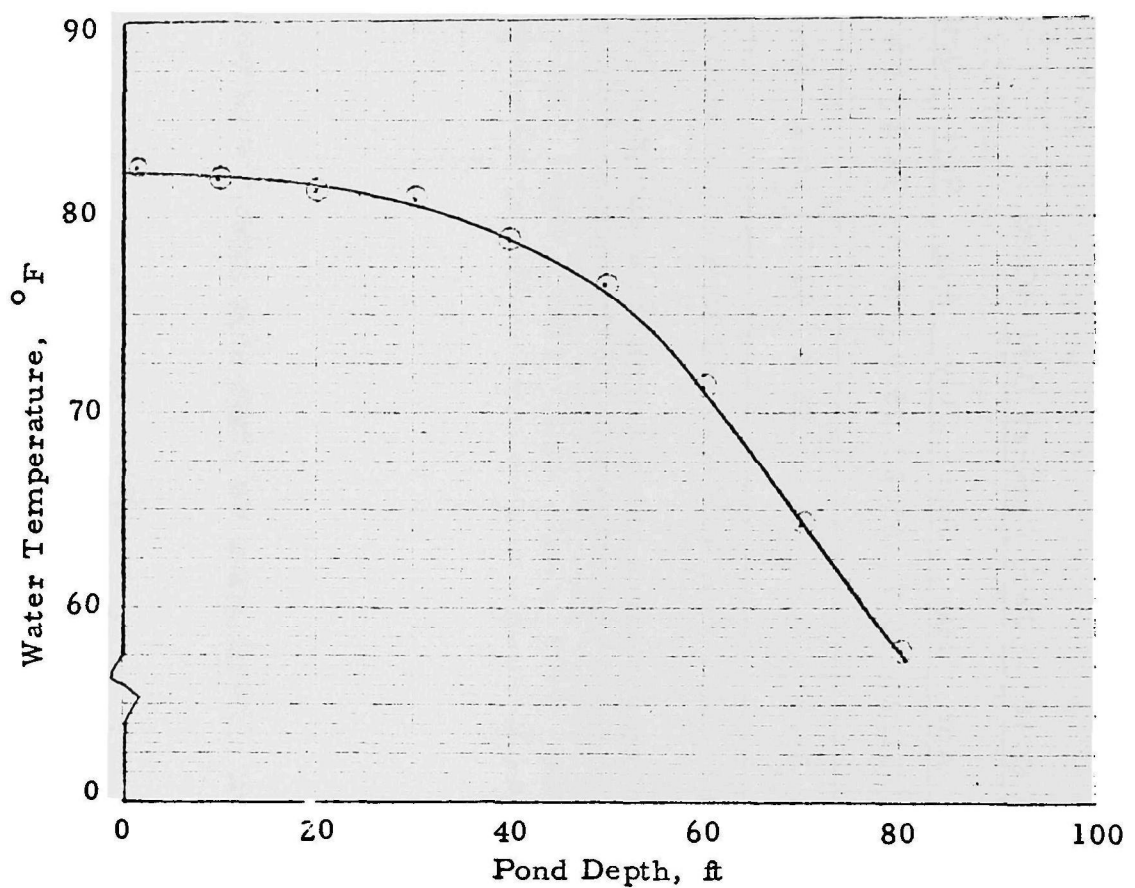
	Jan	Feb.	Mar	Apr	May	June	July	Aug	Sept	Oct.	Nov.	Dec.
Q_N , btu/ ft^2 day												
T_a , °F												
P_a , psia												
W , mph												
$a_{12} + a_{13} W =$ $(3730 + (3730W/10))$ $-3730(1 + W/10)$												
$x[.089 - \theta_a]$ $x(.00473) - P_a]$												
$Q_{pp} = WTE/A$	1282	1245	1268	1090	1440	1392	1570	1498	1400	1347	885	1115
f_1	-585	53	1305	1891	2849	4343	4931	4441	3441	1831	611	-938
$f_1 + \dot{Q}_{pp}$	697	1298	2573	2981	4289	5735	6501	5936	4841	3178	1496	177
$A(\Delta T_c)/WTE$.0140	.0144	.0142	.0164	.0124	.0126	.0114	.0119	.0128	.0133	.0203	.0161
ΔT_c , °F	18	18	18	18	18	18	18	18	18	18	18	18
$(t_{30.5})/C\rho(V/A)$.0122	.0122	.0122	.0122	.0122	.0122	.0122	.0122	.0122	.0122	.0122	.0122
T_{equil} , °F	23.5 will ice	32.2	46.5	50.8	59.9	70.0	76.6	74.3	66.8	53.5	40.6	18.6 will ice
T_{mixed} , °F* (transient)	41.5 41.4 41.4	41.4 43.4 44.8	46.1 51.6 54.3	56.1 57.5 58.1	58.4 64.5 67.9	69.4 74.7 77.0	77.7 82.6 84.8	85.6 84.5 83.8	83.4 79.2 77.6	76.9 71.9 68.2	66.8 60.8 57.8	54.9 49.0 45.7

TABLE C-10 - Four Corners Data (Cont.)

	Jan.	Feb.	Mar	Apr.	May	June	July	Aug.	Sept.	Oct.	Nov.	Dec.
T _{slug Flow'} °F (Transient)	37.0	37.7	43.0	51.2	55.7	65.2	75.0	78.0	74.2	65.0	54.0	46.0
T _{mixed'} °F (steady state)	41.4	47.9	57.8	58.8	70.9	78.3	86.4	83.2	76.2	65.1	50.6	34.0

* The three temperatures correspond to the 1-day, 10. 2-day and 20. 4-day of each month.

NOTE: Predicted transient operation temperatures are based on the assumption that the pond on 1 January has a water temperature at the intake equal to the measured value of 41. 5° F.



Four Corners Plant: Measured Temperature Depth Profile
July 1969

Figure C-7

1 Accession Number

2 Subject Field & Group

Ø5D

SELECTED WATER RESOURCES ABSTRACTS
INPUT TRANSACTION FORM

5 Organization

Littleton Research and Engineering Corporation
Littleton, Massachusetts

6 Title

AN ENGINEERING-ECONOMIC STUDY OF COOLING POND PERFORMANCE

10 Author(s)

Hogan, W. T.,
Liepins, A. A., and
Reed, F. E.

16 Project Designation

FWQA Contract 14-12-521; DFX

21 Note

22 Citation

FWQA, R & D Report No. 16130DFX05/70

23 Descriptors (Starred First)

*Thermal pollution, *Cooling water, *Ponds, *Design, *Economic Evaluation,
 *Energy budget, Heated water, Heat transfer, Thermal Power Plants, Economics,
 Capital costs, Operating costs, Evaporation, Convection, Design data

25 Identifiers (Starred First)

*Cooling ponds

27 Abstract

A procedure for predicting the temperature of a thermally loaded captive pond is presented. Using this information, the cooling pond is shown in a special case to have an economic advantage over a cooling tower and to be not much more expensive than a natural body (stream or ocean) or water. This, with the ecological and recreational assets of a captive cooling pond, would seem to encourage their expanded use with large thermo-electric power plants.

This report was submitted in fulfillment of Contract No. 14-12-521 under the sponsorship of the Federal Water Quality Administration. (Hogan-Littleton)

Abstractor
W. T. HoganWR-102 (REV. JULY 1969)
WRSIC

Institution

Littleton Research & Engineering Corporation

 SEND TO: WATER RESOURCES SCIENTIFIC INFORMATION CENTER
 U.S. DEPARTMENT OF THE INTERIOR
 WASHINGTON, D. C. 20240